



Deliverable D10.2

Report on the initial developments and preparatory works for the integrated demo

Project acronym:	FP3-IAM4RAIL
Starting date:	01/12/2022
Duration (in months):	48
Call (part) identifier:	HORIZON-ER-JU-2022-01
Grant agreement no:	101101966
Due date of deliverable:	M10, July 2024
Actual submission date:	06/07/2025
Responsible/Author:	Strukton Rail Nederland (SRNL)
Dissemination level:	PU
Status:	Issued

Reviewed: (yes)

Document history		
Revision	Date	Description
0.1	01-11-2023	First issue, for work package internal use only
0.2	07-08-2024	Final draft for project internal review (DB)
0.3	15-09-2024	Last work package internal review
1.0	07-10-2024	Final version to send to project coordinator
1.1	19-06-2025	Final version responding to rejection letter including appendix and changes marked in sections

Contributors		
Name	Beneficiary	Details of contribution
Pérez Martinez, Pedro Martin	ADIF	Descriptions of Spanish turnouts to be monitored
Botella Del Valle, Iñigo	ADIF (Ineco)	Descriptions of Spanish turnouts to be monitored
Camacho, Javier	CAF (Cetest)	Onboard monitoring (ABA) and applications: characterization of track geometry parameters' measurement.
Rodríguez, Borja	CEIT	Monitoring turnouts acceleration signals and Detection of missing / loosened fasteners with ABA
Bravo, Imanol	CEIT	Detection of missing / loose fasteners with ABA
Amundarain, Aiert	CEIT	Inspection turnouts: analysing 3-dimensional reconstruction
Iparraguirre, Olatz	CEIT	Occlusion monitoring due to vegetation
Borro, Diego	CEIT	Occlusion monitoring due to vegetation
San Miguel, Mario	CEIT	Rail crack detection using microwaves
Adin, Iñigo	CEIT	Rail crack detection using microwaves
Astiazaran, Alex	CEIT	Monitoring turnouts acceleration signals
Baasch, Bejamin	DLR	Multi-Sensor track monitoring and Digital Twin of Vehicle-Track-Interaction (section 12)
Lähns, Alexander	DLR	Multi-Sensor Track Monitoring
Groos, Jörn	DLR	Structure of the document, Editor
Heckmann, Andreas	DLR	Digital Twin of Vehicle-Track-Interaction
Oselin, Pierfrancesco	DLR	Digital Twin of Vehicle-Track-Interaction
Neumann, Thorsten	DLR	Holistic Monitoring, Diagnostic Models and Decision Support
Reetz, Susanne	DLR	Holistic Monitoring, Diagnostic Models and Decision Support
Boogaard, Anthony	Strukton Rail	Onboard monitoring and applications
Buursma, Douwe	Strukton Rail	Wayside monitoring and applications
Ramaker, Silvester	Strukton Rail	On-board monitoring (GPR) and applications
Samson, Henk	Strukton Rail	Structure of the document, Editor
Tiecken, Jacques	Strukton Rail	On-board monitoring and applications
Bucher, Christian	Voestalpine	Wayside monitoring, applications and pilot sites
Titze, Thomas	Voestalpine	Wayside monitoring, applications and pilot sites
Ebner-Mürzl, Christian	Voestalpine	Wayside monitoring, applications and pilot sites
Kaiser, Sonja	Voestalpine	Wayside monitoring, applications and pilot sites
Velic, Dino	Voestalpine	Wayside monitoring, applications and pilot sites
Pålsson, Björn	Chalmers University of Technology	Wayside monitoring, applications and pilot sites
Theysen, Jannik	Chalmers University of Technology	Wayside monitoring, applications and pilot sites
Heinzleiter, Paul	RISC Software GmbH	Monitoring data preparation

Disclaimer

The information in this document is provided "as is", and no guarantee or warranty is given that the information is fit for any particular purpose. The content of this document reflects only the author's view – the Joint Undertaking is not responsible for any use that may be made of the information it contains. The users use the information at their sole risk and liability.

The content of this Deliverable does not reflect the official opinion of the Europe's Rail Joint Undertaking (EU-Rail JU). Responsibility for the information and views expressed in the therein lies entirely with the author(s).

TABLE OF CONTENTS

1.	EXECUTIVE SUMMARY	13
2.	ABBREVIATIONS AND ACRONYMS	14
3.	BACKGROUND & OBJECTIVE / AIM & INTRODUCTION	16
3.1.	BACKGROUND & CONTEXT	16
3.2.	OBJECTIVE / AIM	16
3.3.	READING GUIDE AND REFERENCE TO PREVIOUS DELIVERABLE (D10.1)	17
3.4.	LINK BETWEEN USE CASES AND APPLICATIONS	18
4.	PILOT SITES	20
4.1.	SPAIN: HIGH SPEED & CONVENTIONAL LINE PILOT SITES	20
4.1.1.	<i>Conventional Line Pilot Site</i>	<i>20</i>
4.1.2.	<i>High Speed Pilot Site</i>	<i>27</i>
4.2.	THE NETHERLANDS	37
4.2.1.	<i>Description</i>	<i>37</i>
4.2.2.	<i>Installed Equipment</i>	<i>38</i>
4.2.3.	<i>Current status mixed traffic demonstrator Netherlands</i>	<i>38</i>
4.2.4.	<i>Current status of wayside monitoring data</i>	<i>38</i>
5.	UTILIZED TOOLS, SOLUTIONS AND SYSTEMS	41
5.1.	MULTI SENSOR & MULTI-VEHICLE TRAIN BORNE SYSTEM	41
5.1.1.	<i>Introduction to the Use of the Leonardo Platform</i>	<i>41</i>
5.1.2.	<i>The LEONARDO platform in a nutshell</i>	<i>41</i>
5.2.	MULTI-SENSOR WAYSIDE MONITORING OF SWITCHES	42
5.2.1.	<i>Using novel multi-sensor systems for infrastructure wayside monitoring</i>	<i>43</i>
5.2.2.	<i>Integrated asset management and monitoring platform</i>	<i>45</i>
5.2.3.	<i>The POSS® System in a nutshell</i>	<i>48</i>
6.	HOLISTIC MONITORING AND DECISION SUPPORT	49
6.1.	INTEGRATED DATA SET FOR HOLISTIC MONITORING AND DIAGNOSTICS	50
6.2.	THE WORK TOWARDS DIGITAL TWIN	50
7.	REALITY MODEL	51
7.1.	INTRODUCTION	51
7.1.1.	<i>Background of this application</i>	<i>51</i>
7.1.2.	<i>Scope / Objective / Aim</i>	<i>51</i>
7.1.3.	<i>Broader context</i>	<i>52</i>
7.1.4.	<i>Description of the technology</i>	<i>52</i>
7.1.5.	<i>Functionality in detail</i>	<i>53</i>
7.2.	PROGRESS	54
7.2.1.	<i>Tests</i>	<i>54</i>
7.2.2.	<i>Next steps</i>	<i>54</i>
8.	HOLISTIC SWITCH MONITORING AND DIAGNOSTIC MODEL	55
8.1.	INTRODUCTION AND METHODOLOGY	55
8.2.	WORK PROGRESS	55
8.3.	ACHIEVED RESULTS	56
8.3.1.	<i>Feature engineering for switch diagnostics</i>	<i>56</i>
8.3.2.	<i>Effects of power supply variations on condition monitoring of point machines</i>	<i>58</i>

8.3.3.	<i>Effects of track geometry on point machines</i>	59
8.4.	STATUS HANDED OVER FROM WP10 TO WP11	61
8.5.	PRELIMINARY RESULTS THAT CAN BE USED	61
9.	MULTI-SENSOR TRACK MONITORING	62
9.1.	INTRODUCTION AND METHODOLOGY	62
9.1.1.	<i>State of the art</i>	62
9.1.2.	<i>Challenges</i>	62
9.1.3.	<i>Our approach</i>	63
9.2.	WORK PROGRESS.....	64
9.3.	ACHIEVED RESULTS.....	64
9.3.1.	<i>Comprehensive Data Collection:</i>	64
9.3.2.	<i>ABA data processing and analysis:</i>	64
9.3.3.	<i>Computer vision:</i>	66
9.4.	STATUS HANDED OVER FROM WP10 TO WP11	68
9.4.1.	<i>Data Integration and Management:</i>	68
9.4.2.	<i>Enhanced Accuracy and Reliability:</i>	68
9.5.	PRELIMINARY RESULTS THAT CAN BE USED	69
9.5.1.	<i>ABA processing and analysis</i>	69
9.5.2.	<i>Switch detection and classification</i>	69
10.	DETECTION OF LOOSE FASTENERS WITH ABA	70
10.1.	INTRODUCTION AND METHODOLOGY	70
10.2.	WORK PROGRESS.....	72
10.3.	ACHIEVED RESULTS.....	74
10.4.	STATUS HANDED OVER FROM WP10 TO WP11	76
10.5.	PRELIMINARY RESULTS THAT CAN BE USED	77
11.	SOUND RECORDINGS FROM ABA FOR DIAGNOSTICS	78
11.1.	SCOPE / OBJECTIVE /AIM.....	78
11.1.1.	<i>State of the art</i>	78
11.1.2.	<i>Challenges / Techniques to be applied</i>	79
11.2.	DEVELOPMENTS / NEXT STEPS	79
11.3.	FURTHER DEVELOPMENTS.....	80
12.	DIGITAL TWIN: DYNAMIC VEHICLE RESPONSE ANALYSIS EXCITATION RAIL SURFACE UNEVENNESS	82
12.1.	INTRODUCTION AND METHODOLOGY	82
12.1.1.	<i>State of the art</i>	83
12.1.2.	<i>Challenges</i>	83
12.2.	ACHIEVED RESULTS.....	84
12.3.	STATUS HANDED OVER FROM WP10 TO WP11	86
12.4.	PRELIMINARY RESULTS THAT CAN BE USED	87
13.	TRACK GEOMETRY MEASUREMENT FROM PASSENGER VEHICLE	88
13.1.	INTRODUCTION AND METHODOLOGY	88
13.1.1.	<i>Scope / Objective /Aim</i>	88
13.1.2.	<i>Description of the technology</i>	88
13.2.	WORK PROGRESS.....	89
13.2.1.	<i>State of the art</i>	89
13.2.2.	<i>Challenges</i>	89
13.2.3.	<i>Developments</i>	90

13.3.	ACHIEVED RESULTS.....	91
13.4.	STATUS HANDED OVER FROM WP10 TO WP11	93
13.5.	PRELIMINARY RESULTS THAT CAN BE USED	94
14.	OCCCLUSION MONITORING DUE TO VEGETATION.....	95
14.1.	INTRODUCTION AND METHODOLOGY	95
14.2.	WORK PROGRESS.....	98
14.3.	ACHIEVED RESULTS.....	105
14.4.	STATE THE STATUS HANDED OVER FROM W10 TO WP11.....	105
15.	MONITORING TURNOUTS ACCELERATION SIGNALS.....	106
15.1.	INTRODUCTION AND METHODOLOGY	106
15.2.	WORK PROGRESS.....	107
15.3.	ACHIEVED RESULTS.....	112
15.4.	STATUS HANDED OVER FROM WP10 TO WP11	116
15.5.	PRELIMINARY RESULTS THAT CAN BE USED	119
16.	RAIL CRACK DETECTION USING MICROWAVES	120
16.1.	INTRODUCTION AND METHODOLOGY	120
16.2.	WORK PROGRESS.....	121
16.3.	ACHIEVED RESULTS.....	122
16.3.1.	<i>System requirements derived from user needs.....</i>	<i>122</i>
16.3.2.	<i>Research on state of the art</i>	<i>124</i>
16.3.3.	<i>Definition of test protocol and development of laboratory test bench</i>	<i>127</i>
16.3.4.	<i>Electromagnetic simulations of the problem (ANSYS).....</i>	<i>128</i>
16.3.5.	<i>Off-line processing of laboratory signals and simulations.....</i>	<i>133</i>
16.3.6.	<i>Proof of Concept at Laboratory</i>	<i>133</i>
16.3.7.	<i>Proposal for system architecture and refining of system requirements</i>	<i>136</i>
16.4.	STATUS HANDED OVER FROM WP10 TO WP11	138
16.5.	PRELIMINARY RESULTS THAT CAN BE USED	139
17.	INSPECTION TURNOUTS: ANALYSING 3-DIMENSIONAL RECONSTRUCTION	140
17.1.	INTRODUCTION AND METHODOLOGY	140
17.2.	WORK PROGRESS.....	145
17.3.	ACHIEVED RESULTS.....	147
17.4.	STATUS HANDED OVER FROM WP10 TO WP11	148
17.5.	PRELIMINARY RESULTS THAT CAN BE USED	149
18.	SWITCH MONITORING.....	150
18.1.	FUNCTION: DATA FUSION METHODS FOR MONITORING DATA	151
18.1.1.	<i>FP3-IAM4RAIL Turnouts Data Pipeline</i>	<i>153</i>
18.1.2.	<i>Visualization of Validated Data</i>	<i>154</i>
18.1.3.	<i>Feature Engineering for Machine Learning</i>	<i>158</i>
18.1.4.	<i>Selection of Relevant Acceleration Channels Based on Data Availability.....</i>	<i>161</i>
18.2.	FUNCTION: MODEL-BASED CONDITION MONITORING OF SWITCHES AND CROSSINGS	161
18.2.1.	<i>Multibody simulation model.....</i>	<i>162</i>
18.2.2.	<i>Waveguide finite element model.....</i>	<i>163</i>
18.3.	FUNCTION: DRIVE/DETECTOR ROD MONITORING	164
18.4.	FUNCTION: SWITCH ASSEMBLY MONITORING	165
18.5.	FUNCTION: TRACK QUALITY MONITORING.....	166
18.6.	FUNCTION: VEHICLE/TRACK INTERACTION AND THE RESULTING DYNAMIC FORCES	170



18.6.1.	<i>Brief introduction to the application.....</i>	<i>170</i>
18.6.2.	<i>Description of the technology.....</i>	<i>170</i>
18.6.3.	<i>Methodology</i>	<i>171</i>
18.6.4.	<i>Description of the data</i>	<i>172</i>
18.7.	FUNCTION: FROG / SWITCH RAIL MONITORING	174
18.8.	FUNCTION: FROG MONITORING	178
19.	CONCLUSIONS	181
20.	WORKS CITED	183

List of Figures

FIGURE 3-1: SCOPE RAIL INFRASTRUCTURE MONITORING, RANGE OF 360 DEGREES	16
FIGURE 4-1: SCHEMATIC ILLUSTRATION OF THE MONITORING SYSTEM ARCHITECTURE FOR THE MIXED TRAFFIC TURNOUT DEMONSTRATOR.	21
FIGURE 4-2: INSTALLED MULTI-SENSORS IN CROSSING PANEL FOR TRACK QUALITY AND WING RAIL / CROSSING NOSE MONITORING.	22
FIGURE 4-3: MULTI-SENSORS INSTALLED IN SWITCH PANEL FOR TRACK QUALITY AND SWITCH RAIL / STOCK RAIL WEAR MONITORING.	22
FIGURE 4-4: SENSOR LOCATIONS AT FIRST DRIVE LEVEL ON POINT RAIL AND HOLLOW SLEEPER	23
FIGURE 4-5: APPLICATION OF STRAIN GAUGE SENSORS	24
FIGURE 4-6: ACCELERATION SENSOR.....	24
FIGURE 4-7: DISPLACEMENT SENSOR	25
FIGURE 4-8: STRAIN GAUGE SIGNALS OF SHORT-TERM VALIDATION MEASUREMENT SYSTEM.....	25
FIGURE 4-9: FEATURES OF ACCELERATION MEASUREMENTS OF SHORT-TERM VALIDATION MEASUREMENT SYSTEM	26
FIGURE 4-10: COMPARISON OF VERTICAL SLEEPER DISPLACEMENTS IN CROSSING AREA RECORDED FOR ONE PASSAGE WITH THE PERMANENT MONITORING SYSTEM (LEFT) AND THE SHORT-TERM VALIDATION MEASUREMENT SYSTEM (RIGHT)	27
FIGURE 4-11: HIGH SPEED LINE TURNOUT DEMONSTRATOR.....	28
FIGURE 4-12: SCHEMATIC SYSTEM ARCHITECTURE OF MONITORING SYSTEM INSTALLED AT SWITCH PANEL OF THE HIGH-SPEED DEMONSTRATOR LOCATED IN SANTA CRUZ DE LA ZARZA.	29
FIGURE 4-13: SCHEMATIC SYSTEM ARCHITECTURE OF MONITORING SYSTEM INSTALLED AT CROSSING PANEL OF THE HIGH-SPEED DEMONSTRATOR TURNOUT LOCATED IN SANTA CRUZ DE LA ZARZA.	30
FIGURE 4-14: INDUCTIVE SENSORS FOR SWITCH POSITION MONITORING OF THE CLOSED SWITCH RAIL AT THE BEGINNING OF THE SWITCH AND MULTI SENSOR FOR TRACK QUALITY MONITORING.	30
FIGURE 4-15: MULTI-SENSORS MOUNTED BOTH STOCK RAILS (BEGINNING OF THE SWITCH) AND INDUCTIVE SENSORS FOR SWITCH POSITION MONITORING AND MULTI SENSOR FOR TRACK QUALITY MONITORING.....	31
FIGURE 4-16: INDUCTIVE SENSORS FOR MONITORING THE NEAREST FLANGEWAY AND THE CLOSED SWITCH RAIL AT THE END OF THE SWITCH PANEL.....	31
FIGURE 4-17: MULTI-SENSORS INSTALLED IN CROSSING PANEL FOR TRACK QUALITY AND WING RAIL / SWING NOSE MONITORING.	32
FIGURE 4-18: ANALOGUE ACOUSTIC SENSOR INSTALLED ON POINT MACHINE CASING FOR POINT MACHINE MONITORING.....	33
FIGURE 4-19: ANALOGUE ACOUSTIC SENSOR INSTALLED ON HOLLOW SLEEPER FOR DETECTOR ROD MONITORING.	33
FIGURE 4-20: SENSOR LOCATIONS AT FIRST DRIVE LEVEL ON POINT RAIL AND HOLLOW SLEEPER	34
FIGURE 4-21: APPLICATION OF STRAIN GAUGE SENSORS	35
FIGURE 4-22: ACCELERATION SENSOR.....	35
FIGURE 4-23: DISPLACEMENT SENSOR	36
FIGURE 4-24: STRAIN GAUGE SIGNALS OF SHORT-TERM VALIDATION MEASUREMENT SYSTEM.....	36
FIGURE 4-25: FEATURES OF ACCELERATION MEASUREMENTS OF SHORT-TERM VALIDATION MEASUREMENT SYSTEM	37
FIGURE 4-26: IMAGE OF THE LOCATION: VIEW FROM THE LEONARDO.....	38
FIGURE 4-27: FORM PRESENTING RESULTS OF THE VERIFICATION	39
FIGURE 5-1: OVERVIEW OF THE SENSORS MOUNTED ON THE LEONARDO PLATFORM	41
FIGURE 5-2: MULTI-SENSOR PLATFORM FOR TRACK QUALITY AND RAIL WEAR MONITORING USED IN VARIOUS LOCATIONS OF THE TWO DEMONSTRATOR TURNOUTS.....	44
FIGURE 5-3: SCHEMATIC ILLUSTRATION UTILISED MULTI-SENSOR WITH INCLUDED SENSOR MODULES AND INTERNAL CHANNEL ORIENTATIONS	44
FIGURE 5-4: ANALOGUE STRUCTURE BORNE NOISE SENSOR	45
FIGURE 5-5: INDUCTIVE DISPLACEMENT SENSOR FOR SWITCH RAIL POSITION MONITORING	45
FIGURE 5-6: SCHEMATIC ILLUSTRATION OF THE ZENTRAK ASSET MANAGEMENT & MAINTENANCE AND INFRASTRUCTURE MONITORING PLATFORM.....	46
FIGURE 5-7: LANDING PAGE OF THE ZENTRAK INFRASTRUCTURE MONITORING MODULE. THE MAP SHOWS THE LOCATION OF THE TWO DEMONSTRATORS LOCATED IN THE ADIF MIXED TRAFFIC AND HIGH-SPEED NETWORK.....	46
FIGURE 5-8: ZENTRAK ASSET MANAGEMENT & MAINTENANCE MANAGEMENT SOFTWARE (MOBILE VERSION).....	47
FIGURE 6-1: STRATEGIC OPTIONS FOR AN OPTIMAL TRADE-OFF BETWEEN COSTS AND QUALITY OF INFRASTRUCTURE ASSET MONITORING BASED ON A HOLISTIC ANALYSIS.....	50
FIGURE 7-1: OVERALL CONTEXT OF THE REALITY MODEL.....	52
FIGURE 7-2: THE SIX STEPS TOWARDS THE REALITY MODEL	54
FIGURE 8-1: TIMELINE OF PREVIOUS, CURRENT AND FUTURE WORK RELATED TO THIS APPLICATION ("HOLISTIC SWITCH MONITORING AND DIAGNOSTIC MODEL.....	55
FIGURE 8-2: SCHEMATIC OVERVIEW PROPOSED DIAGNOSTIC MODEL (TAKEN FROM D12.2, I2S2)	56

FIGURE 8-3: EVOLUTION OF A CURRENT CURVE HUMP IN THE LOCKING SECTION WITH INCREASING HUMP SEVERITY OVER TIME MEASURED BY ITS PROMINENCE (= MAXIMAL VERTICAL DISTANCE BETWEEN CURRENT CURVE AND HUMP BASELINE) (CF [5]).	58
FIGURE 8-4: OVERLAPPING MOVEMENTS OF SEVERAL SWITCHES THAT DRAW FROM THE SAME POWER SUPPLY. DROPS IN THE AVAILABLE VOLTAGE (UPPER PLOT) CAUSED BY THE INRUSH PEAK OF ONE SWITCH ARE RESULTING IN DIPS IN THE MOTOR CURRENT CURVES (LOWER PLOT) OF THE OTHER SWITCHES	59
FIGURE 8-5: TRACK GEOMETRY MEASUREMENTS OF A SWITCH SEGMENT AND POINT MACHINE MOTOR CURRENT CURVES IN THE WEEK BEFORE	60
FIGURE 8-6: POSSIBLE EXAMPLE FOR CORRELATIONS BETWEEN CC MEASUREMENTS AND TRACK GEOMETRY	61
FIGURE 9-1: CONCEPT FOR RAIL DEFECT CLASSIFICATION USING ENSEMBLE LEARNING	63
FIGURE 9-2: ABA PROCESSING SEQUENCE TO RECONSTRUCT SPECTRAL FEATURES OF THE RAIL	65
FIGURE 9-3: TIME-FREQUENCY REPRESENTATION OF RAW ABA DATA	65
FIGURE 9-4: TIME-FREQUENCY REPRESENTATION OF ABA DATA AFTER NOISE REMOVAL	66
FIGURE 9-5: SEMANTIC SEGMENTATION TO EXTRACT RAIL LINES IN LEONARDO CAMERA DATA (EGO PERSPECTIVE)	67
FIGURE 9-6: SWITCH DETECTION AND CLASSIFICATION USING CAMERA DATA FROM THE LEONARDO PLATFORM	68
FIGURE 10-1: METHODOLOGY FOR DETECTION OF MISSING FASTENERS WITH ABA	72
FIGURE 10-2: EXAMPLE OF LOOSEN AND MISSING FASTENERS DETECTED BY THE LEONARDO VEHICLE	73
FIGURE 10-3: LEONARDO INSPECTION VEHICLE CHARACTERISTICS	74
FIGURE 10-4: INSPECTION DATA OF THE TRACK	75
FIGURE 10-5: : LEONARDO ABA DATA	75
FIGURE 10-6: EXAMPLE OF TRACK GEOMETRY INFORMATION AND LOCATION	76
FIGURE 11-1: SHOWS AN EXAMPLE OF ABA SOUND SIGNALS PLAYABLE WITH AN MP3 PLAYER	80
FIGURE 12-1: A DIGITAL TWIN OF THE DYNAMIC VEHICLE RESPONSES EMBEDDED IN A MODERN ASSET MONITORING AND MANAGEMENT CONCEPT	82
FIGURE 12-2: COUPLING DATA-DRIVEN MODELS WITH A PHYSICAL MODEL FOR MODELLING AND ANALYSING DYNAMIC VEHICLE RESPONSES. THE FIRST ANN EXTRACTS THE LONGITUDINAL RAIL PROFILE FROM THE MEASURED ABA DATA. THIS IN TURN IS CONVERTED BACK INTO ABA SIGNALS BY THE SECOND ANN AND THE PHYSICAL MODEL [22]	85
FIGURE 12-3: TRAINING RESULTS. TOP: A COMPARISON OF THE LONGITUDINAL PROFILE OF THE RAIL PREDICTED BY THE ANN (THE BLUE LINE) AND THE REFERENCE PROFILE (THE ORANGE LINE). CENTRE: A COMPARISON OF THE ABA SIGNAL PREDICTED BY THE ANN (THE BLUE LINE) AND MEASURED (THE ORANGE LINE). CENTRE: A COMPARISON OF THE ABA SIGNAL PREDICTED BY THE ANN (THE BLUE LINE) AND MEASURED (THE ORANGE LINE). BOTTOM: A COMPARISON OF THE ABA SIGNAL PREDICTED BY THE PHYSICAL MODEL (THE BLUE LINE) AND MEASURED (THE ORANGE LINE)	86
FIGURE 12-4: OPTIMIZATION WORKFLOW FOR MODEL PARAMETERS TUNING	87
FIGURE 13-1. CAF FEVE SERIES 2700 VEHICLE.	88
FIGURE 13-2. INSTALLATION OF SENSOR IN AXLE BOX FOR TRACK GEOMETRY ASSESSMENT.	89
FIGURE 13-3. REGIONAL CANTABRIA LINE USED FOR VEHICLE INTEGRATED COMPACT TRACK GEOMETRY SYSTEM CHARACTERIZATION.	90
FIGURE 13-4. SCHEME OF VEHICLE ORIENTATION, LEADING TRACK, TRAILING TRACK.	91
FIGURE 13-5. REFERENCE AND CALCULATED PARAMETERS (I).	92
FIGURE 13-6. REFERENCE AND CALCULATED PARAMETERS (II).	92
FIGURE 13-7. REFERENCE AND CALCULATED PARAMETERS (III).	92
FIGURE 13-8. REFERENCE-ESTIMATION DIFFERENCE DISTRIBUTIONS.	93
FIGURE 14-1: PROPOSED METHODOLOGY FOR VEGETATION OCCLUSION DETECTION.	97
FIGURE 14-2: SAMPLE IMAGES OF THE TWO DATASETS USED IN THIS USE CASE: A) GERALD DATASET AND B) CITYSCAPES DATASET.	99
FIGURE 14-3. CLASS DISTRIBUTION OF GERALD DATASET.	100
FIGURE 14-4. IMAGE SIZE ANALYSIS OF GERALD DATASET.	100
FIGURE 14-5. SAMPLE IMAGES OF TRACK ALTERNATIVES: A) STRUKTON'S ORIGINAL VIDEO AND B) SCREENSHOT OF TRAINSIMWORLD RANDOM TRACK.	101
FIGURE 14-6: EVALUATION METRICS FOR RAILWAY SIGNAL RECOGNITION MODEL TRAINED WITH GERALD DATASET.	102
FIGURE 14-7: SAMPLE OF MODEL'S INFERENCE ON A FRAME FROM LEONARDO'S JOURNEY	105
FIGURE 15-1: GENERAL LAYOUT OF A TURNOUT	106
FIGURE 15-2: METHODOLOGY FLOWCH	107
FIGURE 15-3: INSTRUMENTATION OF THE CROSSING	108
FIGURE 15-4: : INSTALLATION OF DISPLACEMENT SENSORS (A) AND ACCELEROMETERS (B)	108
FIGURE 15-5: A SCANNED CROSSING PANEL	109
FIGURE 15-6: BÉZIER CURVES AND PROFILES OF A CROSSING RAIL GENERATED BY SIMPACK.	110
FIGURE 15-7: 60E1 CROSSING RAIL SECTIONS FROM THE BENCHMARK.	110

FIGURE 15-8: SECTION OF A CROSSING NOSE IN A POINT CLOUD.....	111
FIGURE 15-9: : PRELIMINARY STRAIGHT LINE FINITE ELEMENT MODEL.....	111
FIGURE 15-10: PARTITION OF CONTACT PATCH BASED ON FASTSIM ALGORITHM.....	112
FIGURE 15-11: PASSING OF A LONG-DISTANCE TRAIN FROM THE CONVENTIONAL PILOT SITE CROSSING IN RIFÁ.....	113
FIGURE 15-12: ACCELERATION SIGNALS IN 3 DIRECTIONS	113
FIGURE 15-13: FFT OF THE ACCELERATION SIGNALS AT THE CENTRE OF THE FROG	114
FIGURE 15-14: BENCHMARK RESULTS COMPARISON WITH OTHERS	114
FIGURE 15-15: ADVANCED CONTACT PARAMETERS	115
FIGURE 15-16: DISTRIBUTION OF VERTICAL FORCES ON A CROSSING RAIL OBTAINED FROM MBS	115
FIGURE 15-17: CONTACT PATCH ON A FEM RAIL.....	116
FIGURE 15-18: ACCELERATION SIGNALS OBTAINED FROM FEM	116
FIGURE 15-19 NOMINAL CROSSING NOSE DRAWING (ADIF)	117
FIGURE 15-20: CATEGORIZATION OF DEGRADATION LEVEL.....	118
FIGURE 15-21: DEFINITION OF KPI ACCELERATION AVERAGE VALUE.....	118
FIGURE 15-22: DEFINITION OF HEALTH STATUS.....	119
FIGURE 16-1: RAILWAY INSPECTION USING MICROWAVES	120
FIGURE 16-2: HEAD CHECKING GENERATED ON A TRACK WHEN THE TRAIN WHEEL MOVES FROM LEFT TO RIGHT.....	122
FIGURE 16-3: SQUATTING DEFECT EXAMPLE.....	123
FIGURE 16-4: SHELLING EXAMPLES: (LEFT) INITIAL INDICATORS OF SHELLING AND (RIGHT) BREAK PROVOKED BY SHELLING	123
FIGURE 16-5: SIMPLIFIED FLOW DIAGRAM OF THE DETECTION SYSTEM OPERATION	124
FIGURE 16-6: PHOTOGRAPH OF THE POSITIONING SYSTEM.....	127
FIGURE 16-7: THREE STEEL SHEETS USED IN THE SETUP.....	128
FIGURE 16-8: ANSYS MODEL OF A RECTANGULAR WR90 WAVEGUIDE THAT RADIATES A STEEL BLOCK WITHOUT CRACKS	129
FIGURE 16-9: SIMULATED S11 FOR A DISTANCE VALUE OF 26MM BETWEEN WAVEGUIDE AND SURFACE	129
FIGURE 16-10: ANSYS MODEL OF A RECTANGULAR WR90 WAVEGUIDE THAT RADIATES A STEEL BLOCK WITH A RECTANGULAR CRACK ...	130
FIGURE 16-11: SIMULATED S11 FOR A DISTANCE VALUE OF 26MM BETWEEN WAVEGUIDE AND THE SURFACE WITH A CRACK.....	130
FIGURE 16-12: MAGNITUDE COMPONENT OF THE S11 RESULT OBTAINED FOR A DISTANCE VALUE OF 26MM BETWEEN WAVEGUIDE AND THE SURFACE WITH A CRACK.....	131
FIGURE 16-13: IMAGINARY COMPONENT OF THE S11 RESULT OBTAINED FOR A DISTANCE VALUE OF 26MM BETWEEN WAVEGUIDE AND THE SURFACE WITH A CRACK.....	131
FIGURE 16-14: ANSYS MODEL OF THE STEEL SURFACE WITH THREE CRACKS.....	132
FIGURE 16-15: IMAGE OBTAINED FROM THE PROCESSING OF THE S11 DATA USING THE PYTHON SCRIPT	132
FIGURE 16-16: . ROUTE FOLLOWED BY THE WAVEGUIDE WHEN PERFORMING THE MEASUREMENTS	134
FIGURE 16-17: (A) AMPLITUDE AND (B) PHASE RESULTS OF S11 AT 33 GHz (BLUE), 33.25 GHz (ORANGE) AND 36 GHz (YELLOW) ALONG THE ROUTE	135
FIGURE 16-18: OUTPUT SIGNALS OF THE CRACK DETECTION ALGORITHM	135
FIGURE 16-19: DIMENSIONS OF THE STEEL SHEETS USED TO EMULATE CRACKS IN THE LABORATORY SETUP	136
FIGURE 16-20: BLOCK DIAGRAM OF THE PROPOSED SYSTEM.....	137
FIGURE 16-21: SECOND OPTION FOR THE IMPLEMENTATION OF THE PROPOSED SYSTEM	137
FIGURE 16-22: BLOCK DIAGRAM OF THE COMPLETE MICROWAVE INSPECTION SYSTEM	138
FIGURE 17-1: A TURNOUT SCHEME	140
FIGURE 17-2: BLADED WHEEL GEOMETRIC MEASUREMENT	143
FIGURE 17-3: MANUAL SWITCH RAIL MEASUREMENT	143
FIGURE 17-4: TROLLEY KRAB	144
FIGURE 17-5: COMPONENTS OF A TURNOUT (SOURCE CHALMERS UNIVERSITY, PAPER JULY 2010).....	146
FIGURE 17-6: THE MODELS OF THE CROSSING PANEL AND THE SWITCH OF THE TURNOUT	147
FIGURE 17-7: REGISTER CAD MODEL AND CAPTURED MODEL.....	148
FIGURE 17-8: DISTANCES	148
FIGURE 18-1: SCHEMATIC ILLUSTRATION HOW FUNCTIONS ARE LINKED TO EACH OTHER AND HOW THE INTRODUCED TOOLS ARE CONTRIBUTING TO AN INTEGRATED ASSET MANAGEMENT DEMONSTRATOR.....	150
FIGURE 18-2: AN EXAMPLE FOR A PANDERA VALIDATION SCHEMA.....	153
FIGURE 18-3: EXAMPLE OF PANDERA VALIDATION FUNCTIONS FOR THE SCHEMA	154
FIGURE 18-4: PLOT OF ACOUSTIC EMISSION CHANNELS FOR CROSSING AND SWITCHING AREAS.....	155
FIGURE 18-5: PLOT OF MULTI-SENSOR CHANNELS FOR CROSSING AND SWITCHING AREAS.....	155
FIGURE 18-6: PLOT OF MIXED TRAFFIC CHANNELS	156

FIGURE 18-7: NUMBER OF DATA SAMPLES RECORDED BY THE ACOUSTIC SENSOR AT THE CROSSING AREA FROM MARCH TO DEC. 2024 ..	157
FIGURE 18-8: NUMBER OF DATA SAMPLES RECORDED BY MULTI-SENSOR AT THE CROSSING AREA FOR ACC CHANNELS FROM APRIL TO DEC. 2024	158
FIGURE 18-9: SPECTROGRAM OF THE ACCELERATION CHANNEL SWITCH_SL_DISP_ACC_LONG OF THE SWITCHING AREA	159
FIGURE 18-10: COMPARING THE READ SPEEDS OF DIFFERENT FILE FORMATS – PICKLE, PARQUET, HDF5 AND AVRO	160
FIGURE 18-11: MULTIBODY SIMULATION MODEL AND BOGIE MODEL IN SIMPACK.....	162
FIGURE 18-12: VERTICAL WHEEL-RAIL CONTACT FORCES ON WING RAIL AND SWING NOSE FOR LEADING AND TRAILING WHEEL SETS	163
FIGURE 18-13: NORMAL CONTACT FORCES BETWEEN SWING NOSE AND THE FIRST 14 SLIDE CHAIRS/BASE PLATES ALONG THE SWING NOSE. THIS REGION COVER THE DISTANCE FROM THE FIRST TO THE FOURTH LOCK.....	163
FIGURE 18-14: ACOUSTIC EMISSION SIGNALS OF THE ACOUSTIC SENSORS MOUNTED ON THE HOLLOW SLEEPERS FOR DETECTOR ROD MONITORING IN THE CROSSING PANEL.....	164
FIGURE 18-15: ACOUSTIC SIGNALS OF ANALOGUE ACOUSTIC SENSORS MOUNTED ON HOLLOW SLEEPERS IN SWITCH PANEL.....	165
FIGURE 18-16: SWITCH POSITION VALUES FOR LEFT AND RIGHT SWITCH RAIL IN TWO CROSS SECTIONS (FRONT AND BACK).	166
FIGURE 18-17: VERTICAL SLEEPER DISPLACEMENT RECORDED IN TWO CROSS SECTIONS OF SWITCH- AND CROSSING PANEL OF THE HIGH-SPEED DEMONSTRATOR LOCATED IN SANTA CRUZ DE LA ZARZA. ALL FOUR POSITIONS SHOW LOW DISPLACEMENTS (BELOW 1MM) WHICH INDICATES A GOOD BALLAST CONDITION AND HIGH TRACK QUALITY.	167
FIGURE 18-18: VERTICAL SLEEPER DISPLACEMENTS RECORDED AT SWITCH- AND CROSSING PANEL OF THE MIXED TRAFFIC DEMONSTRATOR LOCATED IN RIFA/TARRAGONA (CATALUNIA). HIGH DISPLACEMENTS IN CROSSING PANEL INDICATE POOR BALLAST SUPPORT AT THIS SLEEPER	167
FIGURE 18-19: VERTICAL AND LATERAL ACCELERATION SIGNAL MEASURED IN SWITCH AND CROSSING PANEL OF THE MIXED TRAFFIC DEMONSTRATOR TURNOUT IN RIFA / TARRAGONA. THE VERTICAL AND LATERAL ACCELERATION MAGNITUDES IN THE CROSSING AREA ARE VERY HIGH AND INDICATE A LOW ASSET HEALTH STAT.....	168
FIGURE 18-20: PICTURE FROM MIXED TRAFFIC DEMONSTRATOR TURNOUT FORM JUNE 2023 DURING AN ON-SITE VISIT OF THE DEMONSTRATOR.....	169
FIGURE 18-21: PICTURE FROM DEMONSTRATOR TURNOUT 9 MONTHS LATER IN MARCH 2024. THE RED BOX INDICATES INITIATED SURFACE DAMAGE, A BREAKOUT, AT THE CROSSING NOSE RUNNING SURFACE.	169
FIGURE 18-22: MAXIMUM SLEEPER DISPLACEMENT IN SWITCH AREA PER AXLE FOR (UPPER) MIXED TRAFFIC TURNOUT IN RIFA / TARRAGONA AND THE HIGH-SPEED DEMONSTRATOR TURNOUT IN SANTA CRUZ DE LA ZARZA (MIDDLE AND LOWER PLOT)	170
FIGURE 18-23: MAXIMUM SLEEPER DISPLACEMENT IN CROSSING AREA PER AXLE FOR (UPPER) MIXED TRAFFIC TURNOUT IN RIFA / TARRAGONA AND THE HIGH-SPEED DEMONSTRATOR TURNOUT IN SANTA CRUZ DE LA ZARZA (MIDDLE AND LOWER PLOT)	170
FIGURE 18-24: SIMPACK TRACK MODEL.....	171
FIGURE 18-25: SIMPACK VEHICLE MODEL	171
FIGURE 18-26: TRACK MODEL.....	171
FIGURE 18-27: CROSSING CAD MODEL	172
FIGURE 18-28: FROG SECTIONING.....	172
FIGURE 18-29: CROSSING NOSE VERTICAL ACCELERATION - EXAMPLES AT 65 AND 45 KM/H	173
FIGURE 18-30: SLEEPER VERTICAL DISPLACEMENT AT CROSSING NOSE - EXAMPLES AT 65 AND 45 KM/H.....	173
FIGURE 18-31: VERTICAL BALLAST FORCE AT CROSSING NOSE - EXAMPLES AT 65 AND 45 KM/H	174
FIGURE 18-32: VERTICAL AND LATERAL ACCELERATION SIGNALS FROM SWITCH- AND CROSSING PANEL AT THE MIXED TRAFFIC DEMONSTRATOR LOCATED IN RIFA/TARRAGONA (CATALUNIA). THE SIGNALS ARE RECORDED FROM A COMMUTER TRAIN.	174
FIGURE 18-33: VERTICAL AND LATERAL ACCELERATION SIGNALS FROM SWITCH- AND CROSSING PANEL AT THE HIGH-SPEED LINE DEMONSTRATOR LOCATED IN SANTA CRUZ DE LA ZARZA (TOLEDO). THE SIGNALS ARE RECORDED FROM A REGULAR HIGH-SPEED TRAIN.	175
FIGURE 18-34: ACOUSTIC EMISSION SIGNALS RECORDED IN SWITCH AND CROSSING PANEL OF THE HIGH-SPEED DEMONSTRATOR TURNOUT.	176
FIGURE 18-35: ACOUSTIC EMISSION SIGNALS RECORDED IN SWITCH PANEL AND CROSSING PANEL AT MIXED TRAFFIC DEMONSTRATOR....	176
FIGURE 18-36: MAXIMUM ACOUSTIC EMISSION IN SWITCH AREA PER PASSAGE FOR MIXED TRAFFIC TURNOUT IN RIFA / TARRAGONA (UPPER PLOT) AND THE HIGH-SPEED DEMONSTRATOR TURNOUT IN SANTA CRUZ DE LA ZARZA (MIDDLE – LEFT STOCK RAIL AND LOWER PLOT- RIGHT STOCKRAIL)	177
FIGURE 18-37: MAXIMUM ACOUSTIC EMISSION IN CROSSING AREA PER PASSAGE FOR MIXED TRAFFIC TURNOUT IN RIFA / TARRAGONA (UPPER PLOT) AND THE HIGH-SPEED DEMONSTRATOR TURNOUT IN SANTA CRUZ DE LA ZARZA (MIDDLE – AT SPLICED RRAIL AND LOWER PLOT- AT THE SWING NOSE TIP)	177
FIGURE 18-38: MAXIMUM VERTICAL ACCELERATION SWITCH AREA PER PASSAGE FOR MIXED TRAFFIC TURNOUT IN RIFA / TARRAGONA (UPPER PLOT) AND THE HIGH-SPEED DEMONSTRATOR TURNOUT IN SANTA CRUZ DE LA ZARZA (MIDDLE – LEFT STOCK RAIL AND LOWER PLOT- RIGHT STOCKRAIL)	178

FIGURE 18-39: MAXIMUM VERTICAL ACCELERATION IN CROSSING AREA PER PASSAGE FOR MIXED TRAFFIC TURNOUT IN RIFA / TARRAGONA (UPPER PLOT) AND THE HIGH-SPEED DEMONSTRATOR TURNOUT IN SANTA CRUZ DE LA ZARZA (MIDDLE – AT SPLICED RRAIL AND LOWER PLOT- AT THE SWING NOSE TIP)	178
FIGURE 18-40: NUMERICAL SIMULATION OF A WHEEL RUNNING OVER A TURNOUT FROM LEFT TO RIGHT, SIDE VIEW (TOP) AND TOP VIEW (BOTTOM, THE WHEEL IS HIDDEN). THIS SNAPSHOT SHOWS THE MOMENT WHERE THE WHEEL LEAVES THE LEFT WING RAIL AND IMPACTS THE FROG.....	178
FIGURE 18-41AND 18-42: HEXAHEDRAL ELEMENTS ON (A) THE CONTACT SURFACES OF THE RAIL HEAD AND (B) THE WHEEL.	179
FIGURE 18-43 AND 18-44: TETRAHEDRAL ELEMENTS ON THE WEB AND FOOT OF THE RAIL (TOP VIEW AND BOTTOM VIEW).....	179

List of Tables

TABLE 3-1: REFERENCES TO D10.1.....	17
TABLE 3-2: RELATIONSHIP APPLICATIONS AND USE CASES.....	19
TABLE 4-1: OVERVIEW OF THE SENSORS USED FOR SHORT TERM MEASUREMENTS.....	23
TABLE 4-2: OVERVIEW OF THE SENSORS USED FOR SHORT TERM MEASUREMENTS.....	34
TABLE 13-1: 95 TH CENTILE REPEATABILITY AND REPRODUCIBILITY ASSESSMENT OF CALCULATED PARAMETERS.	92
TABLE 13-2: EXPANDED UNCERTAINTY ESTIMATION BASED ON TEST RESULTS.	93
TABLE 14-1: TOP -10 GERALD DATASET CLASSES DESCRIPTION	102
TABLE 14-2: PRELIMINARY RESULTS OF THE SEMANTIC SEGMENTATION MODEL FOR CITYSCAPES TEST	104
TABLE 15-1: SENSOR LOCATION AND CHARACTERISTICS	108
TABLE 16-1: CURRENT STATUS OF THE DIFFERENT PROCESS STEPS.....	121
TABLE 18-1: SPECIFICATION OF CROSSING PANEL AND TRAFFIC CONDITIONS FOR MULTIBODY SIMULATIONS.....	162

1. EXECUTIVE SUMMARY

The primary aim of this deliverable is to advance short-term asset management strategies for rail tracks and their surroundings through the rigorous testing of new technologies at pilot sites in Spain and the Netherlands. This includes a detailed evaluation of a set of applications specifically tailored to meet the operational needs of infrastructure managers (IM) and maintenance service providers represented by ADIF and Strukton, respectively. These applications are assessed against Technology Readiness Levels (TRL) to ensure they meet the required standards for practical deployment. Several of these applications have already been successfully piloted, resulting in immediate, tangible benefits for the involved end-users. Additionally, other technologies have been installed, and preliminary testing has commenced, laying the groundwork for further research and development.

The work in WP 10 is based on two distinct use cases. Use Case 1 focuses on a high Technology Readiness Level (TRL) the integration of several new monitoring technologies in operational environment aimed at providing rapid solutions to specific asset management challenges, thereby facilitating quick problem-solving. Based on that, Use Case 2 is centred around the fusion of data from these multiple sources to improve fault detection and diagnosis in general by a holistic monitoring approach. This comprehensive holistic approach is designed to provide deeper insights into infrastructure conditions and behaviours. The applications developed under this two-folded approach are guided by the high-level architecture of the prototype platform and will be demonstrated in mixed-traffic and high-speed pilot sites in Spain and the Netherlands.

Out of the 13 applications defined, several have already achieved TRL 6, demonstrating their capability and reliability in operational settings. Predominantly, these applications are related to Use Case 1, proving effective in delivering practical solutions and quick wins. In contrast, the remaining lower-TRL applications, mostly associated with Use Case 2, are being integrated into the innovation funnel for further evaluation and refinement. This strategic approach supports the advancement of high-TRL technologies while ensuring continuous assessment and potential development of lower-TRL innovations, maintaining a dynamic pipeline of advancements.

Furthermore, some applications that currently exhibit high TRL results include additional ideas or approaches at lower TRL levels. With further research and development, these lower-TRL components can also achieve higher TRLs, resulting in applications with broader and more mature functionality. This comprehensive process ensures both immediate practical benefits and sustained innovation, fostering a robust development cycle.

The innovation funnel strategy plays a crucial role in managing and advancing these technologies. By continuously evaluating both mature and emerging technologies, this strategy ensures that resources are allocated to the most promising developments while keeping a pipeline of lower-TRL innovations for future exploration. This methodical approach supports sustained progress in rail infrastructure management and enhances the effectiveness of asset management strategies.

To ensure ongoing success and effectiveness, it is recommended to persist in employing the innovation funnel strategy for the assessment and advancement of technologies at various stages. This strategy will enable a focus on the most promising developments while maintaining a robust pipeline of innovations. By doing so, the project will be well-positioned to achieve continued progress and effective management of rail infrastructure assets, addressing both immediate needs and future challenges.

2. ABBREVIATIONS AND ACRONYMS

Abbreviation / Acronym	Description
ABA	Axle Box Accelerometers
AI	Artificial Intelligence
API	Application Programming Interfaces
ATO	Autonomous Train Operation
BIM	Building Information Modelling
CAD	Computer Aided Design
CCS	Control Command and Signalling subsystem
CDM	Conceptual Data Model
CNN	Convolutional Neuronal Network
CSM	Common Safety Method
DC	Direct Current
DMI	Directional Movement Indicator
DSP	digital signal processing
DT	Digital Twin
DTM	Digital Track Management
DXF	Drawing Interchange Format
DWG	AutoCAD Drawing Database (file extension)
ENE	Energy (subsystem)
ERJU	Europe's Rail Joint Undertaking
ERTMS	European Railway Traffic Management System
EU	European Union
FA	Flagship Area
FEM	Finite Element Modelling
FME	Feature Manipulation Engine
FMU	Functional Mock-up Unit
FP	Flagship Project
GAN	generative adversarial neural network
GIS	Geographic Information System
GNSS	Global Navigation Satellite Systems
GPR	Ground Penetrating Radar
GPS	Global Positioning System
HMI	Human Machine Interface
HS	High Speed
IAMS	Intelligent Asset Management Strategies
IM	Infrastructure Manager
IMU	Inertial Measurement Unit
INF	Infrastructure
InteDemo	Integrated Demonstrator
JU	Joint Undertaking
KER	Key Exploitable Results
KML	Keyhole Markup Language
KPI	Key Performance Indicator
LCC	Life Cycle Cost
LTI	Linear Time Invariant

Abbreviation / Acronym	Description
MAP	Modelica Association Project
MAWP	Multi-Annual Work Programme
MBM	Multi Body Modelling
MBS	Multi Body Simulation
MCA	Model Consortium Agreement
MEMS	Micro-electromechanical system
ML	Machine Learning
MSMP	Multi-Source Multi-Purpose
OPEX	Operational Expense
PCB	Printed Circuit Board
R&I	Research and Innovation
RAMS	Reliability, Availability, Maintainability, Safety
RCF	Rolling Contact Fatigue
RF	Radio Frequency
RST	Rolling Stock
RU	Railway Undertaking
S2R	Shift2Rail
S&C	Switches and Crossings
SP	System Pillar
TMS	Traffic Management System
TRL	Technology Readiness Level
TT	Transversal Topic
UAV	Unmanned Autonomous Vehicle / Unmanned Aerial Vehicle
UXO	Unexploded Ordnances
WP	Work Package
XML	Extensible Markup Language

3. BACKGROUND & OBJECTIVE / AIM & INTRODUCTION

3.1. Background & Context

Deliverable D10.2, titled "Report on the Initial Developments and Preparatory Works for the Integrated Demo," is part of Flagship Project 3 FP3–IAM4RAIL. It represents the outcome of Work Package 10, "Multi-Source/Multi-purpose IAMS Application: Scope Refinement & Quick Wins," and serves as groundwork for Work Package 11. WP10 and WP11 complement each other, with WP11 focusing on main development tasks, including demonstrating applications initiated in WP10, particularly for the multi-source/multi-purpose asset management platform. The objective of D10.2 is to provide a detailed update on the progress and groundwork for the integrated demonstration within WP10 and WP11, emphasizing preparatory steps and immediate substantial progress ("quick wins").

This deliverable should be considered in the context of D10.1. In the previous deliverable, the intent was to ensure conciseness and accessibility, providing a self-contained overview that aligns with the broader MSMP IAMS objectives within the research program and highlighting connections to other research programs and work packages within FP3–IAM4RAIL. For a more detailed background and comprehensive context, please refer to D10.1. This will offer a thorough understanding of the underlying principles and detailed connections to the broader research initiatives. In this deliverable, we will strive to balance brevity and completeness, including essential summaries without unnecessary repetition, to enhance the clarity and utility of our documentation.

3.2. Objective / Aim

The aim of Work Packages 10 and 11 is to enhance technical monitoring solutions for short-term asset management and off-site work preparation using a multi-source/multi-purpose (MSMP) asset management platform. Key objectives include providing continuous, traceable diagnostic and prognostic information using data from embedded wayside and onboard sensors. The scope covers data acquisition for assets within 360 degrees (illustrated in Figure 3-1)and approximately 5 meters around each asset, with special attention to Switches and Crossings (S&Cs) as vital components.



Figure 3-1: Scope rail infrastructure monitoring, range of 360 degrees

3.3. Reading Guide and reference to previous deliverable (D10.1)

The real-world integrated demonstration of the MSMP platform following the generic system architecture and use cases described in D10.1 will consist of specific applications realized at specific pilot sites in the Netherlands and Spain as already indicated in D10.1 and summarized in the following subsections. Within this deliverable the accomplished preparatory work and obtained quick wins are described for the pilot sites in section 7, the applied tools and methods in section 8 and the holistic condition monitoring and diagnostics in chapter 9. In total 13 specific applications are further elaborated and implementation at the different pilot sites is ongoing (see subsections below and Table 3-2: relationship Applications and Use Cases Table 3-2). The applications are described in detail in sections 7 to 18. Conclusions and outlook to the work planned for WP 11 are given in section 19.

The table below outlines the chapters in this deliverable, with corresponding references to the relevant chapters and paragraphs from the previous deliverable, "10.1 High-Level System Architecture.

Table 3-1: references to D10.1

Current Deliverable (10.2)		Previous Deliverable (D10.1)	
#	Chapter Title	#	Chapter Title
4	Pilot Sites	8	Pilot Sites
5	Utilized tools, solutions and systems	7.1 7.2	Utilized Tools, Solutions & Systems
6	Holistic Monitoring and Decision Support	7.3	Holistic Analytics and Decision Support
7	Reality Model	9.7	3D-modelling underground infrastructure: pipes & cables
8	Holistic Switch Monitoring and Diagnostic Model	9.1	Holistic Switch Monitoring and Switch Diagnostic Model
9	Multi-Sensor Track Monitoring	9.4	Track Monitoring Using ABA
10	Detection of loose Fasteners with ABA	9.4	Track Monitoring Using ABA
11	Sound Recordings from ABA for Diagnostics	9.4	Track Monitoring Using ABA
12	Digital Twin: Dynamic vehicle response ANALYSIS excitation rAIL surface unevenness	9.4	Track Monitoring Using ABA
13	Track Geometry Measurement from Passenger Vehicle	9.8	Track geometry measurement from passenger vehicle
14	Occlusion Monitoring due to Vegetation	9.3	Occlusion Monitoring Due To Vegetation
15	Monitoring Turnouts Acceleration Signals	9.5	Turnouts Monitoring: Acceleration Signals
16	Rail Crack Detection using Microwaves	9.2	Crack and surface damage detection in railways using microwaves
17	Inspection Turnouts: Analysing 3-Dimensional Reconstruction	9.6	Inspection of Turnouts: Analysing 3-Dimensional Reconstruction
18	Switch Monitoring	9.9 9.10 9.11 9.12	Drive/Detector Rod Monitoring Switch Assembly Monitoring Track Quality Monitoring Frog / Switch Rail Monitoring

This table provides a clear and detailed mapping of the content between the two deliverables, ensuring that all relevant references are easily accessible.

3.4. Link between Use Cases and Applications

As stated in deliverable D10.1 (section 5.2), two basic use cases to guide the implementation of our specific MSMP asset management platform prototype are defined:

- Use Case 1: Linking (new) monitoring technologies to asset management issues
- Use Case 2: Fusion of monitoring data for an enhanced fault detection and diagnosis

The use cases can be seen as consisting of two distinct steps:

- In the first step, we focus on the direct utilization of technology and its data, linking it to specific rail infrastructure issues. This phase aims to quickly address and tackle targeted problems, potentially leading to immediate benefits and quick wins.
- In the second step, we adopt a more scientific and comprehensive approach. We explore the integration of data from different technologies to achieve more accurate and insightful results. This stage involves a deeper analysis of the data to uncover additional information about the infrastructure's behaviour, condition and potential issues. While this step requires more effort and resources, it promises to provide a more thorough understanding of the railway system and its performance.

In essence, the first step is geared at a higher TRL towards immediate gains, while the second step seeks to unlock a more profound and informed perspective, laying the groundwork for long-term improvements and advancements in rail infrastructure management.

In summary, we will follow a layered approach by developing a set of specific applications (sections 7 to 18) relevant for end-users. These applications will leverage the high-level architecture of the prototype platform (see D10.1) in the two different use cases, contributing to the high-level demonstrator (#4) with several mixed-traffic and highspeed pilot demonstration sites in Spain and the Netherlands (see section 7). The relations of the applications to the two use cases and the specific pilot sites are given in Table 3-2.

The applications address specific real-life asset management issues recognized by end-users (maintenance engineers, asset owners, etc.). Examples include monitoring vegetation due to occlusion, the detection of rail as well as track geometry defects and a set of relevant failures at switches and crossings. The applications are based on a new technology (use case 1), are combining data from multiple technologies (use case 2) or both.

Working with these two use cases, applying diverse and sometimes novel technologies, leads to simultaneous development of various ideas (applications). Each application progresses through different stages of the Technology Readiness Level (TRL) framework, with some failing temporarily while others succeed. This process is managed through an innovation funnel, a mechanism that helps businesses navigate new ideas by streamlining innovation and reducing risk. The funnel prioritizes, screens, selects, refines, and tests proposed solutions, ensuring only the most viable ideas proceed.

Of the 13 applications defined, several have already reached TRL 6, particularly those related to Use Case 1, proving their capability and reliability in operational settings. These high-TRL

applications have delivered practical solutions and quick wins. Meanwhile, lower-TRL applications, mostly tied to Use Case 2, are being evaluated and refined within the innovation funnel. This approach promotes the advancement of high-TRL technologies and continuous assessment of lower-TRL innovations, maintaining a dynamic pipeline of developments.

Additionally, some high-TRL applications incorporate lower-TRL ideas that, with further research and development, can also reach higher TRLs. This results in applications with enhanced functionality and broader scope. The innovation funnel ensures that developments at various stages are continuously assessed and advanced based on their potential for success.

By integrating an innovation funnel, we maintain a steady flow of promising developments and focus resources on the most viable projects. This approach not only achieves high TRLs but also keeps the pipeline filled with lower-level innovations for future exploration. This continuous feed of potential advancements supports sustained progress in rail infrastructure management, delivering quick wins and demonstrating the effectiveness of this comprehensive approach.

Table 3-2: relationship Applications and Use Cases

#	Application	Section	Use Case	Explanation	Pilot sites
01	Reality Model	7	1 & 2	Uses different technologies, however not really data fusion technology	Netherlands
02	Holistic Switch Monitoring and Diagnostic Model	8	1 & 2	Utilizing information from established monitoring (e. g. wayside switch monitoring) and inspection (e.g. track geometry measurements) technologies with new embedded technologies, machine learning and traceable diagnostic models.	Netherlands
04	Multi-Sensor Track Monitoring	9	1 & 2	Fusion of axle-box accelerations with image data and information from ground penetrating radar.	Netherlands
05	Holistic Switch Monitoring and Diagnostic Model	9.4	1 & 2	Development of a reliable signal filtering and processing algorithm for the detection of fastener defects, using tagged image data to select track segments with the desired defects where the ABA signal is to be analysed.	Netherlands
06	Sound Recordings from ABA for Diagnostics	11	2	Sound is an extra parameter to be used only in conjunction with other signals such as ABA	Netherlands
07	Digital Twin: Dynamic vehicle response ANALYSIS excitation rAIL surface unevenness	12	1 & 2	Development of an accurate digital twin of LEONARDO to enhance the vehicle-borne Multi-Sensor Track Monitoring by introducing system knowledge based on enhanced models.	Netherlands
08	Track Geometry Measurement from Passenger Vehicle	13	1	ABA signals are used	Spain
09	Occlusion Monitoring due to Vegetation	14	2	Development of a vision-based monitoring system to detect interferences between trees and critical railway infrastructure elements that could feed a smart maintenance system.	Netherlands
10	Monitoring Turnouts Acceleration Signals	15	2	Development of a non-intrusive monitoring system to estimate crossing degradation using databases generated by computational models.	Spain
11	Rail Crack Detection using Microwaves	16	2	Radiofrequency technology to detect the presence of cracks.	-
12	Inspection Turnouts: Analysing 3-Dimensional Reconstruction	17	1 & 2	Establish the health status of turnouts by analysing their three-dimensional reconstruction	Spain
13	Switch Monitoring	18	1&2	Uses various technologies and functionalities	Spain

4. PILOT SITES

4.1. Spain: High Speed & Conventional Line Pilot Sites

Switches and crossings are sensitive components of the railway infrastructure since the exchange of forces between the wheel and the rails at these points is greater than that generated on the rails in the rest of the track. It is the weakest point of the railway superstructure since there are important discontinuities in them for the support of the wheel profile (gap, needle-counter needle, etc.) that cause strong unwanted wheel load impacts.

For this reason, they require more expensive and specialized conservation, which makes them elements on which maintenance attention must be concentrated.

Currently in the Spanish network managed by ADIF there are more than 15,000 switches and crossings, so their correct maintenance is essential given their high number and importance in safety. A failure in crossings can have major effects on the safety and operation of the railway network.

In this way and given the great scalability that correct maintenance requires and its importance for safety, for ADIF, it is considered necessary to monitor the devices, in order to anticipate a possible incident, with predictive maintenance techniques.

Predictive maintenance will allow us to identify possible failures in infrastructure elements before they occur. This will result in an optimization of maintenance times and costs, since the planning of activities will be carried out in advance.

Currently, more than 50% of the total investments in railway infrastructure of the ADIF network are allocated to maintenance. Real-time monitoring of assets will also allow the useful life of assets to be extended, by being able to anticipate their deterioration, with fewer long-term renewal needs.

In Spain, two distinct pilot sites have been designated: one for conventional rail lines and another for high-speed rail lines. This differentiation stems from the fact that these two types of rail lines have unique requirements and, consequently, necessitate different inspection regimes.

4.1.1. Conventional Line Pilot Site

The switches and crossings on conventional lines are composed of fixed-point crossings made of manganese steel, the manufacture of which is regulated by standards E.T.03.361.141.9 and EN15689. These crossings are one of the weakest parts of the device, since it is where discontinuity of the rolling occurs.

In order to control the behavior of the entire device, inspections are carried out, both geometric and checking the state of the materials, regulated by the Technical Instruction for Inspection and Surveillance of track devices ADIF IT-301-001-VÍA-28, that determines the maintenance tolerances and the general criteria for preventive maintenance of infrastructure and roads ADIF-PE-301-001-005-SC-524-A-06 that establish the inspection frequencies.

In addition, ultrasonic auscultations are carried out on the conventional lines' crossings, on Network A once every two years and on the rest of the network once every three years. In these auscultations, a deep inspection and an ultrasonic auscultation on the crossings are carried out, however, the high manganese cast steel commonly used in the frogs has a granular structure that

makes measurements in any auscultation attenuated, so in the manganese steel frogs ultrasound is not really useful.

Based on ADIF's experience, defects in crossings account for more than 80% of all defects detected in the track superstructure, with 92% of these in the area of the fixed-point crossing.

In order to reduce the number of inspections and try to carry out predictive maintenance instead of current corrective maintenance, ADIF aims to develop innovative technological solutions that are capable of detecting structural damage in track devices at an early stage, also checking its evolution, in such a way that tools are generated to be able to apply predictive maintenance strategies.

4.1.1.1. Definition

The chosen turnout for the mixed traffic line demonstrator is a DSH-P1-60-500-0,071-TC which is a very common turnout in the mixed traffic line. The turnout shown in was installed in 2016 and provided by Voestalpine JEZ. See also D10.1

4.1.1.2. Instrumentation

The equipped mixed traffic demonstrator turnout is monitored by a total of four multi-sensors. Two of them are used for track quality monitoring and are mounted on a sleeper at the beginning of the switch and the other on the sleeper below the crossing point. These are usually the mostly loaded parts of a turnout due to the dynamic forces and abrupt stiffness changes in the system. Figure 4-1 shows a schematic illustration of the system architecture. The demonstrator turnout is operated by a central cabinet, containing the power supply and data acquisition and connectivity system. The sensors are connected via M12 8 pole cables, providing power and data transmission to the multi-sensor system.

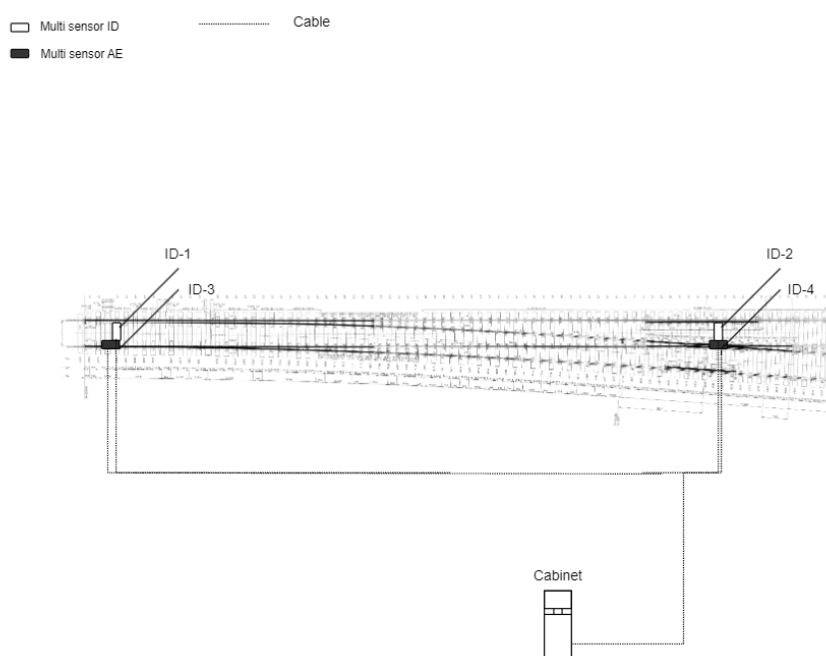


Figure 4-1: Schematic illustration of the monitoring system architecture for the mixed traffic turnout demonstrator

Figure 4-2 shows the two multi-sensors in the crossing panel. The sensor located at the sleeper is used for measuring sleeper displacements and tilt, thereby monitoring the track quality. A second multi-sensors mounted on the wing rail for monitoring the health state of the cast manganese crossing block by detecting wear or cracks. There are also other sensors visible on this picture which are related to an additional short-term installation introduced in the following section.



Figure 4-2: Installed multi-sensors in crossing panel for track quality and wing rail / crossing nose monitoring.

Figure 4-3 shows the two multi-sensors installed in the switch panel, which are used for track quality and switch rail / stock rail monitoring. The sensors are both mounted by adhesive coupling to the monitored component thereby allowing a connection without the need to drill the components.



Figure 4-3: Multi-sensors installed in switch panel for track quality and switch rail / stock rail wear monitoring.

4.1.1.3. Short time validation measurements mixed traffic demonstrator

During a short time of several days an additional measurement system is built up to demonstrate the performance of the long-term monitoring with conventional (acceleration, displacement, strain gauge) technology. This installation is removed after the testing phase completely. Figure 4-4 shows a schematic illustration of the sensor locations of the short-term validation measurement system.

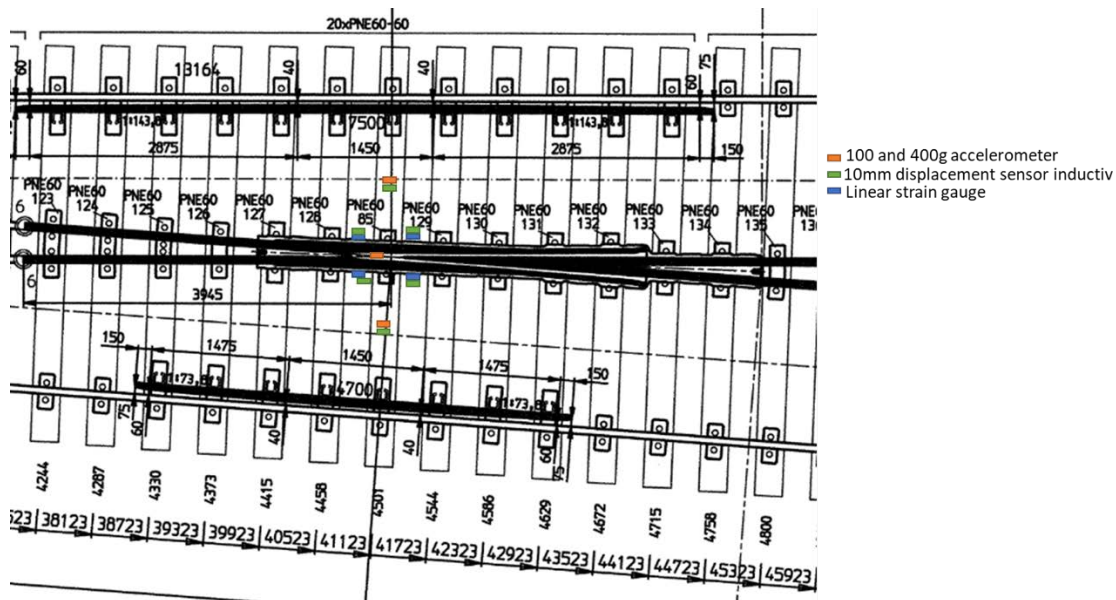





Figure 4-4: Sensor locations at first drive level on point rail and hollow sleeper

The system contains strain gauge, acceleration and displacement measurements. Table 4-2 shows the number of sensors as well as the main specifications.

Table 4-1: Overview of the sensors used for short term measurements

Sensor	Figure	Description	Quantity	Case material	Weight [g]	Size [mm]
Strain gauge		Linear strain gauge 3mm grid length	4	Plastic foil	1g	10x10x1
Acceleration		400g acceleration sensor PJM	3	Plastics and metall	80g	40x40x25
Displacement		Inductive displacement sensor 0-10mm	6	Plastics	20g	20x40x20

Strain gauge sensors with 4 wire technology are used in areas of interest for high stresses. Those thin insulated foils with a measurement grid in it are glued to a polished surface as in the Figure 4-5 below. The cables are fixed with cable ties and stored in the same cable protection tube. At the crossing nose position the sensors are installed on the crossing nose foot side in the sleeper spacing centre. Additionally, displacement measurements are conducted at the same position of the strain gauge to get correlation for the FEA models.



Figure 4-5: Application of strain gauge sensors

The acceleration sensors are glued with 2 component high strength glue to the area of interest. Those measurements are performed to estimation acceleration amplitudes during train passages and correlate those to other sensor signals. The sensors are completely electrically insulated and between the glued surface and the sensor an additional plastic layer is installed to ensure the electric insulation at all times. Figure 4-6 shows a sensor mounted on the wing rail foot.



Figure 4-6: Acceleration sensor

The displacement sensors, shown in Figure 4-7 are mounted with a bolt in the gravel and work contact free to the metallic surface completely electrically insulated. The purpose of those sensors is to serve for validation purposes of the track quality multi-sensor as well as provide additional measurement locations to gain a detailed overview on the track loading in the crossing area.



Figure 4-7: Displacement sensor

4.1.1.4. Results short-term validation measurements mixed-traffic demonstrator

Figure 4-8 shows the maximum stress peaks measured at location e4 for all 180 trains measured during the short-term validation period. The maximum tensile and compression stress due to bending of the crossing nose are displayed for each train.

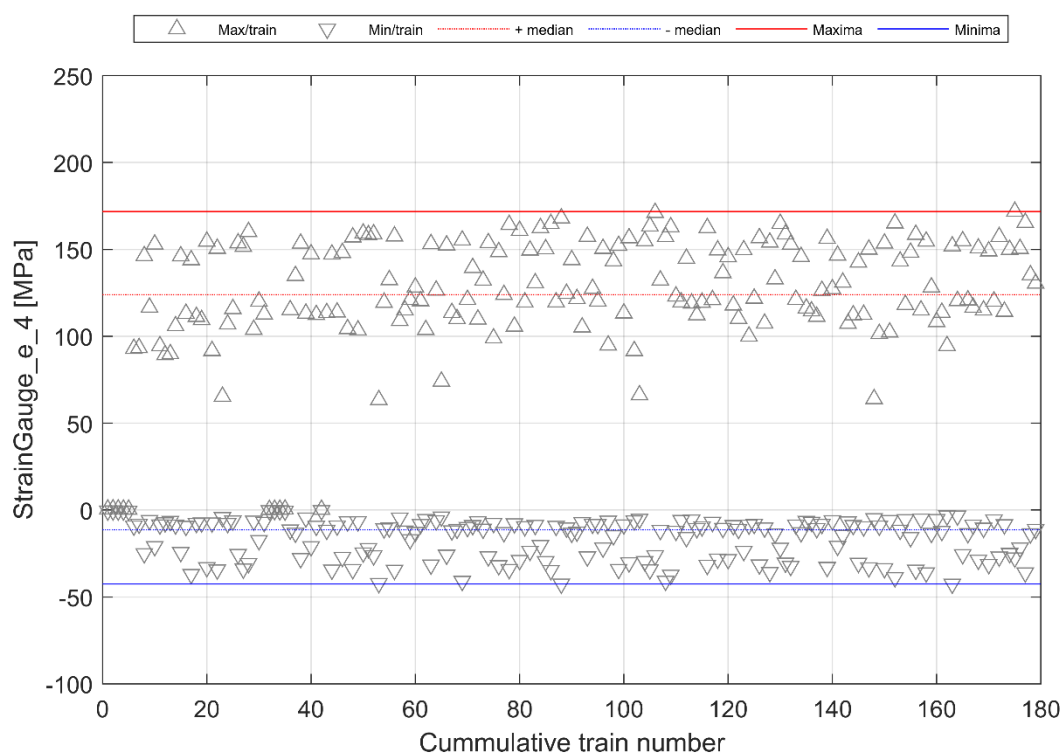


Figure 4-8: Strain gauge signals of short-term validation measurement system

In Figure 4-9 the acceleration peaks per train are displayed in the same way. It is visible that most of the trains is in a peak range of 150g, but several trains show high acceleration in the range of the sensor limit above 400g. Those trains will be evaluated in detail to see where this high acceleration peaks come from.

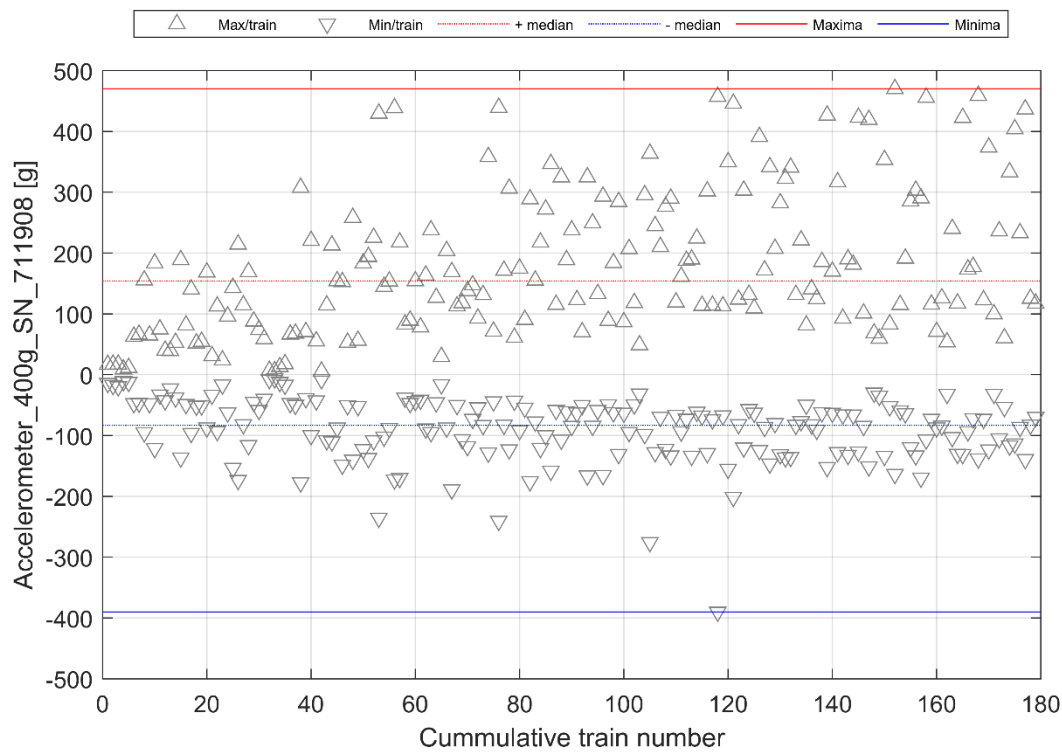


Figure 4-9: Features of acceleration measurements of short-term validation measurement system

4.1.1.5. Comparison of mixed traffic short-term validation measurements and permanent monitoring system

Figure 4-10 shows a comparison of the vertical sleeper displacement for a single train passage recorded in the crossing area of the mixed traffic demonstrator turnout. The left plot shows the data recorded by the multi-sensor system for track quality monitoring compared to the short-term validation measurement system on the right side. Generally, it can be observed that the obtained signals from both systems are comparable and in overall good agreement. Both measurements show the same signal characteristics and the same trend. Within a next step all passages recorded during the time span when the short-term validation measurements were performed will be conducted to provide a detailed view on distributions and maximum errors.

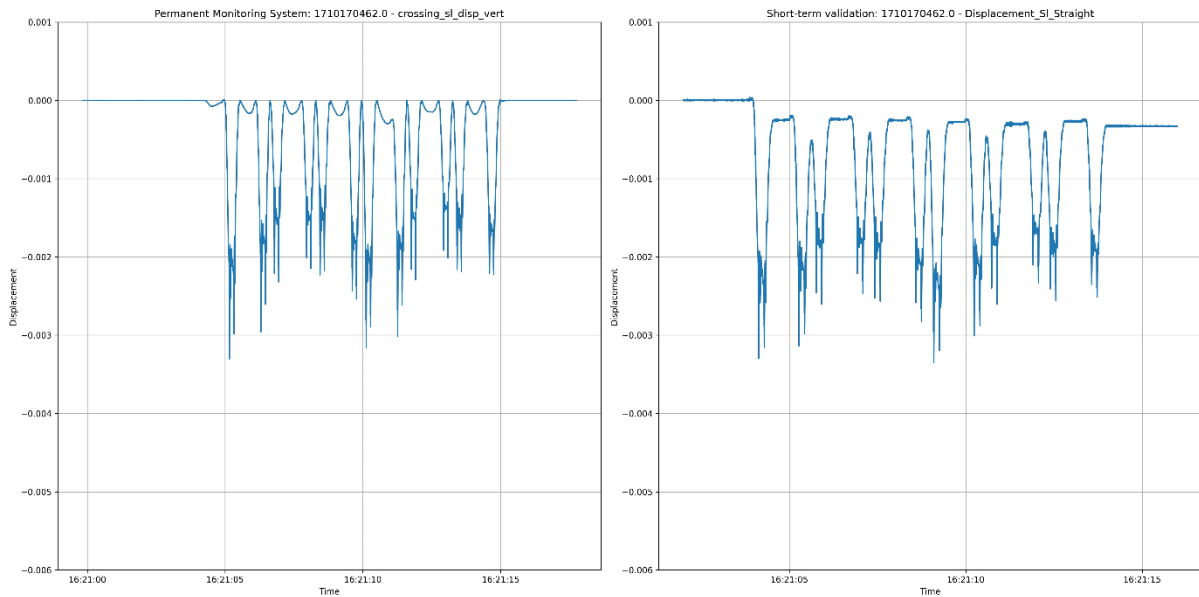


Figure 4-10: Comparison of vertical sleeper displacements in crossing area recorded for one passage with the permanent monitoring system (left) and the short-term validation measurement system (right)

4.1.2. High Speed Pilot Site

The inspections carried out to control the condition of the high-speed track devices are analogous to those on conventional lines, exclusively increasing the inspection frequencies. These inspections are regulated by the Technical Instruction for Inspection and Surveillance of track devices ADIF IT-301-001-VÍA-28 and the General Criteria for preventive maintenance of infrastructure and track ADIF-PE-301-001-005-SC-524 -A-06.

Furthermore, since they do not have fixed-point frogs, they avoid discontinuities in the rolling, and the data from the geometry monitoring trains are valid, so through their analysis it is possible to continuously control the geometry of the track devices.

Finally, ultrasonic auscultations are also carried out, but with greater frequency (annually) than those carried out on the conventional lines' crossings.

The most common incidents in these assets are caused by problems in the mechanical safety installations and the lack of testing of the motors, since the rolling continuity in the moving-point frogs prevents impacts on them.

The monitoring of these devices will make it possible to know the functionality of the assets, the stresses to which the motors are subjected and to better understand their behavior, as well as to anticipate possible incidents by trying to achieve predictive maintenance.

4.1.2.1. Definition

The selected turnout, which is shown in Figure 4-11 is an AV3 provided by Voestalpine JEZ. (3rd evolution in high-speed turnouts).



Figure 4-11: High speed line turnout demonstrator

See for further details and specification D10.1, section 8.2. In the following paragraphs an update of the work and equipment installed.

4.1.2.2. Installed Equipment

The Spanish high-speed demonstrator in the ADIF network had been installed in March 2024. The demonstrator was divided in two separate systems, due to its spatial distance between switch- and crossing panel (over 100m). Therefore, voestalpine Railway Systems installed two control cabinets containing the power supply, data acquisition and connectivity systems for the installed sensors. In total the demonstrator comprises 32 sensors, covering every single setting level (in total 14 setting levels). In the switch panel the installed system includes 4 multi-sensors (2 for switch rail monitoring and 2 for track quality monitoring) as well as 10 analogue acoustic sensors for point machine and detector rod monitoring, see Figure 4-12. Moreover 6 inductive sensors have been installed for switch position monitoring in different cross sections of the switch panel. The most critical locations in a switch are generally its beginning, where the sensors monitor the position of both switch rails, thereby ensuring that the gap between switch rail and stock rail is within a defined tolerance band. The second critical location is the nearest flangeway, which is located shortly after the last setting level in the switch panel. There, a total of 6 displacement sensors is used to monitor both, the closed and the open switch rail position as well as the nearest flangeway, thereby guaranteeing a safe switch operation and detect deviations which need to be corrected before leading to traffic disruptions.

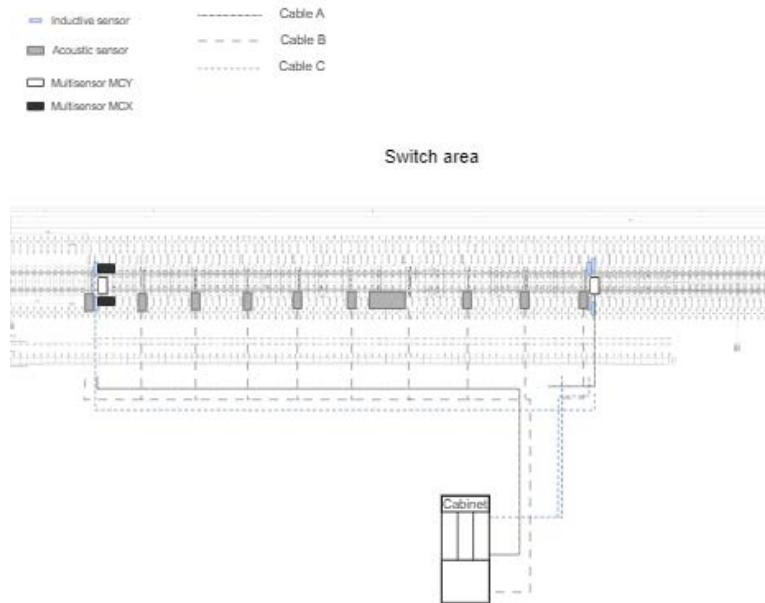


Figure 4-12: Schematic system architecture of monitoring system installed at switch panel of the high-speed demonstrator located in Santa Cruz de la Zarza.

In the crossing panel a total of 4 multi sensors (2 for wing rail / swing nose monitoring and 2 for track quality monitoring) is used as well as 8 analogue acoustic sensors for point machine and detector rod monitoring. As the maintenance teams reported an increased occurrence of breaking detector rods, the installed monitoring system uses even two sensors per setting level to guarantee a detection of any irregularities or faulty vibration levels in the crossing level in order to avoid or immediately recognise breaking rods. Beyond that, a clear focus is laid on the wing rail and swing nose monitoring, as those two components are the most highly loaded ones in the crossing panel and are of outmost importance for a safe operation of the asset. Figure 4-13 shows a schematic illustration of the system architecture in the crossing panel.

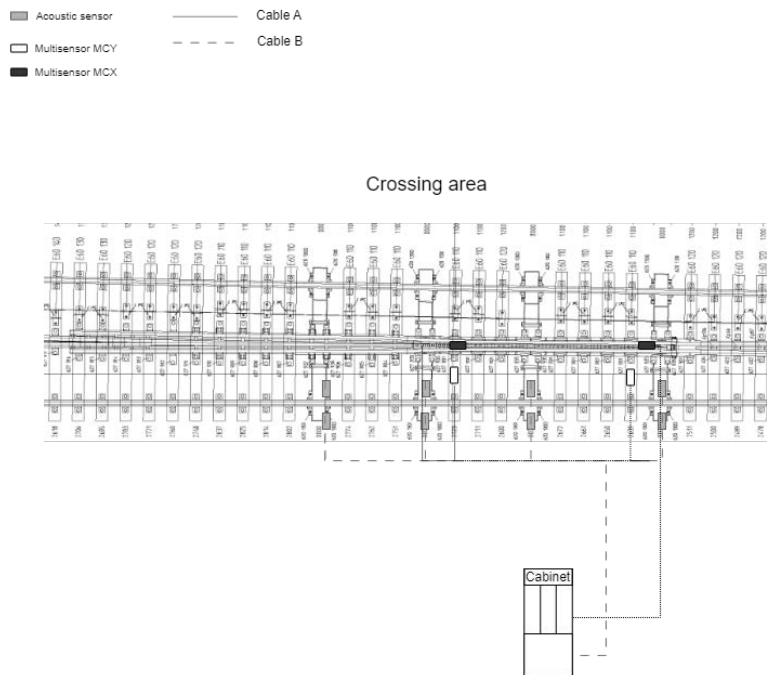


Figure 4-13: Schematic system architecture of monitoring system installed at crossing panel of the high-speed demonstrator turnout located in Santa Cruz de la Zarza.

Figure 4-14 shows the multi-sensor for track quality monitoring in the switch panel, as well as the two inductive sensors for switch position monitoring of the closed switch rail. The inductive sensors are mounted by a mounting frame installed on the switch base plates whereas the multi-sensor is glued to the sleeper. Both sensors are connected by M12 8-pole cables which provide power to the sensor and serve for data transmission.



Figure 4-14: Inductive sensors for switch position monitoring of the closed switch rail at the beginning of the switch and multi-sensor for track quality monitoring.

Figure 4-15 shows the same location from another perspective. This allows a view on the installed multi-sensor for stock rail and switch rail monitoring. The sensor is mounted by adhesive to the rail itself, thereby enabling an evaluation of the structure borne noise signals for rail wear / crack monitoring.



Figure 4-15: Multi-sensors mounted both stock rails (beginning of the switch) and inductive sensors for switch position monitoring and multi sensor for track quality monitoring.

Figure 4-16 shows the four inductive sensors in at the end of the switch panel which are used for monitoring the closed switch rail as well as the nearest flangeway. Both values are crucial for a safe switch operation. Therefore, a continuous monitoring in real time increases both, safety and availability of the turnout.



Figure 4-16: Inductive sensors for monitoring the nearest flangeway and the closed switch rail at the end of the switch panel.

Figure 4-17 shows two multi-sensors installed in the crossing panel, one for track quality and the other for wing rail / swing nose monitoring. The sensor locations are chosen to enable a focus on the through route, as this turnout is mainly used (99%) in the through route.



Figure 4-17: Multi-sensors installed in crossing panel for track quality and wing rail / swing nose monitoring.

Figure 4-18 shows an analogue acoustic sensor mounted on the point machine casing. This sensor is used for both, point machine as well as detector rod monitoring, as it is able to detect any unreasonable vibration levels and thereby indicating faulty operations or component states.

Figure 4-19 shows an analogue acoustic sensor mounted on the hollow sleeper for detector rod monitoring. This position was chosen as it is the closest position which was allowed by the maintenance teams for sensor application, as a direct application on the movable detector rod was too critical for a safe operation. However, the sensor is able to detect any changes in vibration levels and thereby able to detect any faults in this area.



Figure 4-18: Analogue acoustic sensor installed on point machine casing for point machine monitoring



Figure 4-19: Analogue acoustic sensor installed on hollow sleeper for detector rod monitoring.

4.1.2.3. Short-time validation measurements for high-speed demonstrator

During a short period of several days, an additional measurement system is built up to demonstrate the performance of the long-term measurement with conventional (acceleration, displacement, strain gauge) technology. Furthermore, the system provides additional sensor locations which are not covered by the permanent monitoring system for correlation purposes and validation of the FEA simulation models. This installation is removed after the testing phase completely. Figure 4-20 shows a schematic illustration of the sensor locations and types for the high-speed demonstrator short term validation measurements.

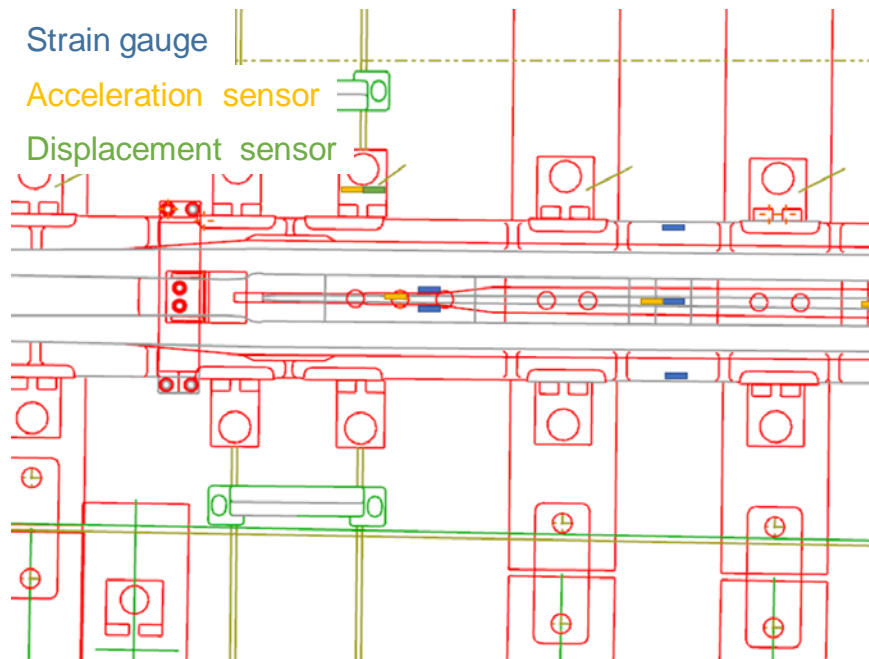





Figure 4-20: Sensor locations at first drive level on point rail and hollow sleeper

Table 4-1 shows the specifications and number of sensors installed in the short-term validation measurement system. The system contains strain gauge, acceleration and displacement measurements.

Table 4-2: Overview of the sensors used for short term measurements

Sensor	Figure	Description	Quantity	Case material	Weight [g]	Size [mm]
Strain gauge		Linear strain gauge 3mm grid length	9	Plastic foil	1g	10x10x1
Acceleration		400g acceleration sensor	6	Plastics and metall	80g	40x40x25
Displacement		Inductive displacement sensor 0-10mm	6	Plastics	20g	20x40x20

The strain gauge sensors with 3 wire technology are used in areas of interest for high stresses. Those thin insulated foils with a linear measurement grid of 3mm are glued to a polished surface as in Figure 4-21 below. The cables are fixed with cable ties and stored in the same cable protection tube. Aim of these measurements is to gain insights in the component loading during operation and provide strain signals for correlation with the permanent monitoring data such as structure borne noise and simulation results.



Figure 4-21: Application of strain gauge sensors

The acceleration sensors, shown in Figure 4-22 are glued with 2 component high strength glue to the area of interest. The measurement is conducted in order to estimate the acceleration amplitudes during train passage and compare those to the accelerations captured by the permanent monitoring system for verification purposes.



Figure 4-22: Acceleration sensor

The displacement sensors shown in Figure 4-23 are mounted with a ground spike in the gravel and work contact free to the metallic surface completely electrically insulated. The aim of this sensor is to serve for validation of the displacement multi-sensor used for track quality monitoring as well as providing additional positions which are not covered by the permanent monitoring system.



Figure 4-23: Displacement sensor

4.1.2.4. Results short term validation measurements high-speed demonstrator

Figure 4-24 shows the maximum stress peaks measured at location e2 for one day with ~39 trains measured during the short-term validation period. The maximum tensile and compression stress due to bending of the wing rail casted frame are displayed for each train. The signal peaks are very homogeneous for all trains.

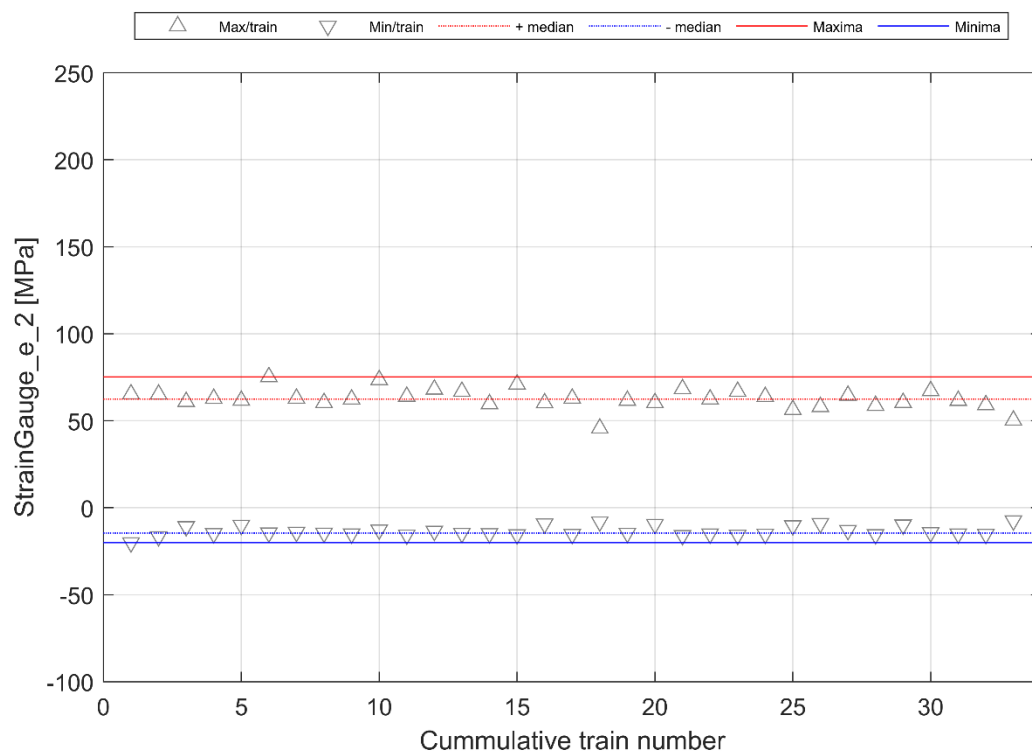


Figure 4-24: Strain gauge signals of short-term validation measurement system

In Figure 4-25 the acceleration peaks per train are displayed in the same way. It is visible that most of the trains is in a peak range next to the maximum peak acceleration. The scatter is very low and covers with the low scatter in stress signal.

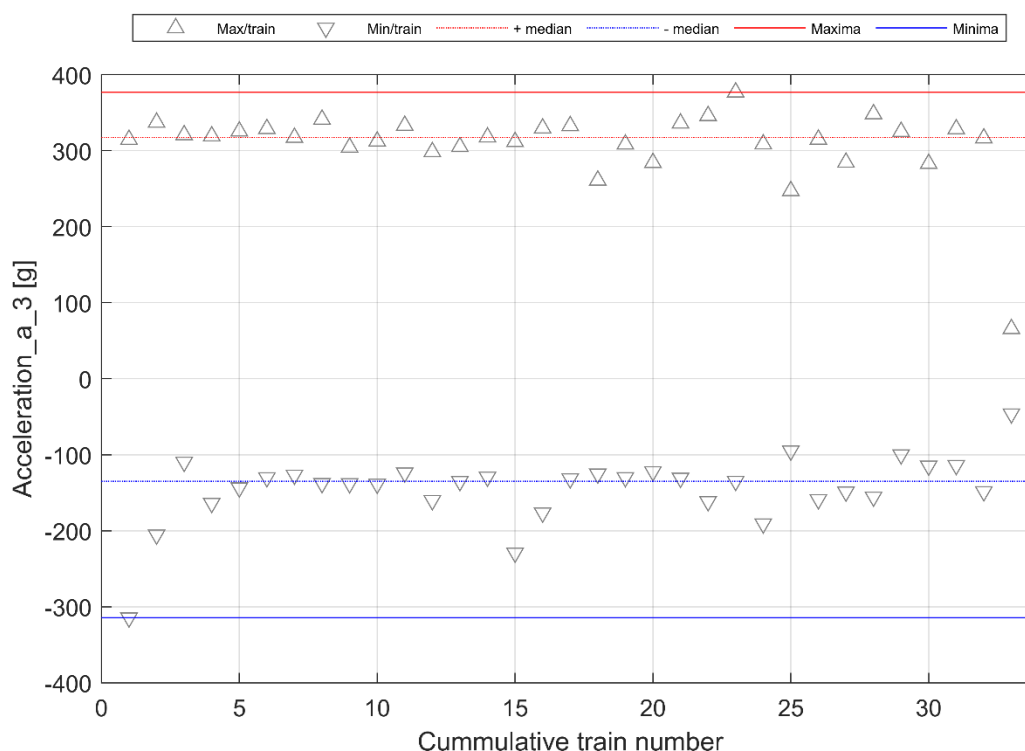


Figure 4-25: Features of acceleration measurements of short-term validation measurement system

4.2. The Netherlands

4.2.1. Description

The pilot sites are detailed in Section 8.1 of D10.1, with a particular focus on the turnouts. Exact details are available in that section. For wayside monitoring, a flexible approach has been adopted, opting for non-fixed locations due to specific data analysis requests. These requests often targeted particular issues, necessitating varied locations to address them. The key requirement was the ability to collect repeated data at the same location to ensure reproducibility and validation of results. The following paragraphs provide updates on this matter.

Turnout

For more details, refer to deliverable D10.1. The selected turnout at the pilot site in the Netherlands is a 1:15 NSE2 turnout, manufactured by WBN (Voestalpine) and installed in 2005.



Figure 4-26: image of the location: view from the Leonardo

Wayside data

Besides the turnout, for the onboard systems various routes have been defined where on a fairly regular basis new data can be obtained. See also D10.1. and a summary in section 5.2.3 in this document.

4.2.2. Installed Equipment

See D10.1. Details of the monitoring equipment for the turnout is fully described. See in this document also additional information.

For the onboard is described as well as the Leonardo platform, see also D10.1 and a summary in section 5.1.2 in this document.

4.2.3. Current status mixed traffic demonstrator Netherlands

Ongoing alignment between PRORAIL, vaTSNL and STRUKTON. The demonstrator in the Dutch mixed traffic line operated by PRORAIL has not been implemented yet, however alignments between the Dutch infrastructure operator PRORAIL, voestalpine Track Solutions Netherlands and STRUKTON are ongoing.

4.2.4. Current status of wayside monitoring data

A comprehensive package containing data from the ABA (Accelerometer-Based Acquisition) system and Trackscan has been shared for the specified test case. This package also includes data related to the 'Train driver' and GPR (Ground Penetrating Radar). The ABA and raw GPS data are provided in their original format, avoiding conversion to HDF5 (h5) to preserve the timing information. Two processing solutions are available, with one based on Python, while other alternatives exist.

The raw data includes live coordinates, but it is recommended to process only the time and acceleration signals. The Applanix exports should be used to achieve more accurate location matching, considering that there is an offset between the center of the IMU (Inertial Measurement Unit) and the instrumented axle, approximately 12 meters. The offset has been verified, and further confirmation has been completed. For a more detailed explanation, see the image below (Figure 4-27). The quality of the stickers on the Leonardo is excellent, so additional measurements can be easily conducted if needed.

Kalibratiespoor Zutphen

Werknummer 21038205010

Versie A

T.o.v. grondslag aangelegd d.m.v. 06-GPS

Meetdatum 31-05 en 30-06 2023

Maatvoerder: J. Detmar

Gemeten met Leica TS 16 / GS 18

Coördinaten in RD en t.o.v. NAP

Kalibratie rapport ter inzage bij meetkundige dienst Strukton Rail

Tel. 06-1172 5512

Uitgewerkt: J. Detmar

Gemeten hart target

Figure 4-27: form presenting results of the verification

The Trackscan information is organized into four measurement runs, with each run labelled by date, run number, and driving direction. Each run's folder contains images and CSV files with various detections performed by the train. Synchronization of these files is facilitated by the section IDs, corresponding to the last six digits of the image filenames. The images have been filtered to include only the specified area, though some section numbers in the CSV files may not have matching images and can be disregarded as they fall outside the specified area.

Various file formats are included for review, with notable extensions as follows:

1. **si**: Files containing section information, useful for quickly mapping locations and selecting areas of interest.
2. **geom**: Files containing geometry information, as previously shared.
3. **f**: Files detailing detected fasteners, including bounding boxes and other specific measurements.
4. **tw** and **jb**: Files indicating the locations of thermite welds and joint bars (insulating rail joints), which can be valuable for correlating with ABA data.



Review of these file formats has been taken place between the various partners. The led to clarification and/or additional requests.

5. UTILIZED TOOLS, SOLUTIONS AND SYSTEMS

In D10.1 the tools are described. Here some updates and/or clarifications.

5.1. Multi Sensor & Multi-Vehicle train borne system

5.1.1. Introduction to the Use of the Leonardo Platform

In this section, we describe the Leonardo monitoring train, and the sensor technologies deployed on board: not as a claim of technological novelty in themselves, but to provide clarity on the tools and infrastructure used within this research. The Leonardo platform serves as a versatile and agile testing environment, enabling the integration, experimentation, and refinement of existing and emerging technologies under real operational conditions. Its key value lies in the ability to combine multiple sensing modalities (such as Axle Box Accelerometers (ABA), Ground Penetrating Radar (GPR), LiDAR, video, and, more recently, audio) within a single, modifiable platform. This setup facilitates repeated testing, side-by-side comparison of tools, and data collection across various conditions, supporting both applied research and high Technology Readiness Level (TRL) development. The platform is not the innovation itself, but a means to rigorously evaluate and evolve the technologies and methodologies central to this work package.

5.1.2. The LEONARDO platform in a nutshell

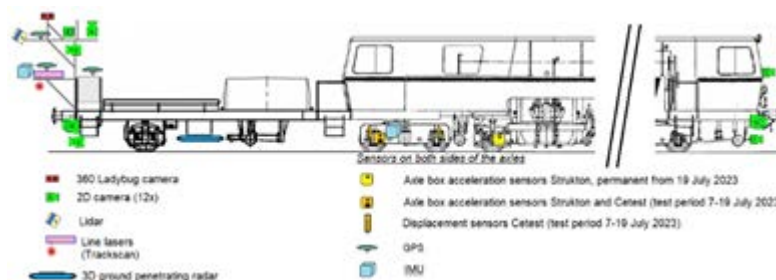


Figure 5-1: Overview of the sensors mounted on the LEONARDO platform

The LEONARDO platform [1] uses a retrofitted tamping machine which has been transformed into an advanced rail measurement train for gathering comprehensive and accurate data on both the rail condition and the environment (cf. Figure 5-1). Its “Trackscan” laser measurement system is employed to measure the railway tracks while a LIDAR (= Light Imaging, Detection and Ranging) sensor is utilized to map the surrounding environment alongside the tracks. Both the railway tracks and the surroundings are captured through an optical camera system which gathers detailed visual information. The LEONARDO also incorporates 3-dimensional ground penetrating radar (GPR) to measure ballast and ground layers, providing valuable data regarding the stability and consistency of the rail infrastructure. Additionally, axle-mounted acceleration and displacement sensors are integrated to record vibration patterns and measure the elongation of primary suspensions, aiding in the assessment of overall rail performance and safety including estimating relevant track geometry parameters.

The LEONARDO platform is comprehensively detailed in Section 7.1 of D10.1, titled "Multi-Sensor & Multi-Vehicle Train-Borne Onboard Monitoring." Furthermore, the subsequent paragraphs will emphasize specific aspects that have raised some requests for clarification.

Level of Innovation Proposed by using the Leonardo platform

The Leonardo monitoring train was developed prior to this research program. However, the innovation lies in the principles behind the LEONARDO platform. This platform facilitates the rapid testing of new technologies and provides easy access to operational data, enabling collaboration with industry and research partners. The primary focus is on acquiring data from infrastructure assets from an on-track perspective within a ± 5 -meter radius, aiming to gather valuable information, including the possibility of detecting underground issues.

The true innovation of the LEONARDO platform is demonstrated through practical applications that move beyond one-off tests, driven by the involvement and needs of end-users. This practical approach ensures that the applications are demand-driven and address real-life issues in rail infrastructure. Additionally, this approach promotes high Technology Readiness Levels (TRLs), as it requires addressing practical deployment issues in operational environments. The diverse data sources also present intriguing challenges for in-depth research, making this setup appealing to researchers. Crucial to its success is the unobstructed access to operational infrastructure. This comprehensive focus on practical, real-world applications and high TRLs makes the LEONARDO platform a valuable component of this work package.

For further details, see also the TRA paper “Agile Multi-Sensor Platform LEONARDO: Evaluation of New Monitoring Technologies in an Operational Environment” [2].

Use of ABA and GPR

Regarding Axle Box Accelerometers (ABA) and Ground Penetrating Radar (GPR), while these technologies are indeed in use, their consistent and effective application in real-life practice remains an area with significant room for innovation. The embedding of ABA in everyday practice and its potential for consistently detecting various issues is still evolving. The true innovation lies in the combination of multiple data sources to enhance detection capabilities and achieve high TRLs. This integrated approach ensures a more comprehensive understanding and resolution of rail infrastructure issues.

The addition of GPR to the data collection toolkit is particularly noteworthy. The latest advancements in GPR technology allow for faster driving speeds, enabling the Leonardo to operate seamlessly between operational train services. While GPR is not yet common practice, its utility in investigating recurring track geometry issues is increasingly evident.

Additional Detail on Potential Explosives

The mention of potential explosives was included as a single example and is not the primary driver of this work. The main focus is on conducting more frequent scans of the underground to identify ballast pockets, badger sets, and other potential issues that could lead to recurring track alignment problems. Given the primary focus, it is acknowledged that the example of explosives may not be the most relevant and could potentially be omitted in future communications.

The application mentioned section 7 in this deliverable is a better example where the use of the ground penetrating radar will be used. The reality model includes 3D-modelling of underground infrastructure.

5.2. Multi-Sensor wayside monitoring of switches

The following section describes to utilised tools, solutions and systems for wayside infrastructure monitoring, introduced in chapter 7 in D10.1. The infrastructure monitoring system is composed

of custom-developed hardware, including sensors and data acquisition system, analytical tools to transform the measured data into information thereby enabling prescriptive maintenance approaches and software tools for visualisation and asset management purposes.

5.2.1. Using novel multi-sensor systems for infrastructure wayside monitoring

In recent years, voestalpine Railway Systems developed a novel multi-sensor platform which can be used to monitor various damage patterns in turnouts as well as in open track. The technology is based on multi-directional vibration and motion measurements and provides additionally a temperature sensor module. Beyond that, the system provides onboard data processing, filtering as well as edge computing capabilities. There are multiple versions of this sensor system which can be chosen depending on the component to be monitored or the operational parameters of the monitored asset.

Within this project, two versions of this sensor platform are used for monitoring purposes. The sensors were as mentioned above developed in the past years, referring mainly to the hardware aspect. However, the firmware and on-board implemented algorithms are still adapted during the current project, especially as these need to be adapted to the requirements of high-speed applications. In addition, the knowledge obtained from simulations, advanced data analytics and reference measurements will be incorporated into the sensor firmware. Part of it was conducted within WP10 and will be also further conducted in WP11. Figure 5-2 shows an image of the utilised multi sensor platform.

The first sensor type which is used for track quality monitoring and is mounted on highly loaded sleepers in a turnout (e.g. at the turnout beginning and in the crossing region). This sensor monitors the displacement and rotation of the sleeper and thereby provides information on stiffness changes and developing voids below the sleeper. The sensor was already tested in previous projects such as Shift2Rail, at the demonstrator turnout in Vienna Liesing (ÖBB track) as well in other projects with ÖBB such as Rail4Future (FFG Project number: 882504). However, within the current project several updates on firmware level have been implemented and a strong focus was on further developing model based and data driven analytical approaches for the estimation of required operational parameters and the overall health state of the monitored asset.

The second version of the multi-sensor system which is used within this project includes a structure borne noise module and serves for monitoring of rails, such as wing rails, stock rails and switch rails or frogs. This sensor has a very high frequent band width (up to 48kHz) and is therefore able to detect even minor changes in the material and detect excessive rail wear or even crack development. This sensor version was also developed from a hardware perspective before the start of the current project. The main innovation conducted during the current project refers to advanced analytical models in order to address different damage patterns of turnouts in both, high speed and mixed traffic area.



Figure 5-2: Multi-sensor platform for track quality and rail wear monitoring used in various locations of the two demonstrator turnouts

The introduced sensor system is utilised within WP10/11 to provide information on the asset health state in real time and serve as an input source for various condition monitoring models, thereby enabling the smart asset management demonstrator.

The sensor includes, depending on its version, multiple sensor modules, for example a three-ax accelerometer, a three-ax gyroscope, a temperature sensor and a structure borne noise module or a displacement sensor module with adjustable sampling rate, measurement range and filter settings. Figure 5-3 shows a schematic illustration of the sensor, its included sensor modules as well as its internal channel orientations.

Sensor Positions & Orientation

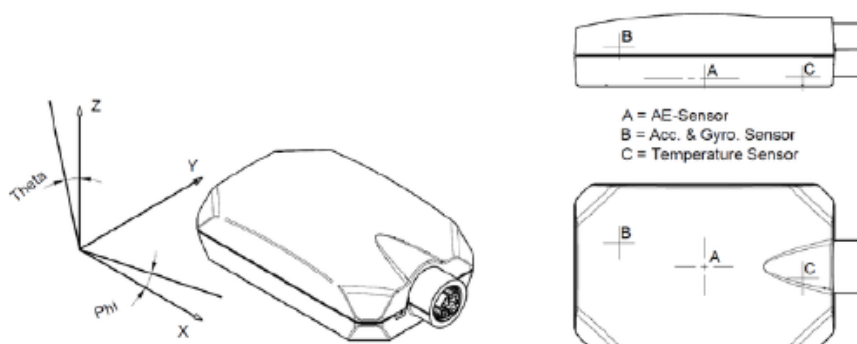


Figure 5-3: Schematic illustration utilised multi-sensor with included sensor modules and internal channel orientations

This multi-sensor can be applied on the component to be monitored either by screwing a mounting frame to the component or by using an adhesive connection. The adhesive coupling is furthermore also required for the structure borne noise measurements.

Moreover, voestalpine Railway Systems uses also further sensor types within this project for infrastructure monitoring purposes. An analogue version of the structure borne noise sensor is

used in the high-speed demonstrator which provides an even higher bandwidth (1 MHz) and is used for monitoring of point machines and detector rod breaks, see Figure 5-4.



Figure 5-4: Analogue structure borne noise sensor

Another sensor which is used in the high-speed demonstrator is an inductive proximity sensor which monitors the gap between switch rail and stock rail, as this is a safety critical parameter and therefore crucial for a safe operation of the turnout, see Figure 5-5. This sensor provides the distance of the two rails in 0.1 mm precision which allows the operator to recognize any positional changes of the rail tip or the nearest flangeway of a switch and react to such changes before they lead to traffic disturbances, thereby increasing the overall availability of the track.



Figure 5-5: Inductive displacement sensor for switch rail position monitoring

5.2.2. Integrated asset management and monitoring platform

voestalpine Railway System provides within this project its integrative asset management & maintenance management (former DTM software) and infrastructure monitoring (former ROADMASTER software) platform called zentrak. Both software solutions have been developed by voestalpine Railway Systems over the past years and are already in use at multiple railway operators over the world. However, the focus within WP10/11 is to integrate these both solutions in one holistic and interacting platform, combining all relevant data sources coming from the operation of the asset, its maintenance teams, providing the general asset structure and history as well as online and real time monitoring data, thereby providing an overall view on the asset health state and pending maintenance tasks. Figure 5-6 shows the schematic structure of the zentrak ecosystem which can incorporate information coming from voestalpine Railway Systems hardware, as well as any third-party hardware, process the incoming data and pass it to the user or any other interface, for example an ERP software used by the operator. zentrak thereby serves as a central platform combining data for multiple incoming streams and guarantees efficient and performance-oriented asset management for an overall improvement of the asset life cycle costs.



Figure 5-6: Schematic illustration of the zentrak asset management & maintenance and infrastructure monitoring platform.

The zentrak infrastructure monitoring module, shown below in Figure 5-7, provides multiple monitoring features and visualisation as well as advanced data analytics capabilities for the asset manager and service teams. By providing information on the location of the turnout, various KPIs which describe the health state even up to a component level, or as an overall asset health state, the user can choose the granularity of information he needs and dive even into signals of single train passages. Furthermore, the system estimates and records operational parameters of the asset, such as the number of passing trains, train types, average / maximum speeds, passing directions and number of switching processes, thereby guaranteeing not only a comprehensive picture of the operation itself, but furthermore allowing a detailed clustering and filtering of the data, thereby increasing the overall effectiveness of the system.

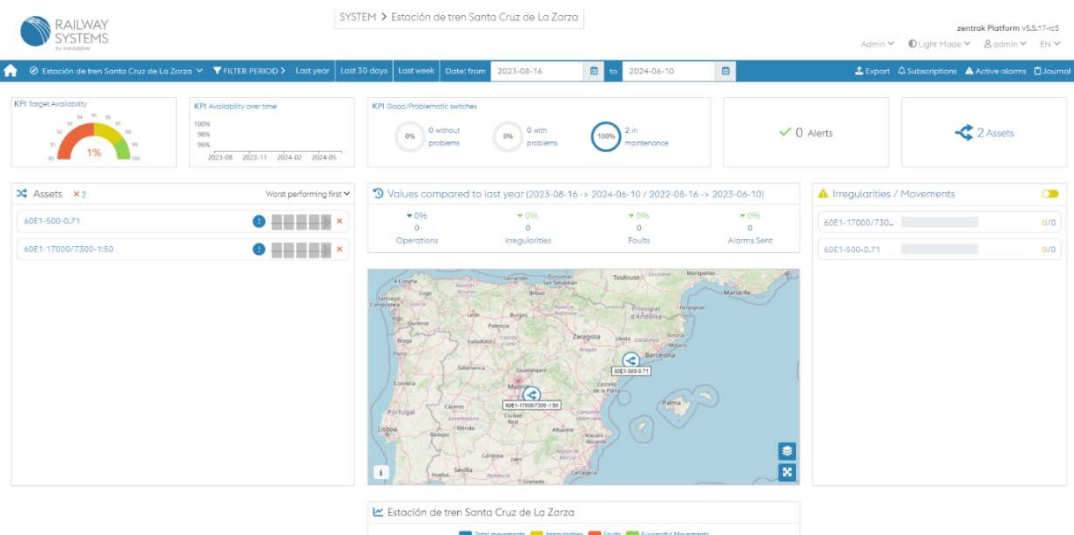


Figure 5-7: Landing page of the zentrak infrastructure monitoring module. The map shows the location of the two demonstrators located in the ADIF mixed traffic and high-speed network.

Figure 5-8 shows the high- speed demonstrator in the zentrak asset management & maintenance

management module. This tool contains all relevant information from contact management including information on the asset (or component) manufacturer, the operator as well as the service and maintenance operator. zentrak asset management & maintenance management provides furthermore a detailed overview of the component structure of the asset, manufacturing and installation dates, the maintenance history as well as possibilities for planning of pending maintenance tasks. The most crucial feature is the ability of data exchange between zentrak infrastructure monitoring and asset management by means of predefined interfaces.

This communication is crucial for both applications as for example a component exchange or recognised defect needs to be reported and considered in both systems as it triggers different actions or changes in the analytics procedure and affects future maintenance actions. Therefore, an integration of both modules is of crucial importance and will lead to a powerful tool for railway operators and their maintenance teams, as it will increase their effectiveness significantly.

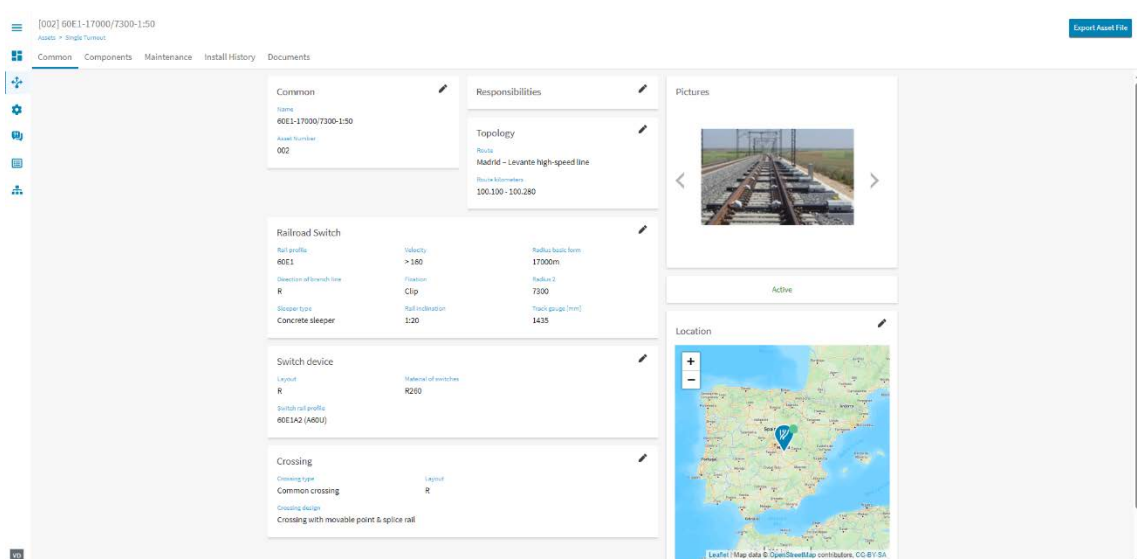


Figure 5-8: zentrak asset management & maintenance management software (mobile version)

Both software modules (infrastructure monitoring and asset & maintenance management) have been developed before the project as unique and independent solutions. The focus of the current development and the main innovation is to provide a more integrated solution which combines these software tools into one platform to provide the infrastructure and maintenance operator with relevant real time monitoring data, which can be used for maintenance planning but also during inspection and maintenance tasks. Furthermore, the data provided within the asset and maintenance management tool will be linked to the monitoring software, providing necessary input for its algorithms and models. As an example, if the maintenance staff adjusts anything in the turnout – this change of the asset state will affect the monitoring data and hence could lead to a false alarm in the monitoring tool. On the other hand, if this information is available to the monitoring software with the information which parameter was changed (and how much) – the monitoring system will be capable to provide significantly better predictions and action recommendations while the false positives will be reduced. Another major advancement will be to incorporate developed models and algorithms into the software so that it will provide the infrastructure operator with better recommendations and suggestions which type of failure he can expect and until when he needs to fix it before it leads to breaks downs and availability issues

of the turnout.

5.2.3. The POSS® System in a nutshell

POSS® [3] is a condition monitoring system for assets in the railway and power industry. It consists of local dataloggers and sensors that collect measurements and send the data to a central server where it is visualized in a User Interface. The main focus of POSS® is the monitoring of point machines which includes measuring the consumed current during a throw, as well as the state of some related relays and the ambient temperature. When anomalies are found in these measurements (e.g., through the exceedance of predefined thresholds), the system triggers a warning or alarm, indicating to a team of maintenance experts that the behaviour of the switch deviates from the expected patterns. The maintenance experts then go on to further analyse the data to see if any maintenance or repair activities are required.

For more detailed information on POSS, refer to Section 7.2.4.2 in deliverable D10.1, as well as several previously published papers [3] [4] [5] [6]. The ongoing work on POSS will build upon these earlier developments and findings, leveraging the established research and results to inform current and future efforts.

6. HOLISTIC MONITORING AND DECISION SUPPORT

Holistic monitoring and decision support directly refers to the multi-sensor use case within FP3–IAM4RAIL WP10/11 as described in D10.1 (Section 5.2.1). The railway infrastructure is a complex combination of various components such as rails, ballast, switches and crossings (S&C), point machines (PMs), catenary, interlocking etc., all having their own fault types and therefore often being maintained separately in practice. However, components often do not operate independently, and also their health condition and degradation may depend on each other. Holistic railway infrastructure monitoring thus aims at explicitly taking such dependencies into account for the purpose of enhanced diagnostics and health prediction including considering the connections to train operations. As for advancing digitalization and AI (= Artificial Intelligence) research, this requires systematic and synchronized data covering all relevant components including manual and automatic inspection data and maintenance reports as well as structured data from embedded sensors together with information about environmental conditions.

The project partners of FP3–IAM4RAIL WP10/11 have therefore been starting to collect such a comprehensive data set for a 22 kilometres long main line with mixed traffic on four parallel tracks and about 40 switches between Amsterdam and Utrecht in the Netherlands as well as data from a second pilot site in Spain. Data are now being shared bilaterally among the partners upon their specific needs and handled and synchronized using their respective data management tools to fit to their individual research and development tasks as described later in the application section (see section 8) of this deliverable D10.2 (see also [7]).

An essential aspect of the holistic approach as described above is that parallel measurements for the same infrastructure asset or the same track element using various wayside and/or onboard sensors are likely to contain redundant information about the respective health conditions. While data fusion can help then to increase the reliability of the estimated health states, the data at the same time allow for analysing which sensors or combinations of sensors (together with their positioning) are the most informative ones or, on the contrary, could be dropped from the overall sensor layout without too much loss of information. Even more, transferring knowledge as obtained from a few highly equipped and comprehensively monitored infrastructure assets could reduce the sensor needs for the large rest of similar assets in the rail network. As a result, sensors can be selected and positioned in a more optimal way considering both statistical power of the data and cost efficiency, thus (hopefully) providing better decision support at still reasonable costs. Figure 6-1 depicts the principles of the possible options in a graphical way.

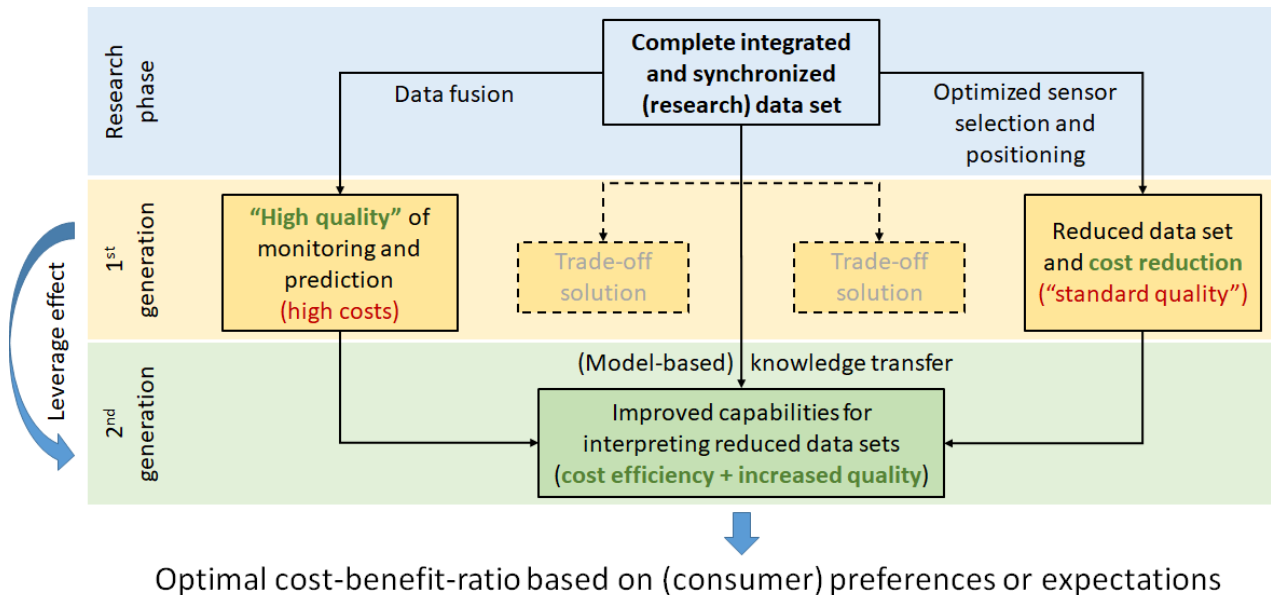


Figure 6-1: Strategic options for an optimal trade-off between costs and quality of infrastructure asset monitoring based on a holistic analysis

6.1. Integrated Data set for holistic monitoring and diagnostics

Intending to foster the development of enhanced tools for integrated health monitoring and fault diagnostics via (simulation-oriented) physical models and/or modern data-driven approaches, various kinds of train-borne data have been and are being collected via the so-called LEONARDO platform (cf. Section 5.1.2). All this is accompanied by continuously recorded current curve (incl. control circuit) and sometimes also power supply measurements for the point machines together with environmental data such as temperature (cf. Section 5.2.3). For a dedicated switch, also sleeper displacements (per axle) and blade positions via inductive sensing are going to be measured. In addition to that, by using different modelling techniques and simulation frameworks, synthetic data sets will be generated by means of virtual sensors to complement the data obtained by means of real sensors in field test campaigns. Synchronized maintenance and manual inspection reports will help to validate and interpret the automatically generated measurements as well as the results that are going to be derived from them algorithmically.

Within WP 10 relevant preparatory steps to obtain and create such an integrated data set for further research and demonstration in WP 11 supporting and combining several of the described applications were successfully completed.

6.2. The work towards digital twin

As described in D10.1 a vital interface to the research on digital twins in FP1_Motional exists and is realized by several applications related to train-borne and wayside modelling and simulation of the vehicle-track interaction (see sections 8 and 12) as well as the comprehensive modelling of complex assets such as switches (see section 17).

7. REALITY MODEL

7.1. Introduction

7.1.1. Background of this application

According to the current schedule, the last railway section in the Netherlands to be equipped with ERTMS will not be completed until 2050. To accelerate this process, ProRail has established an innovation partnership. The goal of the ASAP ERTMS innovation partnership is to bring this completion date forward to 2040, with an ambition to accelerate it even further to 2035.

The innovation partnership provides a space for market parties to collaborate with ProRail in developing innovative and effective solutions that are not yet available on the market. This partnership has outlined specific challenges, one of which is: "Smarter design: develop solutions to accelerate the creation of integrated railway designs."

To address this challenge, it is essential to understand the current situation. This involves leveraging developments from FP3–IAM4RAIL WP10 to use the technology of the Leonardo. Additionally, to optimize the results, the developments of the Leonardo will be refined and enhanced. The synergy between these two initiatives includes:

- Responding to a concrete question from FP3-IAM4RAIL
- Extensive testing of the technology
- Ensuring the technology will be used in practice

The drive to create this Reality Model stems from the national innovation partnership with ProRail to accelerate the rollout of ERTMS. FP3–IAM4RAIL provides support by making the data available and optimizing and validating the data capturing techniques used. This synergy between FP3–IAM4RAIL WP10 and the innovation partnership ASAP-ERTMS ensures that the developments meet the needs and achieve a high Technology Readiness Level (TRL). The ASAP-ERTMS partnership offers a testbed and an opportunity for deployment of the technology developed.

7.1.2. Scope / Objective /Aim

To achieve a successful execution of the designed and planned work, it is necessary to have a prior understanding of the actual situation. On one hand, the actual situation is documented in the drawings of the existing infrastructure. However, it is also necessary to verify if these drawings reflect the current situation. Additionally, it is important to know the condition of the infrastructure. Therefore, a digital model of the actual situation in the field is necessary. This is crucial for creating a practically feasible axle counter and balise design for a railway section.

The goal is to display as much current information about a rail track as possible using a 3D model. This 3D model provides a highly accurate representation of the actual rail track, creating what's called a "Reality Model."

The more up-to-date the information in the Reality Model, the greater its added value. By using the information for the design, balises can be projected at locations where they can actually be placed in practice. This gives the possibility if what is designed fits the actual situation outside. The design can be adjusted accordingly avoiding last minute decisions outside, avoiding failure costs in the execution phase. The design is immediately practically executable.

To have truly current information available, the LEONARDO platform, as described in D10.1 is being used.

7.1.3. Broader context

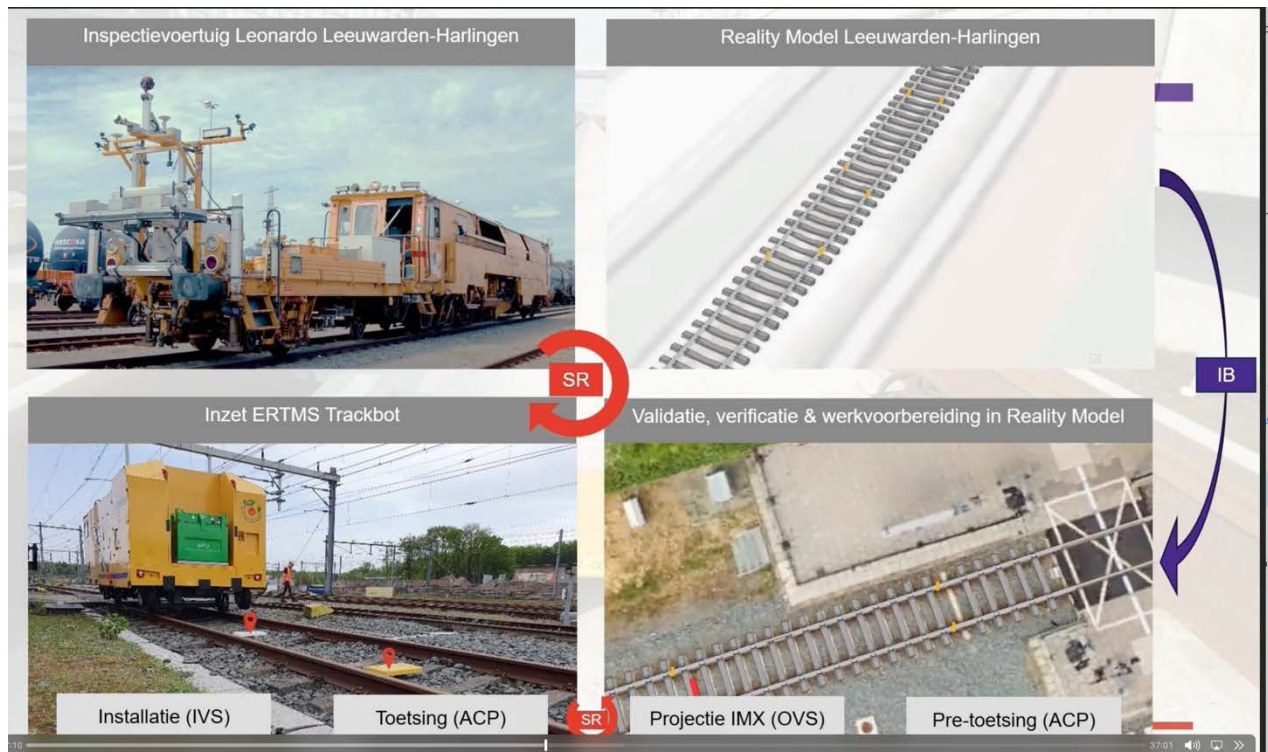


Figure 7-1: overall context of the reality model

7.1.4. Description of the technology

Although the Leonardo has various technologies on board as explained, the Reality Model currently uses only the following:

- LiDAR: Using a LiDAR system, a 360-degree point cloud of the environment is created.
- Trackscan: Using the Trackscan, a detailed point cloud of the track is created, roughly between the ballast shoulders.
- Ground Penetrating Radar

In addition to the current information collected with the Leonardo, the Reality Model utilizes available rail data from the ProRail databases as much as possible. For example, KS-bladen and GIL are used for the underground infrastructure. This underground infrastructure is also cross-checked with the results of ground-penetrating radar to ensure the drawings are accurate and no other objects are present.

7.1.4.1. Challenges

The ERTMS configurator, which uses numerous data points to create a 3D model of the existing situation. This "Reality Model" allows for viewing the design within the current environment

before any work begins. This is highly beneficial as encountering issues during the execution phase leads to costly mistakes.

Significant progress has been made in object recognition over the past two years. Detecting objects within a 3D point cloud requires innovative technology. The computer can now recognize the contours of a railway object from a 3D environmental scan, although this wasn't always flawless. Initially, there were challenges, such as mistaking a pole for a tree or a signal for a traffic sign. However, with continuous training and advancements in AI, the accuracy has improved considerably. The results are now professional and reliable.

7.1.4.2. Validation of data and reaching required accuracy

The processing of collected data into a Reality Model has been validated based on location accuracy and object detection certainty. This was done for datasets gathered by the LiDAR scanner (environmental point cloud) and the Trackscan (detailed railway point cloud). A proprietary software model was developed for processing the point cloud data from the LiDAR scanner. Different model versions were compared during this validation, focusing mainly on the Kampen-Zuid test area. An initial check on the impact of scaling up to the Hanzelijn on data quality was also conducted.

Validation of location accuracy and object detection certainty was performed using fixed reference points, allowing for comparison of different datasets. Objects registered in Railmaps were used for this purpose. A Strukton surveyor manually measured several relevant objects near Kampen-Zuid station with a Leica GS18 GNSS system:

- 47 overhead portal masts
- 4 variable signals
- 4 ES joints, including 40 collar bolts
- 6 balises

The locations of these objects were compared with their known geographical positions in Railmaps, showing they were within 5 to 10 centimetres of the expected locations. This indicates that Railmaps data is suitable for an initial validation of the Reality Model and can be used for validating the Reality Model of the Hanzelijn.

7.1.5. Functionality in detail

In general, the process to develop the Reality Model follows these six steps:

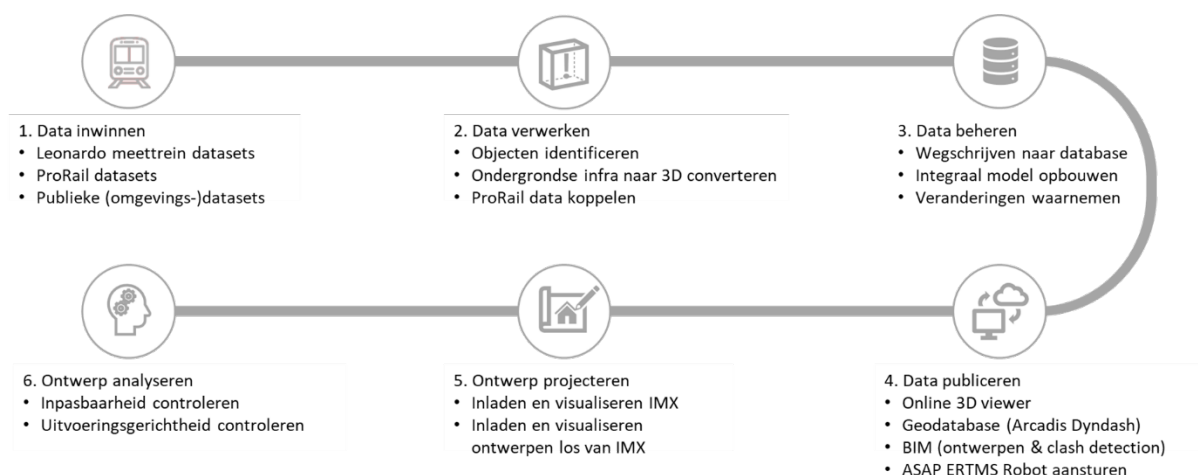


Figure 7-2: the six steps towards the Reality Model

The first step in the process is data collection. This is done using the Leonardo measurement train and sources available from ProRail. Additionally, public datasets such as the Actueel Hoogtebestand Nederland (AHN) are used to supplement ground level data for areas not visible to the measurement train.

The second step involves processing the collected data into usable information.

In the third step, the processed data is stored in a database, creating a comprehensive view of the environment.

The fourth step is the publication of the data in various formats, such as a Geodatabase, to serve as input for Arcadis design tools.

In the fifth step, the completed design is loaded and visualized in the Reality Model.

The final step is to analyze the design and check it for practical feasibility.

7.2. Progress

7.2.1. Tests

The Reality Model is currently undergoing testing. This test will take place and is expected to be used in a pilot project later this year. This pilot involves the installation of balises, utilizing actual designs and data.

In addition, during the preparation phase, we used the Strukton Reality Model to check whether axle counters and balises could be installed in practice in accordance with the design (IMX). This makes the added value of the Strukton Reality Model tangible. The test is considered to be at TRL 7, which corresponds to a system prototype demonstration in an operational environment.

7.2.2. Next steps

In the coming years, several tenders are planned that will support the advancement of the Reality Model from TRL 8 to TRL 9. This progression marks the shift from demonstration to full-scale deployment, enabling implementation in real-world operational contexts. Strukton has already secured one of the initial projects, meaning that practical application of the Reality Model will begin late 2026.

8. HOLISTIC SWITCH MONITORING AND DIAGNOSTIC MODEL

8.1. Introduction and methodology

As already mentioned in section 6, data from various sensors and their combination are the foundation for the holistic monitoring of railway assets such as switches and crossings. Often, there are relations (or relations can be expected) where parts of the infrastructure directly and physically interact with each other but are still monitored separately in practice. Ballast condition and general track geometry, for instance, usually lack of an integration with the health monitoring of the point machines (including mechanical switch elements such as slide chairs and rods etc.) in context of maintenance and fault diagnostics.

Starting from current curve measurements as a single-sensor approach (use case 1), holistic diagnostics Figure 8-2 combine these data with other measurements such as power supply voltage or track geometry data (cf. Section 8.3.2 and 8.3.3). By that, the multi-sensor use case in FP3–IAM4RAIL WP10/11 (use case 2) is addressed in a natural way, too.

8.2. Work progress

Figure 8-1 shows the current state of progress for this application with a short review of relevant work done in the past (SoA) and a rough preliminary outlook to Wave 2 and 3 of the current series of ERJU FA3 projects.

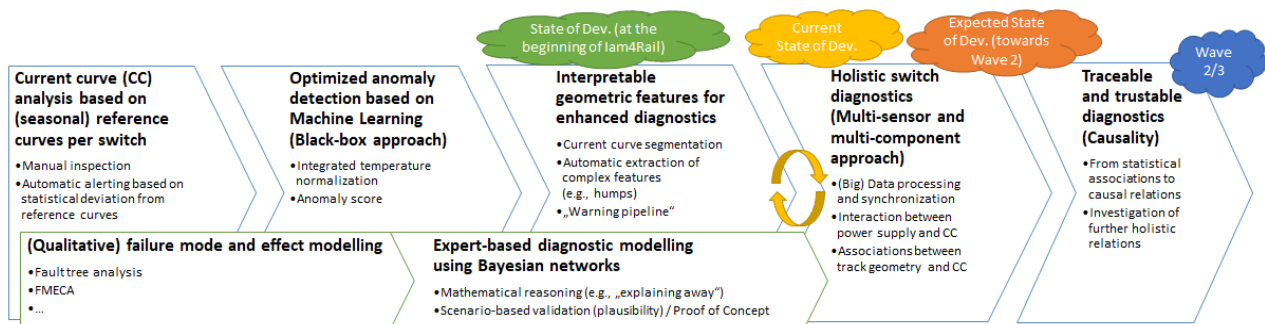


Figure 8-1: Timeline of previous, current and future work related to this application ("Holistic switch monitoring and diagnostic model")

As can be seen, current curve (CC) analysis is a well-established approach for switch health monitoring. In the past, practitioners started with manual CC inspection based on the comparison with reference curves per season, for instance. Automatic alerting, when curves deviate from the expected patterns (typically based on simple thresholding), was implemented then (see 5.2.3). Later, (black-box) machine learning was introduced to *detect* abnormal curves while automatically compensating the temperature variations in the CC [8]. For better *diagnostics*, then some first, more specific and complex features (e.g., humps in the switch movement phase) have been introduced that are related to more specific faults [4]. Here, also (automatic) CC segmentation became more and more important. At the same time, system-oriented qualitative modelling approaches (such as FMECA) evolved in terms of more complex expert-based (quantitative) diagnostic models (i.e., Bayesian networks, see Figure 8-2) with a first proof of concept and a simple scenario-based validation at the time when FP3–IAM4RAIL started [9]. Here, the switch

drive with its mechanical and electric parts is linked to other components and external influencing factors for the purpose of mathematical reasoning (including so-called „Explaining away“). By that it is taken into account that, at least theoretically, anomalies in the CC could be caused not only by switch drive defects, but also by other components (e.g., power supply, track geometry, ...) or other external factors. This, of course, (if true) would directly affect the effectiveness and optimization of maintenance planning and actions.

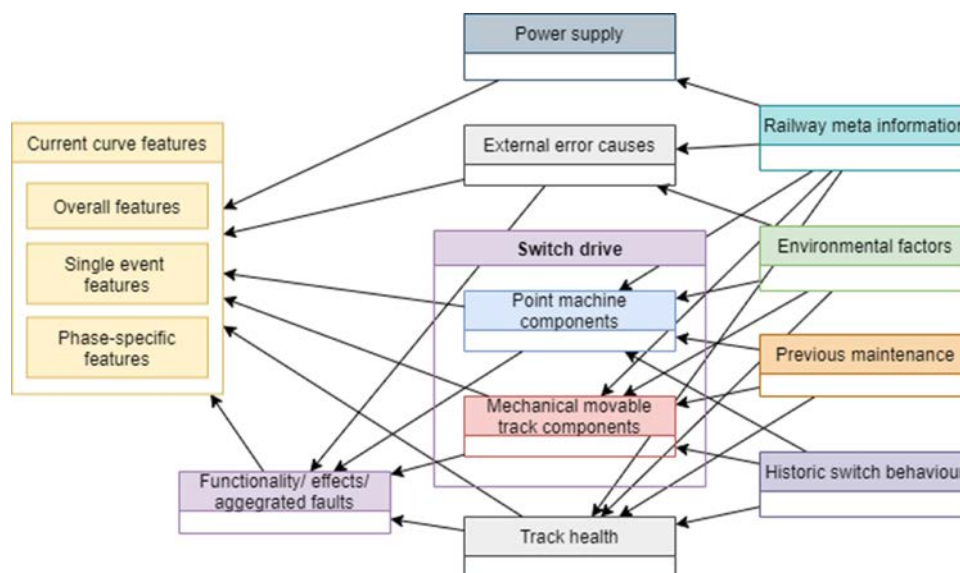


Figure 8-2: Schematic overview proposed diagnostic model (taken from D12.2, I2S2)

With the purpose of studying (some of) these inter-component (i.e., *holistic*) relations in more detail, WP10 therefore started with collecting, processing, and synchronizing (multi-sensor) long-term data on power supply voltage and track geometry data together with the respective POSS (i.e., CC and relay) measurements required for that. First results of an initial data exploration are described in Section 8.3. In parallel, the necessary computerization of the extraction of human-interpretable and very specific features from the CC measurements (besides the already existing basic features) was continued.

8.3. Achieved results

8.3.1. Feature engineering for switch diagnostics

General statistical features (e.g., mean, variance) as easily derived from data are often just a first step towards a diagnostic understanding of complex data and systems. Not without reason, switch maintenance engineers usually also take the geometrical characteristics of the current curves as one of the currently most important measurements for the condition monitoring of point machines into account. However, the automatic computation of such features becomes much more difficult compared to standard statistics because they usually are much more specific to the given type of data and asset.

Initial work on such geometrical current curve features for so-called NSE switches (as widely used in the Dutch FP3–IAM4RAIL pilot site) addressed humps in the movement phase of the current

curves and possible flat spots as part of such humps related to a slipping clutch (cf. Section 8.2). In combination with some basic statistical features per phase (i.e., inrush, unlocking, movement, locking), these automatically computed features already help to identify anomalies and possible defects in the point machines [4, 5]. As part of FP3–IAM4RAIL WP10/11 with relation to its single-sensor use case (Use case 1), the set of relevant features that can be computed automatically from the data (instead of visual inspection of the current curves) is now being expanded to also include humps during the (un-)locking phase Figure 8-3as well as, for instance, dips and oscillations in the current curves all being essential evidences for holistic diagnostics (cf. [6]).

Figure 8-3, for instance, shows the evolution of a critical hump in the unlocking phase of a given switch with hump features (e.g., size and prominence) computed automatically by the algorithm. Note that such interpretable and transparent features are very helpful not only for diagnostics itself, but also for the systematic data-based analysis of the multi-component relationships between switch engine and other switch or rail components (cf. Sections 8.3.2 and 8.3.3) in general.

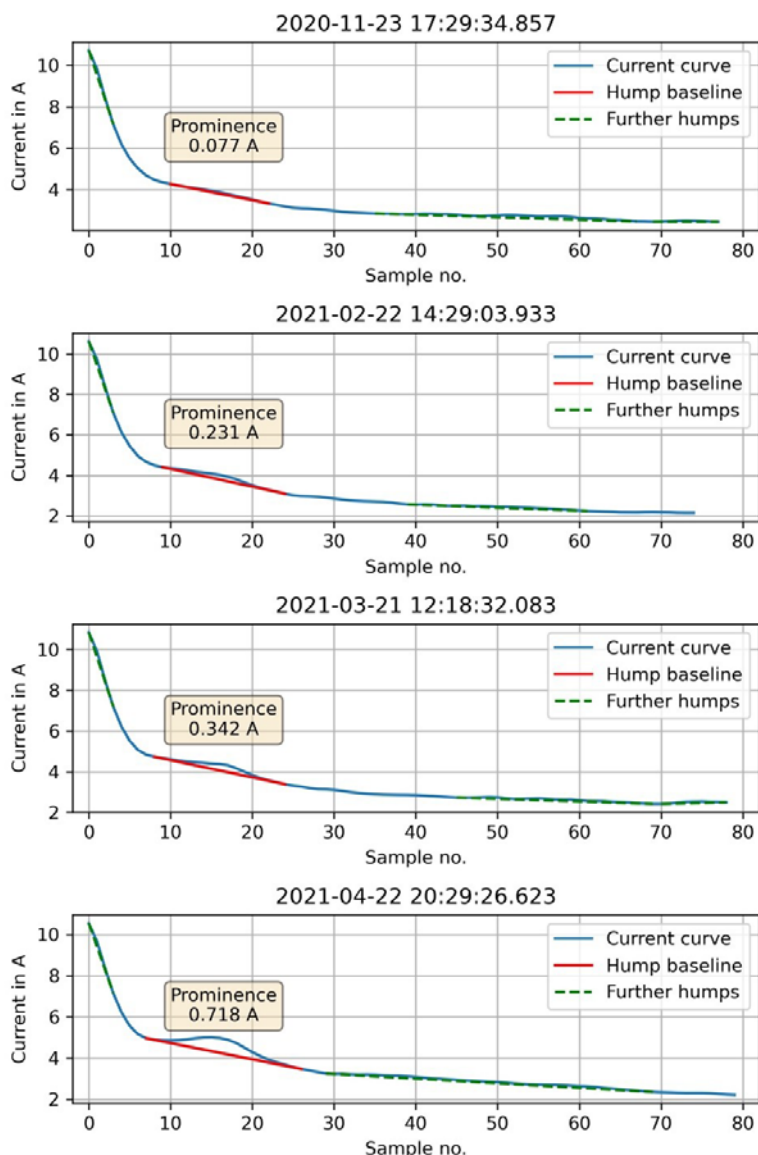


Figure 8-3: Evolution of a current curve hump in the locking section with increasing hump severity over time measured by its prominence (= maximal vertical distance between current curve and hump baseline) (cf [5]).

8.3.2. Effects of power supply variations on condition monitoring of point machines

As mentioned before, recent fault diagnostics for point machines often rely on motor current curve measurements, which are then interpreted by maintenance practitioners for triggering suitable maintenance actions. To improve the reliability of results, algorithmic approaches sometimes control for influencing factors such as temperature [5]. [8]

As a part of the Dutch pilot site installations, now also the voltage measurements of several switches that all draw from the same power source were collected for a deeper analysis. A first exploration of the data shows that power supply fluctuations caused by simultaneous switch movements can indeed influence the shape and level of motor current curves (see Figure 8-4) and thus should be considered during the manually and/or algorithmically conducted diagnostic

interpretation of the current curves. In fact, without taking the power supply effect into account here, it would not be possible to decide whether small humps or dips in the current curves, for instance, are simply normal or if they are indicating the early stage of an evolving failure as would be relevant to know for predictive maintenance instead.

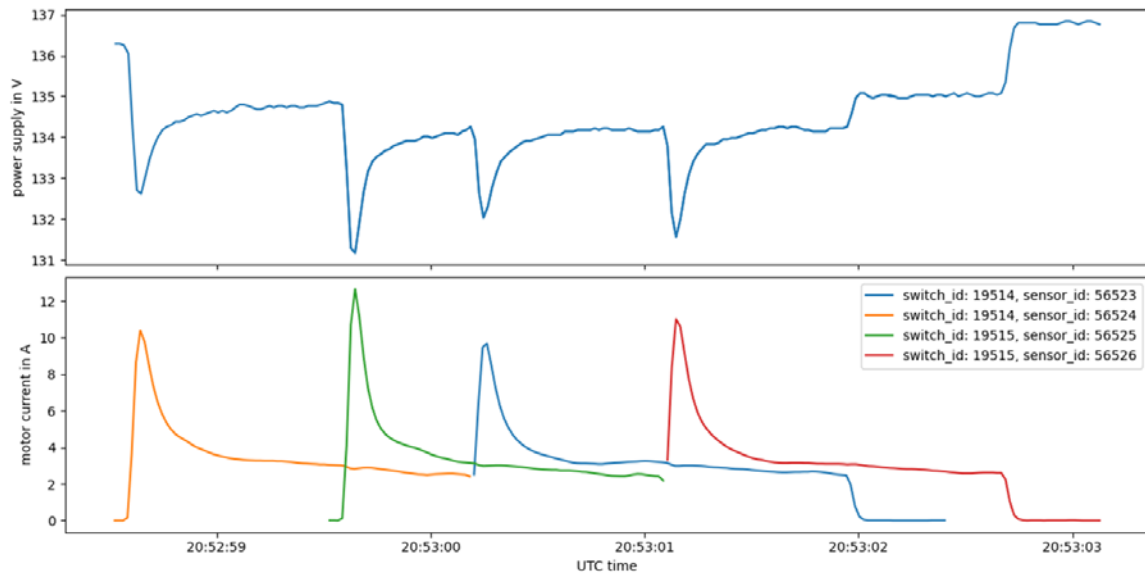


Figure 8-4: Overlapping movements of several switches that draw from the same power supply. Drops in the available voltage (upper plot) caused by the inrush peak of one switch are resulting in dips in the motor current curves (lower plot) of the other switches

In the next steps, data collection will be continued with a deeper exploration of the respective dataset. The goal is to see how power supply fluctuations might impede currently used condition monitoring approaches (e.g. by causing false alarms) and how this new measurement data could be used to improve them.

8.3.3. Effects of track geometry on point machines

Besides other factors, track geometry can be expected to be related to several issues in context of point machine health monitoring and diagnostics. To uncover these relations, data from the Dutch pilot site (cf. section 4.2) are synchronized and compared to each other. In particular, the following data have been synchronized so far for a deeper analysis:

- Track geometry measurements of switch segments (see Figure 8-5: small plots with one plot for each geometry parameter).
- Monthly train statistics (axles, tons, number of trains per switch).
- Wayside measurement data from point machines collected by POSS, e.g. relay data and point machine motor current curves (see Figure 8-5: larger plots showing current curves separated by switch movement direction) with features derived according to Section 8.3.1.

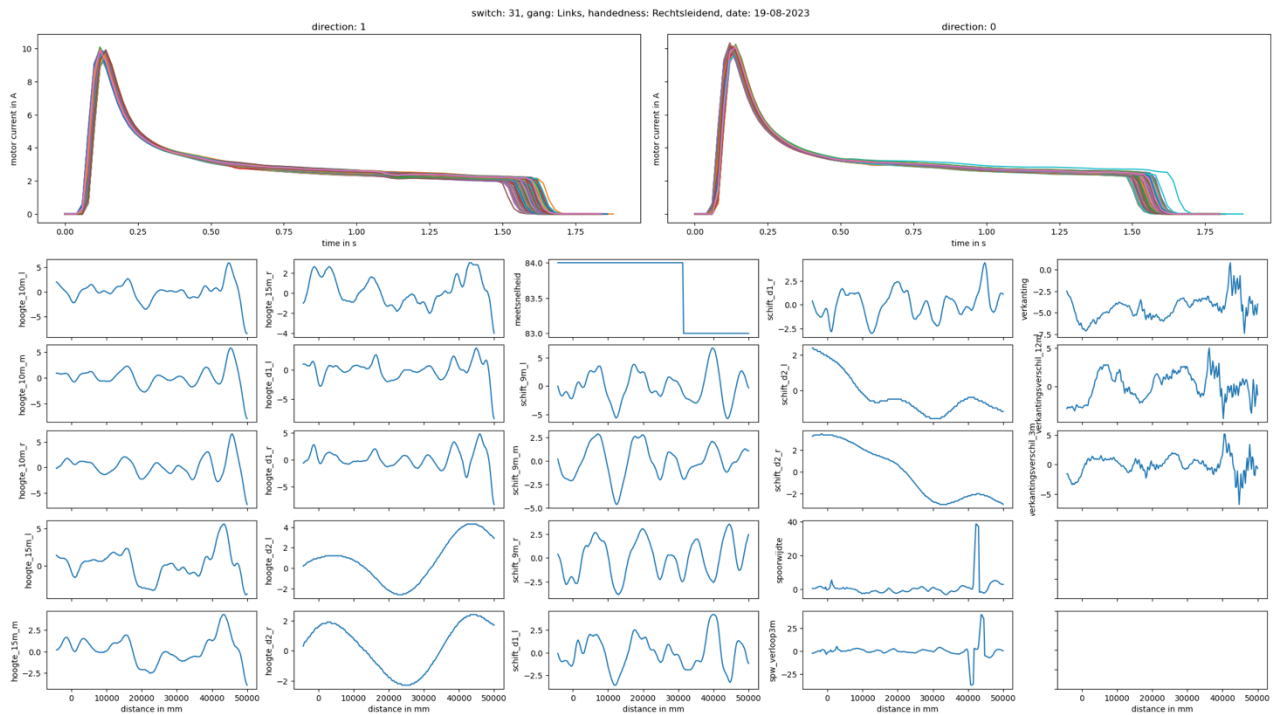


Figure 8-5: Track geometry measurements of a switch segment and point machine motor current curves in the week before

This data is now available from 2023 onwards for the switches of the Dutch pilot site and can be scaled easily. Additional to the track geometry measurements of the switch segments, more detailed measurement data collected by the LEONARDO train could be considered, and results from the processing of said data could be integrated as well. The next steps are further work on data management, data exploration and feature engineering for this newly combined, holistic dataset.

As part of an initial data exploration at the transition between WP10 and WP11, Figure 8-6 indeed shows a promising example where a strong correlation between changes of some track geometry features (i.e., cant, twist) and changes in the CC for one of the movement directions of the given switch over time can be conjectured.

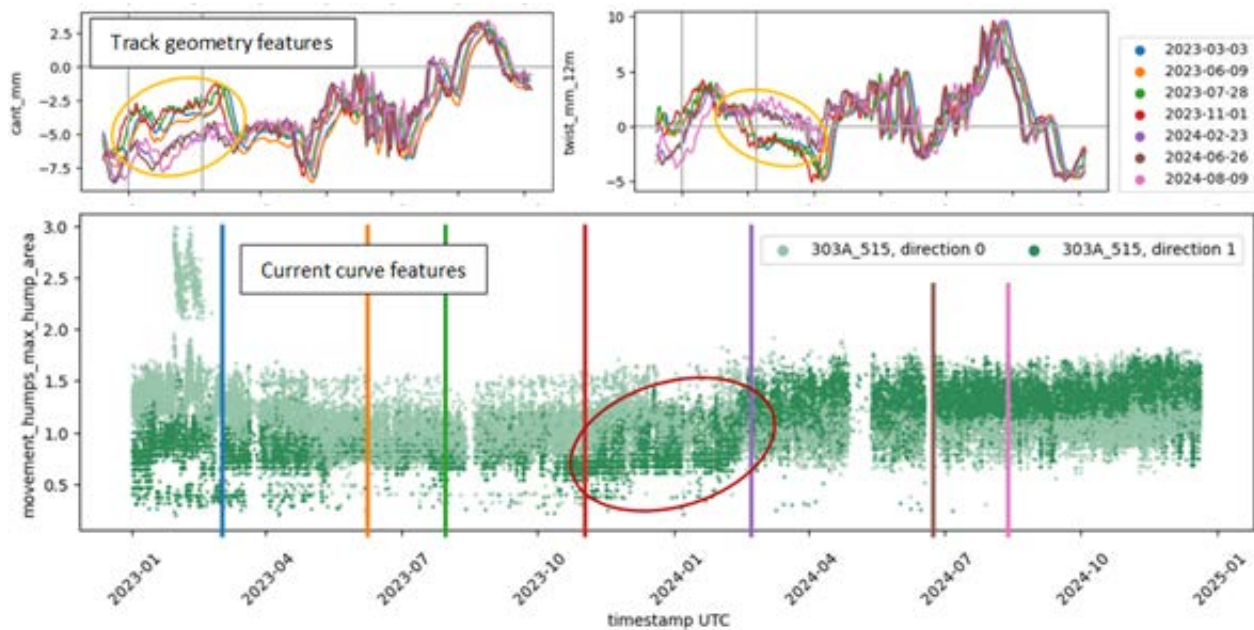


Figure 8-6: Possible example for correlations between CC measurements and track geometry

8.4. Status handed over from WP10 to WP11

Practically, there is a very smooth transition between WP10 and WP11 concerning the presented application (“Holistic switch monitoring and diagnostic model”). Nevertheless, one major achievement of WP10 is that all data collected for this application so far, are now available in synchronized form via a common database with automatic processes for updating the data if required. Needless to say, this is an indispensable prerequisite for all the upcoming (big) data analysis. That is, the analyses of the relation of power supply and track geometry on the CC are going to be continued to better understand and quantify the respective effects (cf. Sections 8.3.2 and 8.3.3). This also includes and requires to further automatize and optimize the extraction of specific, interpretable CC features (beyond standard statistical features) in terms of Section 8.3.1 and to investigate them for the existing large-scale data.

8.5. Preliminary results that can be used

Based on the preliminary results in WP10 (see Section 8.3), already a small number of scientific publications related to the presented application (“Holistic switch monitoring and diagnostic model”) have been submitted. Further journal and/or conference contributions are in preparation. Moreover, new CC features as described in Section 8.3.1 could help to increase the TRL of previous demonstrators for switch diagnostics in the progress of WP11. Later in wave 2/3, it is planned to widen the data analysis to further inter-component effects related to CC diagnostics (as laid out in the diagnostic model from Figure 8-2) and to formally address the important question of causality more explicitly, which is mostly ignored by standard AI methods today. Of course, this research is likely to benefit from the current results and the growing experience with the data from the holistic perspective in the progress of FP3–IAM4RAIL.

9. MULTI-SENSOR TRACK MONITORING

Multi-sensor condition monitoring provides a robust and comprehensive approach to maintaining track health, improving operational efficiency, and reducing costs.

The Leonardo vehicle, as a multi-sensor platform is able to acquire data from various onboard sensors at the same time. This provides the unique opportunity to fuse sensor information for a holistic overview of the track condition.

9.1. Introduction and methodology

The aim of this application is to provide a better understanding on the condition of the track by fusing information from various synchronized onboard-sensor data.

The integration of data from multiple sensors helps in diagnosing the root cause of issues more effectively. Multi-sensor data can reveal correlations and patterns that are not apparent with single-sensor data, leading to better decision-making. A good example is an anomaly on the rail head detected by an image classifier. This could be a rail surface defect such as corrugation or just dirt on the track that visually appears quite similar. Integrating information on the wheel-rail interaction measured with ABA sensors will help to classify the detected anomaly.

Specifically, the objective is to enhance the accuracy and reliability of onboard track monitoring by using multiple sensors and suitable processing and analysis algorithms.

The “Leonardo” measurement vehicle conducts precise measurements using various sensor technologies. An overview of this technologies can be found in section 7.1 of deliverable D10.1.

9.1.1. State of the art

Modern track recording and automated inspection machines from different manufacturers deliver track status and condition monitoring from different data sources and in recent years numerous research and development activities have been carried for automated condition monitoring for individual sensors systems such as those used by the Leonardo platform (GPR, lidar, camera, ABA, etc.). However, there is a lack of approaches that fuses different complementary information from the wide range of parameters that the combination of several sensors can provide for a holistic overview of the condition of the track in a programmatic way.

In the previous Shift2Rail project INS2SMART-2, a data-driven approach for detecting rail surface defects and estimating their severity using camera data and axle-box acceleration was developed [9]. However, the different data sets were analysed individually.

To combine camera and ABA data from the Leonardo platform, the rail line needs to be extracted from the images. A promising state of the art tool for that is semantic segmentation [10].

Data-driven anomaly detection for railway tracks is best performed using supervised machine learning methods. However, these algorithms rely on a large amount labelled data, which is rarely available. In this case, unsupervised learning methods can be used to detect anomalies. A state-of-the-art approach for unsupervised anomaly detection and diagnoses is the combination of autoencoders and clustering algorithms [11].

9.1.2. Challenges

Implementing multi-sensor condition monitoring, while beneficial, poses several challenges that

must be addressed for effective operation. Data integration and management are complex, requiring synchronization and accurate correlation of diverse data formats. Designing such systems demands a deep understanding of the equipment and sensor placement, adding to the complexity. The sheer volume of data can lead to overload, necessitating advanced data management tools. Specialized technical expertise is required for implementation and interpretation. Ensuring interoperability between different sensors and existing systems can be difficult, necessitating standardization. Sensor data are inherently noisy, environmental factors can impact sensor performance and data quality, requiring careful consideration of data processing algorithms. Sophisticated data analysis algorithms and expertise are needed to accurately interpret the data and to balance sensitivity to minimize false positives and negatives. Data-driven approaches rely on huge amount of labelled data, which are in most cases not available. In contrast, physics-based algorithms do not need labelled data, but a deep understanding of the physical processes and systems involved, yet this information is often lacking.

9.1.3. Our approach

An ensemble learning approach was conceptualised that combine classifiers using different sensor data from the Leonardo. The novelty is to combine information fusion (combining multiple classifiers for different sensor data) with sensor fusion (combining sensor data for multimodal classification) to create a super-learner that can detect and classify defects more accurately than conventional methods according to the ensemble learning theory. In addition, the scarcity of labelled data can be addressed with this approach. The following figure shows the ensemble classifier approach based on ABA and camera data.

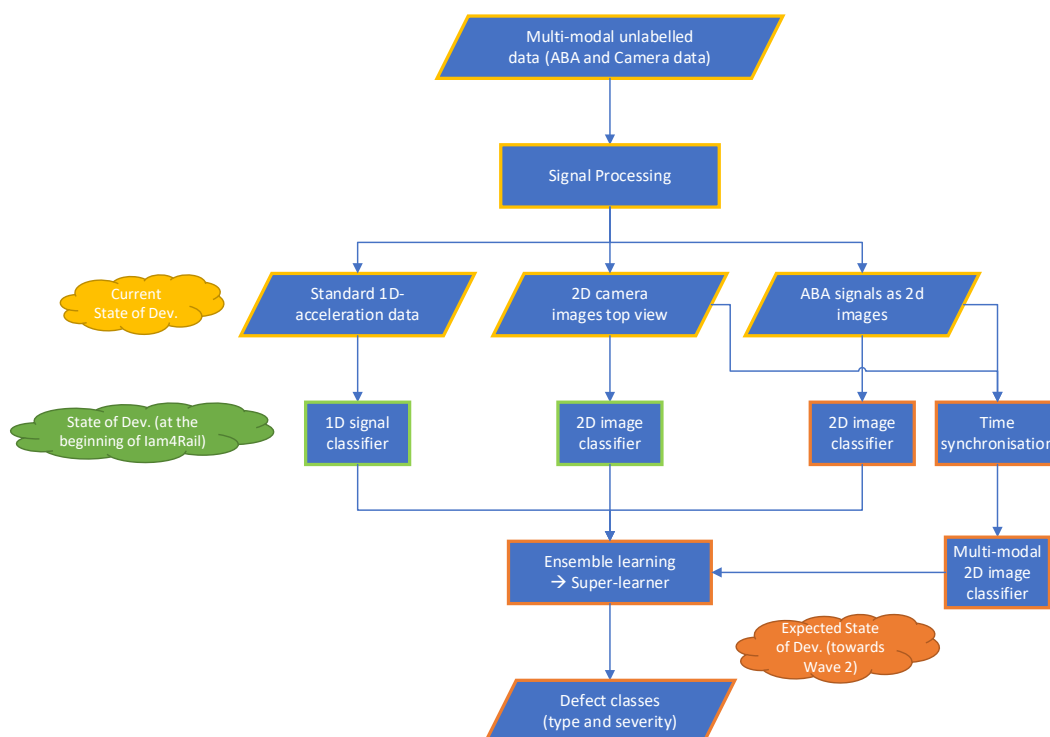


Figure 9-1: Concept for Rail defect classification using ensemble learning

9.2. Work progress

The current state of development with regards to the ensemble learning approach is indicated in Figure 9-1 (boxes with dark yellow frames).

A comprehensive data set was created and shared by the project partners involved. The data set consists of multi-sensor measurements from the Leonardo platform, which were acquired on two consecutive measurement runs in 2024.

An ABA data pre-processing pipeline was developed based on the Leonardo data. It can be used for vehicle-dynamics-based anomaly detection and provides a 2D representation of the ABA data that can be used as input for 2D image classifiers.

To detect surface defects on the rail head and to combine the video data and ABA data from the Leonardo platform, it is necessary to extract the rail line from the video data. In this context a semantic segmentation approach was tested. Transfer learning was employed to use the semantic segmentation model initial trained on driver's perspective data (source domain) with rail top view data (target domain).

For a holistic monitoring approach of infrastructure objects such as switches, which combines onboard and wayside data, it is first necessary to detect this object in the onboard data. Therefore, an object classification algorithm for switches was tested on the Leonardo data.

9.3. Achieved results

The following sections describe the results that have been achieved within WP10, which provide the basis for the ongoing work in WP11.

9.3.1. Comprehensive Data Collection:

A comprehensive data set was created and shared by the project partners involved. The data set consists of multi-sensor measurements from the Leonardo platform, which were acquired on two consecutive measurement runs in 2024.

9.3.2. ABA data processing and analysis:

The data pre-processing pipeline for ABA data was tested on the Leonardo data. The processing sequence aims at removing unwanted signal components and noise and to extract features based on the spectral characteristics of the rail surface. It is based on spectral analysis, time-frequency representations and unsupervised feature extraction. The sequence is detailed in Figure 9-3.

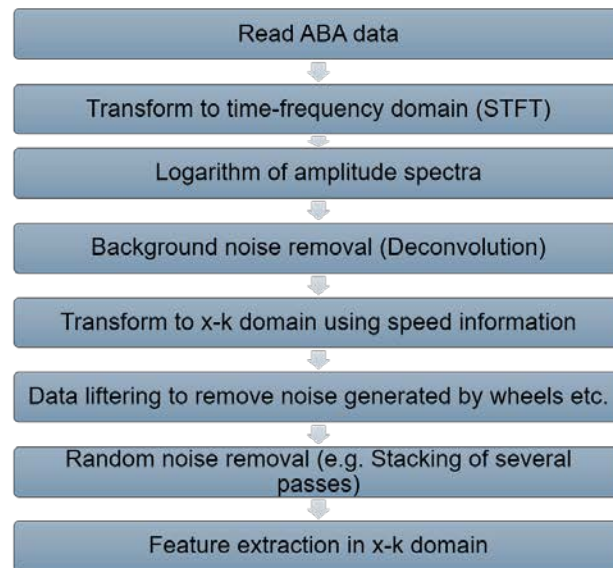


Figure 9-2: ABA processing sequence to reconstruct spectral features of the rail

The following two figures show time-frequency representations of the ABA data before and after noise removal. The harmonics related to the vehicle response are clearly removed with only little leakage of signal energy.

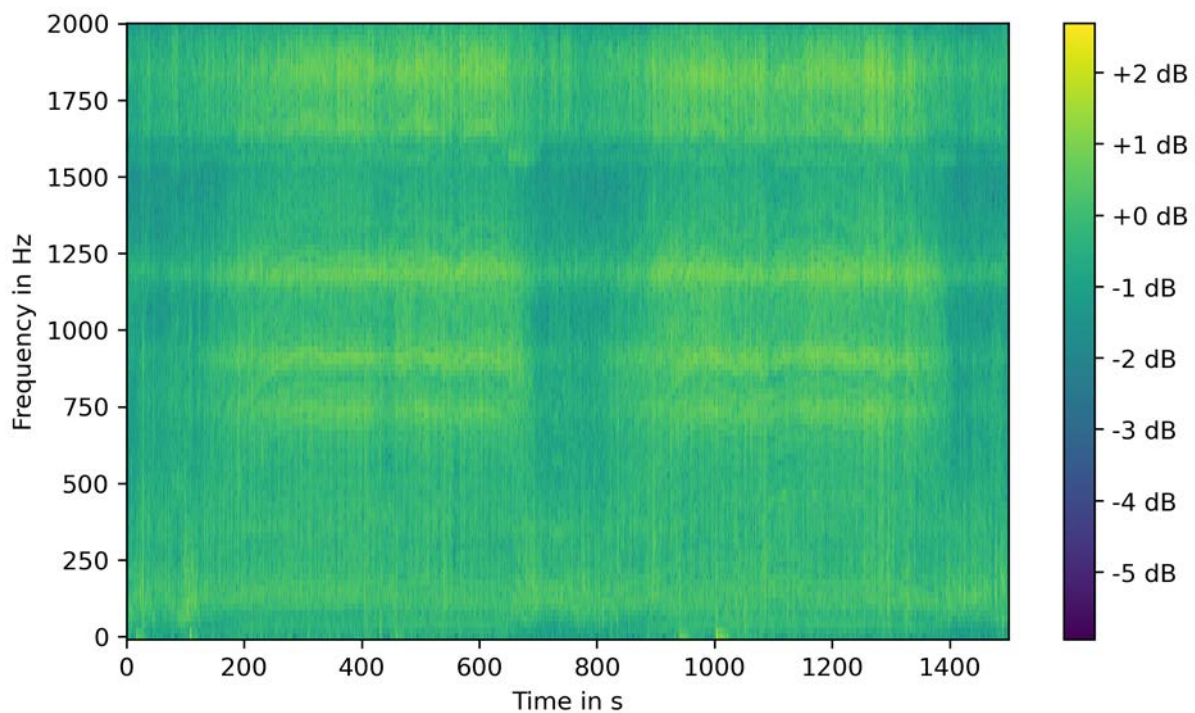


Figure 9-3: Time-frequency representation of raw ABA data

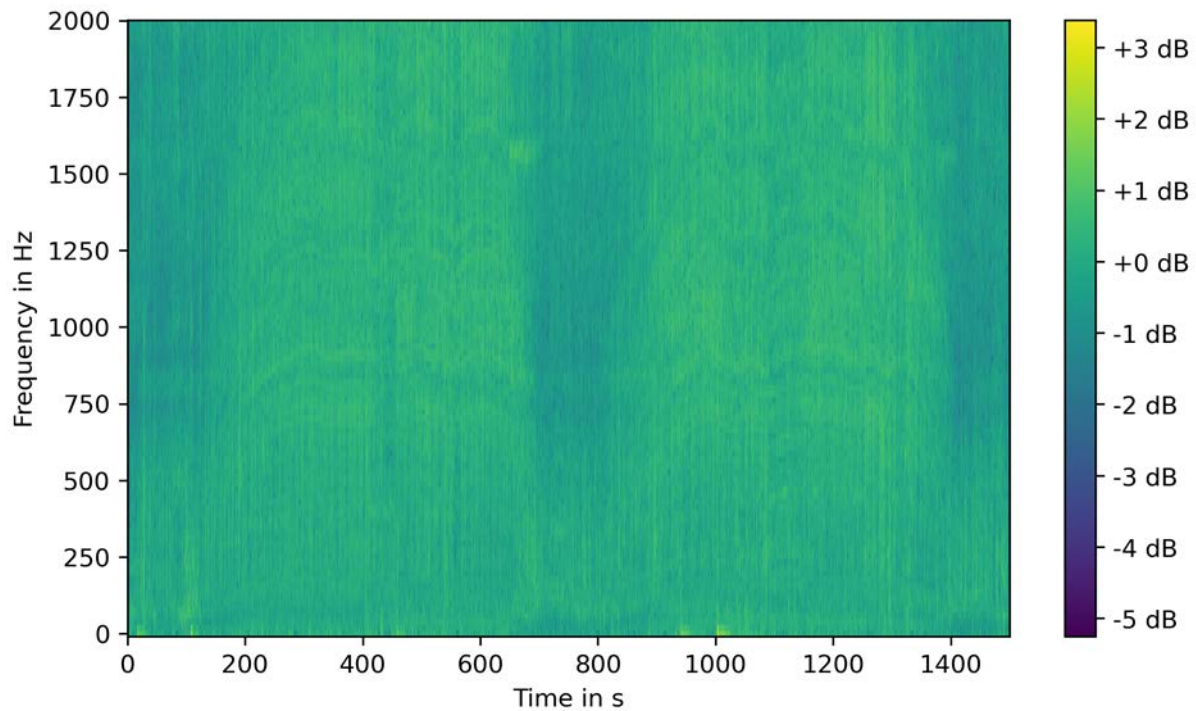


Figure 9-4: Time-frequency representation of ABA data after noise removal

9.3.3. Computer vision:

The results of the semantic segmentation approach in different domains (driver's perspective and top view) are depicted in the following figure. It can be seen that the rail lines can be accurately separated from the background.



Original image

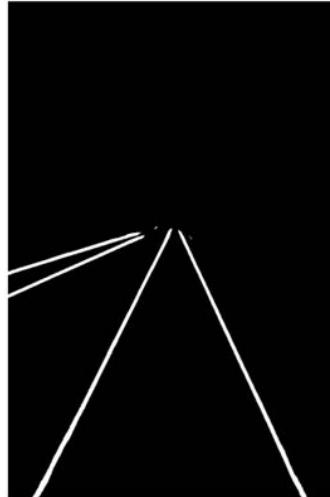


Image segmented into rails and background



Detected rail pixels drawn on original image

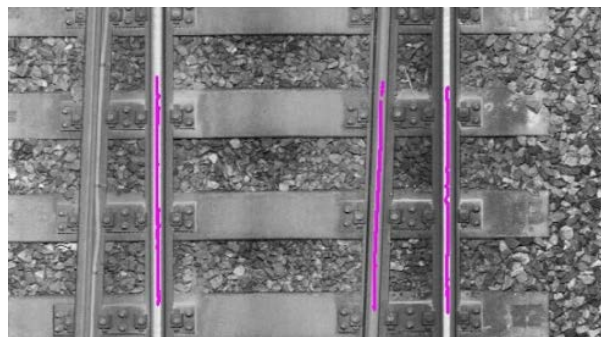


Figure 9-5: Semantic segmentation to extract rail lines in Leonardo camera data (ego perspective)

The results of the object classification algorithm for switches tested on the Leonardo data are exemplified in the figure below. Using only a small amount of manually labelled data, the algorithm could detect and classify switches with high accuracy.

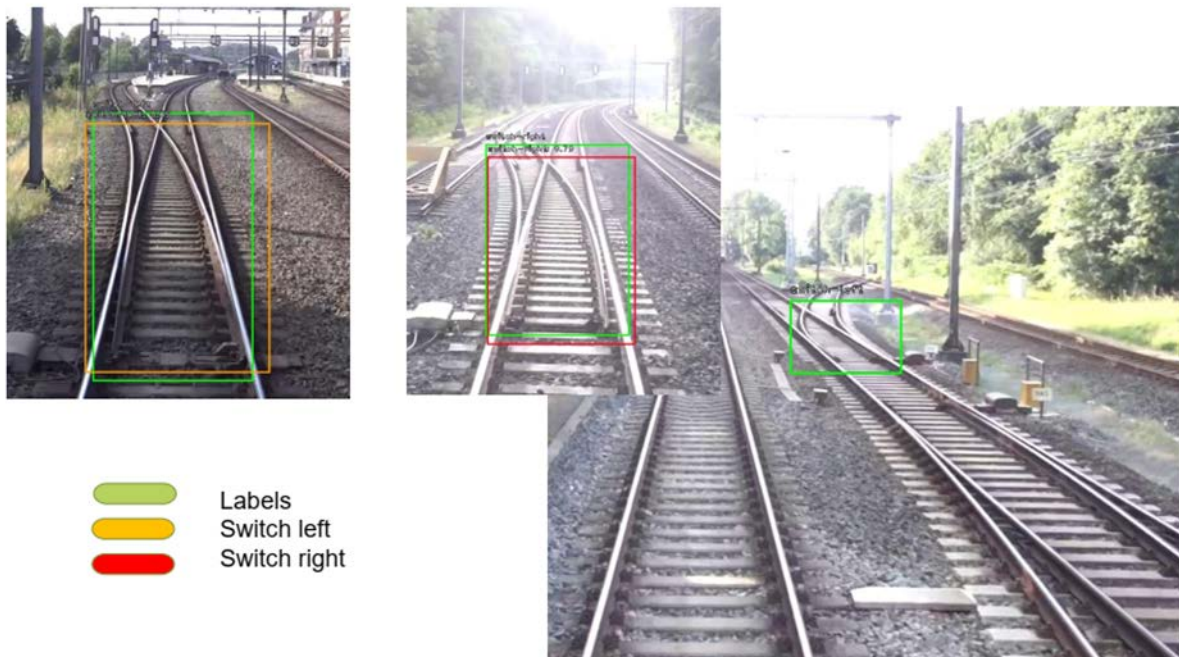


Figure 9-6: Switch detection and classification using camera data from the Leonardo platform

9.4. Status handed over from WP10 to WP11

The work progress from WP 10 to WP 11 and the direct relation of the specific sub-task can be seen in Figure 9-1 indicated by the links between the yellow-framed boxes (developments in WP 10) and orange-framed boxes (developments aimed for in WP 11). The following sections highlight the key aspects.

9.4.1. Data Integration and Management:

Within WP 11 the Leonardo will acquire rich multi-sensor data sets on the Dutch pilot site on a regular basis. This means that large amounts of data need to be managed. Therefore, the handling and integrating of big data from multiple sensors is a key task in WP11 to ensure that data from various sensors are synchronized and accurately correlated. The data processing and synchronisation sequences developed in WP 10 are integral parts for the integration of onboard data into a holistic data analysis.

9.4.2. Enhanced Accuracy and Reliability:

By using multiple sensors, the system can cross-validate data, leading to more accurate and reliable condition assessments. Redundancy in data collection reduces the chances of errors caused by sensor malfunctions or inaccuracies.

In WP 11 the ensemble learners conceptualised in WP 10 will be implemented. That will lead to better performance than a single classifier (state of the art). In addition, the scarcity of labelled data can be addressed with this approach.

9.5. Preliminary results that can be used

Besides providing the basis for the ongoing work in WP11, some results can readily be used. The relevant applications are described in the following sections.

9.5.1. ABA processing and analysis

The developed ABA processing sequence can be used to find anomalies on the track with respect to the vehicle dynamics. These points of interest can be further analysed by means of other Leonardo sensor data (e.g. Camera, GPR) and inspection data and can be labelled based on this analysis. Labelled data is essential for defect classification. However, it is a time-consuming task and labelling guided by ABA analysis reduces this effort dramatically.

9.5.2. Switch detection and classification

The camera-based switch detection and classification can be used to extract relevant sensor data for switch monitoring that can be used and integrated in the holistic switch monitoring approach.

10. DETECTION OF LOOSE FASTENERS WITH ABA

This section describes the monitoring of the track and its components using Axle Box Accelerations. In particular, CEIT is interested in the detection and diagnosis of anomalies in rail fasteners, such as fasteners looseness detection, and their implication in track geometry and the apparition of other defects (e.g. squats, rail corrugation).

This is one of the ABA developments undertaken within WP10, though it has a distinct objective. At a later stage, the various developments will be coordinated, including those from other ABA projects within cluster D.

10.1. Introduction and methodology

The aim of monitoring, condition-based, and predictive maintenance techniques is to optimise the life cycle of the entire railway infrastructure, i.e., to improve reliability by having continuous information on assets, resulting in a reduction of both maintenance costs and operational disruptions. However, the inspection of certain track elements, such rail fastenings, is currently carried out manually, by walking along the track, and the assessment of their condition is based on a visual evaluation. This makes the process non-efficient and potentially unreliable, as it is subjected to the operator's subjectivity [12].

For that reason, as described in D10.1 (7.1.3), the continuous acquisition of track condition data using ABA (Axle Box Accelerations) and its subsequent analysis is a key factor in maintenance decision making by asset and maintenance managers. As mentioned there, the accuracy of the predictions can be significantly improved by fusing information derived from different sensors (for example, a combination of ABA based rail surface and fastener defect classification and video image classification) and machine learning models.

Based on the State-of-the-Art, where more than 90 references were studied [13], it is possible to develop signal processing techniques for the detection of specific track problems based on the analysis of accelerations (ABA).

Track-side systems are commonly used to monitor critical areas of the infrastructure, such as switches and crossings [13], whilst on-board [14] systems can be used to monitor any section of the track. This second line will be the focus of the research, mainly based on the acquisition of acceleration data by using accelerometers installed in the axle boxes of rail vehicles in service [15] [16].

Finally, according to the type of track defects or problems to be detected and the main types of sensors used, different signal filtering techniques and algorithms may be implemented to analyse the recorded signals. In this work, we will use ABA data to assess the condition of rail fasteners [17], investigating the related impact on the condition of track geometry (e.g. misalignments) and the apparition of other defects in the track (e.g. corrugation).

While studies on detecting torque looseness in fasteners have been conducted, there remains a gap in the research. This gap justifies the need for further development in this area. Various studies have utilized modal analysis of the track as a starting point in research, along with vibration-based looseness detection studies. A modal test was recently conducted. The key factor is not only detecting missing fasteners but also identifying partial looseness before it impacts the track geometry or rail head integrity.

Although ABA is primarily sensitive to geometric errors in the track or rail surface, making it seem less efficient from a physical standpoint, it has also been shown to react to varying torque conditions in rail fasteners. A lower-than-required torque reduces the stiffness between rails and sleepers, which in turn alters the modal shape. This change affects the deformation of the rails under a moving load and consequently impacts the acceleration signals in the axle boxes.

While eddy current sensors, such as the lindometer, may seem like a simpler method for detecting anomalies in rail fasteners, the lindometer primarily detects the absence of a clip rather than issues within the fastener itself. The advantage of ABA-based systems lies not only in their lower cost but also in their ability to be installed on passenger trains, providing daily data collection, providing more frequent access to the railway track, as opposed to other systems installed in inspection vehicles, such as the aforementioned lindometer or vision systems.

The case study is focused on the detection of loosen fasteners, so that new methodologies and algorithms will be developed for obtaining relevant information and features from the data captured by the sensors.

The methodology that will be used to implement this application can be summarized as follows (Figure 10-1):

- Develop a simulation framework able to generate synthetic data by means of virtual sensors, representing realistic ABA. To do that it is necessary:
 - Get the most accurate input data related to the vehicle where the accelerometers are installed, as well as the kind of track where the real datasets are going to be generated. With the support of DLR, a multi-body model of the Leonardo inspection vehicle will be created (see detailed information on digital twins in Chapter 13 of this document).
 - Develop a mathematical model that represents the defects and anomalies to be detected and diagnosed, in order to integrate those effects in the simulation framework [18]. Previously, the response of the track to excitation with different patterns of failed rail fasteners must be studied [19].
 - Generate scenarios that represent realistic operation in different conditions (speed, track irregularities, etc.), including faulty conditions owed to the anomalies to be detected and diagnosed and obtain datasets (i.e. synthetic data) for the generated scenarios. SIMPACK, the multibody simulation software, and ABAQUS, the finite elements model software, will both be used.

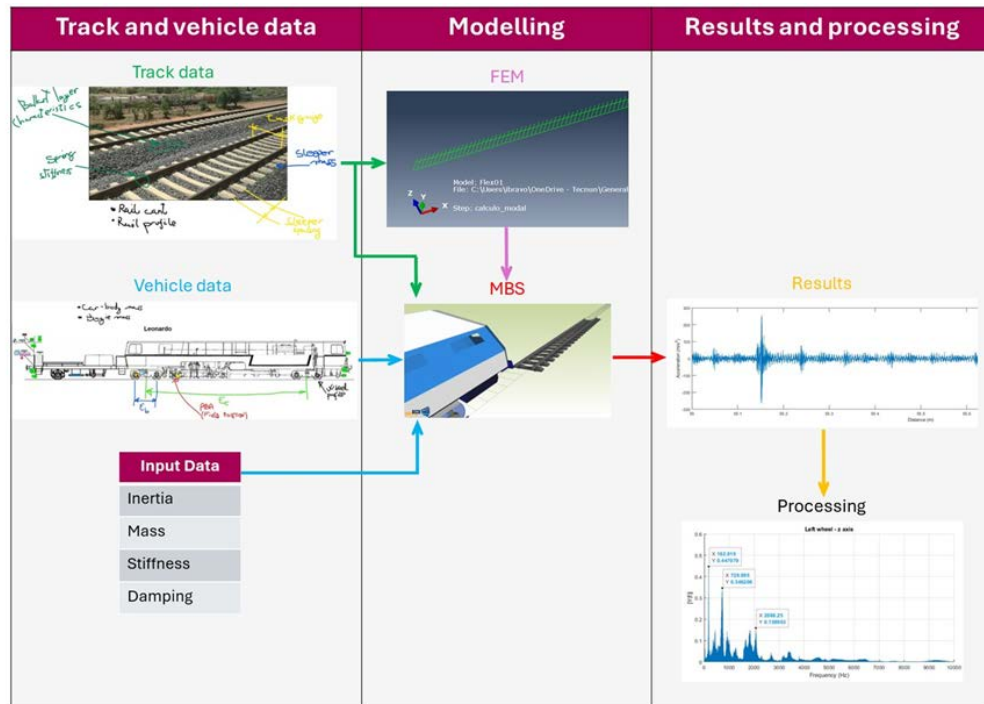


Figure 10-1: Methodology for detection of missing fasteners with ABA

- Develop signal processing techniques and algorithms that are suited to axle box accelerometers that will allow obtaining a set of features that will potentially contribute to the detection and diagnosis of failures and anomalies.
- Explore Machine Learning or Deep Learning algorithms for the detection and diagnosis of anomalies in the track, potentially exploring the condition of rail fasteners and its impact in the track geometry (e.g. misalignment) and the rail (e.g. apparition of corrugation), for example by utilizing image analyses methods on spectrograms of ABA data.
- Validation of results. First using the synthetic dataset to assess the detection and diagnosis of well identified failures and anomalies. Then, the technology will be demonstrated using real data provided by Leonardo platform, up to TRL5/6.
- Fusion of different approaches (e.g. ABA and vision, ABA and GPR and track geometry) for the classification and detection of defects.

10.2. Work progress

Initial steps in the time and frequency domains are shown with the analysis of the ABA and Trackscan data provided by Strukton Rail in June 2024.

The condition of the track and its components is being monitored using accelerometers placed on the axle box of the Leonardo inspection vehicle', owned and operated by Strukton Rail, who has installed two PCB 604B31 type triaxial accelerometers.

The first steps were dedicated to the application of filtering algorithms to acceleration signals for track geometry control (e.g. longitudinal level). Signal filtering techniques are applied to ABA signals in areas where faulty fasteners have been detected by the vision systems of the LEONARDO

inspection vehicle.

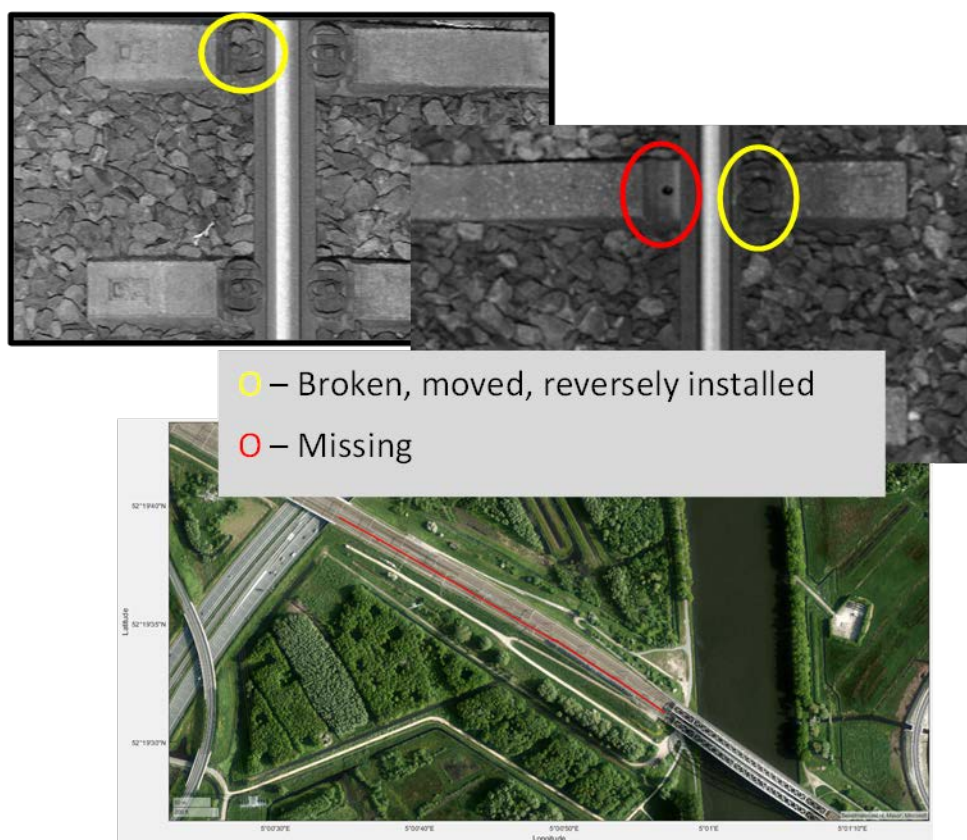


Figure 10-2: Example of loosen and missing fasteners detected by the Leonardo vehicle

All the information related to the track is collected. CEIT has asked for information of the inspection vehicle to advance with DLR in the creation of the MBS model of LEONARDO.

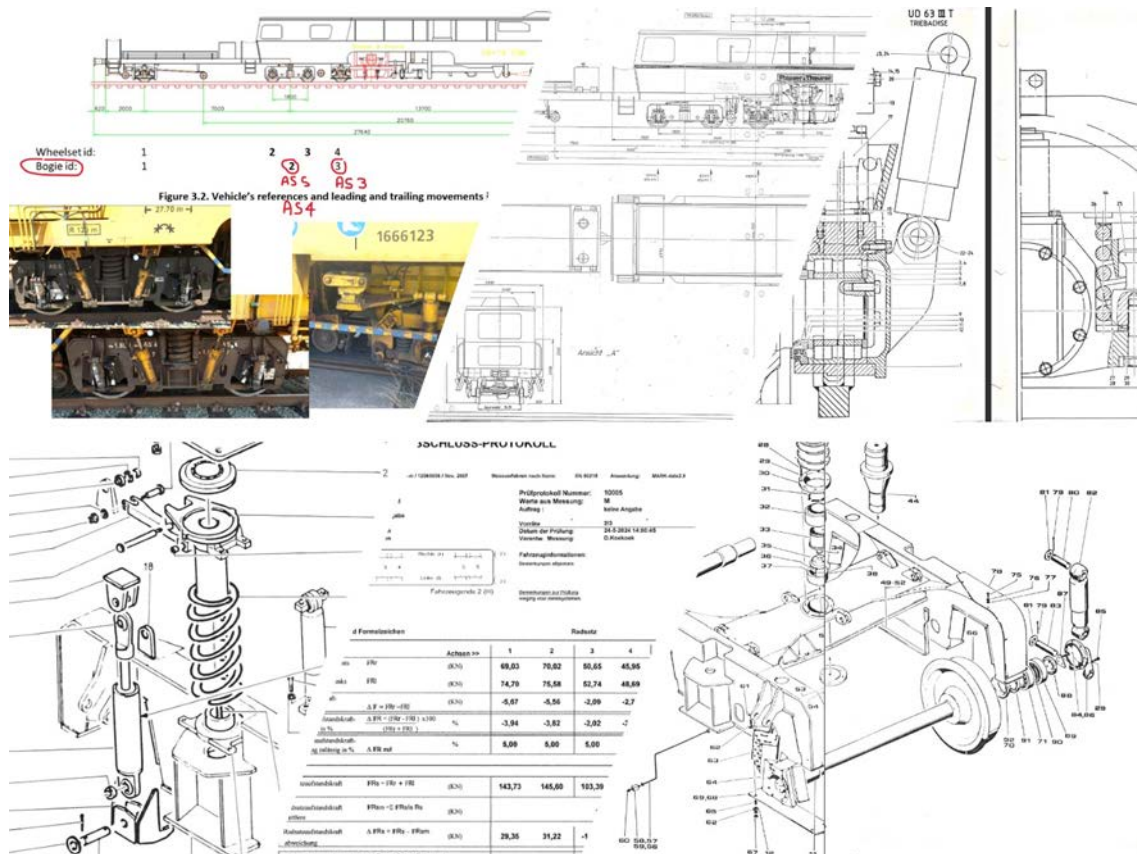


Figure 10-3: Leonardo inspection vehicle characteristics

To study the rail response under an impact excitation, a modal test of the track with a dynamometric hammer will be carried out in Q4 2024, with the support of ADIF accessing a relevant environment in Spain.

The field test will follow the methodology described in previous papers related to the study and detection of failed fasteners [12], [20] and damaged railways [19], based on the idea that a damage in the fastener will change system's stiffness, inertia, or energy dissipation properties, and therefore, the measured dynamic response of the system. The experiment will be conducted by applying different torque conditions in one of the fasteners.

A script to easily identify the track segment to be studied has been developed, considering that the track information of the dataset comes from different sources:

- Trackscan geometry data.
- Trackscan geographical location data.
- Dewesoft raw acceleration data.
- Tagged images with track defects.

10.3. Achieved results

Different approaches to represent the defects and anomalies are studied, waiting for access to the track to perform an experimental modal test.

Meanwhile, inspections and monitoring data are being studied:

- Inspection data of the track, including track geometry, visual inspection reports, detection of defects, etc. (see Figure 10-4).

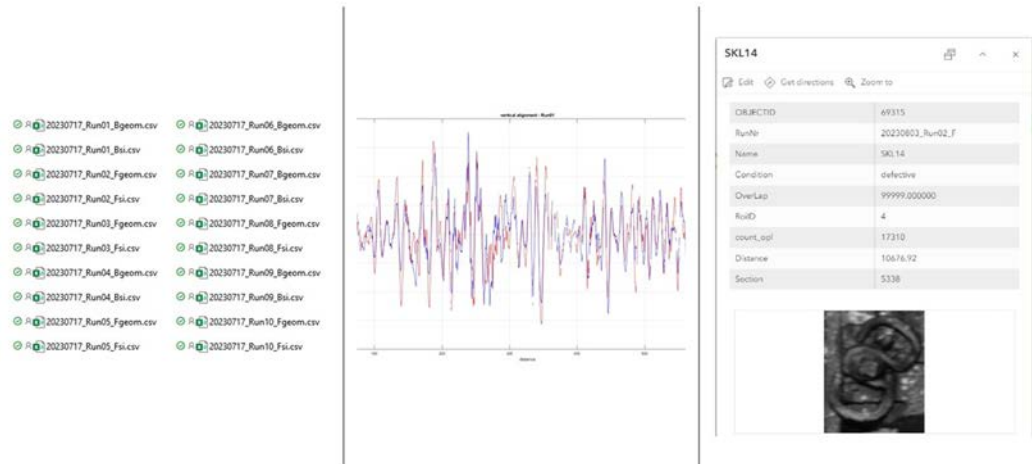


Figure 10-4: Inspection data of the track

- ABA data captured with Leonardo platform in different measurement campaigns along the project (see Figure 10-5).

`hdf5File = 'Leonardo_ABA_2023_07_17_084141.h5'; info = h5info(hdf5File);`

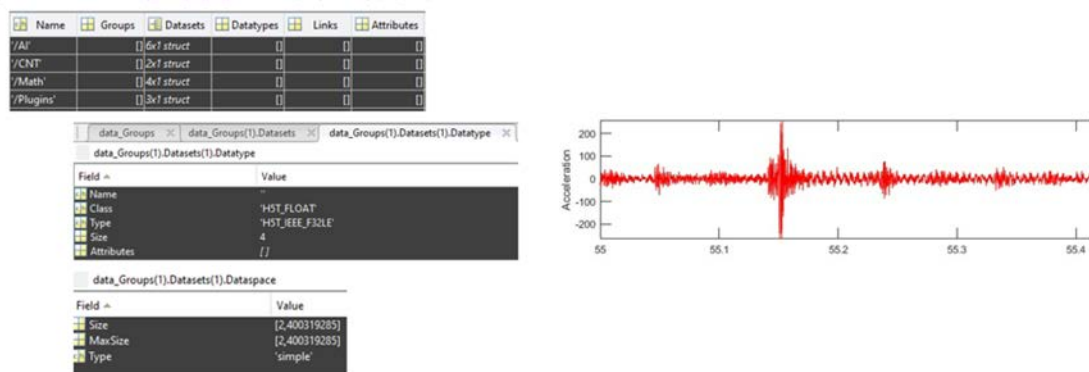


Figure 10-5: Leonardo ABA data

By applying the developed script, we can easily match the Trackscan data (track geometry information and defective fasteners location) with the ABA data (see Figure 10-6).

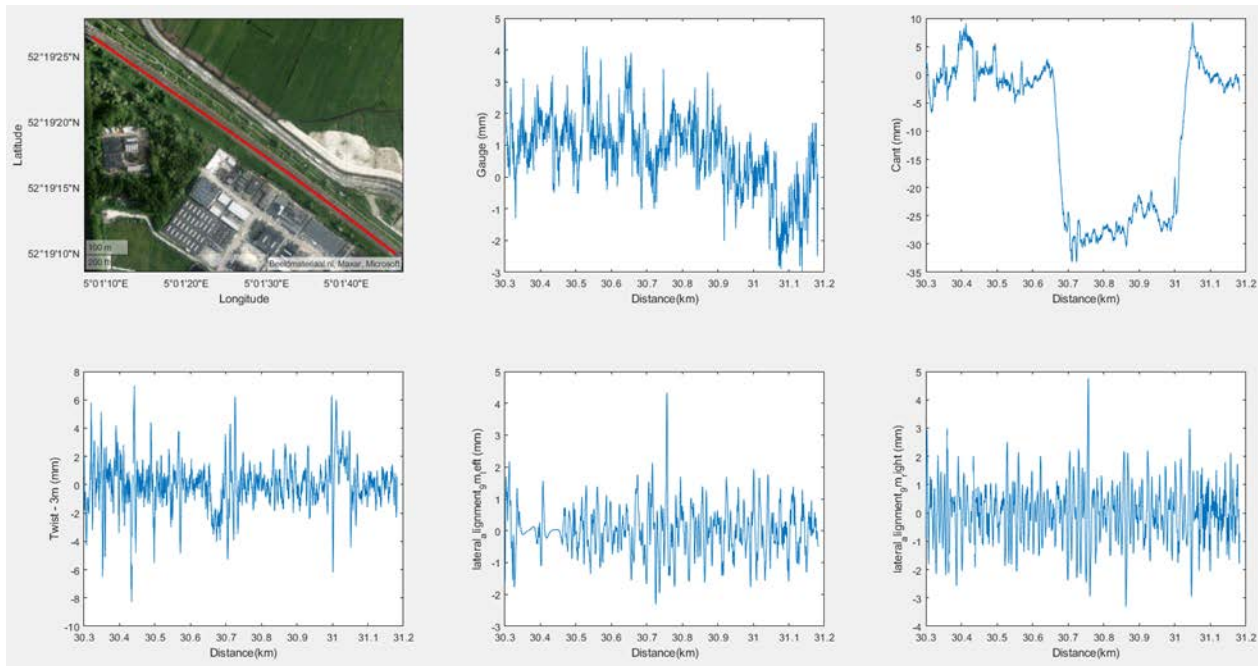


Figure 10-6: Example of track geometry information and location

To develop anomaly detection/diagnosis algorithms, synthetic data representing the conditions of the NED scenario will be used. Synthetic datasets will be generated and used as inputs.

10.4. Status handed over from WP10 to WP11

After analysing the results of the SoA, where more than 90 references were studied, initial steps in the time and frequency domains are shown with the analysis of the ABA and Tracksan data provided by STRUKTON RAIL in June 2024.

Preliminary works are dedicated to creating an optimal simulation framework to increase the required data for the development of algorithms. Working only with the MBS models is not enough to achieve our goals, because track dynamics plays an important role. Thus, the combination of the FEM and MBS is presented.

As mentioned in the methodology, the response of the track to excitation with different patterns of failed rail fasteners must be studied. To do so, an experimental modal test is going to be carried out on an Adif facility in Spain, following the protocol described in the Work Progress section.

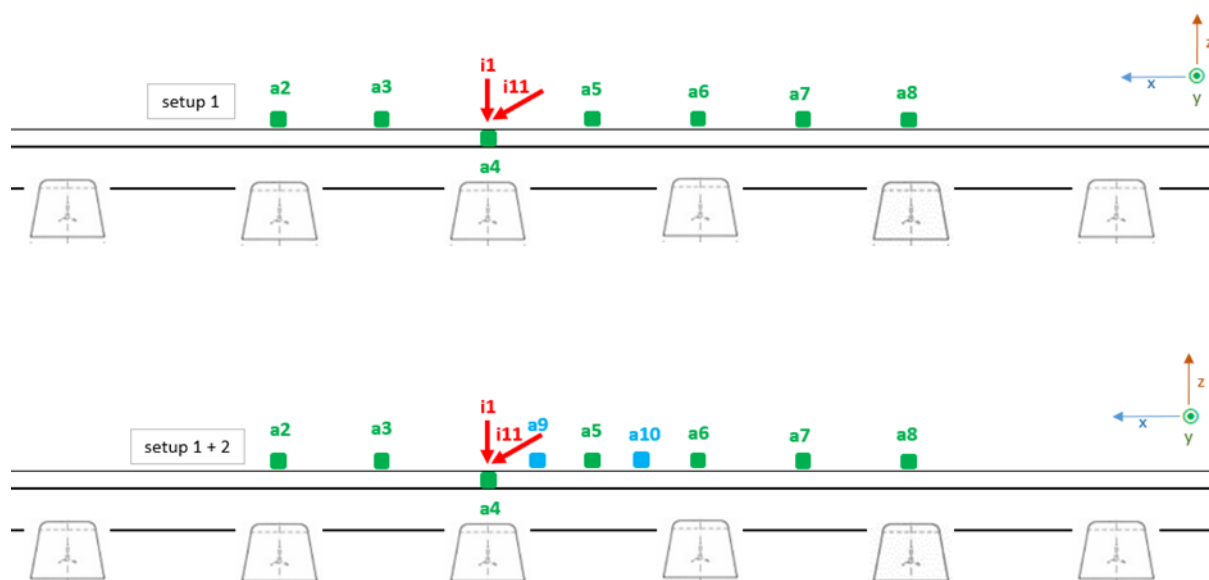


Figure 10-7: Experimental modal test proposed layout

This experiment will allow us to extract some features when applying different torque conditions.

10.5. Preliminary results that can be used

It has been found that a correct choice of accelerometers to be installed in the axle box of the vehicle is crucial. If the acceleration acquisition range is not wide enough, signal clipping is recorded, which makes correct signal processing difficult, but future improvements in the acquisition of ABA signals will allow a correct detection of track defects.

11. SOUND RECORDINGS FROM ABA FOR DIAGNOSTICS

11.1. Scope / Objective /Aim

Introduction:

The video footage and measurement data from the measurement train, De Leonardo, are increasingly being made available for practical use. New developments in the Geoconda Rail View software are making the video footage and measurement data more suitable for digital inspections and analyses.

In March 2024, training began for approximately 35 rail specialists on the effective use of Geoconda Rail View v2.04. These training sessions not only received very positive feedback but also generated 20 new ideas for further development. Of these ideas, 18 have already been implemented in the latest Geoconda Rail View v2.1, which was launched on July 17, 2024. In August 2024, training will commence for 100 maintenance technicians on conducting inspections using Geoconda Rail View.

One of the ideas that has yet to be realized is the addition of sound to the images.

Problem:

End-users with field experience often rely on sound during outdoor track inspections to detect potential irregularities. By incorporating sound alongside other data, this approach could replicate that experience, prompting a closer examination of the available data. It could be particularly valuable during the research phase, allowing end-users with field expertise to collaborate with data scientists in exploring the potential of the data, and may also prove useful for future applications.

In the Netherlands, many maintenance activities and inspections can only be conducted at night during short track closures, limiting daytime inspections to viewing the track from the inspection path. This restricts technicians' ability to perform thorough inspections, though they can often detect issues by the sound of a passing train. However, they are not permitted to access the track during the day to investigate further.

In Geoconda Rail View, technicians can visually detect issues but lack the necessary sound to fully assess the situation. Although all cameras on the Leonardo are equipped with microphones, the captured sound is not always suitable due to wind noise and ambient sounds. Experienced technicians believe that by combining sound with visual observation, they can more accurately identify specific track irregularities, allowing them to make informed decisions about the necessary repair actions.

11.1.1.State of the art

Is this the type of language used by technicians, and has it ever been researched?

The article [11] discusses traditional inspections based on images and sound. In Pakistan, railway engineers manually inspect the tracks by analysing acoustic sounds and images. This method is cumbersome, labour-intensive, and prone to errors. The study suggests improving the performance of traditional acoustics-based systems with deep learning models to reduce the number of errors (train accidents). Thus, sound in images could contribute to the quality of digital inspections if supported by deep learning models.

The article [12] describes a study where sound is used to identify track components and their defects. This article examines the feasibility of Acoustic Track Monitoring (ATM), which involves extracting realistic information about the track condition from the interface noise of the rail from in-use high-speed trains. ATM could enable continuous track analysis, detecting abrupt or prolonged changes in the track, thus meeting the expected need for fast and automated track maintenance. Based on recordings in the suburban railway of Athens, a database of noise in the area of rail joints between tracks and wheels was created. The aim was to assign acoustic signatures to as many track components and defects as allowed by the dataset's content and quality.

The research was conducted on 33 km of local track in Athens using prepared microphones. The results indicate that sound alone is insufficient for accurate inspections. Support from images and data recognition models is necessary.

11.1.2.Challenges / Techniques to be applied

First approach is to use the ABA signal emulating sound. The main challenge is converting ABA vibrations into sound. If the sound from the video cameras is not directly suitable, can the ABA vibrations be converted into a usable sound, or can a combination of sound and vibration data be made? Initial tests converting data from ABA vibration sensors into sound show that each sensor produces a usable sound. This sound is free from wind noise and ambient sounds. However, the vibrations of the motor and the drive transmitted through the chassis to the sensors on the axle can be heard.

The ABA sensors measure vibrations (500-5,000Hz) on the two axle boxes of a bogie axle in the X, Y, and Z directions. Together, these vibrations contain frequencies that fall within the hearing range (20-20,000Hz). However, the sound has a different timbre than the sound heard when standing next to the track. One possible reason is the frequency range of the vibration sensors used. There is a lack of approximately 480Hz in the low-frequency range and 15,000Hz in the high-frequency range.

The second approach involves using shielded microphones, which more accurately reflects real-world conditions. The ABA signal for sound is more closely related to the forces between the wheel and rail and thus does not provide the full spectrum of sound that microphones can capture. This option is being considered. In an article published in the journal of Elsevier [13], microphones in the passenger compartment of a high-speed train were used as an alternative to ABA vibration sensors. This research showed that similar anomalies could be recognized from the sound signal as from the ABA signal.

11.2. Developments / next steps

The request for the reliable sound of rail wheel contact in Geoconda Rail View has been present for some time. During the development of Geoconda Rail View, tests were conducted with the microphone sound of different cameras, but the results were not satisfactory.

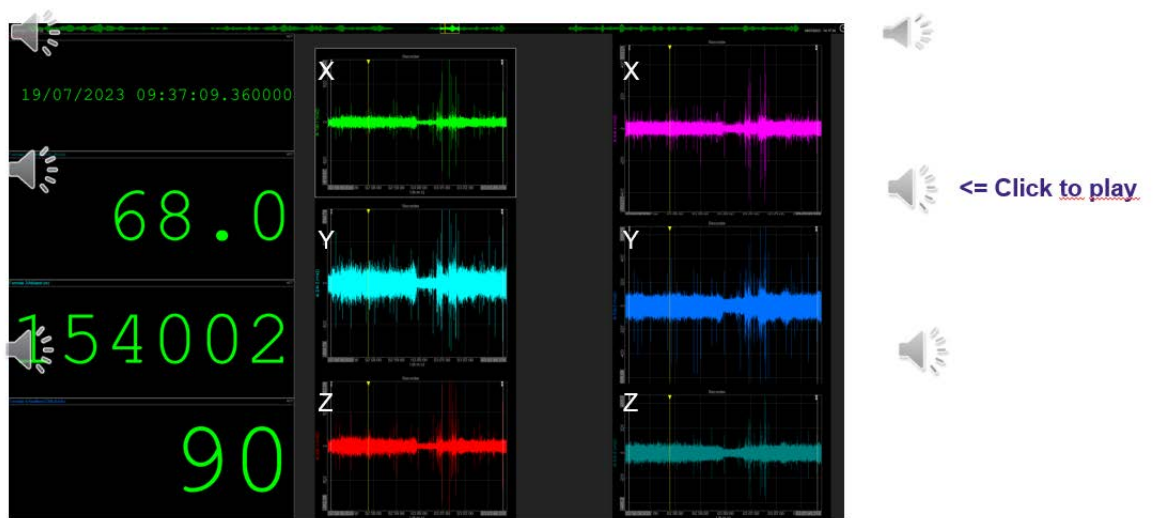
Following the installation of ABA sensors on the Leonardo last July, a test was conducted to see if the vibration signal could be converted to a standard MP3 sound file. The Python library Pydub was used for the conversion, offering a simple interface for editing audio files.

The initial question was whether the result sounded adequate for use. The first results did not sufficiently match the actual sound that maintenance technicians hear outside. Due to the lack of

good objective sound references for comparison, the actual differences between the converted ABA sounds and the real sound remain unknown.

Additionally, it is not yet clear how to handle the three separate sounds arising from the x, y, z vibration signals. It is uncertain whether these should be simply merged, used partly, or used in proportion. The next step involves conducting a thorough analysis of the actual sound, which should provide more insight for specifying the next development step.

ABA-sounds passing a track switch



#Leonardo

3

Figure 11-1: shows an example of ABA sound signals playable with an mp3 player

11.3. Further developments

For further developments, the following steps are a guidance to create a sound suitable for use in Geoconda Rail View:

Step 1:

Identify the sounds that technicians hear along the railway. An audio library with labelled sounds and images will be set up for this purpose. Both a video camera and a sound camera will be used. This is expected to provide insight into the characteristics of the sounds that technicians need for inspections.

Step 2:

Convert the ABA data into sound, attempting to isolate the influence of the measurement train using a 'Leonardo measurement train' filter that will be developed.

Step 3:

Use the sound from videos that have been used in Geoconda Rail View since 2022 to train an audio model. Over 400 hours of suitable videos are available for this purpose.

Step 4:

Blend and verify the filtered sounds from the ABA sensors and video cameras using the audio library. Based on the results, the filters will be adjusted to achieve the best possible outcome.

Step 5:

Conduct a user study to determine whether the sound in Geoconda Rail View leads to better acceptance of digital inspections.

12. DIGITAL TWIN: DYNAMIC VEHICLE RESPONSE ANALYSIS EXCITATION RAIL SURFACE UNEVENNESS

Digital twins, as a digital representation of a physical asset or process, have become popular tools for a variety of asset management and monitoring applications. Specifically, a digital twin is a digital, indistinguishable copy of a real asset that allows to provide information on the past and current condition of its counterpart. It simplifies the analysis and the condition monitoring, leading to effective forecasting of the status of the physical asset and its predictive maintenance. A more detailed description can be found in Section 6.2.1 of the deliverable D10.1.

12.1. Introduction and methodology

As a part of the critical infrastructures, rail transportation systems require comprehensive and frequent monitoring. For this reason, digital twins are particularly interesting for the railway sector and offer the potential to improve the reliability and safety of rail transport. Specifically, the vehicle-track-interaction monitoring is important for maintaining ride quality, reducing wheel-rail impacts, rolling noise and improving safety and reliability. The usage of digital twin, therefore, could lead to strong improvements in the context of track monitoring, reducing inspection and maintenance costs, by means of a continuous monitoring and comparison of acquired data against the ideal response of the system.

The digital twin used here is based on a digital model that links the dynamic vehicle responses with the rail profile. The digital twin approach makes it possible to check the quality of the model in real time. To do this, the model is regularly validated using the measured sensor data. If the digital twin no longer adequately reflects reality due to any changes in the system, e.g. after the revision of the wheelset or changes to the sensor system, the underlying model can be updated with the help of conventional inspection data.

The model should be able to be used for modelling in both directions (forward and inverse). This means that, on the one hand, it should be possible to determine the expected vehicle reactions or ABA data from a longitudinal rail profile (forward modelling) and, on the other hand and of much greater interest for rail condition monitoring, to determine the longitudinal rail profile from the measured ABA data (inverse modelling). The rail's condition can thus be permanently determined during operations and transmitted to a central asset management system. The condition information obtained from the measurement data can in turn be used to continuously update more comprehensive digital twins for asset management, e.g. a digital twin of the track infrastructure. The integration of a digital twin to analyse dynamic vehicle reactions in an asset management system is shown in the figure below.

Concept:

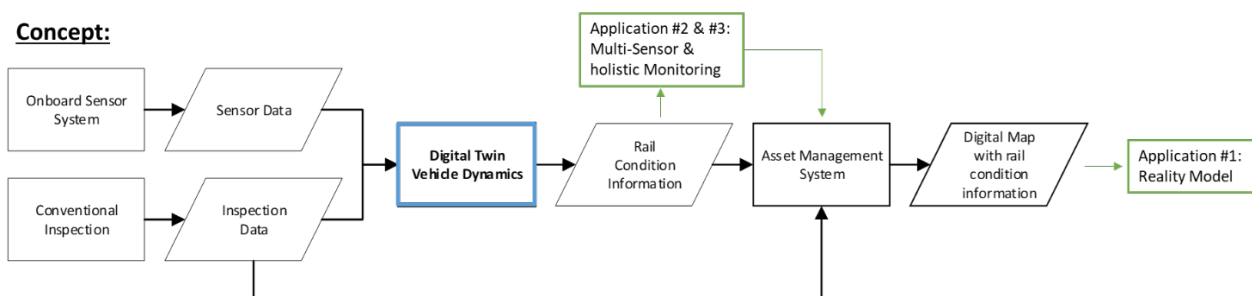


Figure 12-1: A digital twin of the dynamic vehicle responses embedded in a modern asset monitoring and management concept

12.1.1.State of the art

Digital models and twins for dynamic vehicle responses can be divided into deterministic (“physics-oriented”) and “data-driven” approaches, as well as hybrid approaches that combine both.

As digital twins are digital, indistinguishable copies of a real assets, it is difficult to describe them with one unique definition, due to the broad topic they cover. Indeed, they can represent the real counterparts in different ways, from states or ongoing processes (e.g. digital twins for Industry 4.0) to dynamics.

A physics-oriented digital twin of Leonardo has to describe the multi-body interactions, the wheel-track contact and spring-damper effects.

Particularly, tools such as Simpack, Dymola and OpenModelica allow to describe the vehicle by means of multibody simulation via differential equations that govern its dynamics. Once the modelling is completed, Software-in-the-loop (SIL) simulations can be assessed to predict system outputs and fulfil monitoring tasks.

The current state of the art regarding physics-oriented digital twin is its manipulation via the Functional Mock-up Interface, the leading standard to exchange dynamic simulation models. Particularly, once a system has been correctly modelled with one of the previously mentioned tools, it has to be exported and compiled as Functional Moke-up Unit (FMU), a binary file that allows to interact with more complex simulations in Software-in-the-loop (SIL) implementations, by exchanging input and generating outputs, accordingly. Additionally, the simulation of distributed systems and the agents involved can be done by following the System Structure and Parametrization (SSP) standard.

With this technology, interoperability between different companies and software is guaranteed, leading to faster development and collaborations for digital twins.

The model parameters of a data-driven digital twin are learnt using real-world examples of input and output data. Prior knowledge of the physical models and their parameters is therefore not necessary. These models are also referred to as surrogate models. They especially offer decisive speed advantages in inverse modelling that make near-real-time applications possible. Data-driven methods range from simple linear models to artificial neural networks (ANN) with a large number of intermediate layers known as deep learning models.

There are also hybrid approaches, which combine data-driven models with physical models.

On the one hand, the advantage of these models lies in the fact that simple physical models, which only require a limited number of model parameters, can be used and the resulting reduced accuracy is compensated for by the data-driven model component. On the other hand, data-driven models are supported by the integration of physical information. This is particularly relevant if an insufficient amount of training data leads to an increased generalisation error in the data-driven models. Furthermore, the data-driven models are made plausible by physical constraints and thus gain in interpretability and reliability.

12.1.2. Challenges

The main challenge when developing a physics-oriented digital twin is the level of accuracy that is wanted or can be achieved. For high-complexity systems, describing every component and its interactions can easily lead the system design to explode. For this reason, simplifications and

approximations have to be introduced, by reducing the system complexity by means of lumped components, linearized equations and equivalent but simpler effects.

Once the design choices are completed, the second noticeable challenge is the parameters tuning.

Purely physics-based modelling is only suitable to a limited extent for the approach presented here, as the model parameters that describe the mechanical mass-spring system are not known. In addition, the wide frequency range of the ABA signals is associated with a high computational effort for the simulation.

A disadvantage of data-driven especially of deep neural networks is their so-called black box character. This means that the reasoning of the model and its parameters cannot be easily interpreted. There is a general conflict between the objectives of the interpretability and accuracy of a model.

12.2. Achieved results

A primarily data-driven surrogate model that incorporates physical knowledge for dynamic vehicle responses has been developed. The vertical vehicle dynamics can be described using a Linear Time Invariant (LTI) system. However, the wheel-rail interaction is known to be non-linear. In contact mechanics, wheel-rail contact is often described as a Hertzian contact problem [10]. It is therefore important to use a model that represents this non-linearity. Furthermore, inversion is only causal and stable for LTI systems with minimum phase, which cannot be guaranteed for dynamic wheel-rail interactions.

These requirements have motivated the use of ANN. These are powerful tools for modelling non-linear time-invariant systems. They therefore form the basis of the model used in this study. The layers of the ANN use non-linear activation functions to account for the non-linearity. The model consists of two sub-models, each consisting of an ANN. The first ANN represents a surrogate model for the inverse problem, namely the prediction of the longitudinal rail profile from the ABA data. The second ANN is a surrogate model for the forward problem, which reconstructs the ABA data from the rail profile. Both models are trained together but can be used separately during inference. A physical constraint is imposed on the model in order to obtain physically meaningful results. The simplest physical model that does not depend on the parameters of mechanical systems involves the assumption that the movement (displacement) of the axis corresponds to the rail profile or, in mathematical terms, that the accelerations measured at the axle bearings (ABA data) are equal to the second derivative of the rail profile with respect to time. This simple model is independent from any vehicle parameters and can hence be readily applied to any railway vehicle.

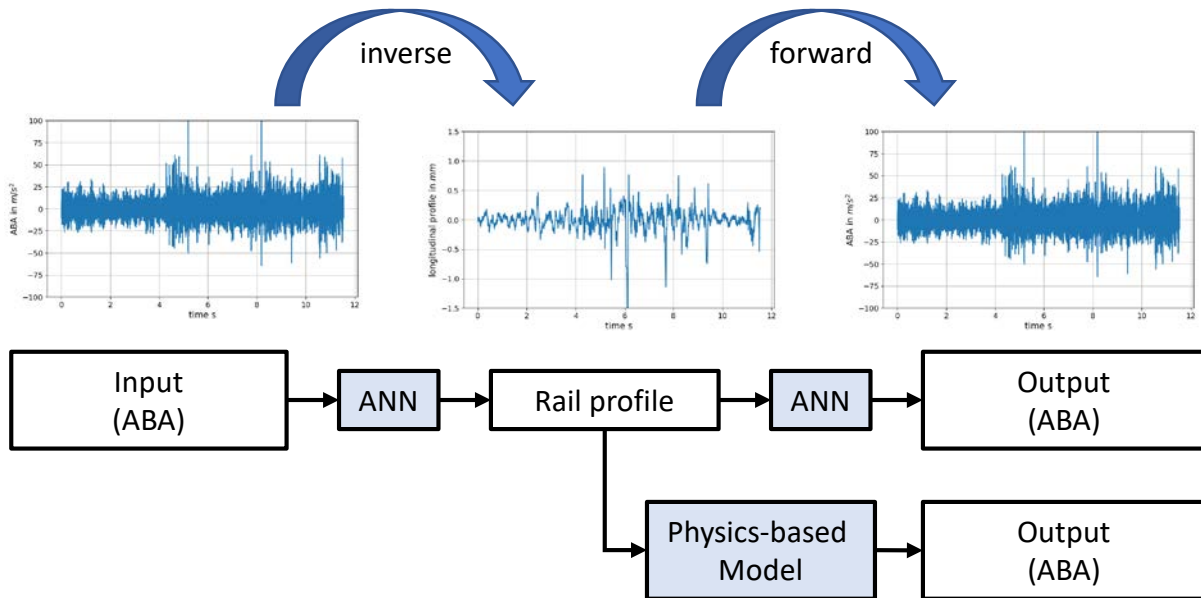


Figure 12-2: Coupling data-driven models with a physical model for modelling and analysing dynamic vehicle responses. The first ANN extracts the longitudinal rail profile from the measured ABA data. This in turn is converted back into ABA signals by the second ANN and the physical model [22]

Initial training and testing of the model were performed using data from the Braunschweig harbour railway. ABA data was recorded with sensors on a shunting locomotive for this purpose. The longitudinal profile of the rails was measured with a hand-pushed device and used as reference data for training and testing the models. Figure 12-3 shows the results of training the models. The top figure clearly shows that the longitudinal profile obtained from the ABA data (the blue line) is a very accurate representation of the reference profile (the orange line) measured with the hand-held measuring device. The line diagram in the middle compares the output of the second ANN, i.e. the reconstructed ABA signal, with the measured (input) ABA data. Sufficiently accurate results were also achieved here. The output of the physical model is shown by the line diagrams at the bottom.

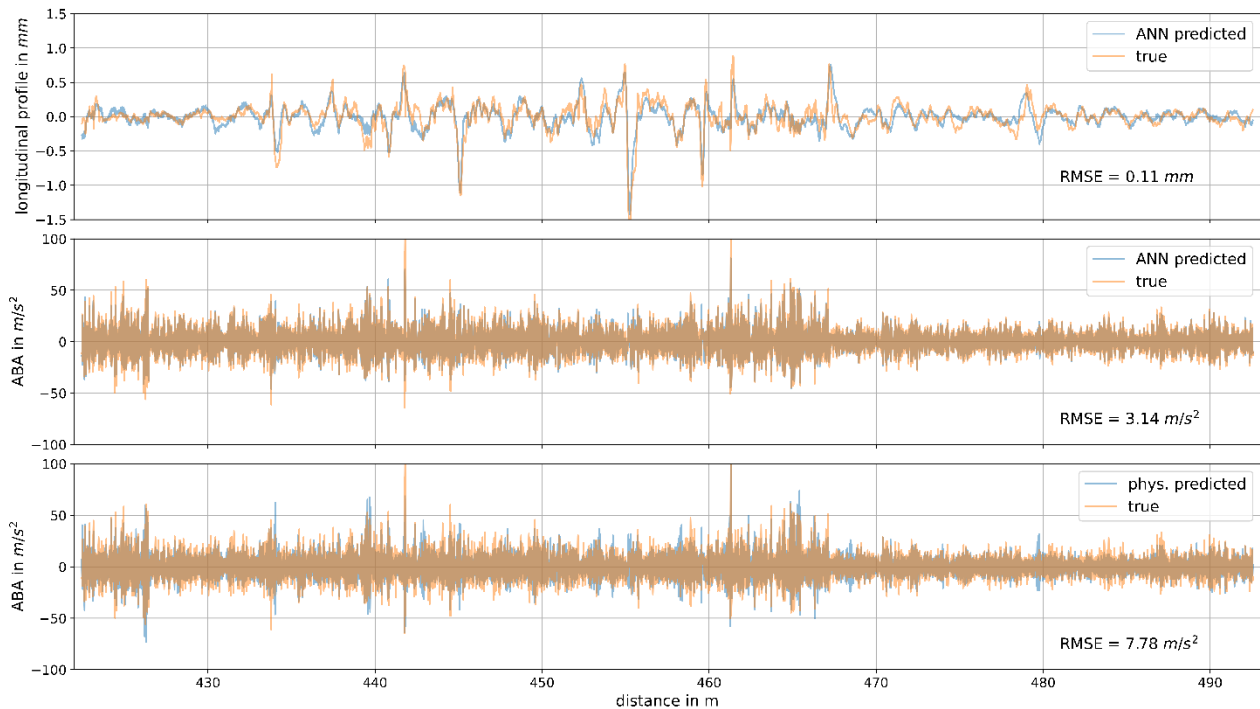


Figure 12-3: Training results. Top: a comparison of the longitudinal profile of the rail predicted by the ANN (the blue line) and the reference profile (the orange line). Centre: a comparison of the ABA signal predicted by the ANN (the blue line) and measured (the orange line). Bottom: a comparison of the ABA signal predicted by the physical model (the blue line) and measured (the orange line)

12.3. Status handed over from WP10 to WP11

To further improve the hybrid model presented above, the goal within WP 11 is, to replace the very simple physical model by an accurate digital twin of the Leonardo.

In the case of approximated modelling, in which there is no exact correspondence between a real component and its digital or mathematical counterpart, or in the case of some information such as inertia, masses, spring-damper coefficient are not available, it is necessary to find the missing or unknown values via optimization processes. Particularly, for this task high quality input and output data is necessary to correctly obtain the right parameters.

This process is known as data-dependent, meaning that the quality of used data directly affects the quality of the estimated parameters. Figure 12-4 illustrates the optimization logic: real input data is fed into the model, along with an initial guess of the parameters. The obtained estimation of the output is compared with the real output data and evaluated based on a loss function. Eventually, a minimization step is performed, and the new parameters are estimated and fed backward for the next optimization step.

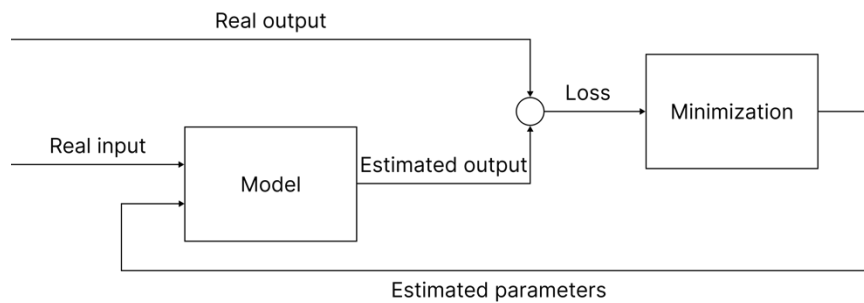


Figure 12-4: Optimization workflow for model parameters tuning

12.4. Preliminary results that can be used

It has been shown that so-called hybrid models, which combine data-driven and physical approaches, can be used to obtain relevant condition information from the sensor data. The longitudinal rail profile could be reconstructed with sufficient accuracy for asset management from dynamic vehicle responses (acceleration measured at the axle box). The presented digital twin approach allows the quality of the model to be monitored during operations. The model can be readily applied to other railway vehicles and tested on the Dutch pilot site and retrained based on the Leonardo data.

13. TRACK GEOMETRY MEASUREMENT FROM PASSENGER VEHICLE

13.1. Introduction and methodology

This work provides a detailed continuation of the efforts described in D10.1, specifically in section 9.8 (Track Geometry Measurement from Passenger Vehicle), incorporating input from CETEST, an affiliated entity of CAF.

While section 9.8 in D10.1 depicted the strategy for implementing a track geometry measurement system in a passenger vehicle, this section in D10.2 outlines a first approach for validating a simplified and vehicle-integrated measurement system in terms of measured results performance and European standard compliance.

13.1.1. Scope / Objective / Aim

The aim of this approach is to characterize a track geometry measurement system able to be integrated into a passenger vehicle, that is, the intention is to quantify the ability of a compact system to obtain track geometry parameters.

The scope of the characterization involves main geometry parameters, or their estimation based on a simple and compact instrumentation that in the future could be fitted in a very non-invasive manner onto a passenger vehicle.

In order to characterize those parameters, EN13838-2 has been followed.

This characterization has been performed using Leonardo platform (see section 5.1.2) and results from a specific test campaign in Spain.

Tests in Spain were conducted in a regional vehicle from CAF manufacturer FEVE series 2700.



Figure 13-1. CAF FEVE series 2700 vehicle.

The outputs and results in this section will allow to transform the compact measurement set-up into an onboard integrated system aligned with EN13848-2 specifications with a higher level of maturity, which will be developed in WP11.

13.1.2. Description of the technology

Considering the objectives of this task, the first step intended is to evaluate and validate the measurement performance of a compact track geometry measurement system integrated in a passenger vehicle. The goal, therefore, will be to evaluate the performance of different sensing solutions.

At the current state of the development, commercially available devices have been installed in the CAF FEVE 2700 vehicle. Therefore, the technology of the sensors used are well known accelerometers and displacement measurement devices.



Figure 13-2. Installation of sensor in axle box for track geometry assessment.

Future development in WP11 will consist of the adaptation or creation of these sensors and the suitable hardware (for onboard calculation of parameters) for a non-invasive installation onto any passenger vehicle. The sensors used in the evolution of this HW will be based on the systems used during the test campaign (ABA) and needed design and conditioning will take place in order to develop a robust measurement system for the railway environment.

The experimental campaign for the obtention of characterization data has been performed as described in section 5.1.2 (see also D10.1 section 9.8.2. Refer to D10.1 section 9.8.2 for further information).

13.2. Work progress

13.2.1.State of the art

Although plenty of literature exists about track geometry measurement based on similar approaches, publicly available information does not include information about the quality of the obtained results in a representative manner.

While the utility of the calculated data has been demonstrated for infrastructure managers or vehicle operators, there is no available information concerning the quality (accuracy or reproducibility) of the calculated track geometry parameters. Quality of the measurement and results is assessed by comparing or evaluating the results with specifications in the available standards or related literature. EN13848-2 provides specifications for track geometry measurements and addresses the quality requirements of these data and results.

That is, sources limit their conclusions to specific short-length routes, specific defect identifications, qualitative identifications, or other limited applications. Additionally, track geometry parameters themselves are limited to Vertical Level mostly and Lateral Alignment.

13.2.2.Challenges

Current developments intend to expand the state of the art by:

1. Extending measured track geometry parameters of systems to be mounted onto passenger trains, including: Vertical Level, Lateral Alignment, Twist, Cross Level.

These parameters are key track geometry evaluation parameters addressed by EN13848-2 and are used to monitor and assess the overall status of the track in terms of geometry. The challenge is to measure and assess such parameters with a compact sensing solution which will eventually lead to a native onboard system for passenger vehicles.

2. Quantifying the quality of obtained results according to standard procedure, as described by EN13848-2.

The goal is to assess the overall performance of the measurement system against requirements in EN13848-2 and set the potential of compact sensing solutions meeting European standards.

13.2.3. Developments

The experimental test campaign has been conducted over a 26km long route. Note that this site does not correspond to neither the Netherlands site nor the Spanish site as per chapter 4.

These tests were held in the regional line **C-2 Cercanías Cantabria** (Santander – Cabezón de la Sal), in the north of Spain, between the train stations Santander and Torrelavega – Centro. Tests took place between May 29th 2023 and June 6th 2023.

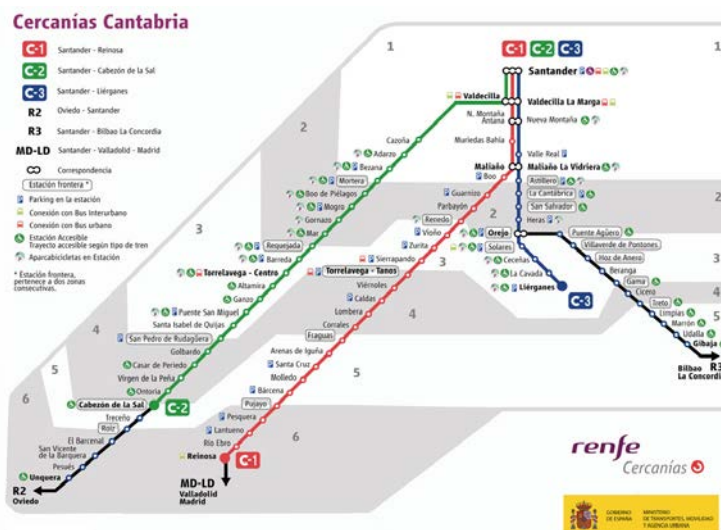


Figure 13-3. Regional Cantabria Line used for vehicle integrated compact track geometry system characterization.

The passenger vehicle was in normal operation condition. Tests were performed without passengers, in ready to run load condition. The sensors have been placed in different positions in the vehicle (axle, bogie, vehicle frame) to evaluate the impact of the different measurements in the results sought. However, final results shown in this chapter are aimed at evaluating the overall performance of the sensing positioned in the axle box, which is also referred to as ABA in this document (section 5.1.2). Although a single bogie is enough for the analysis, three bogies were instrumented for research and comparison purposes.

Therefore, the instrumentation was analogue to that described for Leonardo's bogies in 5.1.2.

Test runs were performed in both running directions, that is, with one end of the vehicle in leading position, and also with that same end in trailing position. It must be noted that these two riding directions could not be performed onto the very same track due to circulation limitations. Normal

circulation directions had to be followed and thus, leading test runs were performed over track I and trailing runs over track II of the same line.

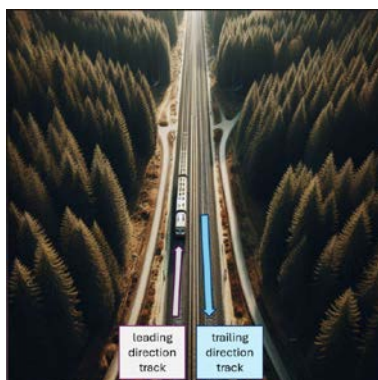


Figure 13-4. Scheme of vehicle orientation, leading track, trailing track.

Test runs were repeated at different speeds: commercial speed and around 40 km/h, always avoiding stopping at stations if possible.

Afterwards, track geometry parameters were calculated. Reference track geometry values have been provided by Infrastructure Manager.

In the following section, the main results obtained from this task are detailed.

13.3. Achieved results

EN13848-2 establishes a procedure for assessing both repeatability and reproducibility of each parameter. For both characteristics, two criteria are defined:

1. Distribution of the absolute value of differences, by establishing a limit value for the 95th centile.
2. Frequency response criteria, by determining a valid tolerance band and a coherence limit.

However, current quantification is restricted by now to criterion on the absolute differences distribution.

In addition, and deviating from EN13848-2 due to the fact that IM Cross Level data is provided this way, Cross Level has been calculated for a D1 range wavelength (between 3 and 25 m). Thus, the limits for the 95th centile do not directly apply, although they are included in the results and comparison for informative purposes.

Figure 13-5 to Figure 13-7 show graphical representation of calculated and reference parameters overlapped in KP at different horizontal zoom levels. For all three figures, horizontal axis represents Kilometric Point (KP) [km] and vertical axis are:

- | | |
|---------------------------------|--|
| 1 st graph (top): | Twist in [mm/m] on a 3m long base. |
| 2 nd graph: | Vertical level [mm] in D1 wavelength range. |
| 3 rd graph: | Lateral alignment [mm] in D1 wavelength range. |
| 4 th graph (bottom): | Crosslevel [mm] in D1 wavelength range. |

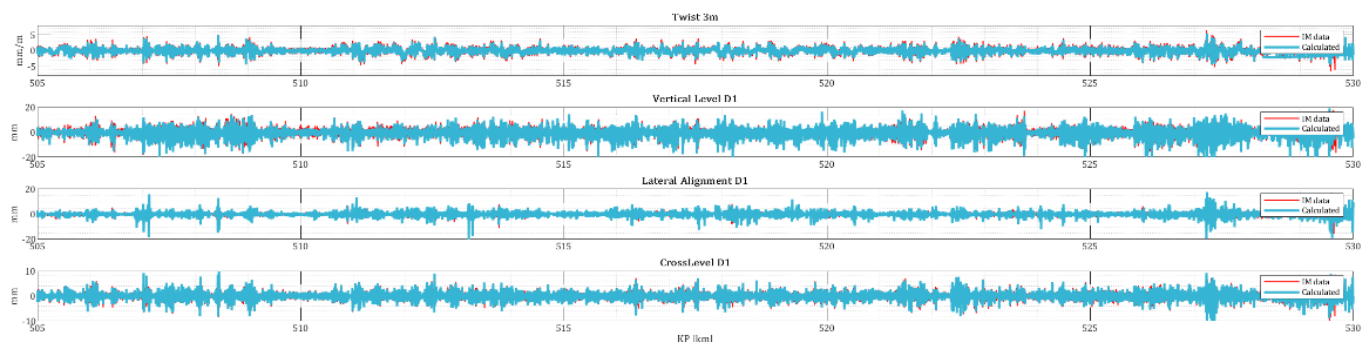


Figure 13-5. Reference and calculated parameters (I).

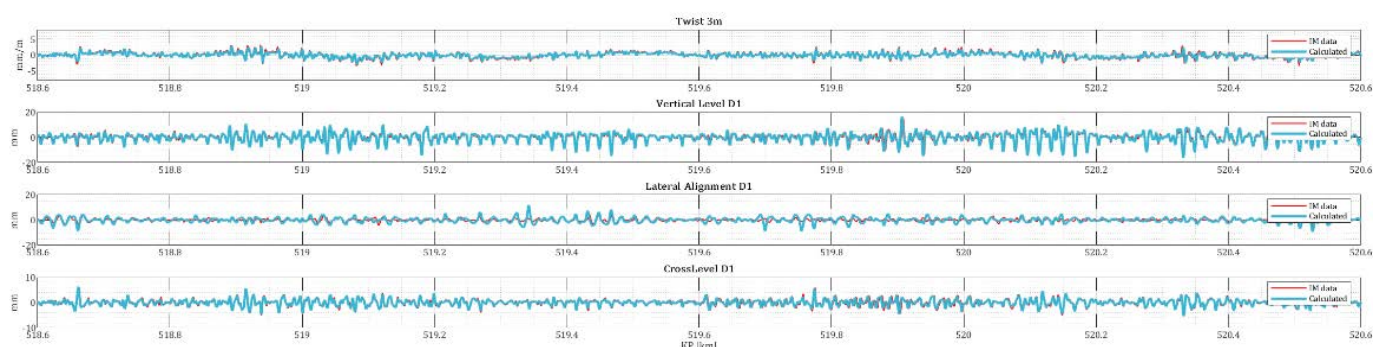


Figure 13-6. Reference and calculated parameters (II).

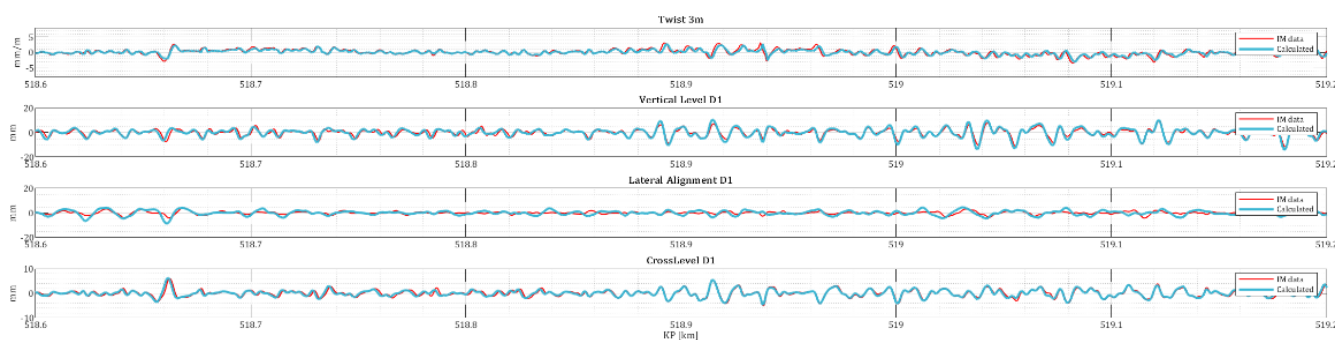


Figure 13-7. Reference and calculated parameters (III).

Table 13-1: 95th centile repeatability and reproducibility assessment of calculated parameters.

	repeatability Criterion P95		reproducibility Criterion P95	
	Calculated P95	EN13848-2 Limit	Calculated P95	EN13848-2 Limit
Twist	0.17	0.23	0.30	0.33
Vertical Level D1	0.49	0.50	0.80	1.76
Lateral Alignment D1	1.25	0.70	0.66	0.80
Cross Level D1	0.27	1.50 ¹	0.47	1.50 ¹

¹ This limit applies to full wavelength range, not to D1 range only. It is shown for informative purposes.

Finally, reproducibility analysis has also been used as a method to estimate the uncertainty of measurement, by comparing reference IM values with calculated ones. Note that this obtained values of measurement uncertainty are only an estimation. For example, the uncertainty of the reference values directly affects the resulting estimation after the comparison. Nevertheless, the obtained estimation is considered a significant quantification of measurement uncertainty of the system. Uncertainty estimations are summarized in Table 13-2, and distributions are showed graphically in Figure 13-8.

Table 13-2: Expanded uncertainty estimation based on test results.

	Expanded Uncertainty
Twist	0.3 mm/m
Vertical Level D1	1.6 mm
Lateral Alignment D1	0.7 mm
Cross Level D1	0.5 mm

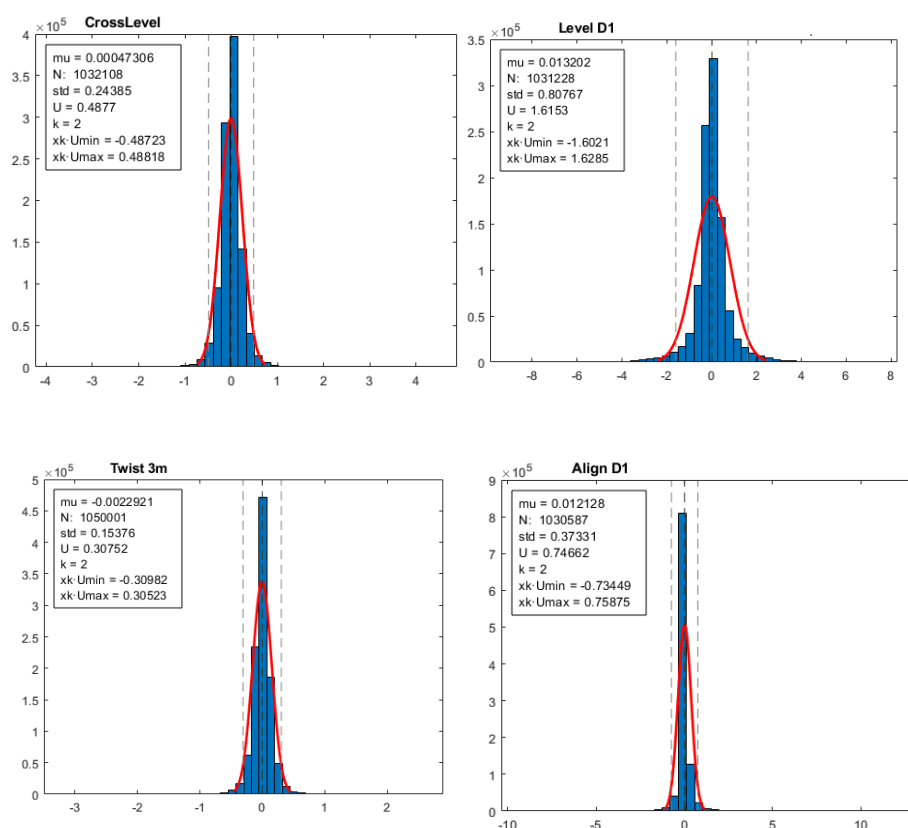


Figure 13-8. Reference-estimation difference distributions.

13.4. Status handed over from WP10 to WP11

The ability of a simple, compact, non-invasive track geometry measurement system has been

quantified based on EN13848-2 standard. Although the fulfilment of EN13848-2 criteria is not established as a requirement for compact measurement devices (because it is intended to provide more frequent information, although not as precise as a track geometry measurement vehicle), the system has proven its ability to provide useful information.

The quality of the information is now quantified by the absolute difference criteria and shall be extended by a frequency content analysis too in further developments.

The following conclusions can be drawn by the obtained results:

- A compact sensing system based on acceleration measurements in axle box can provide assessment of track geometry aligned with EN13848-2 requirements.
- A compact sensing system could potentially reduce the need for complex monitoring systems as dedicated auscultation vehicles for the evaluated parameters.
- Integrating the solution in a passenger vehicle would additionally provide more frequent information and be used to programme full track inspection and maintenance activities.

The results will allow to evolve the sensor solution into a more robust device to be integrated in passenger vehicles. During WP11 activities, research on developing this hardware and software for its installation as an unattended system on a passenger vehicle will be considered. The HW will be intended to ease its installation and maintainability on the vehicle whereas the SW will allow to perform the necessary calculations for online diagnosis of track geometry evolution.

13.5. Preliminary results that can be used

As for today, the outputs of this task allow that these measurements could be used as on-demand track geometry assessment services. The test execution would be fast, and the quality of the results would meet harmonized requirements for the parameters assessed in this chapter.

14. OCCLUSION MONITORING DUE TO VEGETATION

This work has been carried out by CEIT, using public data sources (eg. GERALD and Mapillary image datasets, see [section 15.4](#)) for algorithm training and validation. Moreover, the system is being tested on the data provided by Strukton.

14.1. Introduction and methodology

The unchecked growth of trees and vegetation along roadsides and railways presents a significant challenge to transportation safety and efficiency. One of the most critical issues associated with such overgrowth is the occlusion of traffic signs. Traffic signs serve as vital communication tools for drivers, operators, and pedestrians, delivering essential information such as speed limits, directional guidance, warnings, and regulatory instructions. Ensuring their visibility is paramount for the safety and smooth operation of transportation networks. Traffic signs are designed to be easily visible and legible from appropriate distances, allowing road users sufficient time to react appropriately. Vegetation encroachment is a problem particularly pronounced in areas where rapid vegetation growth is common, or where maintenance activities are insufficient or irregular. This can lead to several safety hazards and impact also on operational efficiency and costs:

- **Obscured Information:** Key information such as speed limits, upcoming stops, pedestrian crossings, and warnings may be hidden from view.
- **Reduced Reaction Time:** Drivers and operators may not have adequate time to respond to critical signage, increasing the risk of accidents, collisions, and traffic violations.
- **Damage Costs:** Overgrown trees can physically damage traffic signs, necessitating repairs or replacements.
- **Operational and service disruptions:** Vegetation can obstruct tracks and interfere with signalling systems; those can hinder the navigation causing delays and disruptions in service.

State of the art – application and sensors

The main application fields where occlusion due to vegetation is handled for maintenance purposes are agriculture, forestry, environmental conservation and infrastructure inspection, urban planning and maintenance.

The experimental setup from the literature consists of sensors placed in front of obstacles, including a thermal camera; RGB camera; 360° camera; light detection and ranging (LiDAR); and radar. These sensors were used either individually or together on ground and aerial vehicles. The thermal camera was able to successfully detect hidden objects like barrels, human mannequins, and humans, similar to how LiDAR perform. On the other hand, the RGB camera and stereo camera were less effective at finding hidden objects and did better with protruding ones. Radar could detect hidden objects easily but had low resolution. Finally, hyperspectral sensors could identify and classify objects but required a lot of storage space [25]. To obtain clearer and more robust data of hidden objects in vegetation further experiments should be performed.

Challenges

Occlusion handling in object detection poses several challenges due to various factors [26]:

- **Variability in Occlusion Types:** Occlusions can occur in different forms, such as intra-class occlusion (hidden by objects of the same class) and inter-class occlusion (occluded by objects of different classes).
- **Complexity of Object Categories and Instances:** The large variety of object categories and instances makes it impractical to collect and label datasets with all possible occlusions for each instance in every category.
- **Insufficient Annotated Data:** The lack of annotated occluded data hinders the training of models to effectively handle occlusions.
- **Incorrect or Insufficient Annotations:** Amodal segmentation, used to determine if an object is occluded, may be ineffective if the annotations are incorrect or insufficient.
- **Limited Real-World Data:** Relying solely on synthetic datasets or automatically generated examples may not capture the complexity of real-world occlusions.
- **Variability in Object Sizes and Scales:** In indoor scenes, the relatively smaller size of objects compared to outdoor scenes can lead to insufficient information in the visible region when objects are occluded, making it harder to recognize and regenerate occluded objects.
- **Robustness of Deep Learning Classifiers:** Deep neural network-based classifiers are less robust in the presence of partial occlusion, impacting the performance of detectors.

Techniques

These factors collectively contribute to the complexity of occlusion handling in object detection and requires specialized techniques to handle the complex and dynamic nature of foliage. Some approaches to address occlusion could be:

- **Multi-Sensor Fusion:** Integrating data from different sensors, such as LiDAR, radar, and RGB cameras, can provide a more comprehensive view of the environment, helping to detect objects behind or within vegetation.
- **Multi-View Fusion:** Integrating information from multiple viewpoints or sensors to reconstruct occluded regions and improve object detection accuracy.
- **Semantic Segmentation:** Utilizing semantic segmentation algorithms can help differentiate between vegetation and objects of interest, enabling the system to focus on detecting objects that are partially or fully occluded by vegetation.
- **Amodal Segmentation:** Amodal segmentation aims to predict the complete shape of an object, including occluded parts, by inferring the object's full extent even when parts are hidden.
- **Dynamic Object Tracking:** Implementing dynamic object tracking algorithms that predict the movement of occluded objects as they navigate through vegetated areas can improve detection accuracy.
- **Generative Adversarial Networks (GANs):** GANs can be used to generate realistic data to fill in occluded regions, aiding in the reconstruction of occluded objects and enhancing detection accuracy.
- **Feature Enhancement:** Enhancing features in regions affected by occlusion to improve the discriminative power of the model and facilitate accurate object detection.

- **Contextual Information:** Leveraging contextual information, such as the spatial relationship between vegetation and objects, can help infer the presence of occluded objects and improve detection performance.

Proposed Methodology

Some of the techniques mentioned above aim to reconstruct the occluded object while others just identify the occlusion. Focusing on the scope of the project, the aim of this use case is to evaluate the visibility of the railway infrastructure elements regarding occlusion due to vegetation to support pruning maintenance decisions.

However, techniques such as multi-view fusion or dynamic object tracking are not applicable to this use case due to its particularities. This approach will be based in a fixed camera position installed on the train head that will count only on that perspective. Additionally, is the camera position the dynamic one but the objects in the infrastructure are static.

Therefore, this use case will be based on environment monitoring at a normal driving speed while collecting geospatial data. Deep learning frameworks demonstrated that they are sufficient to recognise elements such as traffic signs or vegetation. Therefore, the methodology proposed in D10.1 (section 9.3) is presented below and has been refined to add new steps necessary for a more accurate occlusion study and to serve as a support tool for infrastructure maintenance personnel. It is decomposed in the following steps (see Figure 14-1).

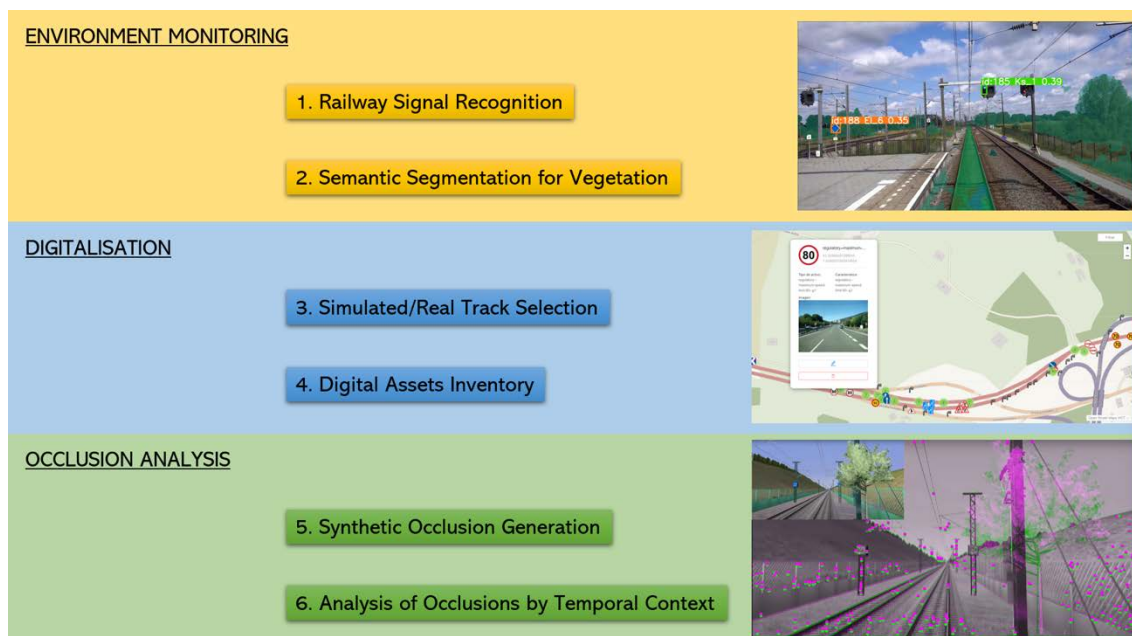


Figure 14-1: Proposed methodology for vegetation occlusion detection

1. **Object Detection Algorithm for Railway Signal Recognition:** Develop or integrate a deep learning-based object detection algorithm specifically trained to identify railway signals. By using publicly available datasets, the algorithm can be evaluated to ensure its accuracy in various conditions, such as different lighting or weather scenarios. However, it will not be trained to detect partially or totally occluded signals.

2. **Semantic Segmentation Algorithm for Vegetation Identification:** Develop a semantic segmentation algorithm capable of identifying and classifying different types of vegetation. By applying this algorithm to historical videos, each frame can be annotated to indicate the presence of vegetation and track its growth over time. This helps in determining if an increase in vegetation is responsible for occluding railway signals.
3. **Simulated/Real Track Selection:** Curate a selection of both simulated and real-world track videos. Simulated tracks allow controlled experimentation with various occlusion scenarios, while real-world tracks provide actual data for analysis. This dual approach ensures that the algorithms are robust against both idealized and practical conditions. Historic real-world videos are particularly valuable for identifying real growth patterns affecting signal visibility.
4. **Digital Assets Inventory:** Create and maintain a digital inventory of all critical assets, related to railway signals and vegetation by analysing historical georeferenced videos. This inventory should be meticulously catalogued to support efficient querying and retrieval.
5. **Synthetic Occlusions Generation:** Create synthetic occlusions to simulate the growth of vegetation. This can be done by digitally superimposing new elements, such as branches or leaves, onto the video frames or simulated environment.
6. **Analysis of Occlusions by Temporal Context:** Perform a temporal analysis of occlusions by comparing the visibility of railway signals at various points in time. Overlay historical detection results to pinpoint when an obstruction begins to affect signal visibility.
7. **Maintenance tasks prediction:** Machine learning techniques can be used to predict future occlusions based on historical growth trends (if data available). This can help in planning maintenance to clear vegetation before it becomes a problem and ensure consistent signal visibility.

By integrating these elements, one can develop a comprehensive framework for analysing how vegetation growth impacts the visibility of railway signals over time. This framework would facilitate proactive measures to maintain clear lines of sight and ensure the safety and reliability of railway operations.

14.2. Work progress

Data availability study

To train the two algorithms for environment monitoring (Object Detection for Railway Signals and Semantic Segmentation for Vegetation identification) annotated image datasets are needed (see Figure 14-2).

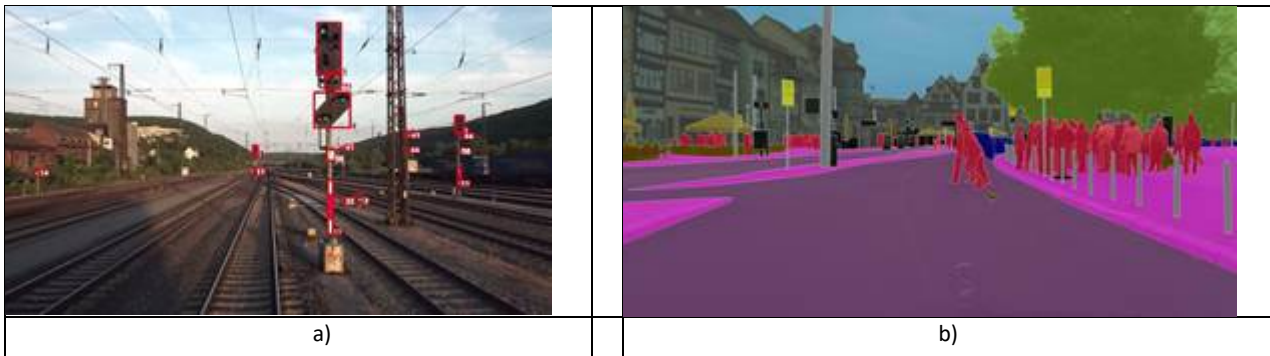


Figure 14-2: Sample images of the two datasets used in this use case: a) GERALD dataset and b) Cityscapes dataset.

The datasets that were identified in D10.1 have been explored in D10.2. For the assets detection it was decided to go for railway signs and lights. For this task OSDaR23, FRSign and RailSem19 datasets were discarded due to the following reasons:

- OSDaR23: does not contain railway sign specific classes. Just “signal” class available, and all videos were recorded in Germany.
- RailSem19: does not contain railway sign specific classes. Just “traffic light” and “traffic sign” general classes where available and for different countries over the world. Additionally, the labels are coarse (not manual) for vegetation class there are better labels in road domain datasets.
- FRSign: just traffic lights were labelled, and their geometry differ from the ones seen in Netherlands.

Thus, it was decided to use GERALD dataset [27] (German Railway Light Signal Dataset) to train Railway Signal Recognition. The GERALD dataset comprises 5000 individual images and annotations for 33,554 occurring objects. Annotations primarily focus on light signals but also include other objects (mostly static signs) to provide a more comprehensive understanding of the environment. Images were collected from the H/V and Ks signalling systems, which are two of the three signalling systems used in Germany. The HI signalling system, used only on some tracks in the former East Germany, was not included due to limited available videos. Nevertheless, other signal types were labelled to obtain a more complete dataset regarding German mainline railway signals and to enable detection of mast signs, hectometre signs etc. The following figure shows all classes and their corresponding number of labelled instances (see Figure 14-3).

However, after a first analysis of the dataset, we have seen that apart from the class imbalance this dataset has other drawback, many samples are of very small signals since they are taken from YouTube videos and are distant objects (see Figure 14-4).

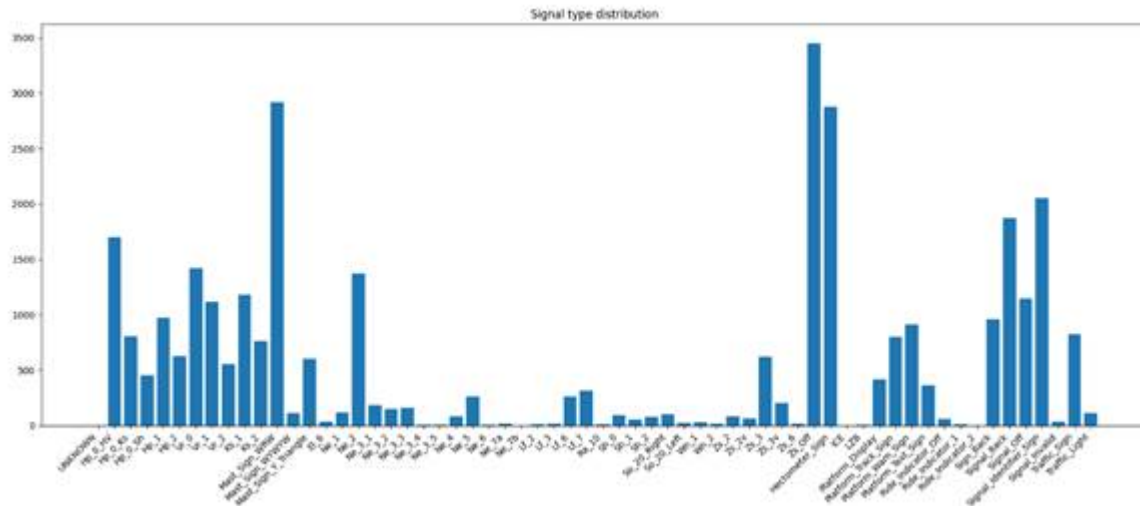


Figure 14-3. Class distribution of GERALD dataset.

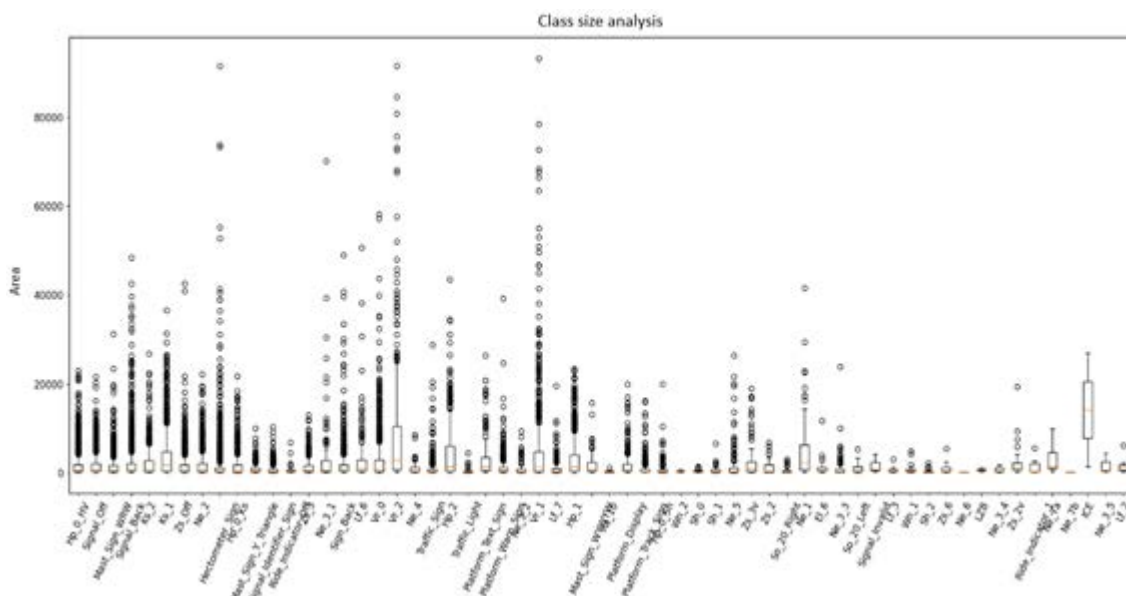


Figure 14-4. Image size analysis of GERALD dataset.

For Semantic Segmentation of Vegetation identification, a deep learning model was trained with RailSem19, but it was observed that vegetation labels were better in datasets such as CityScapes. Thus, RailSem19 was discarded and the popular large-scale dataset CityScapes [28] has been used. It contains a diverse set of stereo video sequences recorded in street scenes from 50 different cities (Germany), with high quality pixel-level annotations of 5 000 frames in addition to a larger set of 20 000 weakly annotated frames. The dataset is thus an order of magnitude larger than similar previous attempts. The Cityscapes Dataset is intended for assessing the performance of vision algorithms for major tasks of semantic urban scene understanding: pixel-level, instance-level, and panoptic semantic labelling. It should be noted that these images are for road scene segmentation, however in this use case we will try if these images are valid for vegetation segmentation in railway scenes.

Regarding Geospatial data, a defined track is needed to create a digital inventory that will be used as reference to detect incidences (occlusions) on successive journeys. It could also be valid to save historical growth trends.

For this use case two alternatives are proposed (see Figure 14-5):

- Real track data: from Leonardo's data collection campaign. This would require adapting the Railway signal recognition model to the specific signalling system of Netherlands.
- Simulated track data: simulators such as OpenRails or TrainSimWorld can be used to obtain video sequences where the country, environment conditions, driving speed, camera zoom, etc. parameters are configurable.



Figure 14-5. Sample images of track alternatives: a) Strukton's original video and b) Screenshot of TrainSimWorld random track

As for the moment CEIT has used the two datasets mentioned in before for model training and testing. Additionally, some extra tests were done with a video provided by Strukton.

Railway Signal Recognition model – GERALD Test

The object detection model was trained based on a YOLOv8 architecture and demonstrated acceptable accuracy for the most common railway signs. However, this model has troubles for small/distant objects, thus, the original architecture was modified to add a P2 head, this implies utilizing a finer-scale feature map in the network's Feature Pyramid Network (FPN) thus providing more detailed information necessary for accurately localizing and classifying small objects. Despite the limited number of instances, the results improved and reached a mean Average Precision (mAP50) of 0.77 across all categories and exceeded 0.9 for the top 10 classes (see Figure 14-6, Table 14-1.)

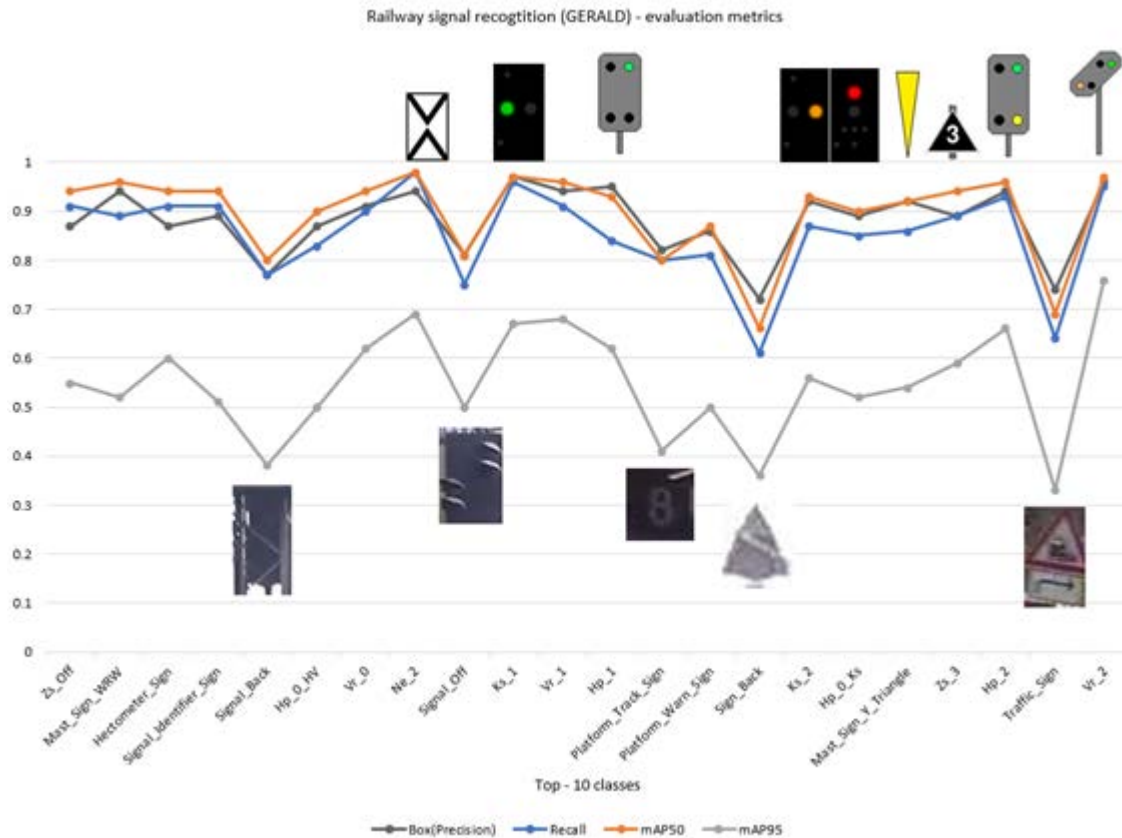


Figure 14-6: Evaluation metrics for Railway Signal Recognition model trained with GERALD dataset

Table 14-1: Top -10 GERALD dataset classes description

Class name	Signal description	System description
Zs_Off	Signal off	Zs additional signals that complement the instructions given by the main signals. They may also be independent
Mast_Sign_WW	Trains may only pass a light signal marked with this mast signal in Zs 1, Zs 7, Zs 8	Special signals
Hectometer_Sign	Shows the driver the position on the route	Special signals
Signal_Identifier_Sign	Identification sign	Others
Signal_Back	Sign at the rear	Others
Hp_0_HV	Two red lights, do not proceed	H-System Block entry signalling
Vr_0	Two yellow, caution wait for stop	V-System Indicate that you should wait for the next active signalling to occur
Ne_2	Identification of the location of a distant signal. For example, in construction, as an indication of a distant signal that is not on the right-hand side or above the track.	Ne (other signals) secondary signals which cannot be assigned to a special category.
Signal_Off	Sign off	Others
Ks_1	Green light, proceed at line speed	Ks-System Same function as the H-system, but more modern

Class name	Signal description	System description
Vr_1	Two green, wait for clear	V-System Indicate that you should wait for the next active signalling to occur
Hp_1	Green, proceed with caution	H-System Block entry signalling
Platform_Track_Sign	track signs, e.g. platform number	Platform
Platform_Warning_Sign	Caution signs on platform	Platform
Sign_Back	Sign at the rear	Others
Ks_2	Yellow light, caution wait for next signal	Ks-System Same function as the H-system, but more modern
Hp_0_k_s	Red light, do not proceed	Ks-System Same function as the H-system, but more modern
Mast_Sign_Y_Triangle	With this mast signal are marked the signals Ks and Hl with white, red and white mast signal, which also have a far signal function.	Special signals
Zs_3	The speed shall not exceed ten times the digits from the signal onwards.	Zs additional signals that complement the instructions given by the main signals. They may also be independent
Hp_2	Yellow and green, proceed with caution. Speed limited 40 km/h	H-System Block entry signalling
Traffic_Sign	Traffic signal	Others
Vr_2	Green and yellow, wait for caution with 40 km/h speed limit.	V-System Indicate that you should wait for the next active signalling to occur

Semantic Segmentation of Vegetation identification – CityScapes Test results

The model was trained based on a HRNet+OCRNet architecture and demonstrated a good accuracy for scene semantic segmentation. The test set showcased a mean Intersection over Union (IoU) of 93.15 and a classification accuracy of 97.01% for vegetation class (see Table 14-2). The model is robust and maintains consistent performance for railway scenarios. However, the temporal coherence needs to be improved to avoid flickering from one frame to the next.

Table 14-2: Preliminary results of the Semantic Segmentation model for Cityscapes test

Class	IoU	Acc
road	98.52	99.16
sidewalk	87.65	93.56
building	93.66	97.0
wall	59.23	68.37
fence	65.27	73.94
pole	71.4	82.16
traffic light	75.39	86.11
traffic sign	82.99	89.83
vegetation	93.15	97.01
terrain	66.35	75.85
sky	95.49	98.27
person	84.0	92.88
rider	64.15	76.63
car	96.02	98.2
truck	86.39	89.99
bus	91.35	95.07
train	84.59	90.48
motorcycle	70.21	79.09
bicycle	79.86	89.74

Leonardo's track – Visual analysis results

A video recorded on Leonardo's vehicle was downloaded from Geoconda (camera Machinist Voor). This is a track from Amersfoort to Amsterdam done the 19/12/2023. We run the inference of the models presented above for this video and get the results (see Figure 14-7).



Figure 14-7: Sample of model's inference on a frame from Leonardo's journey

14.3. Achieved results

Railway signal recognition: Despite the limited number of instances, after the modification of YOLOv8 architecture, the results improved and reached a mean Average Precision (mAP50) of 0.77 across all categories and exceeded 0.9 for the top 10 classes.

Vegetation segmentation: The test set showcased a mean Intersection over Union (IoU) of 93.15 and a classification accuracy of 97.01% for vegetation class. The model is robust and maintains consistent performance for railway scenarios.

General conclusions: vegetation segmentation model can be used for railway domain. However, railway signal recognition model's functionality is limited since it is missing samples of the Dutch signals. It would be convenient to build our own dataset with these signals.

14.4. State the status handed over from W10 to WP11

Those are the tasks planned for WP11:

- Generate a new dataset of Dutch signals and train a proprietary recognition model.
- Look for examples of vegetation occlusions in Leonardo's data or other videos.
- If there are no examples of real occlusions, study methods to generate synthetic occlusions (simulators, diffusion models, GAN, etc.).
- Study different techniques for occlusion detection (historical image registration, amodal segmentation, etc.).

15. MONITORING TURNOUTS ACCELERATION SIGNALS

This section describes the preparatory work carried out by CEIT at the pilot site in Spain, provided by ADIF, for the monitoring system being developed to establish the health status of turnouts using acceleration signals.

15.1. Introduction and methodology

Turnouts are a critical asset of the railway system, enabling train vehicles to take different directions. A turnout is split into two main parts (switch and crossing) and has up to four possible running modes (through or diverging direction and facing or trailing move). The dynamic forces due to wheel-rail contact are heavily affected by the degradation of the crossing nose and/or wing rail mainly by wear degradation. Figure 15-1 shows a general layout of a turnout.

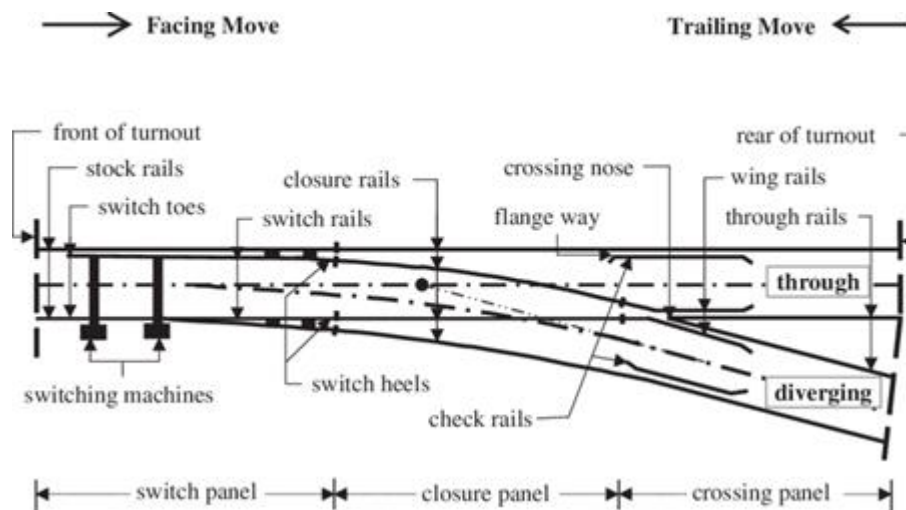


Figure 15-1: General layout of a turnout

The technology to develop aims to detect the health status of the crossing by means of some accelerometers. The objective is to optimize the number of sensors and their characteristics at different locations of a crossing, using computational models based on physical models capable of replicating the dynamic response. At the end, signals acquired by a first prototype should identify the degradation index of the crossing.

According to the literature, in [15] the authors provide a very detailed description of the different ways to monitor a railway crossing and explore measurements using accelerometers. Liu et al [16] install an accelerometer at the nose of the crossing and, using measurements at different levels of degradation, attempt to predict the track's condition.

Fan et al [17] have used recently co-simulations to vehicle track interaction with a multibody system (MBS) and a finite element method (FEM) model. Milosevic et al [18] use a similar methodology, designing a method for continuous monitoring of railway switches and crossings using accelerations. The technology developed in the project will allow to perform the analysis to optimise the positioning of the sensors and work in high and medium frequencies. Another basis for this work is documented by Reetz et al. [19], where the findings suggest that filtering data to narrow frequency bands around specific natural track frequencies could improve the detection of impact events. However, distinguishing between individual impact event origins requires

broadband signals. Therefore, a multi-sensor setup with time-synchronised acceleration sensors distributed over the switch is recommended.

The methodology to define the location of accelerometers and which are the required KPIs is based on simulations, signal processing and field tests. The flowchart of Figure 15-2 shows the methodology (explained in the next section) where several technologies that are going to be developed can be identified:

- Multibody models considering profile sections of a crossing to obtain wheel-rail contact parameters.
- FEM model is based on crossing geometry to calculate acceleration signals at high frequencies.
- Signal processing algorithms for identifying the KPIs from acceleration signals, both synthetic and real.
- A prototype as a demonstrator of the capabilities of computational models to design the monitoring system that is being developed to establish the health status of turnouts using acceleration signals.

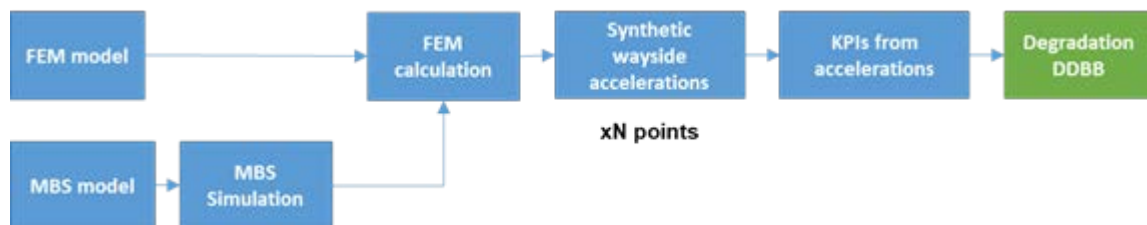


Figure 15-2: Methodology flowch

MBS models are suitable for obtaining wheel-rail contact parameters with low computational cost in comparison to FEM models. To perform an MBS analysis of a turnout, it is crucial to accurately input the sections of the variable rails. For this, it will be necessary to know the rail section in the plane perpendicular to the direction of travel and its longitudinal position.

15.2. Work progress

This section outlines the progress and work made through the development of the project. A preliminary instrumentation of the crossing panel using dynamic sensors was developed to know and evaluate the dynamic response of the crossing panel under a train passage. In parallel, progress has also been made in developing both multibody and finite element (FEM) models of the turnout system, providing complementary approaches for simulating its dynamic performance.

To validate the MBS and FEM models that are being developed, preliminary on-track tests have been carried out in the pilot site of Spain in Rifá on March 2024. The conventional crossing managed by ADIF was instrumented according to Figure 15-3 and Table 1 using up to 16 channels (14 accelerations and 2 displacements). These tests aim to know the dynamic responses of a crossing panel under various rolling stock types and to assess the suitability of the sensors used. Additionally, initial steps in signal processing in the time and frequency domains are given.



Figure 15-3: Instrumentation of the crossing

Table 15-1: Sensor location and characteristics

Location ID [#]	Sensor type	Direction	Range	Channel used	Sensor
1	Accelerometer	Vertical	±500g	1	PCB352C03
2	Accelerometer	Vertical	±500g	2	PCB352C03
3	Accelerometer	Vertical	±500g	3	PCB352C03
4	Double accelerometer	Vertical + Lateral	±500g	4, 5	PCB352C03
5	Accelerometer	Lateral	±500g	6	PCB352C03
6	Accelerometer	Vertical	±50g	7	PCB333A31
7	Triple accelerometer	Longitudinal + Lateral + Vertical	±500g	8, 9, 10	PCB352C03
8	LVDT	Vertical	±2.5mm	11	RDP DCTH100AG
9	LVDT	Vertical	±2.5mm	12	RDP DCTH100AG
10	Double accelerometer	Lateral + Vertical	±500g	13, 14	PCB352C03
11	Accelerometer	Vertical	±500g	15	PCB352C03
12	Accelerometer	Vertical	±50g	16	PCB333A31

Figure 15-4 shows how the installation of displacement sensors (a) and accelerometers (b) was done.



(a)



(b)

Figure 15-4 : Installation of displacement sensors (a) and accelerometers (b).

After the instrumentation, the next two days several acquisitions were performed. Within these

days up to 5 different types of vehicles were running through the crossing:

- Medium distance.
- Long distance.
- Freight vehicle.
- Single locomotive.
- Regional unit.

Real degraded geometry of a specific turnout at different degradation levels is obtained using 3D scanners. In Figure 15-5 the 3D point cloud obtained with a 3D scanner of the crossing panel at the pilot site conventional turnout is shown. The actual state of the crossing is obtained using this technology to work with **degraded geometries** in MBS and FEM models.

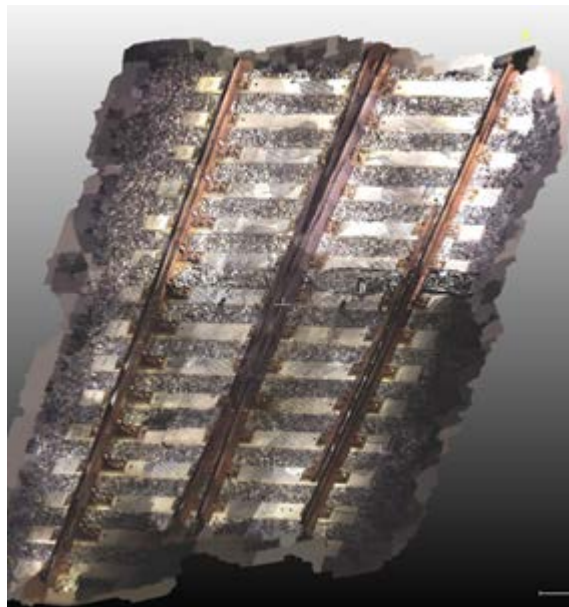


Figure 15-5: A scanned crossing panel

In Simpack, the MBS software used, to obtain the complete geometry of the rails, rail sections are introduced at regular intervals, and interpolation between the sections is performed using Bezier curves. Figure 15-6 shows the Bezier curves generated by Simpack using as input different sections of a crossing. A top view and the profile of the crossing frog are shown.

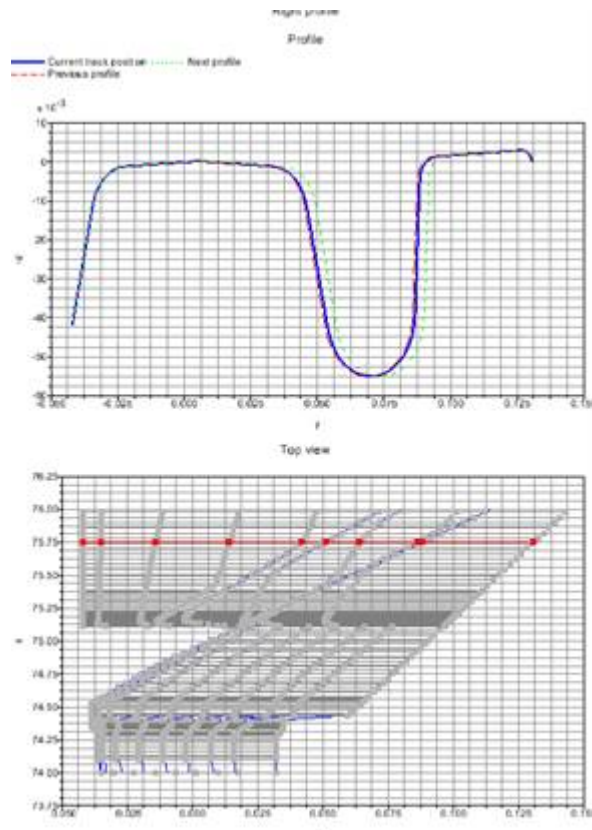


Figure 15-6: Bézier curves and profiles of a crossing rail generated by Simpack

In the benchmark of S&C in 2021 [20], two different types of tracks are analysed: 54E1 and 60E1. Figure 15-7 shows 60E1 crossing rail sections given by the authors of the benchmark. The output of the simulations is dynamic behaviour of the rolling stock and contact parameters. Additionally, the results are analysed for both the switch panel and the crossing panel in direct circulation cases and diverging circulation cases. As a first step with MBS models the results using SIMPACK have been replicated. Therefore, from sections available for a certain crossing it is possible to obtain reliable results.

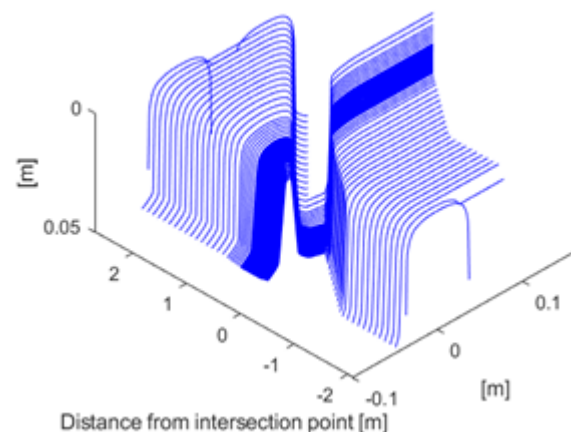


Figure 15-7: 60E1 crossing rail sections from the Benchmark

From the scanned railway crossing point cloud, degraded state rail sections can be obtained to

obtain contact parameters as an output from multibody simulations. Figure 15-8 shows the obtention of a degraded rail section from a scanned point cloud. These sections are used to perform preliminary multibody simulations, using the Benchmark vehicle.

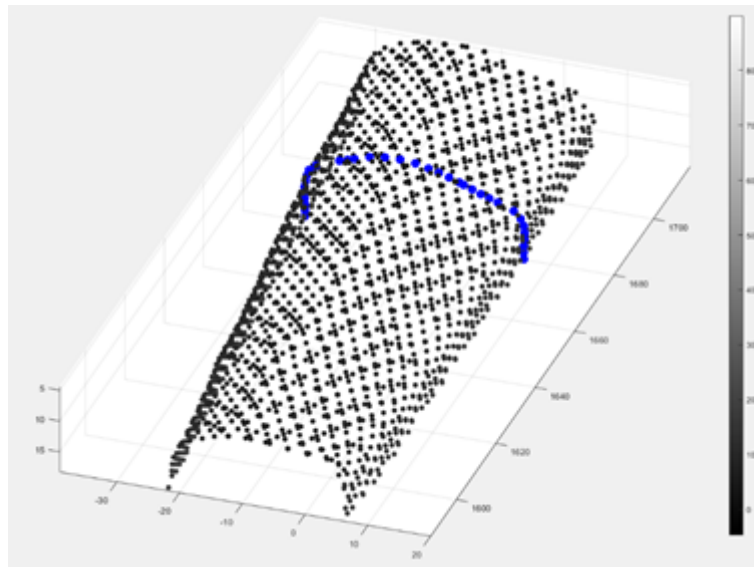


Figure 15-8: Section of a crossing nose in a point cloud

Outputs from MBS model can be used as inputs in FEM models. It is necessary to have an equivalent geometry of the track. This involves modelling the sleepers, rails, and the connections between the elements. The elastic behaviour of these connections is then modelled using special joint elements. A preliminary finite element model of a straight track section (Figure 15-9) has been developed as a first step toward simulating the dynamic behaviour of the railway crossing.

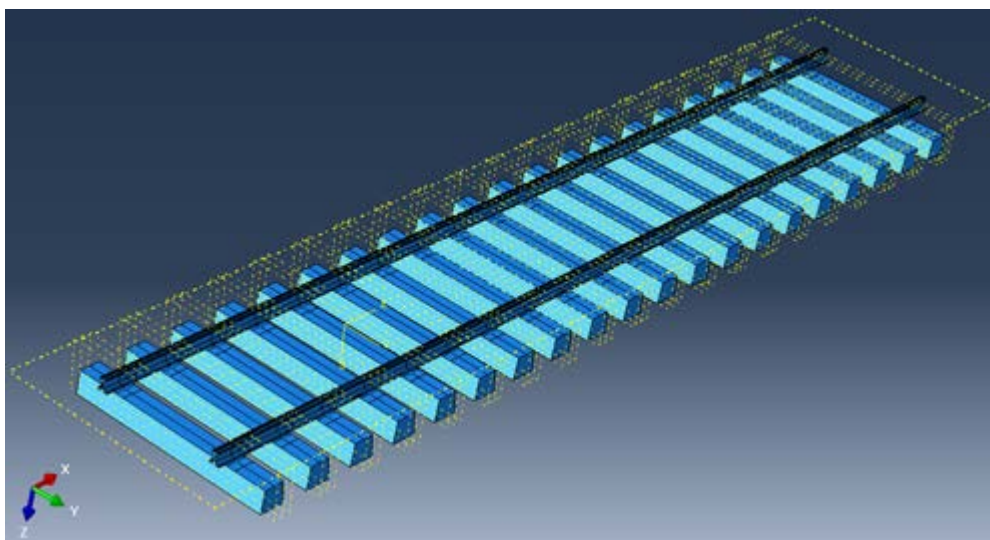


Figure 15-9: Preliminary straight line Finite Element model

To incorporate contact inputs into the finite element model, it is necessary to develop user-defined subroutines in the FORTRAN programming language to reproduce the contact patch. The patches are computed using the FASTSIM algorithm, which is based on Kalker's rolling contact

theory and widely used to estimate tangential contact forces between wheel and rail. It allows for an efficient approximation of the creepage-dependent frictional behaviour within the contact patch, without the high computational cost of full nonlinear models. Key parameters describing the contact conditions are extracted from the multibody simulations of the benchmark scenario. These parameters are then used to reconstruct the contact patch at each time step, enabling a more detailed and realistic representation of the contact mechanics throughout the simulation. By discretizing the contact area into smaller elements, FASTSIM computes local slip and traction distributions, enabling the estimation of forces and moments generated at the interface. Its balance between accuracy and computational efficiency makes it particularly suitable for dynamic simulations where contact conditions evolve rapidly over time. Figure 15-10 shows the partition of the elliptical contact patch based on FASTSIM algorithm.

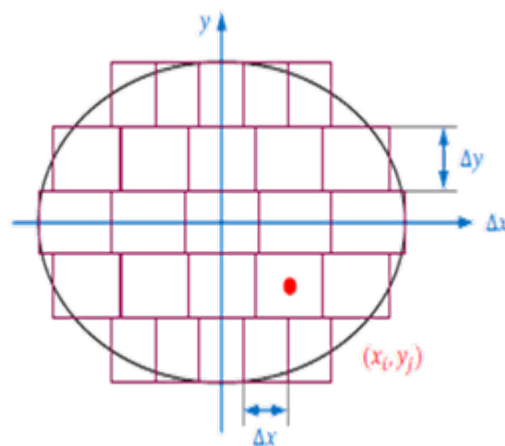


Figure 15-10: Partition of contact patch based on FASTSIM algorithm

The reconstructed contact patch is introduced in FEM environment as a boundary condition in order to obtain acceleration signals in the track model.

15.3. Achieved results

The results obtained from the turnout monitoring have provided valuable information of dynamic behaviour after doing preliminary signal processing in time and frequency domain. In the multibody simulation (MBS) analysis, benchmark turnout results are compared to others and degraded rail sections are used to obtain contact parameters. In the finite element (FEM) model, a synthetic acceleration signal was generated for the track model using the methodology developed.

The results obtained in the monitoring of the crossing panel were acceleration and displacement signals at different points for different types of rolling stock. Figure 15-11 shows an image of the videos that were taken using an action camera to identify the vehicles.



Figure 15-11: Passing of a long-distance train from the conventional pilot site crossing in Rifá

At the end of the tests, the signals are being processed to identify their dynamic behaviour in the time and frequency domains. On the one hand, Figure 15-12 shows an example of the accelerations in three different directions on the crossing nose in the time. On the other hand, Figure 15-13 shows the FFT in the centre of the frog.

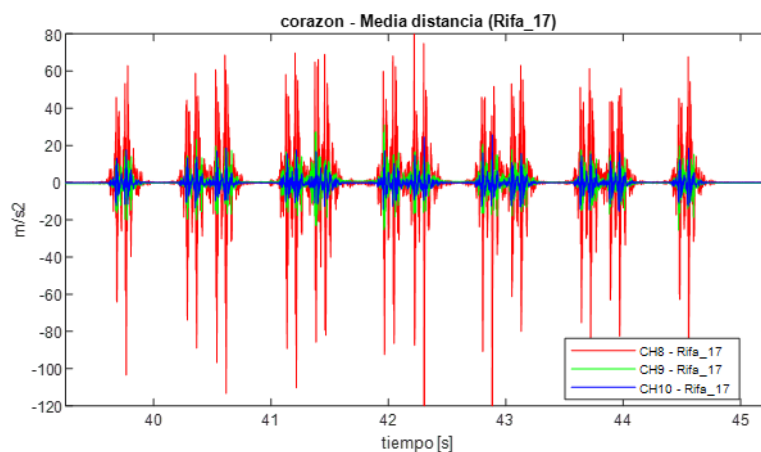


Figure 15-12: Acceleration signals in 3 directions

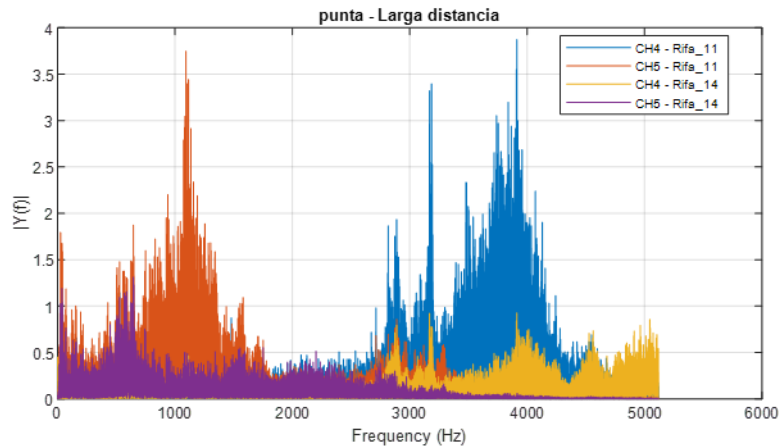


Figure 15-13: FFT of the acceleration signals at the centre of the frog

Regarding the multibody simulations carried out to replicate the switch and crossing benchmark, it can be stated that the modelling capability for switches and crossings has been successfully learned and demonstrated within the multibody simulation framework. In Figure 15-14 a comparison of benchmark results with others is shown and Figure 15-15 shows the advanced contact parameters obtained from the simulations.

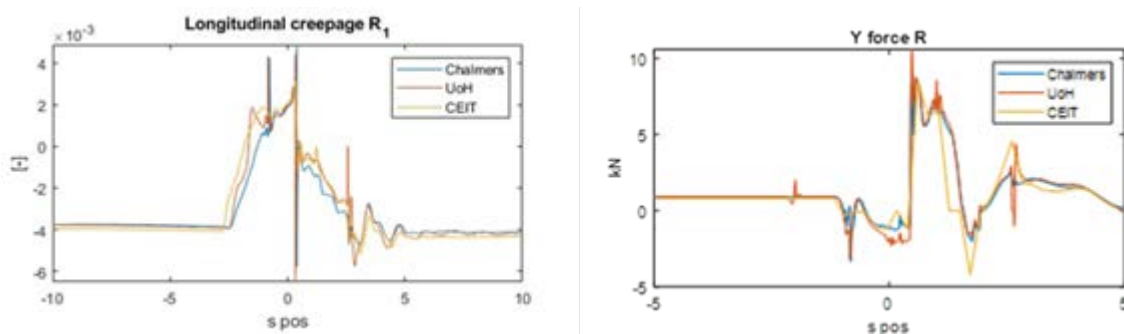


Figure 15-14: Benchmark results comparison with others

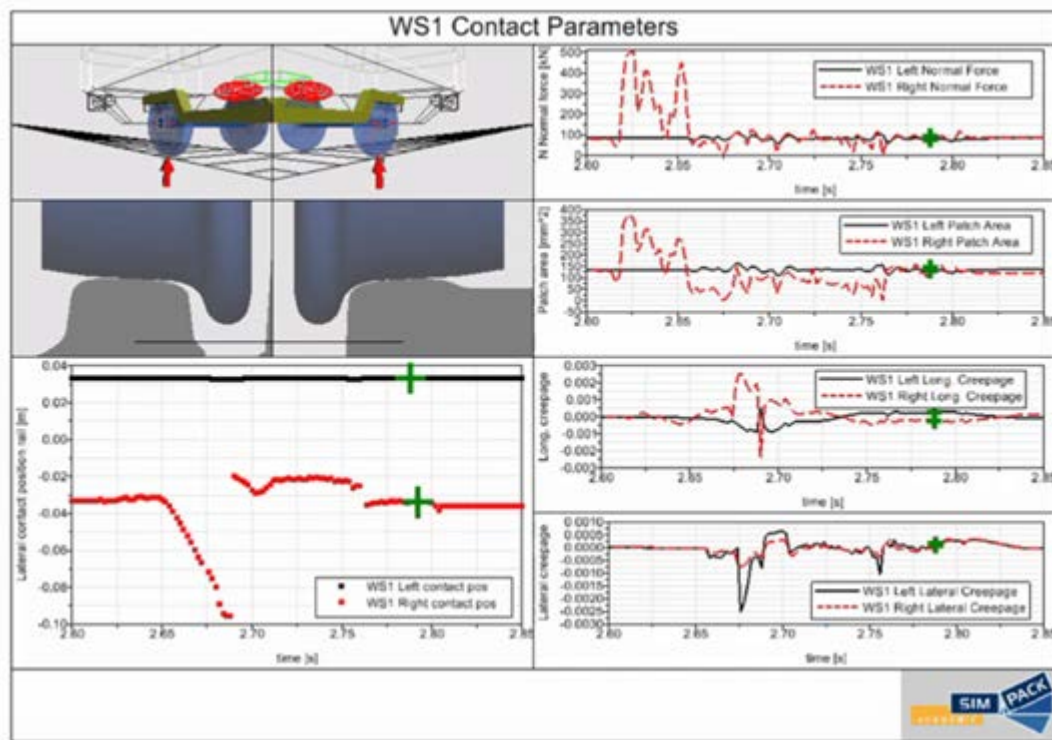


Figure 15-15: Advanced contact parameters

From multibody simulations performed with degraded crossing sections, the contact patch information is obtained. These results include some parameters like contact forces, contact patch dimensions and contact position on the rail. In addition, vehicle overall dynamics is also studied. In Figure 15-16 the force distribution in the scanned crossing frog is shown under the passage of the Benchmark vehicle.

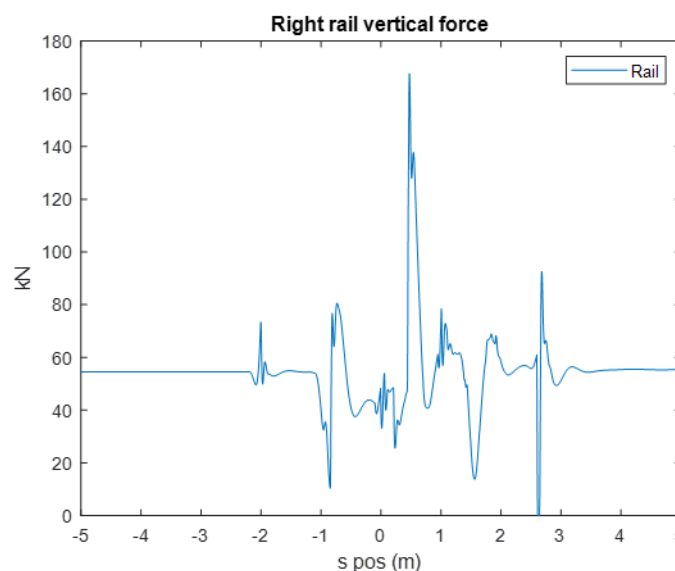


Figure 15-16: Distribution of vertical forces on a crossing rail obtained from MBS

Using this data and following the developed methodology to insert contact patch data in FEM

simulations, synthetic rail accelerations are obtained in preliminary straight-line simulations. In Figure 15-17 the contact patch in Finite Element environment is shown. Figure 15-18 shows an example of those acceleration signals measured in mm/s^2 .

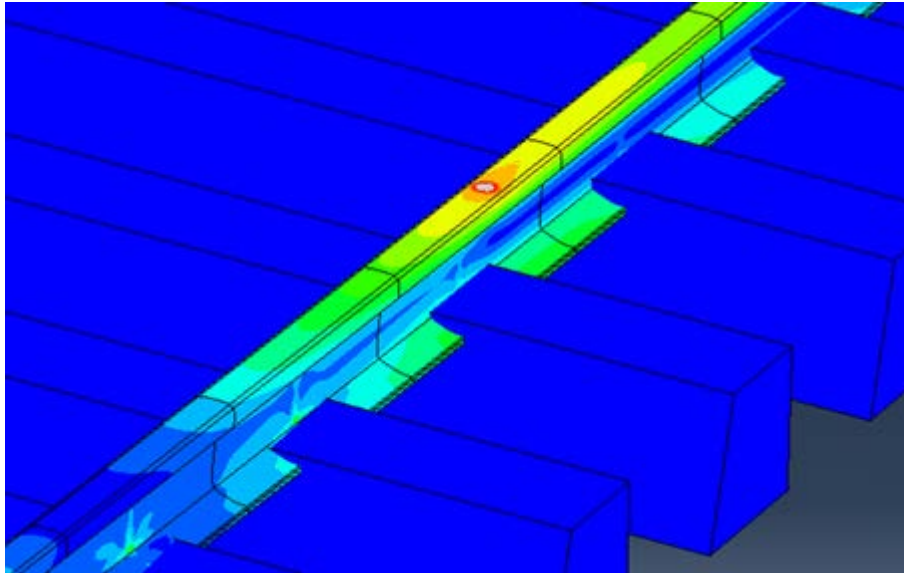


Figure 15-17: Contact patch on a FEM rail

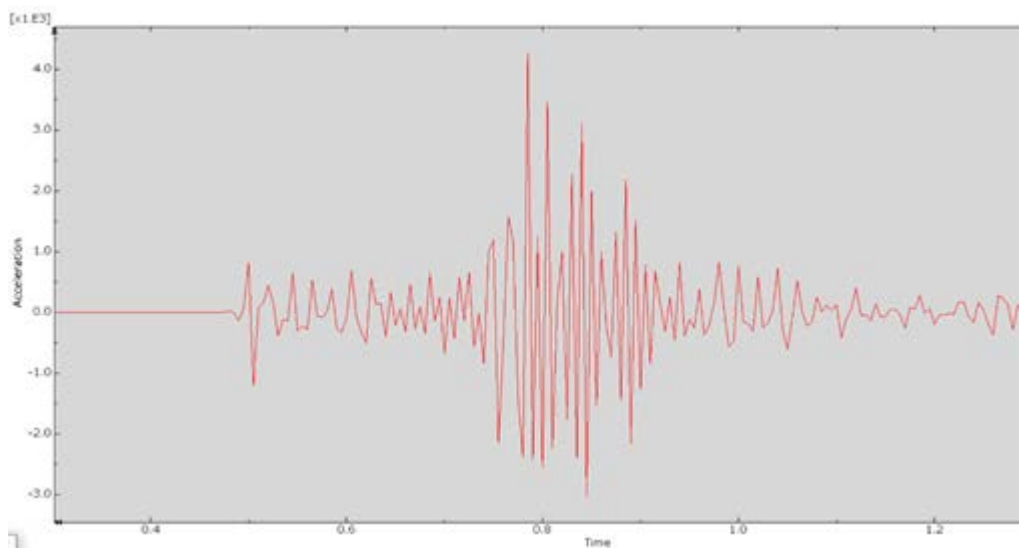


Figure 15-18: Acceleration signals obtained from FEM

15.4. Status handed over from WP10 to WP11

In WP11, the full assessment of the most relevant signal acquisition will be performed for medium-distance and long-distance rolling stock in time and frequency domain by means of FFT, RMS, PSD and spectrograms.

In multibody, simulations using the nominal and degraded geometry of the conventional line turnout in Spain will be performed, modelling the vehicle and the crossing geometry, which is crucial to perform valid simulations. A medium-distance train will be modelled, similar to those in

circulation at the pilot site.

The obtention of nominal (CAD) geometry of a specific turnout is very complicated due to the confidentiality of switch and crossing manufacturers. To obtain this geometry, the starting point is a set of drawings (Figure 15-19) of the crossing nose provided by ADIF.

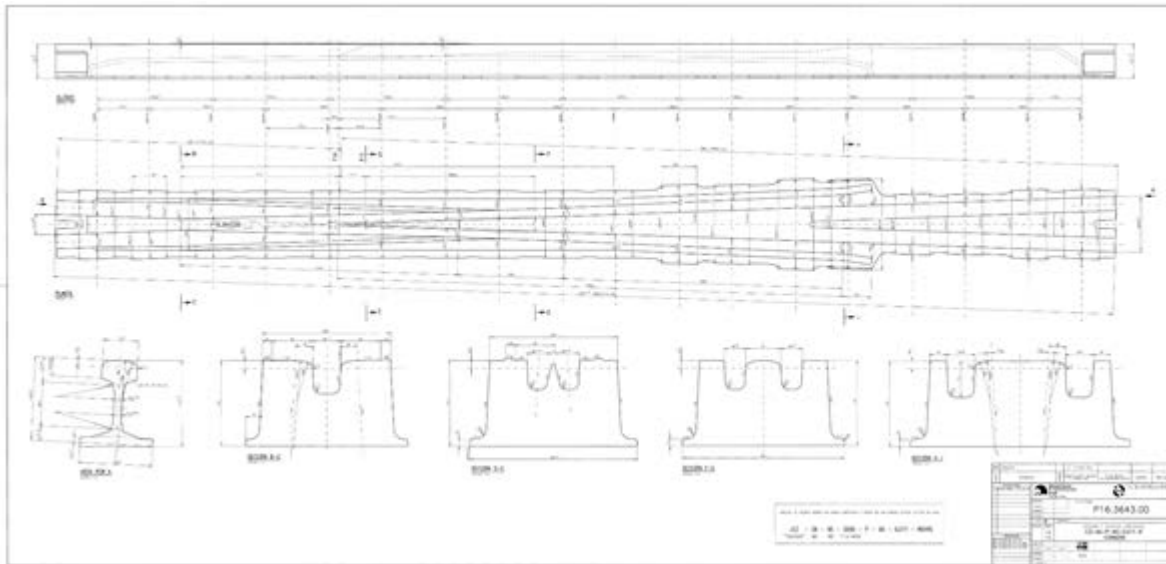


Figure 15-19 Nominal crossing nose drawing (ADIF)

The geometry of the crossing nose will be used to develop a complete model of the crossing panel, modelling sleepers and rails. The connections between components will be modelled using coupling elements, representing the joints as spring-damper elements.

Multibody simulations will be performed using nominal and degraded rail geometries combined with the equivalent rolling stock model. The contact parameters obtained will be introduced in the complete model of the crossing panel as boundary conditions in Finite Element environment, obtaining synthetic accelerations based on the previously described methodology. The output obtained from these simulations will be medium and high frequency synthetic acceleration signals that will help assess KPIs in the future.

Accelerations on pilot site are obtained using accelerometers and will be used to determine the health status of the crossing. These measurements will be used to validate the FEM model.

Furthermore, machine learning techniques will be applied using features extracted from both nominal and degraded vehicle-turnout interactions to identify those most closely associated with degradation levels. This approach will also help define the optimal characteristics and placement of sensors. Within the model, the most informative sensor locations will be determined to effectively monitor the turnout's degradation status and Key Performance Indicators (KPIs) such as peak-to-peak values and RMS will be developed to efficiently assess the condition of the turnout. The eventual data generated are databases using acceleration KPIs to establish a degradation level or index. Using these databases a categorization of degradation level will be created. Figure 15-20 shows an example of how this categorization might be. This will allow to

categorize crossings with different degradation levels when the monitoring solution is created. Parameters that will be analysed can be those related to:

- Train speed.
- Load condition.
- Wheel type.
- Friction coefficient.

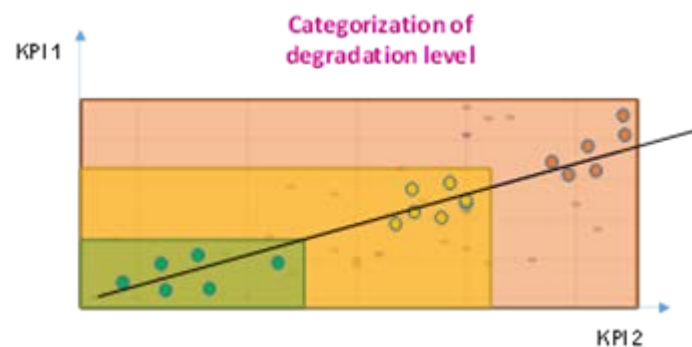


Figure 15-20: Categorization of degradation level

Once the low-cost monitoring solution is developed each KPI from the real acceleration signal will be defined from an average value using a certain time window. In Figure 15-21 this definition of average value is shown. Crossings will be classified based on the categorization defined previously. Finally, the output generated is the definition of health status. Figure 15-22 shows the degradation index of the monitored crossing.

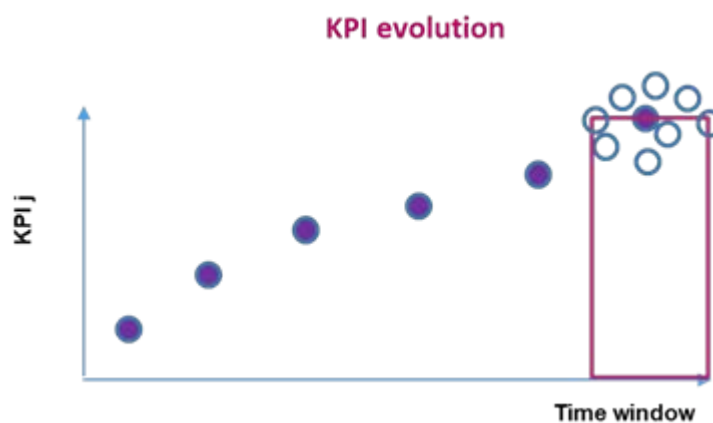


Figure 15-21: Definition of KPI acceleration average value

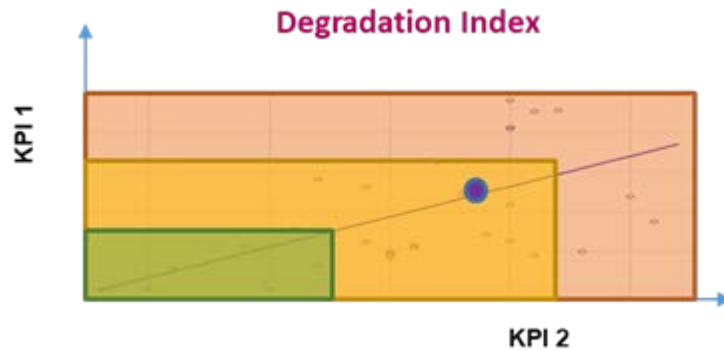


Figure 15-22: Definition of health status

Based on that, a new trackside prototype of an acquisition system will be developed, easy to install and compliant with geometrical characteristics required for track installation and will be installed at the pilot site crossing in Rifá. The system will measure acceleration signals at some previously defined points. The expected result in the validation is to obtain the degradation level of the actual crossing using measurements by means of monitoring.

15.5. Preliminary results that can be used

Although there are no initial results yet that can be used, methodologies have been defined that will be used in the next steps. A methodology that allows to obtain synthetic accelerations in finite element simulations is already proven. Additionally, the first signal processing indicates that sensors used, and acquisition procedure are suitable for monitoring the crossing.

16. RAIL CRACK DETECTION USING MICROWAVES

This section describes the preparatory work carried out by CEIT for the detection of cracks in rail by means of microwave techniques. This activity is performed in CEIT's lab for this project applying the basics of the technology and techniques to this challenge.

16.1. Introduction and methodology

Inspecting the railways for the detection of defects such as cracks is a crucial activity, needed to guarantee the safety of the infrastructure and determine maintenance activities such as repairs or even railway replacement. Cracks of depth deeper than 4mm and/or length over 30 mm are already considered severe and need corrective actions, while if the depth is larger than 5mm, railway replacement is required. These cracks are produced, mainly, both in ruptures of the welds, and in specific locations due to rolling contact fatigue.

This application addresses this problem, by proposing a method based on autonomous inspection of the railway using microwaves. A basic diagram of the proposed system is depicted in Figure 16-1. At a high level, the detection principle to be analysed here is based on radar technique using radiofrequency/microwave technologies, with the ability to illuminate the moving lane when placed on a measurement vehicle or similar platform. The reflections received by this radar must be treated and processed to detect the presence of cracks and ideally be able to diagnose their severity, in order to execute the required mitigation actions (e.g., grinding).

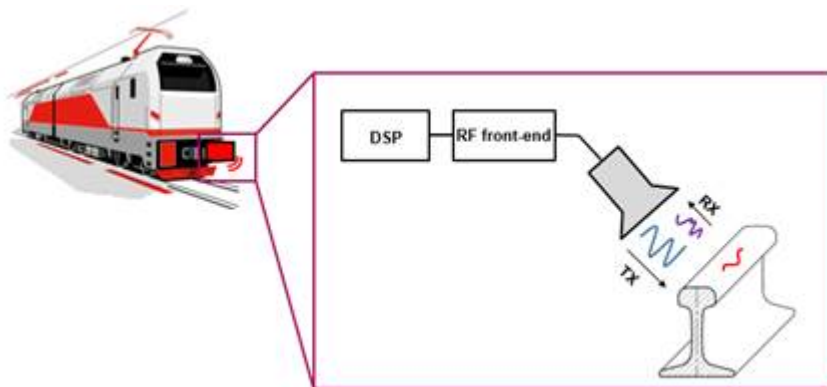


Figure 16-1: Railway inspection using microwaves

Beyond the basic principle in RF (Radio Frequency), several other challenges have been identified for an appropriate solution. These are the mechanical constraints of positioning of the reading and receiving head with respect to the rail, the implementation of the system, embedding it on a moving platform and the processing capability of the data to be analysed. These points influence the viability of the potential product, so it is convenient to consider them from the initial stages of analysis. In this work package, these aspects have been considered and worked on in order to assess the future steps, as it will be demonstrated in the following sections.

In Deliverable 10.1, an iterative process was proposed to draft the inspection system, which consisted of the following steps:

1. System requirements derived from user needs
2. Research on State of the art

3. Definition of test protocol and development of laboratory test bench
4. Electromagnetic simulations of the problem
5. Off-line processing of laboratory signals and simulations
6. Draft for the proof of Concept at Laboratory
7. Proposal for potential system architecture and refining of system requirements.

16.2. Work progress

An initial loop of the process has been completed, at the moment of presenting this deliverable. So far, it has yielded interesting results which help progressing and foreseeing further testing and development. The following table will briefly cover the advancements done so far in each point and the work progress.

Table 16-1: Current status of the different process steps

Process step	Current status
1. System requirements derived from user needs	A careful analysis has been carried out to identify the requirements demanded by the industry and the current status of the literature of application of microwave signals for non-destructive testing of metallic surfaces, oriented towards the inspection of railway tracks.
2. Research on State of the art	An initial and simplified testbench was assembled in a controlled laboratory environment to demonstrate the concept proposed in this activity. Also, representative samples of cracks have been created for their assessment.
3. Definition of test protocol and development of laboratory test bench	Initial models of the propagation of signals at different frequencies being propagated from a waveguide at certain distances of metals with different hole and crack sizes have been performed in ANSYS RF as an initial validation step of the concept.
4. Electromagnetic simulations of the problem	The data collected from the initial simulations, as well as the results of the initial measurements, have been collected and processed to draw relevant conclusions for the progress of the project.
5. Off-line processing of laboratory signals and simulations	The conditions of the initial simulations have been replicated in a laboratory environment using the setup and test protocols defined in point 3 to determine how the concept proposed in this project should be assessed. Initial results point to the suitability of microwave signals for NDT testing of railway tracks and propose the challenges on the implementation on-board.
6. Proof of concept at laboratory	A preliminary system architecture has been defined based on the concepts demonstrated through simulation and preliminary laboratory testing throughout the previous steps.
7. Proposal for system architecture and refining of system requirements.	

A more detailed look into each point, as well as the results of each one, is provided here below throughout different subsections. Additionally, the current challenges in each activity will be described, as well as the next steps for the next phase of the project.

16.3. Achieved results

16.3.1. System requirements derived from user needs

Metal components are widely used in many safety-critical structures across various industries. However, they are prone to surface and subsurface cracks due to factors such as service loads, environmental stresses, and manufacturing irregularities [14] [15] [16]. These cracks can significantly impact on the structural integrity and performance of metal components. Therefore, reliable inspection of metallic structures throughout their life cycle is crucial to prevent failures.

To avoid structural failure, it is essential to reliably detect cracks during routine inspections and repair them before they reach a critical fracture point. The repair strategy depends heavily on the geometrical parameters (or morphology) of the detected crack [17]. Additionally, understanding these geometrical parameters is vital for assessing the component's lifespan and fitness for service, also known as residual life assessment. Hence, inspections should not only detect the presence of cracks but also provide quantitative information about their characteristics, such as spatial extent, orientation, and tip location/size. Inspection tools should also allow for monitoring the crack after repair to evaluate the effectiveness of the repair method in stopping further crack growth.

Rails, as a key component of the railway system, are subjected to intense bending, shear, contact, thermal, and residual stress during operation [18]. These complex loading conditions can lead to the deterioration of the infrastructure and the formation of various defects, mainly originating from manufacturing, improper handling, and rolling contact fatigue or corrosion [19].

The most common type of wear found on a track is generated by the friction between the train wheels and the rail surface, and it can be observed in the head, side or flange of the track. Two examples of head checking defects are presented in Figure 16-2. As it can be seen, this defect consists of tiny cracks spaced between a millimetre up to several centimetres, depending on the contact conditions and the quality of the materials of the track. These cracks occupy several millimetres in the head surface at an angle of 10-15°, and they can grow parallel to the rolling surface, connecting and generating flaking in the track, which subsequently leads to larger issues, like breaks in the tracks or derailments.



Figure 16-2: Head checking generated on a track when the train wheel moves from left to right

Another common defect that can be detected in the tracks is squatting, which can be identified as a widening and sinking in the rail tread, accompanied by arc-shaped fissures and a darkening of the surface, as seen in Figure 16-3. When the fissure depth reaches 3-5mm, the cracks expand transversally, causing the breakage of the rail.



Figure 16-3: Squatting defect example

Finally, another important defect that needs to be considered is shelling, which occurs on the surface of the rail head. It is characterized by the detachment of small, shell-shaped pieces of the rail material, typically in the running surface where the wheel contacts the rail. This defect is a form of rolling contact fatigue and is associated with the high stresses exerted by train wheels passing over the rails repeatedly over time. These generate cracks just below the surface of the rail head, which grow parallel to it due to the cyclic loading of the rail and eventually propagate towards the surface, leading to the detachment of small, shell-like pieces of the rail material.



Figure 16-4: Shelling examples: (left) initial indicators of shelling and (right) break provoked by shelling

Based on the analysis of the defects commonly found in the rails, the early detection of small cracks in the head of the rail, both external and internal, is a critical aspect that will be the target in this activity. Being able to properly identify these cracks and their characteristics (position in the head, length, width, depth, angle) would be an invaluable asset for the maintenance of the infrastructure and avoidance of accidents or large costs in the upkeep of the railway network. In addition to the early detection of these defects, tagging their location and providing relevant information to the maintenance crews would also be highly beneficial. Figure 16-5 shows a flow diagram of the intended system operation.

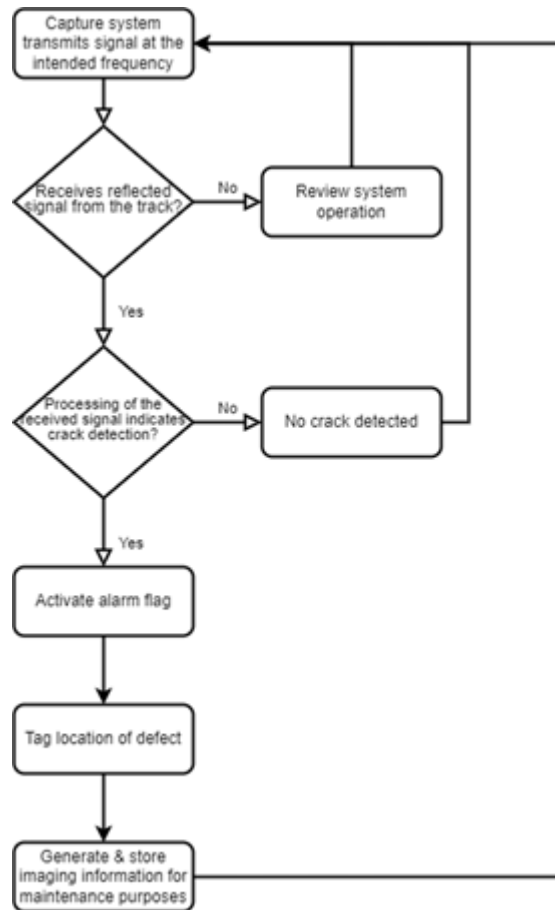


Figure 16-5: Simplified flow diagram of the detection system operation

Therefore, several key characteristics need to be properly defined for the proposed system, including the aforementioned crack characteristics, the sampling and processing speeds of the system, as well as its accuracy in the detection of the cracks and the tagging of its location.

16.3.2. Research on state of the art

For this deliverable, we have centred the analysis of the state of the art on the technologies themselves and not on the equipment that already performed this task as there are no commercial cases of microwave application in trains or wagons. The main goal has been to assess the integrity of metallic structures that requires inspection tools capable of reliably detecting and evaluating cracks. For this purpose, numerous nondestructive testing and evaluation (NDT&E) techniques have been developed. Standard techniques include visual inspection, dye penetrant testing, ultrasonic testing, eddy current testing, magnetic particle testing, and radiography [15]. Additionally, nonstandard techniques such as microwave and millimeter-wave NDT&E methods have also been successfully developed and applied [20] [21] for generic applications. Microwave and millimeter-wave NDT&E methods have significantly advanced in terms of sensitivity, resolution, and utility since their introduction [20] [21].

The aim of this research project is to assess the capability of this technology to perform a better job on the crack detection as it could potentially operate at a further distance from the track, reducing equipment wear and allowing less intrusive inspections.

Today, there is a wide range of microwave and millimeter-wave methods for crack detection and characterization. These methods are generally categorized into far-field techniques [22] [23] [24] [25], near-field techniques [26] [27] [28], and resonator techniques [29].

Microwave and millimeter-wave near-field techniques have shown great potential for various NDT&E applications [30]. Near-field probes developed and demonstrated for crack detection include coaxial probes [25] [31], open-ended rectangular waveguides (RWG) [32] [33], and open-ended circular waveguides (CWG) [34] [35]. A probe is typically used as both a source and detector, with the presence of the crack manifesting as a change in the complex reflection coefficient (scattering parameter S_{11}) measured at the probe input and referenced to the background.

Open-ended RWG probes have been prominent in applying near-field techniques for crack detection and evaluation, demonstrating practical utility in detecting and characterizing exposed, covered, and filled cracks [36]. These simple near-field probes have been extensively studied over the past three decades and can be used with a simple battery-operated system, detecting the crack by observing the characteristic signal acquired using a standing wave reflectometer when the probe is scanned over the crack [37]. The characteristic signal of the crack depends on the geometric parameters of the crack, the size of the probe aperture, the operating frequency, and the location where the standing wave is measured [38]. Using this approach, open-ended waveguides in the K and Ka bands operating at 24 and 33 GHz, respectively, have been developed to characterize fatigue cracks with widths ranging from 3 to 50 μm [39].

In another application, the resonant behavior of the crack was used to determine the depth of surface cracks [35]. To validate this technique, a notch was made through a 12 mm thick aluminum sheet. The considered probes were K-band CWG with an aperture diameter of 6.25 mm operating with the dominant TE₁₁ mode. This study compared rectangular and circular probes for near-field imaging at 24 GHz. The results indicated that the loaded circular probe had higher resolution, and the images confirmed that circular probes produced better images of corrosion due to their near-field pattern without significant side lobes, improving image quality compared to rectangular probes [35].

Based on these analyses, it can be concluded that in terms of the change in the magnitude and phase of the reflection coefficient, rectangular and circular apertures show distinctive behaviors. It is evident that the general shape of the crack indication varies with increasing elevation, especially in the magnitude response. Additionally, while the sensitivity of $|S_{11}|$ to the notch monotonically decreases as the elevation increases for all probes, this pattern is not necessarily observed in the phase change of S_{11} .

In far-field methods, the sample with cracks is placed in the far field of the used microwave sensor, where the elevation is greater than the sensor's far-field limit. That is, with an antenna of larger dimension D operating at a wavelength λ , the crack will be in the far-field region if the elevation is

greater than $\frac{2D^2}{\lambda}$ [40]. The current perturbation initiates a scattered (reflected) signal that differs from that generated by an undisturbed current on a crack-free surface. Essentially, the scattered fields, which are proportional to the radar cross-section, will differ in a cracked metal compared to one without cracks. This technique is based on classical radar measurements and can be performed in monostatic and bistatic configurations (reflection and transmission, respectively), both in the frequency and time domains. When a crack is in the far field of an antenna, its presence does not alter the current distribution in the antenna itself. Early mode conversion methods

introduced in the 1960s and 1970s belong to this category [23] [41]. These methods demonstrated the capability to detect and characterize slots 50 μm wide and depths ranging from 25 μm to 5 mm [42]. Far-field methods also include recent techniques for detecting covered/exposed cracks based on synthetic aperture radar (SAR) imaging [43] [44] [45] [46].

The general sensitivity of these methods is moderate because the radiator is far from the target. However, they are not sensitive to small elevation variations and can detect small cracks with high accuracy. For example, a Ka-band SAR imaging system (26.5–40 GHz) was recently used to detect and characterize cracks of various lengths and widths ranging from 0.25 to 0.875 mm with an elevation of 20 mm [43].

A recent study explored the possibility of using SAR to detect surface defects in rails and measure the parameters of their joints [47]. Experimental data was obtained using a two-coordinate electromechanical scanner and a radar emitting a stepped frequency continuous wave signal in the range of 22.2 - 26.2 GHz. Narrow gauge rail fragments with surface defects of various sizes and depths were used as the study object. A radar signal processing method based on the inverse propagation of its wavefront was developed, with which radar images of the rails with defects were obtained. Experimental studies demonstrated that the developed method allows detecting the presence and measuring the characteristics of cracks in the rolling surface, head separations, joint space width, and the magnitude of the vertical step at the rail joint.

With SAR images, cracks can be detected from great distances and through thick dielectric covers. However, to maintain resolution limited by diffraction, the scan domain size should be approximately twice the elevation or greater [48]. Recently, polarimetric SAR methods have been applied to detect cracks of arbitrary orientations. A K-band (18-26.5 GHz) system with a dual-polarized circular aperture antenna was used to detect covered cracks under thick insulators [35]. Cracks were reliably detected from a 10 mm elevation. The SAR image was constructed from measurements of two copolarizations and one cross-polarization. Using cross-polarization measurements suppresses unpolarized background noise, increasing the system's sensitivity, which is crucial in high distance and coverage conditions [23] [41] [43] [45].

Using dual orthogonal polarization allows estimating the orientation of the crack. However, the choice of polarization type is critical. Using orthogonal linear polarizations results in orientation errors when the crack is parallel to one of the polarizations. In contrast, circular polarization is not dependent on the crack orientation and its effectiveness to detect short cracks at a 20 mm elevation in the Ka-band has been demonstrated in [43].

In summary, near-field techniques, especially those using RWG and CWG probes, have demonstrated high sensitivity and lateral resolution capability in detecting and characterizing cracks in terms of depth, width, and length, even under coverage conditions. These techniques remain fundamental in the field of non-destructive inspection and material evaluation. The sensitivity of near-field reflection methods can be quantified in terms of the measured change in the complex reflection coefficient (phase or magnitude) for a given crack geometry (e.g., width/depth). Like far-field methods, the sensitivity of these methods is also a function of frequency. However, their sensitivity is relatively higher than that of far-field methods and decreases at large elevations. Additionally, they are sensitive to elevation variations.

On the other hand, far-field techniques, such as Ka and K band SAR methods, along with

polarimetric and circular polarization techniques, have shown great potential for detecting and characterizing cracks in terms of depth, length, and width, even under adverse elevation and coverage conditions. The sensitivity of these methods depends on frequency, being more sensitive when the crack resonates at the operating frequency. These techniques are ideal for detection applications where the structure cannot be brought close to the antenna or when the crack is covered by a thick insulator.

In conclusion, both near-field and far-field techniques, using non-destructive testing methods with microwaves and millimeter waves, are highly effective for crack detection. These techniques would be particularly useful for detecting cracks in train rails, providing accurate and reliable evaluation under various operational conditions.

One final aspect to consider is that in railway environments, there is also the issue of the changes in the distance between the antenna element and the surface due to the movement of the frame of the rolling stock and their effect on the results. To address this challenge, lift-off compensation techniques can be applied [49] [50].

16.3.3. Definition of test protocol and development of laboratory test bench

To carry out the validation of the main concepts of the application, a test protocol and a setup had to be generated. In this case, the system consists of a positioning system, VEVOR CNC 3018 Pro, that has been modified to mount a waveguide. This way, the position of the waveguide along the x, y and z axes can be modified relative to a fixed surface.



Figure 16-6: Photograph of the positioning system

On top of the surface of the positioning system, different sheets of F114 steel with laser cuts of different widths and angles to emulate cracks with different orientations, like the ones shown in Figure 16-7, were placed. The use of steel sheets was motivated by the availability and ease of acquisition over real railway tracks, and also commodity for the performance of measurements. Typically, R260 steel would be used, but it is more difficult to obtain flat mechanized ideal samples. This is the reason why this research project has worked with F114 Steel, which has similar electromagnetic properties, which are the key components of the simulations and test once

illuminated by the microwave signal.

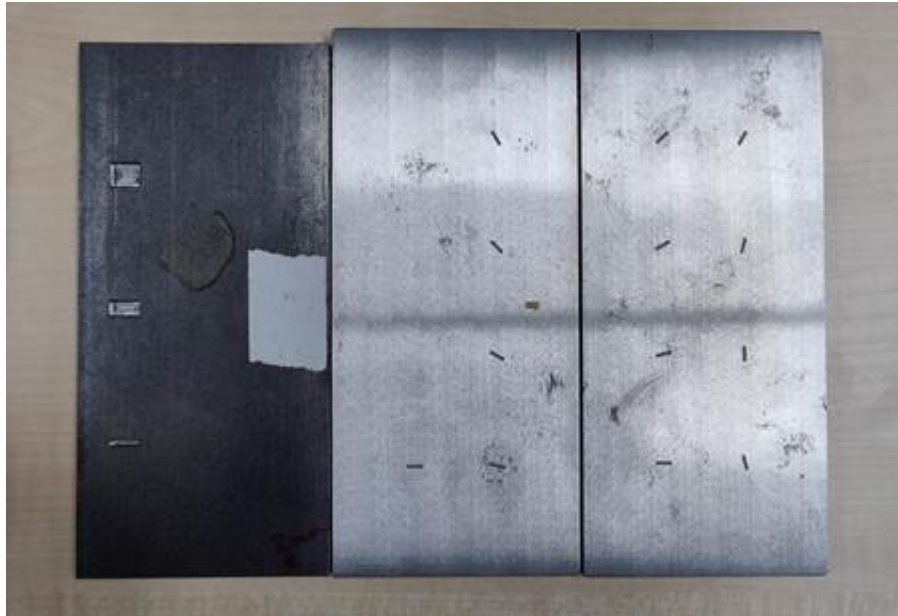


Figure 16-7: Three steel sheets used in the setup

With this setup, a set of varied measurements will be performed to validate the system, as well as test different characteristics of it, such as the impact of using different antennas, the effect of antenna-to-surface separation, changing the measurement acquisition speeds or sample spacing, among others. The test bench is expected to evolve as the system is developed, before eventually moving to field measurements in subsequent projects.

16.3.4. Electromagnetic simulations of the problem (ANSYS)

Before starting with laboratory work, the concepts that were going to be exploited for the implementation of the system had to be validated in a controlled environment. Therefore, specific EM software was selected to simulate the different aspects of the system in a way as close as possible to reality. In this case, ANSYS was chosen. The ANSYS software environment and, specifically, the HFSS 3D suite allowed for the accurate modelling of waveguides and horn antennas and the simulation of the effects when radiating with them on surfaces with and without cracks.

For example, Figure 8 shows the Ansys 3D environment with a model of a rectangular waveguide (in blue), which is used to irradiate a steel material sample without cracks (in green) from a distance that can be varied. This allows us to observe its behaviour and compare it with that of the metal plate with a rectangular hole of 20x20 mm and a depth of 10mm which emulates a fairly large crack, depicted in Figure 16-10, to identify the differences in the results. This probe is typically used as both a source and detector, with the presence of the crack manifesting as a change in the S11 scattering parameter. For this particular test, several distance values were tested and Figure 9 shows the S11 result for a distance value of 26mm. In this case, it can be observed that there is a more resonant response at frequency values of 32.2GHz and 37.46GHz. The same behavior can be observed for the case with the crack, as evidenced by Figure 16-11. In that case, the resonant behavior is observed at 30.99GHz and 35.74GHz, with a large valley at the

first frequency value.

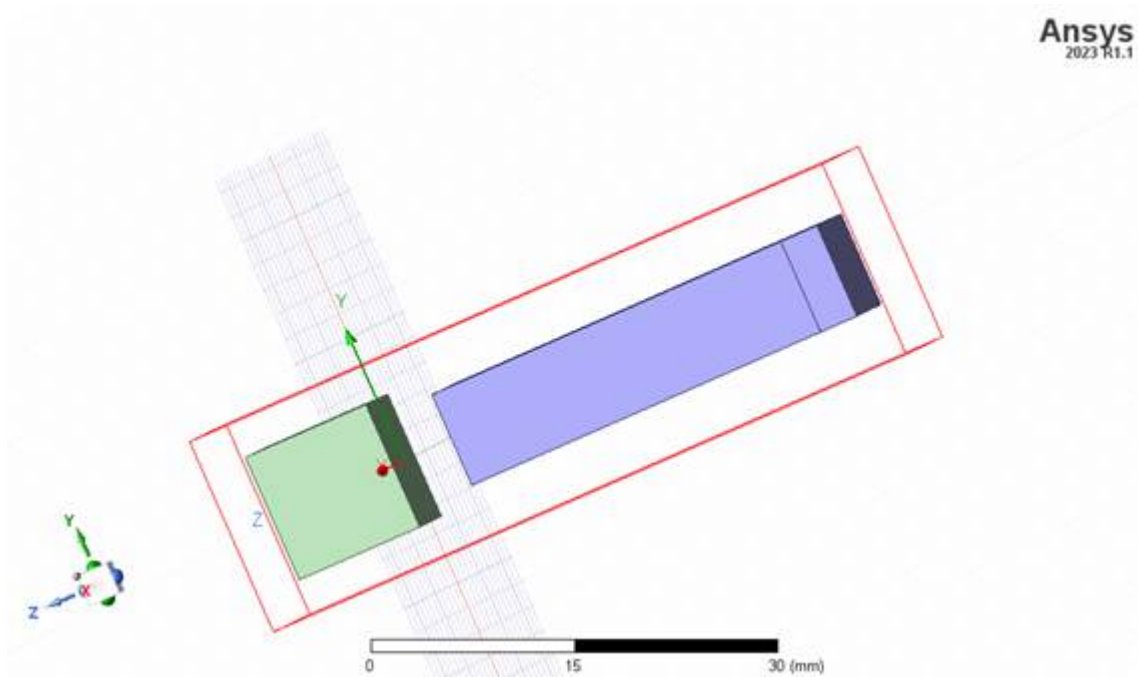


Figure 16-8: ANSYS model of a rectangular WR90 waveguide that radiates a steel block without cracks

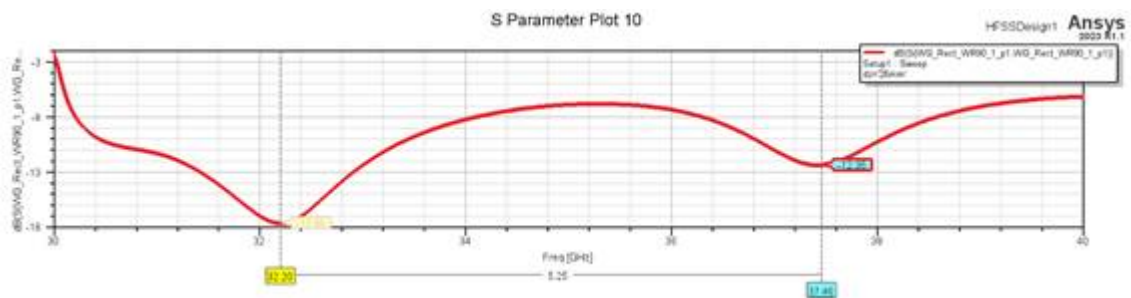


Figure 16-9: Simulated S11 for a distance value of 26mm between waveguide and surface

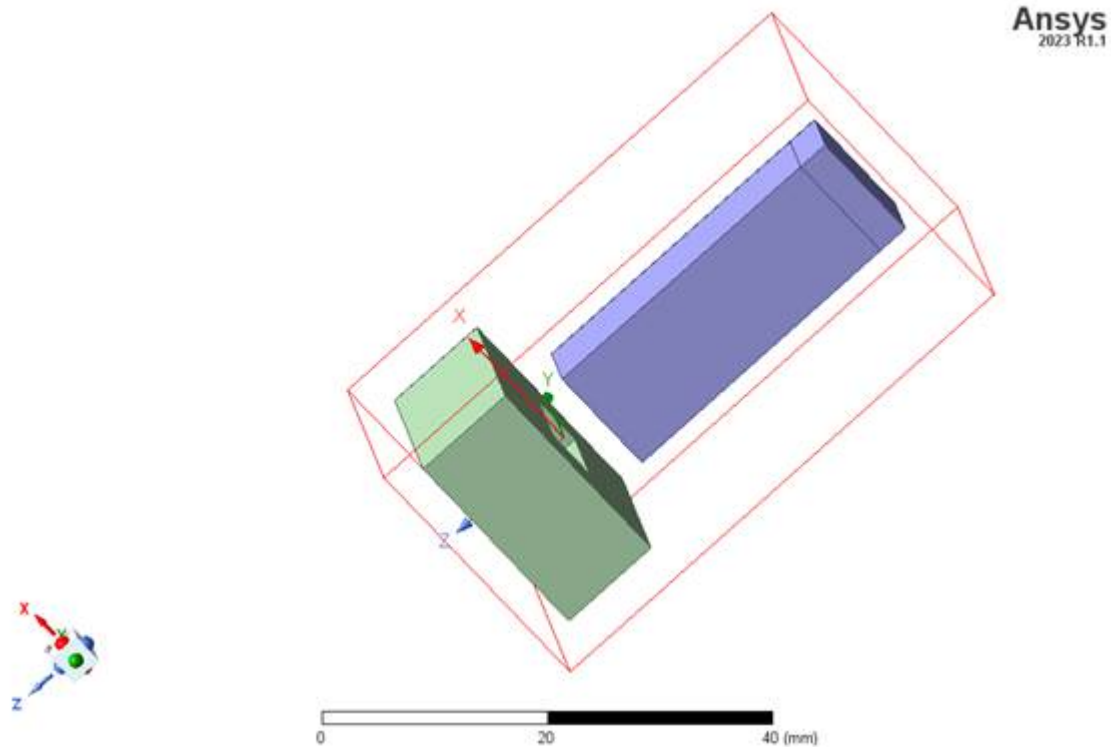


Figure 16-10: ANSYS model of a rectangular WR90 waveguide that radiates a steel block with a rectangular crack

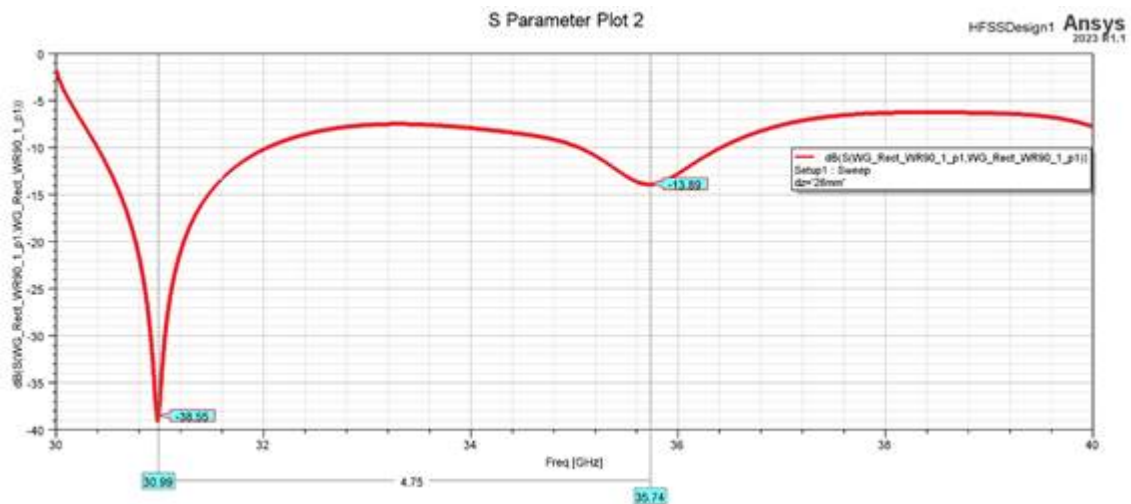


Figure 16-11: Simulated S11 for a distance value of 26mm between waveguide and the surface with a crack

To further analyse the response of the material with the crack, the S11 was broken down into its magnitude and phase components, shown in Figure 16-12 and Figure 16-13. The graph of the magnitude of the reflection coefficient shows the following: values close to 0 indicate good impedance matching, meaning that almost all the incident wave energy is transmitted beyond the input port and very little is reflected. In the context of crack detection, a low value could indicate that there are no significant discontinuities affecting the wave transmission. On the other hand, values close to 1 indicate almost total reflection, which can result from a strong discontinuity or very poor impedance matching. In material testing, a high value indicates that most of the signal is reflected by the material. Small variations in this value at different points in the surface may

suggest the presence of a crack or significant defect.

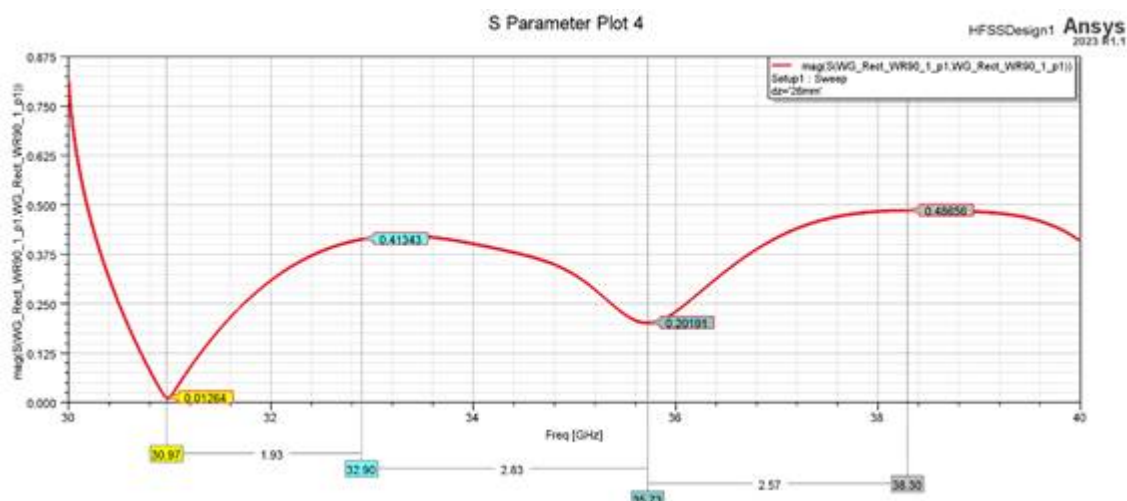


Figure 16-12: Magnitude component of the S11 result obtained for a distance value of 26mm between waveguide and the surface with a crack

Regarding the imaginary part of the reflection coefficient, values close to 0 suggest that there is no large reactive component in the reflection, which may indicate that the waveguide environment is relatively homogeneous, while significant positive or negative values may indicate the presence of inductive or capacitive elements in the environment, respectively. Changes in these values could indicate variations in the material characteristics that might be related to cracks. We can observe that the frequencies at which these changes could be more representatives are 32.9 GHz, 35.04 GHz, and 38.3 GHz, which are in the frequency range selected for the real environment.

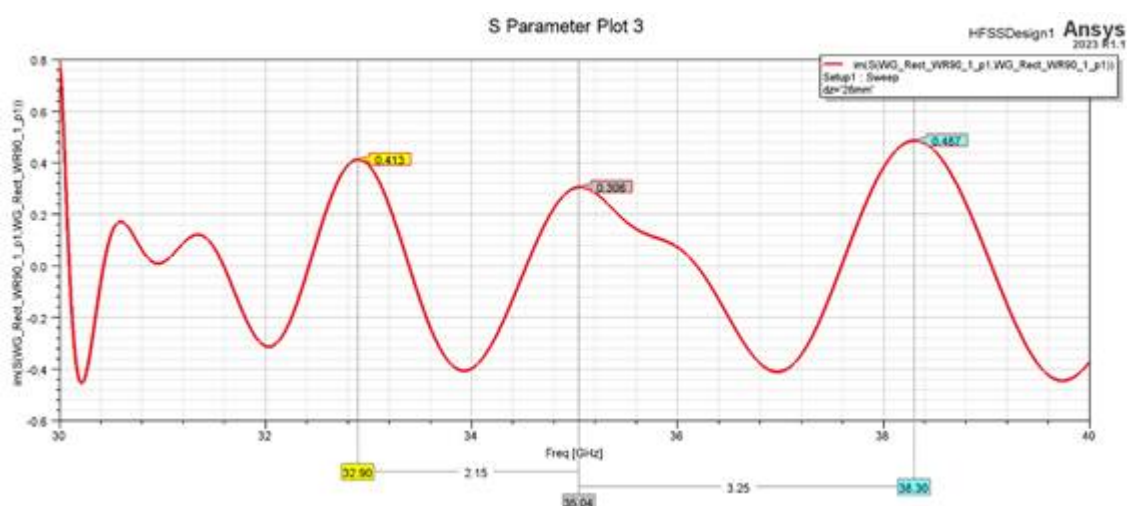


Figure 16-13: Imaginary component of the S11 result obtained for a distance value of 26mm between waveguide and the surface with a crack

In addition to these results, the simulation environment also allows for the testing of the imaging algorithms that will be used to provide an image of the crack once it is detected. An example can be seen in Figure 16-14, where a steel surface with three cracks of different depths has been

irradiated with the simulated waveguide and the S11 results of the scan have been processed using a Python script to obtain the image shown in Figure 16-15, where the crack depth is given by a shaded scale.

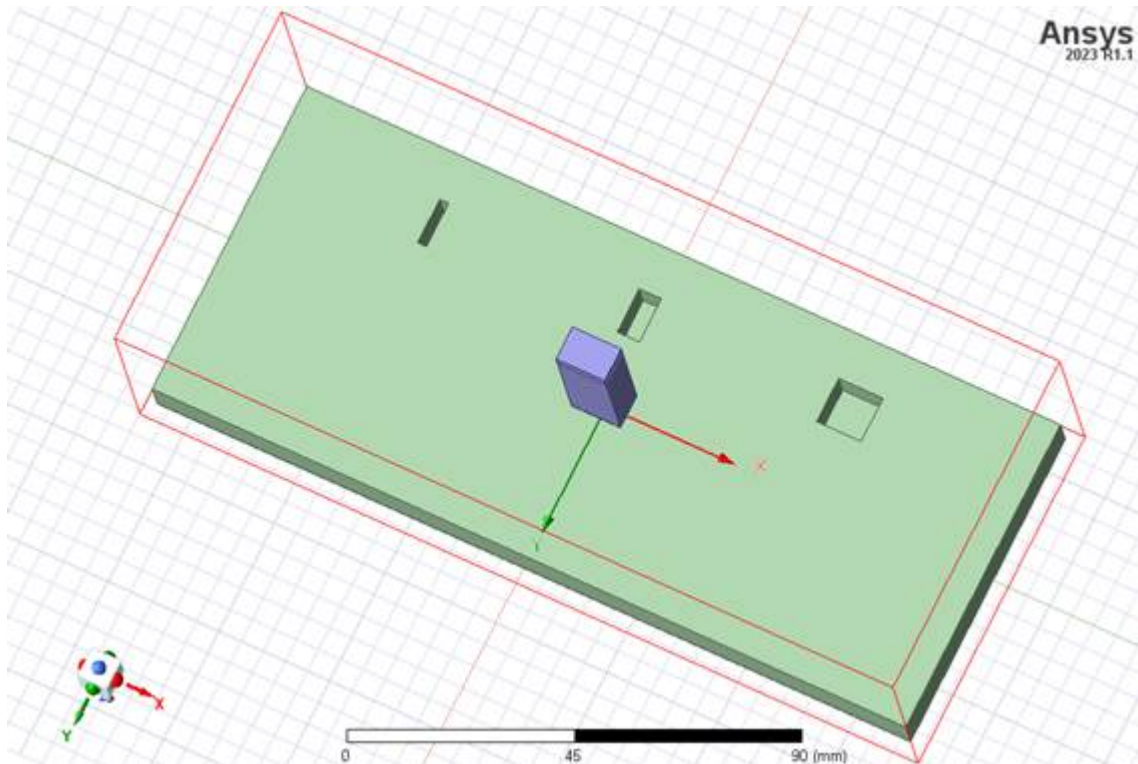


Figure 16-14: ANSYS model of the steel surface with three cracks

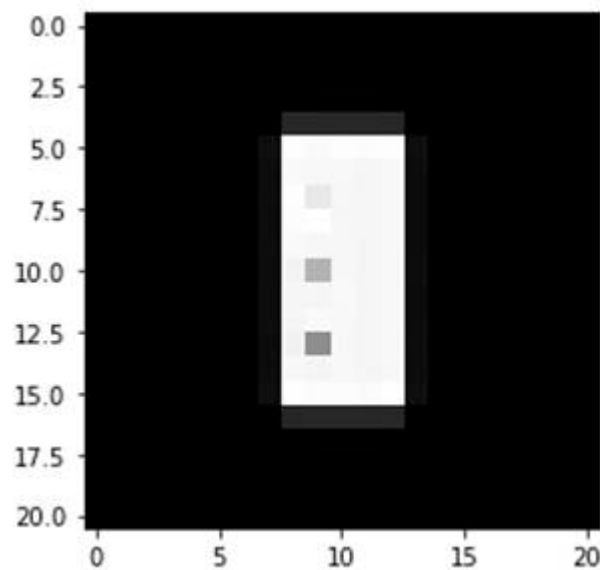


Figure 16-15: Image obtained from the processing of the S11 data using the python script

16.3.5. Off-line processing of laboratory signals and simulations

The data collected from the simulations and measurements performed so far has been stored physically on computers in the laboratory, with backups online for the most sensitive or relevant information. Regarding its processing, several programs have been used, depending on the case:

- ANSYS simulation data was processed using the software to plot relevant results and exported to other formats, like CSV files, S-parameter files or graphs.
- Measurement data has been processed using different means, such as Matlab or python scripts to obtain graphs and imaging data of the physical defects on the steel surfaces.

The relevant outputs and data sets have been properly catalogued and time-stamped in order to facilitate access to them in case they are needed in the future.

Regarding the data storage and management once the system is operating on the field, it will be defined as the prototype is being developed, but a system with both physical and cloud storage for the relevant data will be put in place. The data will be properly catalogued and protected, meeting the established legislation and guidelines.

16.3.6. Proof of Concept at Laboratory

This subsection describes the progress and results obtained so far using the setup described in the previous paragraphs. This is a key part of the process, as its results will determine the path to the more realistic implementation of the project and the decisions taken at this stage will impact the draft system architecture.

As it could be observed in Figure 7, the initial steel sheet used for the laboratory tests had larger markings to facilitate the validation of the concept of whether it was possible to identify the presence of cracks by using microwaves. However, further validation steps and cracks includes mor realistic cracks as a progress for the validation of the technology on this application.

For the first version of the assessment, a WR28 waveguide probe was set to transmit over the 26.5 GHz to 40GHz (Ka band) range, using a Vector Network Analyzer (VNA) to capture the reflected signal coming back from the material, represented as the S11 in terms of magnitude and phase. The first measurements were performed manually over certain points of the material to determine the optimal frequencies for crack detection. These frequencies were 33GHz, 33.25GHz and 36GHz.

Once the frequencies of interest had been identified, a U-shaped route was swept over the initial steel sheet, as seen in Figure 16-16, taking measurements every 0.1mm over the yellow and red lines and skipping performing measurements over the blue line. Considering that the total length of the sheet is 26cm, 2600 measurements were taken, taking approximately 2 hours to complete the sweep. This should not be a case of alarm, since the process can be simplified as the system evolves, and a thorough approach was being sought at this point.

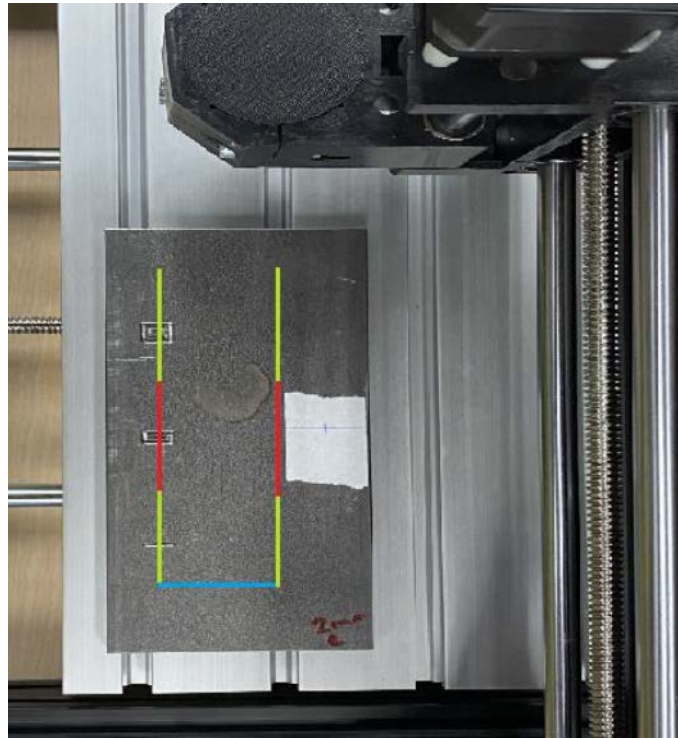
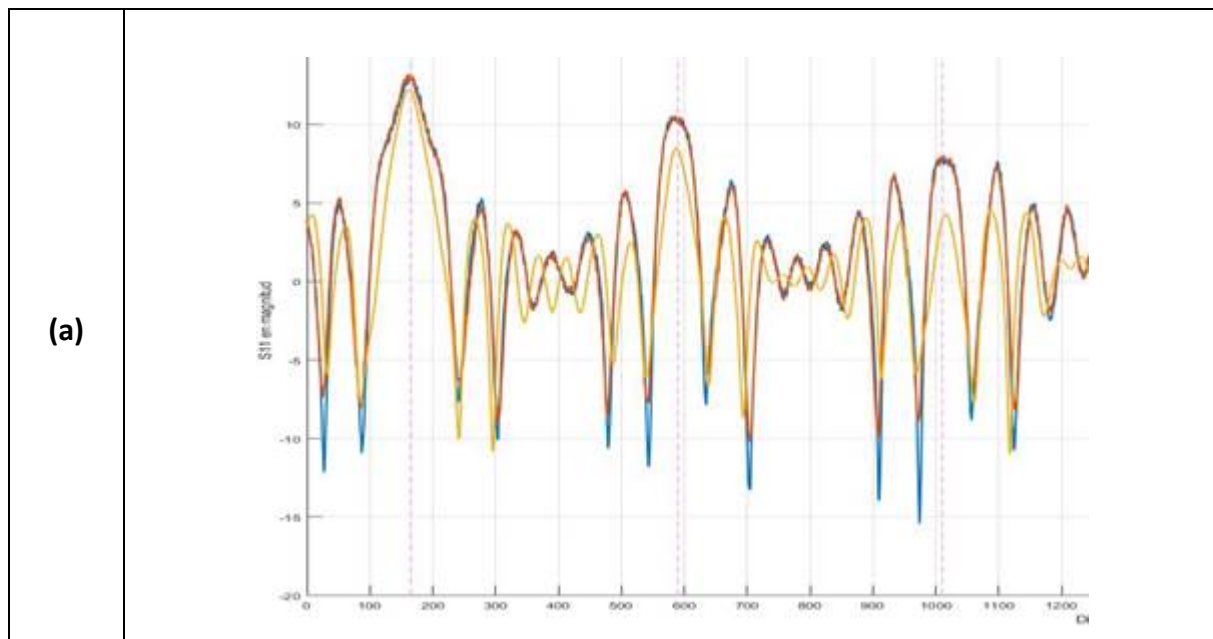


Figure 16-16: . Route followed by the waveguide when performing the measurements

Upon completion of the sweep and once the results were processed using Matlab, it was observed that the magnitude and phase of the S_{11} at the selected frequencies showed changes at the points where the modifications had been done to the sheet, as it can be observed in Figure 16-17.



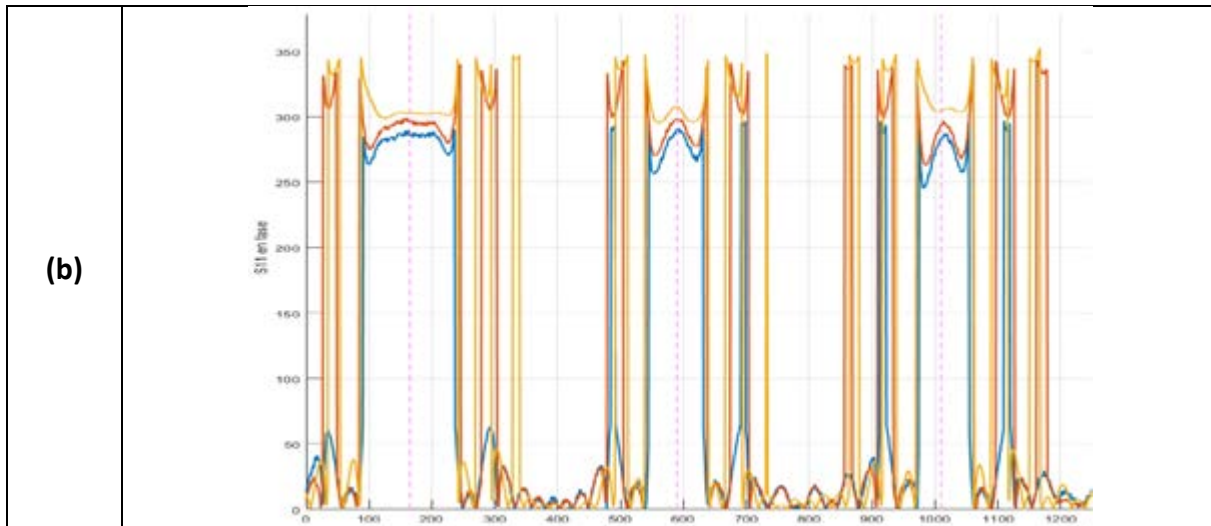


Figure 16-17: (a) Amplitude and (b) phase results of S11 at 33 GHz (blue), 33.25 GHz (orange) and 36 GHz (yellow) along the route

Cleaning up the measurement data and using a proprietary algorithm, the graph shown in Figure 16-18 was obtained, clearly delimiting the areas where the cracks were observed.

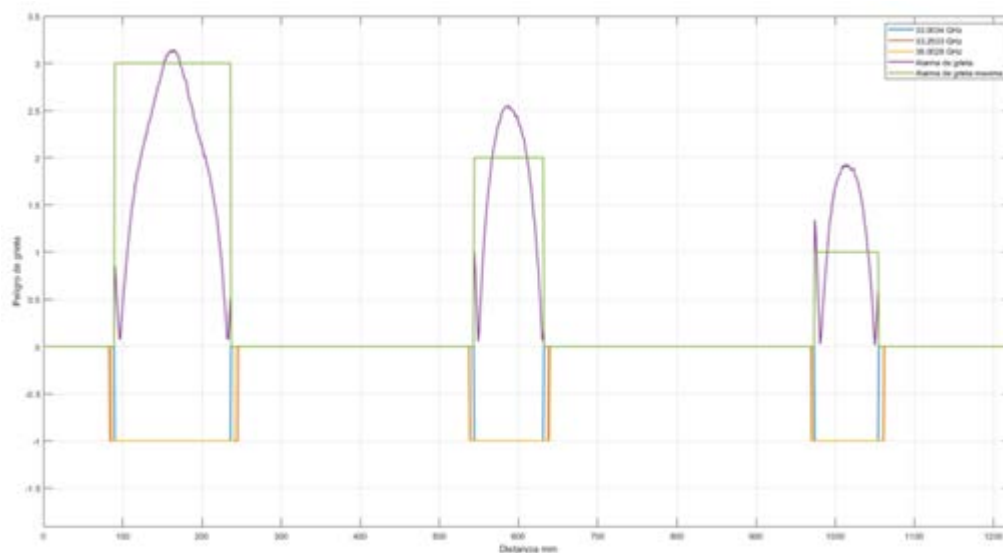


Figure 16-18: Output signals of the crack detection algorithm

Once the initial hypothesis has been demonstrated, the next step is to validate the system performance with smaller cracks (5mm length, 1mm width and 500 μ m depth), as represented in Figure 16-19.

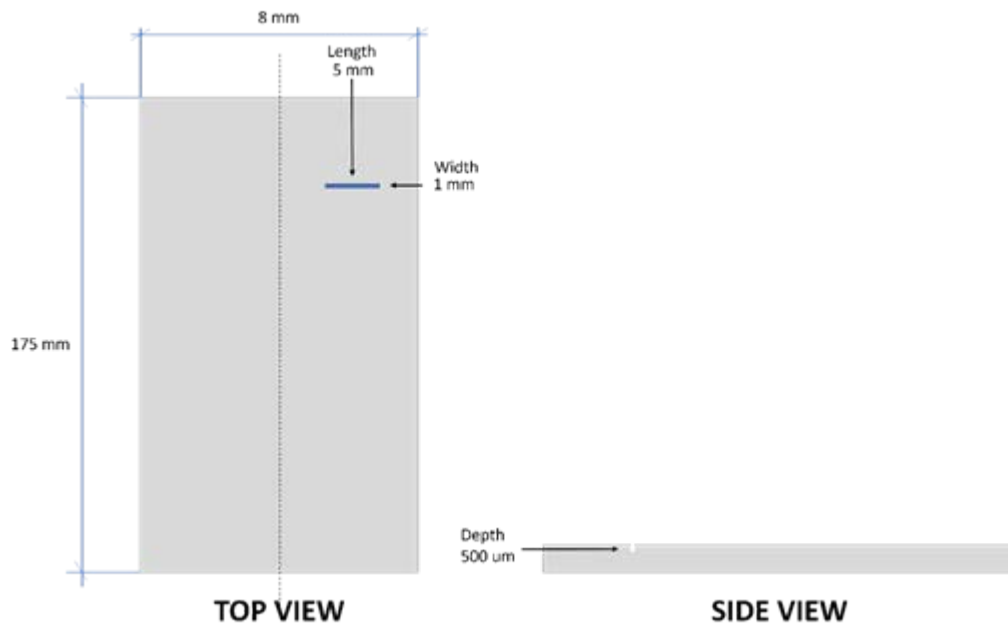


Figure 16-19: Dimensions of the steel sheets used to emulate cracks in the laboratory setup

16.3.7. Proposal for system architecture and refining of system requirements.

Based on the work carried out so far and the extensive literature analysis, the 36 GHz frequency has been identified as the most promising for the detection of defects on the surface of railway tracks. With this target in mind, it has been decided to keep experimenting in the laboratory environment with a deeper focus at this frequency and its immediate range and with enhanced tools and probes. To do so, several options that consider the use of a VNA are currently being explored.

However, when considering a portable prototype of the system that can be installed in an inspection wagon, the concept of integrating a specialised VNA operating up to 50GHz seems ludicrous from a cost and assembly point of view. Therefore, one solution would be to use a VNA that operates at lower frequencies and upconvert the transmitted signals to the 36GHz frequency and then downconvert the reflected signal to the desired frequency value, in a solution that could be close to the one shown in Figure 16-20.

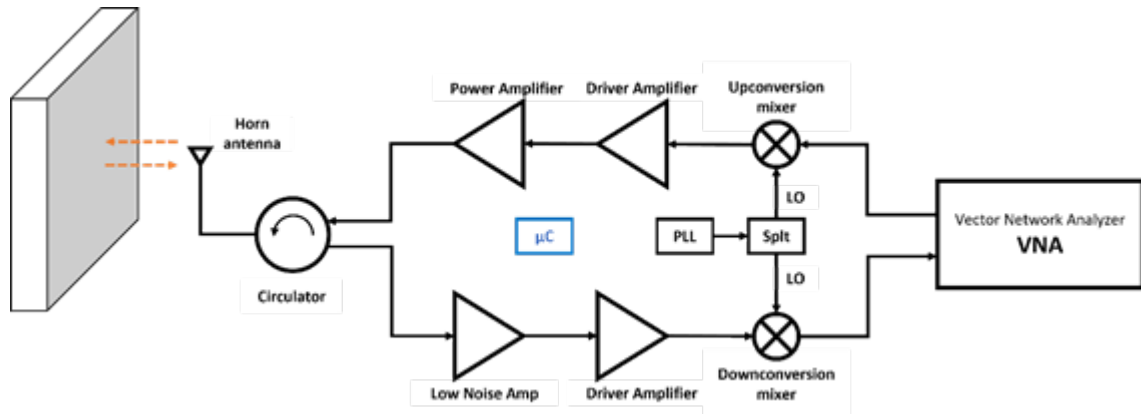


Figure 16-20: Block diagram of the proposed system

As it can be observed, this solution keeps the working principle applied in the initial tests of using a single antenna element, although in this case the waveguide has been replaced by a horn antenna operating in the target frequency range. Given the circuitry that has been added, a circulator has also been placed to isolate the TX and RX signal paths and prevent leakage that could negatively impact the results. In case the isolation between the two paths cannot be guaranteed, another solution is presented in Figure 16-21, where two separate and highly-directive horn antennas would be used for each TX and RX paths. This solution would be more costly and implies a slight increase in complexity due to the placement of the two antennas close together so the measurements can be performed.

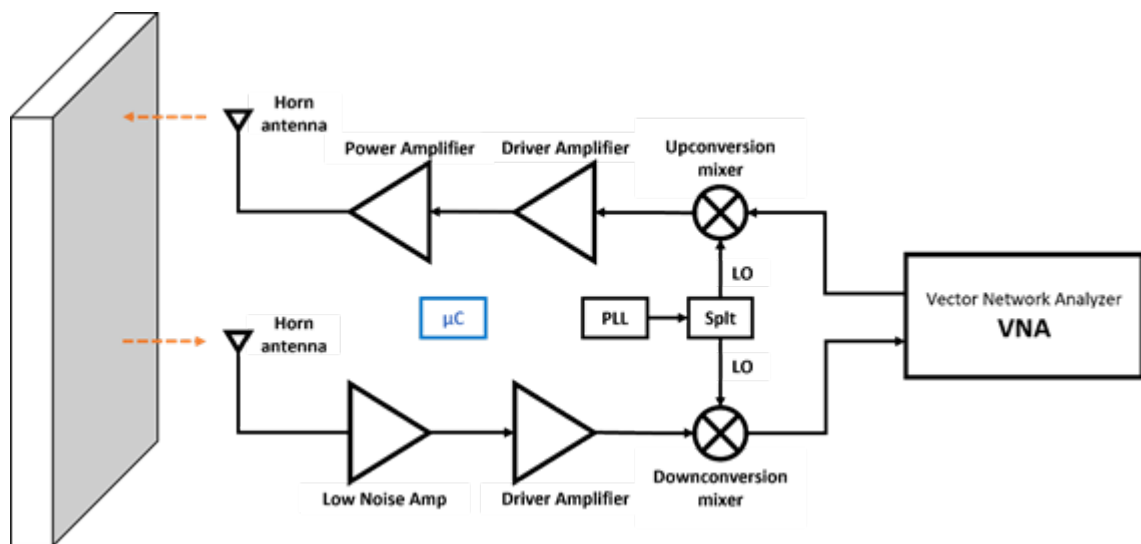


Figure 16-21: Second option for the implementation of the proposed system

Once these two system concepts are analysed and validated, independently of the monostatic and bistatic solution for the antennas, steps will be taken towards the implementation of the portable prototype, which will follow a diagram like the one presented in Figure 16-22. This architecture needs to be better understood in order to be considered as a subsystem for an inspection vehicle.

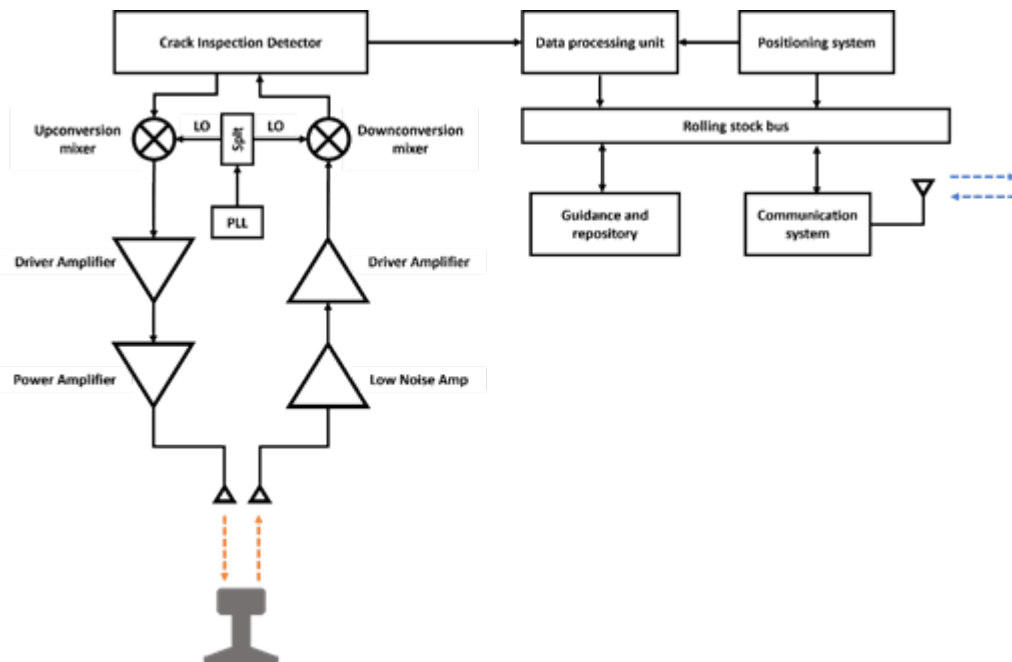


Figure 16-22: Block diagram of the complete microwave inspection system

With this diagram, the goal is to provide a system that can process the electromagnetic signals in real time and tag the location of defects along the track as the train goes along its route.

Regarding the system requirements for the proposed system, the low TRL of the activity, up to now, and its current highly experimental nature does not allow to provide a closed set of specifications. However, based on the literature analysis and the performed tests so far, it has been decided that the system will operate in the K- and Ka-band frequency bands, with the goal to detect cracks on the rail from a distance of less than 15cm. Regarding the dimensions of the cracks that will be detected, the length will be in the range of 1 to 5mm. As for the width of the cracks, 1mm would be the typical value for detection, although the capacity of detecting smaller widths will be pursued. Finally, the detectable crack depth will be set to 500µm.

It must be noted that these requirements have been set as a baseline to guarantee the correct operation and integrability of the system. Additional requisites, such as scan and processing speeds, imaging resolution and location accuracy will be defined at a later stage in the project, depending on the next steps to be performed in WP11.

16.4. Status handed over from WP10 to WP11

Considering the conclusions and follow up activities described in the previous section, the next steps to undertake in the development of the project and moving forward to WP11 will be the refinement of the simulations in order to represent a system closer to the architecture that would be validated for it use. That will explore its potential integration in future concepts of autonomous inspection and monitoring vehicles of any kind and will also reveal its limitations.

To do so, a simplified draft of a crack detection system will be simulated and built following the proposed architectures and its performance will be evaluated regarding the set requirements. Once these simulations and tests are completed, the integration of the design and algorithms will be adapted for the system in a train environment on the field with real tracks to inspect, as it will be done in subsequent projects. Additionally, other functionalities such as the generation of crack

images from the acquired measurement data in the lab will be also developed as WP11 progresses.

16.5. Preliminary results that can be used

As presented in the previous subsections, the performed simulations and laboratory tests produce some relevant data that are the base of the results that can and will be used in the following steps. Namely, we could find the following:

- Ideal data from electromagnetic simulations. This data consists in S-parameter files from ANSYS simulations, such as reflection at the antenna port (S_{11}) for the single antenna scenario simulations.
- Raw S-parameter data obtained from quasi static measurements of steel samples in the laboratory. Data is and will be obtained for setups with different antenna types and placements. When considered for all the steps, this data covers the whole sample of metal and a wide range of frequencies, focusing on those that are of interest for the detection of cracks on the surface of the metal sample used for the simplified testing. At later stages of the project, this data will come from the measurements performed on pieces of real railway tracks, with and without defects, also performed in the lab.
- Outcomes of the digital processing of both the simulation and laboratory data, which will include refinement, filtering, etc, to help in determining the presence of a defect. An example of this will be the imaging data obtained from the S-parameter file processing.

17. INSPECTION TURNOUTS: ANALYSING 3-DIMENSIONAL RECONSTRUCTION

This section describes the inspection system being developed at CEIT to establish the health status of turnouts by analysing their three-dimensional reconstruction. The preparatory work has taken place at the pilot site in Spain, provided by ADIF.

17.1. Introduction and methodology

Turnouts are a critical asset of the railway system, enabling train vehicles to take different directions. A turnout is split into two main parts (switch and crossing) and has up to four possible running modes (through or diverging direction and facing or trailing move). The dynamic forces due to wheel-rail contact are heavily affected by the degradation of the crossing nose and/or wing rail mainly by wear degradation.

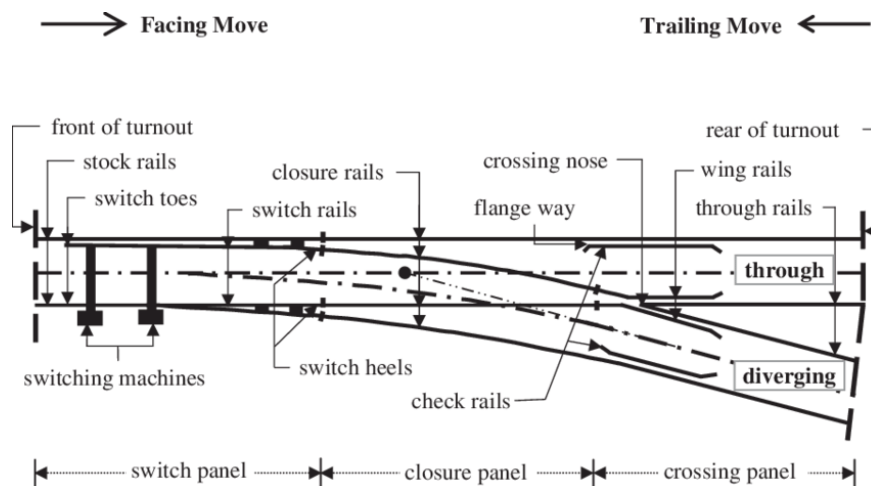


Figure 17-1: A turnout scheme

Turnouts are critical components of railway infrastructure, and their condition is essential to ensuring the safe and efficient operation of trains.

An automatic inspection system will be proposed with the aim of carrying out three-dimensional reconstruction of train crossings. After creating detailed 3D models of turnouts, this information will be used to identify defects and track their development over time. The technology to develop aims to detect the health status of the crossing by means of 3D vision inspection system. Vision systems have qualities that allow for the reconstruction of 3D geometry with great precision. The use of this technology to inspect train rails is widespread [71] [72]. The advantage with the rails is that they have a very simple geometry, which facilitates the implementation of this technology. However, as their name suggests, vision inspection systems can only reconstruct geometry that is visible under certain conditions (occlusions, shadows, ambient lighting, etc., can degrade or prevent the reconstruction of some areas). These problems become more pronounced when inspecting complex geometries, such as railway turnouts.

Railway turnouts are essential for network flexibility but represent complex, high-stress points susceptible to wear and failure. Their integrity is paramount for safety and operational efficiency. Traditional inspection methods, relying heavily on manual visual checks and handheld tools, face

limitations in speed, objectivity, consistency, and the ability to capture comprehensive data. These limitations, coupled with the safety risks for inspectors, have driven the adoption of automated technologies. Among these, vision-based systems, utilizing cameras and laser scanning, have emerged as powerful tools for detailed, objective assessment of turnout conditions. The following paragraphs focus on the state-of-the-art vision-based inspection technologies for railway turnouts. Not only in the literature, but also in the current inspection techniques in the pilot site.

Vision-based systems employ cameras, often combined with laser projection or LiDAR, to capture detailed visual and geometric information about turnouts and their components.

- **Cameras:** High-speed line-scan or area-scan cameras acquire detailed 2D images of the track surface, capturing visual details of components and potential surface defects [73]. Artificial lighting (strobes, lasers) is often used to ensure consistent image quality regardless of ambient conditions.
- **Laser Scanning / 3D Profiling:** Systems project laser lines or patterns onto the track structure. Cameras record the shape of the projected light, allowing for the reconstruction of precise 3D profiles or point clouds of rails, fasteners, and other components. This enables accurate geometric measurements.
- **LiDAR:** LiDAR systems use pulsed laser light to measure distances, creating extensive 3D point clouds of the track and its surroundings, useful for clearance measurements and overall geometric context.

The rich data captured by vision systems enables automated detection and measurement of numerous turnout features and defects. Several companies offer commercial inspection solutions heavily reliant on vision technology for turnouts:

- **ENSCO:** Provides the **Point Asset Inspection System (PAIS)**², integrating laser profiling and machine vision to assess turnout condition, measure wear (frogs, switch blades), and detect component defects. They also offer various imaging systems (RCIS, TCIS, RSIS) applicable within turnouts.
- **Pavemetrics:** Offers the **LRAIL** system³ [\[5\]](https://www.pavemetrics.com/applications/rail-inspection/laser-rail-inspection-system/), using high-resolution laser scanning and AI for automated inspection of turnouts (points, frogs, guard rails, flangeways, geometry) and components like ties and fasteners. It captures 2D images and 3D profiles simultaneously.
- **Plasser & Theurer:** Provides "**Complete turnout measuring including video**"⁴, using non-contact laser sensors and cameras to capture geometry and component condition (fastenings, sleepers, drives) under load, employing AI for analysis.
- **DMA:** Offers the **Turnout & Crossing Measurement System (TCMS)**⁵, an automated optical (camera/laser) and inertial system measuring key turnout parameters like

² <https://www.ensco.com/rail/point-asset-inspection-system-pais>

³ <https://www.pavemetrics.com/applications/rail-inspection/laser-rail-inspection-system/>

⁴ <https://www.plassertheurer.com/en/pt-research/artikel/complete-turnout-inspection-in-four-minutes>

⁵ <https://dmatorino.it/tunout-crossing-measurement-system/>

Free Wheel Passage (Fwps), Nose Protection (Npof), Flangeway Depth (Hfw), gauge, wear, and alignment.

- **Harsco Rail / ZETA-TECH (Wabtec):** Developed the **Automated Switch Inspection Vehicle (ASIV)**⁶ using high-sampling-rate laser rail profiling and **SwitchWear** software for detailed 3D analysis of switch points, stock rails, frogs, and closure rails, identifying wear, damage, and geometric deviations.
- **voestalpine Railway Systems:** While primarily a turnout manufacturer, offers intelligent turnouts with integrated monitoring systems (e.g., **Roadmaster**) that utilize sensors (potentially including vision) for continuous health tracking and predictive maintenance.

ADIF is responsible for inspecting the site where the pilot tests will take place, performing a comprehensive series of **geometric** evaluations that include both traditional **manual** measurements and advanced **ultrasonic**-based assessments to ensure that all dimensions, alignments, and tolerances meet the required specifications before testing begins.

These activities are part of the broader preventive maintenance procedures defined in ADIF's technical instruction ADIF-IT-301-001-VIA-28, which establishes the framework for the inspection and monitoring of switches and crossings. This framework is aligned with the guidelines set forth in the "Criterios Generales de Mantenimiento Preventivo de Infraestructura y Vía" and coordinated through digital platforms such as MPI and SIOS.

Each method has specific advantages, limitations, and areas of application, often conditioned by the materials used in switches and crossings components. Manual inspections focus on geometric parameters and material condition through direct measurement tools and visual inspection, while ultrasonic methods are used for internal defect detection. The technical instruction specifies tolerances and frequency of measurements depending on the switch and crossing type and location and dictates the classification of defects according to severity and urgency of intervention. Results are logged in digital systems to ensure traceability and follow-up.

➤ **Manual geometric inspections:** This method follows the procedures established in the ADIF Standard Vía NAV 7-3-8.2, particularly using wear control rules and specific gauges for inspecting switch blades and stock rails in the turnout assemblies.

Its main characteristics are:

- A cylindrical rule with interchangeable templates (templates No. 11, 12, 6, and grinding templates) is used to simulate wheel profiles (new or worn).

⁶ <https://etheses.bham.ac.uk/id/eprint/7348/1/Rusu17PhD.pdf>



Figure 17-2. Bladed wheel geometric measurement

- The measurements assess:
 - Lateral and vertical wear.
 - Wheel-rail contact angle.
 - Distance between the switch point and the stock rail.
 - Alignment and adjustment of key components (visual and contact verification).
- Measurements are taken at specific points of the turnout:
 - In curved alignments (radius < 1500 m), template No. 11 is used.
 - In straight alignments or with larger radii, template No. 12 is used.



Figure 17-3. Manual Switch Rail Measurement

- Critical areas measured include:
 - Tip of the switch Blade.
 - Area 30–50 mm before the tip.
- Gauges of 3, 4, and 5 mm are used to assess compliance with minimum geometric tolerances (e.g., a minimum qR of 6.5 mm for the flange face).

This method is versatile and applicable to all parts of the turnout, including those made of manganese steel, which is common in monoblock crossings.

An additional technique commonly used during manual inspections is the **KRAB method**, a semi-automatic measurement system employing a lightweight wheeled trolley equipped with electronic sensors. The KRAB system allows precise measurement of key geometric parameters such as:

- Track gauge.
- Cant (superelevation).
- Longitudinal level.
- Alignment (versines).
- Warping (twist).

These measurements are recorded digitally as the operator rolls the trolley along the track. Data is transmitted via Bluetooth to a mobile application (e.g., KrabDroid 2.0) and analyzed using dedicated software (Krab 11), allowing integration into digital platforms like MPI and SIOS for long-term monitoring and traceability.

The KRAB method is especially valuable in complex turnout zones and in materials such as **manganese steel**, where ultrasonic inspection is not reliable. Its portability and precision make it an essential complement to traditional manual tools, enhancing both efficiency and accuracy in routine geometric inspections.



Figure 17-4. Trolley KRAB

- **Ultrasonic Geometric Inspections:** In this method, ultrasonic inspection equipment is mounted on self-propelled vehicles (such as track inspection cars or specialized vehicles). Allows automatic measurement of geometric parameters without direct manual intervention.

Continuous data is collected on parameters such as:

- Flangeway between rail and guard rail.
- Track gauge.
- Guard rail spacing.
- Alignments and superelevation.

Ultrasonic sensors are designed to operate on standard rail materials that are compatible with ultrasonic wave propagation.

Geometric inspection using onboard ultrasonics faces significant limitations in railway turnouts, mainly due to the incompatibility of the method with manganese steel, a common material in monoblock crossings. This type of steel attenuates and disperses ultrasonic waves, preventing reliable measurements in those areas. Additionally, factors such as the complex geometry of the turnout, the presence of dirt or burrs, and the need for precise sensor positioning can affect the quality of readings. Therefore, this technique must be complemented with manual inspections to ensure a comprehensive assessment of the turnout's geometric condition.

Currently, the inspection combines both manual and automatic techniques. Manual inspection, although more labor-intensive, is irreplaceable in certain critical areas made of materials unsuitable for ultrasonic techniques (such as manganese steel). On the other hand, automatic ultrasonic inspection enables rapid and large-scale data collection in compatible sections, contributing to more efficient maintenance management. The complementarity of both methods ensures complete and reliable coverage of the inspections needed to maintain railway turnouts in optimal safety conditions.

In the methodology of this application, two different parts can be found; on the one hand, the three-dimensional reconstruction of the turnout and on the other hand, the analysis to identify defects.

17.2. Work progress

In D10.1, the groundwork for inspection of railway turnouts by analysing their 3-dimensional reconstructions was outlined. This section highlighted the importance of automated, high-precision monitoring techniques compared to traditional manual methods. The initial description in D10.1 covered the fundamental concepts, the expected use of various sensor technologies (cameras, LiDAR, etc.), and briefly mentioned the methodological framework, including:

- General concept of using vision inspection systems for 3D reconstruction.
- Intention to use mobile scanning systems integrated on vehicles.
- Basic approaches for reconstruction (relative pose estimation through sensors and synchronization, and model-based reconstructions using existing CAD data or previously captured models).

The main intention at this stage was to establish the viability of using advanced vision technologies to automate the inspection of railway turnouts, without going into significant detail about specific implementations or test results. The work progress significantly extends the groundwork laid in D10.1, demonstrating concrete advancements and detailing specific actions undertaken.

Field testing at Rifa

While the inspection technology and method in D10.1 were primarily conceptual, an actual field implementation has been carried out at the Rifa pilot site in Spain, provided by ADIF. Due to the unavailability of a dedicated inspection vehicle, a practical, manual 3D reconstruction method was conducted. The chosen solution was a dynamic area scanner capable of capturing structured light patterns, allowing detailed geometry mapping. It utilized SLAM techniques for real-time position tracking, facilitating the integration of multiple scans. Constraints identified included limited computer memory and physical factors like cable length, which required multiple scanning passes,

each covering approximately 2x2 meters, later merged using ICP algorithms. An area scanner was used to reconstruct the turnout. An area scanner works by projecting structured light patterns onto a surface and capturing the reflected light with high-speed cameras to generate detailed 3D images. This process enables precise measurement and mapping of the scanned area, making it ideal for applications in industrial inspection, robotics, and quality control. The scanner used is a dynamic area scanner, which allows capturing the environment without the need for the scanner to remain stationary. This scanner comes with software designed for real-time generation of high-quality 3D meshes from point cloud data. For reconstruction, the scanner must move around the entire environment to capture it fully, ensuring visibility of hard-to-reach areas. The software tracks the scanner's position by using the geometric information from the captured images with techniques known as SLAM (Simultaneous Localization and Mapping). Knowing the position of the scanner makes it possible to integrate all captures into a single coordinate system and generate a mesh with that information. To avoid losing the tracking of the scanner, it is necessary to move it very smoothly over the surface to be captured. Due to constraints such as computer memory, cable length, and the need to maintain tracking, the entire rail switch was not reconstructed in a single pass. Multiple passes were made, with each pass capturing an area of approximately 2x2 meters. It was ensured that there is common geometry between passes, allowing the integration of all passes into a common model during post-processing using ICP algorithms.

Turnout Health Analysis

This subsection explicitly describes methodological refinements, such as the definition of specific areas where defects are most common and detailed explanations of defect identification processes. The geometry and operation of the turnouts causes that the defects are generated in specific areas. The type of defect in each area is different and has its own characteristics. This means that the algorithms to be developed to identify them must be adjusted to these characteristics.

Therefore, the first step is to identify the different areas where wear and defects appear.

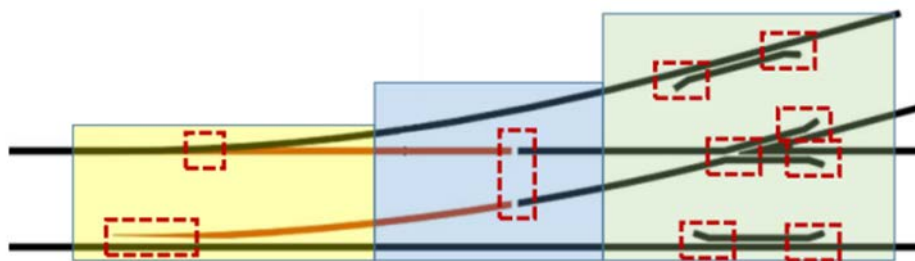


Figure 17-5: Components of a turnout (source Chalmers University, paper July 2010)

Once the different zones are identified, an analysis will be carried out to identify the defects associated with each zone.

Comparative Analysis with CAD models: A detailed workflow for defect quantification is presented, where the 3D reconstruction obtained in the field is compared with the original CAD model or previous reconstructions.

A critical new phase, the registration of these models into a common coordinate system, was explicitly introduced to enable precise comparisons and defect tracking over time. The main errors will be worn and the way to identify and quantify it will be by comparing the 3D reconstruction with the original CAD model. Before the comparison can be made, a registration phase is necessary where the CAD model and the 3D reconstruction are positioned in a common coordinate system. In the case that the original CAD model is not available, a time-based analysis can be performed by comparing the evolution of defects in reconstructions carried out at different times. In this case, a registration phase will also be performed between the reconstructions made at different times, allowing the estimation of the evolution of previously detected defects and the identification of new ones.

The purpose of having the 3D model was to be able to use it in:

- The turnouts monitoring using acceleration signals. The 3D model will be used to correlate the signals from the accelerometers with defects present in the railway turnout.
- Turnout health analysis, the models will be used to identify defects and track their development over time.

17.3. Achieved results

3D Reconstruction of Turnout at Rifa: After the manual 3D reconstruction was performed at the Rifa pilot site, all scan passes are carefully merged, integrating a unified 3D model. This process results in detailed point clouds of the crossing panel and switch panel in both positions: through and diverging routes (Figure 17-6). These point clouds provide a comprehensive view of the turnout's geometry and condition, facilitating precise analysis and comparison.

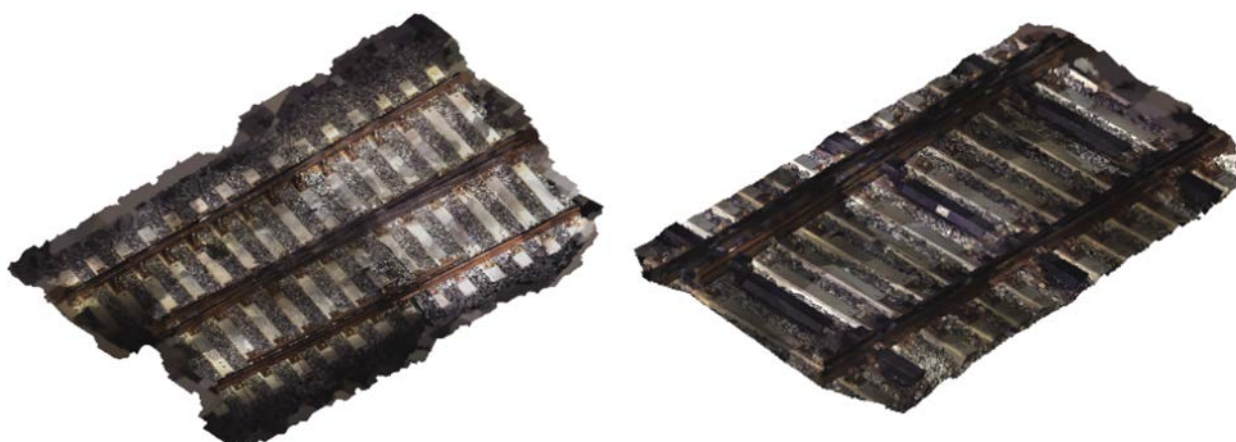


Figure 17-6: The models of the crossing panel and the switch of the turnout

Analytical Results: A preliminary CAD model is used to obtain the first results of the turnout health analysis.

Identification of Specific Defect Areas: Explicit definition of areas prone to wear and defects was conducted to allow targeted defect detection.

Wear and Defect Quantification:

A workflow was established involving a registration step aligning the acquired 3D model with either the original CAD design or previous reconstructions. Following alignment, quantitative metrics (e.g., distances indicating wear or deformation) were computed, allowing accurate measurements of the degradation of railway components over time.



Figure 17-7: Register CAD model and captured model

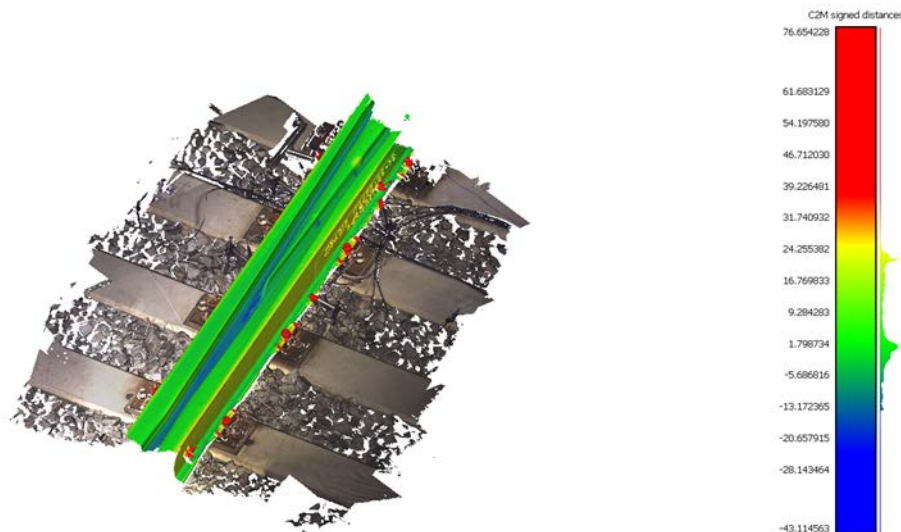


Figure 17-8: Distances

17.4. Status handed over from WP10 to WP11

In WP10, various approaches have been developed and worked on, such as:

- A detailed methodology for automated, vision-based, 3-dimensional reconstruction of railway turnouts was successfully established. The practical implementation validated the use of dynamic area scanners, including structured light projection combined with SLAM-based tracking and ICP-based point cloud integration.
- Demonstrated Field Implementation: A real-world demonstration at the Rifa pilot site was successfully completed.
- A proven data processing workflow was defined and implemented, covering:

- Data collection (raw point clouds and associated sensor metadata).
- Integration and refinement into processed, ready-for-analysis 3D models.
- Registration of obtained data to original CAD models or previously obtained 3D reconstructions.
- Proven Defect Detection and Quantification Approach:
- Clear identification of critical defect-prone regions within railway turnouts.
- Methods to quantitatively measure and track turnout degradation (wear, deformation) by comparing 3D reconstructions against reference models.

In WP11, a vision inspection system will be designed and tested virtually to inspect turnouts. The System will be placed on a vehicle that will travel on the railway track. Different types of scanners (line scanners, area scanners, cameras, LiDARs, etc.) will be considered as potential components of the inspection system. Additionally, the possibility of moving the scanners relative to the vehicle will be considered, which may allow access to difficult-to-reach areas due to the complex geometry of railway turnouts. The inspection system will capture the environment at regular intervals. To obtain the three-dimensional reconstruction of the turnout, all these profiles must be integrated into a 3D model. This requires knowledge of the relative pose of the scanner among all the captures. Two methods will be used to obtain this information:

The virtual vehicle will be equipped with a series of sensors that capture its speed and orientation. By synchronizing the information from these sensors with the instant of capture, an estimate of the relative pose can be made.

If a 3D model of the turnout is available, this model can be used as the basis for the new reconstruction. This model can be the original CAD of the turnout, or a reconstruction made during a previous inspection. Even if the shape is not exactly the same due to wear, this information is useful.

17.5. Preliminary results that can be used

To date, a comprehensive point cloud scan of a railway turnout has been successfully completed, focusing on its most critical components, such as the switch panel and crossing panel. This scan serves several important purposes.

The scan allows for the extraction of precise rail sections, which are essential for calculating contact points in multibody simulation environments. These simulations help in understanding the dynamic interactions and wear patterns of the turnout under various operational conditions.

The initial scan provides a detailed baseline that can be used for future comparisons. By having this reference, it is possible to monitor changes and degradation over time, ensuring that maintenance can be planned proactively.

The scan enables a thorough comparison of the current wear state of the turnout against its nominal geometry. This comparison is crucial for identifying areas that require maintenance or replacement, thereby enhancing the safety and efficiency of railway operations.

A robust methodology has been defined through this scanning process, which will be used for future studies of any turnout. This methodology includes best practices for scanning, data processing, and analysis, ensuring that similar studies can be conducted with high accuracy and reliability.

18. SWITCH MONITORING

This application comprises many different functions and thus data from multiple sources. Therefore, the data management part will play an essential role for an efficient data fusion approach.

The main tools which will be used for switch monitoring are the following:

- Wayside sensor data
- MBD models of the demonstrator turnouts
- FE models of the demonstrator turnout as well as sub models of certain components
- Analytical models (model based and data driven) applied on both “real” sensor data and output data generated by the simulations which can be considered as “virtual” sensor data

Most of the above-mentioned tools have been developed in the past in different projects such as In2Track2 (Grant agreement number: 826255), In2Track3 (Grant agreement number: 101012456) as well as Rail4Future (FFG Project number: 882504) or PredictiveRailwayMonitoring4.0 (FFG Project number: 871512). The main goal of the current project is to integrate those tools and models into a holistic tool for switch monitoring with the clear purpose of increasing availability and safety, reducing LCC, and enhance maintenance processes by means providing digital solutions.

Within WP10, the generic approach was developed how the individual tools will support each other and how they are linked to each other. The following figure shows how the separate functions are integrated into the smart asset management demonstrator.

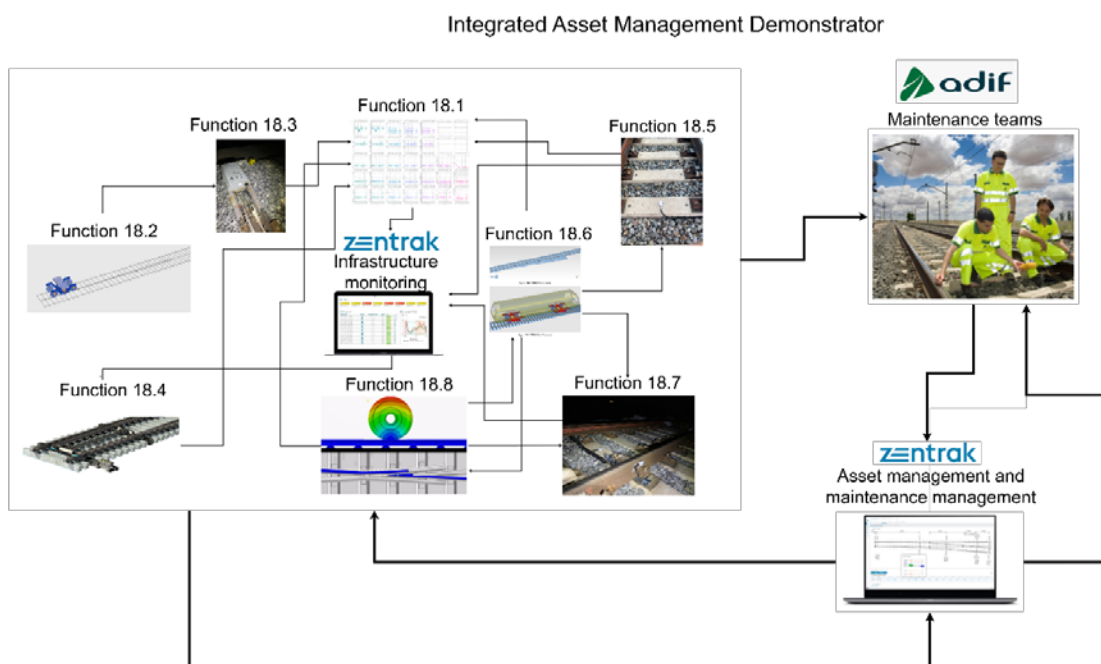


Figure 18-1: Schematic illustration how functions are linked to each other and how the introduced tools are contributing to an integrated asset management demonstrator

The functions introduced in the following subsections are all contributing to the overall integrated

asset management demonstrator. The subfunctions have the aim to cover different damage patterns of the core components of a turnout such as the crossing, the switch device or the point machine with the linked rods which enable a safe operation of the turnout. While each function is focusing on a specific problem, using certain technologies and tools – the overall aim of the function switch monitoring is to provide maintenance teams with information about the current and upcoming health state of the main components of a turnout. The functions which are linked to simulation applications shall serve as a support for advanced data analytics and signal processing, adding physical knowledge to the developed algorithms and thereby improving the capabilities and accuracy of the same. The data management function will combine and clean the data coming from all the different sources and apply machine learning techniques for anomaly detection and data driven decision support. The data coming from the introduced sensor technologies will be used for both data analyses and validation and calibration of the simulation models. Finally, the condition monitoring tool (zentrak infrastructure monitoring) and the asset and maintenance management tool (zentrak asset management & maintenance management) will support the maintenance planning and enable faster fault clearance, thereby improving the overall efficiency of the maintenance processes.

Status handed over from WP10 to WP11

The functions introduced in the following subsections are all contributing to the overall integrated asset management demonstrator. The subfunctions have the aim to cover different damage patterns of the core components of a turnout such as the crossing, the switch device or the point machine with the linked rods which enable a safe operation of the turnout. While each function is focusing on a specific problem, using certain technologies and tools – the overall aim of the function switch monitoring is to provide maintenance teams with information about the current and upcoming health state of the main components of a turnout. The functions which are linked to simulation applications shall serve as a support for advanced data analytics and signal processing, adding physical knowledge to the developed algorithms and thereby improving the capabilities and accuracy of the same. The data management function will combine and clean the data coming from all the different sources and apply machine learning techniques for anomaly detection and data driven decision support. The data coming from the introduced sensor technologies will be used for both data analyses and validation and calibration of the simulation models. Finally, the condition monitoring tool (zentrak infrastructure monitoring) and the asset and maintenance management tool (zentrak asset management & maintenance management) will support the maintenance planning and enable faster fault clearance, thereby improving the overall efficiency of the maintenance processes.

Preliminary results that can be used

First results of the installed monitoring system have already detected certain faults, such as surface defects at a crossing nose, excessive displacements due to poor ballast support as well as increased forces in certain setting levels of the high-speed demonstrators which could be also observed in the simulation results. This information can be already used by the maintenance teams to actively counteract and set appropriate maintenance actions. After the conduction of the proposed maintenance action, such as track tamping, or adjustment of certain components, the change in the monitoring data will be analysed and rated.

18.1. Function: Data fusion methods for monitoring data

The general idea of data fusion is given by validating and merging source sensor data from

different sources such as binary and text files, networked services and databases. The integration of data is typically performed over the following steps:

- Data validation
- Data cleansing
- Data merging

Raw machine data can be stored in classical SQL databases such as PostgreSQL or time series databases such as Influx or Timescale-DB. Besides that, data can also simply be stored in a structured text format such as CSV or in an open binary format such as Apache Parquet or ORC. Using a database or a structured binary format has the advantage that the data itself already contains a data schema, which only permits data in the correct format to be stored there, thus automatically reducing the probability of data errors to occur.

The detection of data errors is done in a *data validation* step. This involves checks for basic data validity, such as if all data fields are filled and have the correct data type or if the values are within a valid range. If such validity criteria are not fulfilled, then during the *data cleansing* process, either the data record could possibly be removed from the data set or corrected based on relevant input from the domain experts. Another option is to raise an error condition for the given data sample. Removing or correcting erroneous data is specifically useful in applications, where the data is used for training purposes in machine learning and enough datasets are available.

Data validation and data cleansing form the basis for merging data from different sources into one data model. Automated *data merging* from different sources can be performed using techniques based on different kinds of similarities from the data channels:

- Unique identifiers, like foreign keys in a relational model ;
- Geographic or temporal vicinity ;
- Domain-specific relations, such as temporal sequences or vicinity of machines in manufacturing processes.

A typical example of data merging is given by combining the data from different sensors in a larger table by means of identifying and matching similar timestamps. If all data sources use the same sampling rate and timestamps, they can easily be transformed into a single table with multiple columns, with a timestamp identifying a row.

However, if the sensors deliver data with different timestamp sampling rates or shifted starting times, matching up the data involves processes such as resampling or adding an offset to the measurement timestamps. In addition, timestamps with missing values for certain sensors can require resampling including the interpolation or forward filling of sensor values. Depending on the use case, missing values can be fine but may also indicate that the overall data model – like a table containing all sensor data – needs to be revised to improve query or processing performances. Also, disallowing null values can also help with automatic data quality improvement through enabling automatic data validation.

A possible approach to prevent a massive number of null values due to mismatched timestamps is to use a so-called *long* table format. While a wide format represents the data from every sensor in a different column, a long format contains the sensor metadata like the identifier or name in a

separate column, putting each measurement identified by a unique combination of sensor and timestamp into a separate row of the table.

18.1.1.FP3-IAM4RAIL Turnouts Data Pipeline

Within the FP3-IAM4RAIL project, the turnouts dataset is categorized into two distinct groups: datasets for high-speed turnouts and datasets for mixed traffic turnouts. For high-speed turnouts, data is collected from two specific regions of each crossing — the crossing area and the switching area — with each region equipped with two types of sensors: the analogue acoustic sensor and the multi-sensor.

All datasets associated with both high-speed and mixed traffic turnouts have been made available via an Amazon Web Services (AWS) S3 bucket, where they are stored in Parquet format. However, the data still requires retrieval, validation, and integration before it can be used for further analysis.

To facilitate this process, a Python module has been developed to automate the download of Parquet files from the S3 storage. The module performs data validation using the Pandera⁷ Python package, which allows the definition of target data schemas and the enforcement of constraints such as valid value ranges, presence checks for columns, and detection of null or missing values.

```
class Iam4RailSchema(pa.DataFrameModel):
    switchconfig_id: int = pa.Field(coerce=True)
    min_timestamp_passage: float = pa.Field()
    channel_name: str = pa.Field(str_matches=r"^[-0-9A-Za-z_]+$")
    samples: float = pa.Field(coerce=True)
    timestamps: float = pa.Field()

    @pa.check("switchconfig_id", name="__switchconfig_id_check_type")
    def __switchconfig_id_check_type(cls, s: pd.Series):
        return _switchconfig_id_check_type(s)

    @pa.check("min_timestamp_passage", name="_min_timestamp_passage_not_zero")
    def _min_timestamp_passage_not_zero(cls, s: pd.Series):
        return _min_timestamp_passage_not_zero(s)

    @pa.check("min_timestamp_passage", name="_min_timestamp_passage_all_same")
    def __min_timestamp_passage_all_same(cls, s: pd.Series):
        return _min_timestamp_passage_all_same(s)

    # This fails for every file:
    # @pa.check("timestamps", name="timestamp_ascending")
    def __timestamp_ascending(cls, s: pd.Series):
        return check_ascending(s)
```

Figure 18-2: An example for a pandera validation schema

⁷ <https://pandera.readthedocs.io/en/stable/>

```
def _switchconfig_id_check_type(s):  
    return str(s.dtype) == "int64" or str(s.dtype) == "float64"
```

```
def _min_timestamp_passage_all_same(s: pd.Series):  
    a = s.to_numpy()  
    return (a[0] == a).all()
```

```
def _min_timestamp_passage_not_zero(s: pd.Series) -> bool:  
    b = s.eq(0)  
    return b.sum() == 0
```

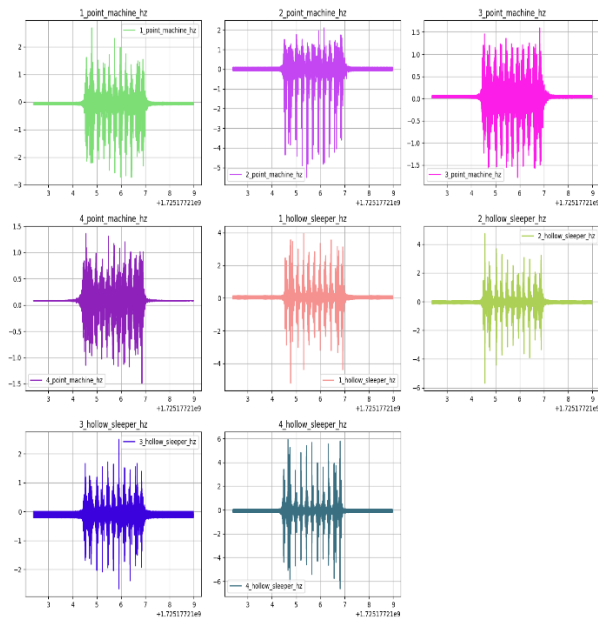
Figure 18-3: Example of Pandera validation functions for the schema

The entire preprocessing workflow has been integrated into an Apache Airflow pipeline. This pipeline is automatically triggered upon the arrival of new data in the S3 storage, ensuring that any newly available source data is systematically downloaded and validated using the Pandera validation framework.

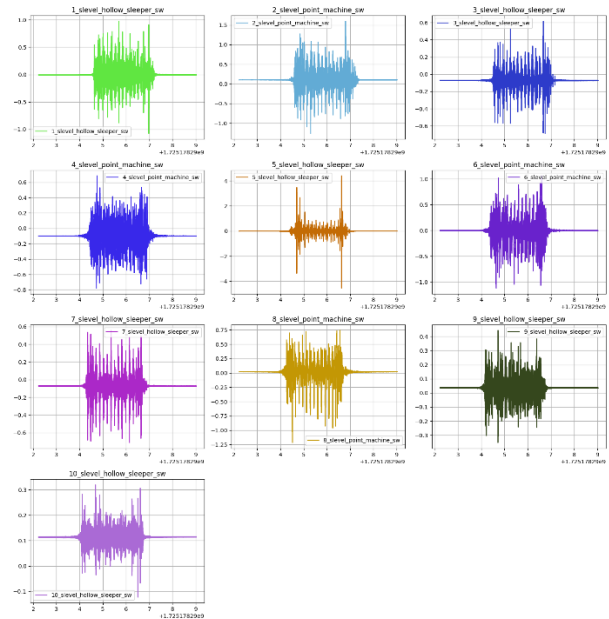
18.1.2. Visualization of Validated Data

Before utilizing the validated datasets for specific artificial intelligence (AI) applications, the collected data for each sensor channel undergoes an initial visualization step. This visualization provides an overview of the sample distribution recorded per channel for each turnout. It also identifies channels that exhibit consistent data acquisition over a defined observation period.

The figures below present plots illustrating the channel activity for both the crossing and switching areas of selected high-speed turnouts, as well as for selected mixed-traffic turnouts, recorded on September 1st, 2024. In particular, each of the colour code represents the data for the corresponding channel name.

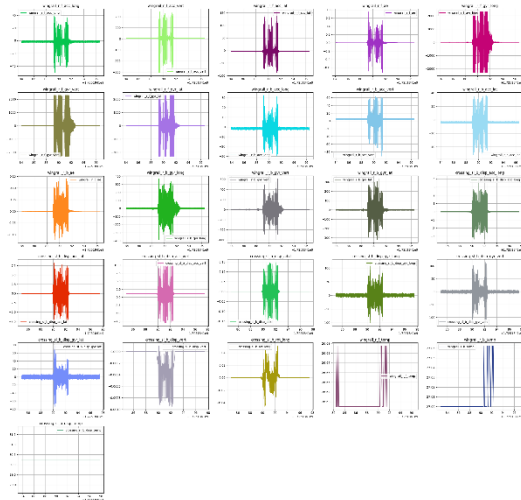


Crossing Area – Acoustic Emission



(b) Switching Area – Acoustic Emission

Figure 18-4: Plot of acoustic emission channels for crossing and switching areas



Crossing Area – multi sensor (b) Switch Area – multi sensor

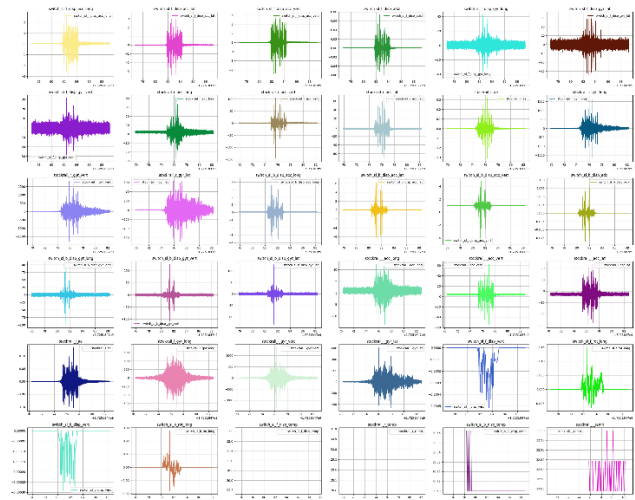


Figure 18-5: Plot of multi-sensor channels for crossing and switching areas

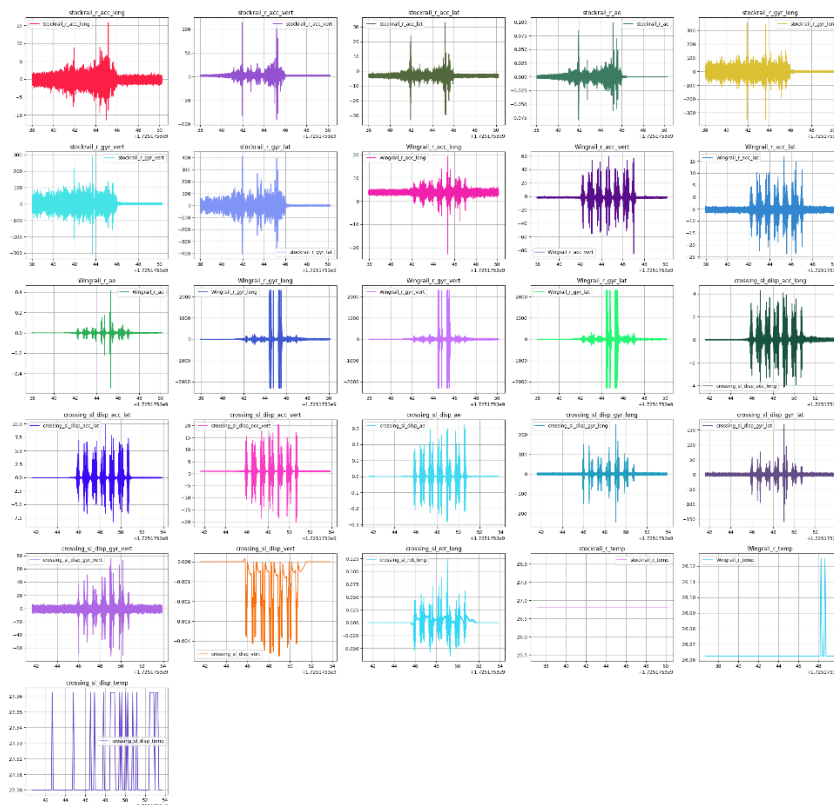


Figure 18-6: Plot of mixed traffic channels

In the Figures below, we present visualisations of the number of data samples recorded from March 2024 to December 2024.

For the acoustic emission sensor for high speed turnouts at the crossing area, the plot in Figure 18-4 shows there is a consistent recording of the number of samples for all eight features:

- 1_hollow_sleeper_hz
- 2_hollow_sleeper_hz
- 3_hollow_sleeper_hz
- 4_hollow_sleeper_hz
- 1_point_machine_hz
- 2_point_machine_hz
- 3_point_machine_hz
- 4_point_machine_hz

Also, one can observe that August recorded the majority of the sensor data on the crossing, followed by September. Figures 18-6 and 18-7 below present a visualisation of the number of data samples recorded per channel name. Specifically, each column depicts the number of samples recorded per channel over time.

For the acoustic channels, the data spans from March 2024 to December 2024, while for the multi-sensor channels, the data covers the period from April 2024 to December 2024. In each plot, the x-axis represents the recording date for a specific turnout, and the y-axis indicates the number of samples recorded on that date.



Figure 18-7: Number of data samples recorded by the acoustic sensor at the crossing area from March to Dec. 2024

For the dataset collected by the multi-sensor at the crossing area for the high-speed turnouts, we only visualize the acceleration (i.e., all channels with the string 'acc') due to the large number of channels (43).



Figure 18-8: Number of data samples recorded by multi-sensor at the crossing area for acc channels from April to Dec. 2024

From Figure 18-5, one can observe that not all the acceleration channels were recorded constantly over the observed period. After the data cleaning step, the following acceleration channels are used for further processing:

- crossing_sl_b_disp_acc_lat
- crossing_sl_b_disp_acc_long
- crossing_sl_b_disp_acc_vert
- wingrail_r_b_acc_lat
- wingrail_r_b_acc_long
- wingrail_r_b_acc_vert
- wingrail_r_f_acc_lat
- wingrail_r_f_acc_long
- wingrail_r_f_acc_vert

These show a consistent recording of data from April until December 2024. In the context of machine learning (ML), it is essential to ensure consistent data recording across all relevant sensor channels from which the features will be extracted for subsequent analysis. Inconsistent or incomplete data can introduce noise, bias, and instability into feature engineering and model training processes. Therefore, all channels exhibiting inconsistent data acquisition will be systematically excluded from further analysis to maintain the quality and reliability of the dataset.

18.1.3.Feature Engineering for Machine Learning

Due to the uneven distribution of the number of samples recorded across channels, it is not

feasible to directly utilize the raw data for any ML task. To ensure compatibility and comparability across channels, further preprocessing is required to achieve a uniform data distribution.

A classical approach for standardizing the number of samples per channel involves the use of spectrograms. Accordingly, spectrograms were computed for each channel in every data file corresponding to both high-speed and mixed-traffic turnouts. This computation was performed using the ShortTimeFFT⁸ class implemented within the SciPy library.

However, spectrograms were not computed for the temperature channels (i.e., channels with the suffix "_temp"). These channels exhibit low sampling frequencies, and their recorded data are nearly constant over time. Following consultation with domain experts, it was decided to represent these channels using the average value of the recorded data, rather than applying time-frequency analysis.

A critical preprocessing step involved addressing the dimensionality of the spectrograms per channel. Since the sampling frequencies differ across channels, discrepancies in the time dimension were observed even among channels with identical sampling rates. To resolve this, spectrograms were discretized by rescaling the time axis to a common target time dimension, ensuring a uniform shape across all processed channels.

Figure 8 below illustrates a sample spectrogram generated for one of the acceleration channels.

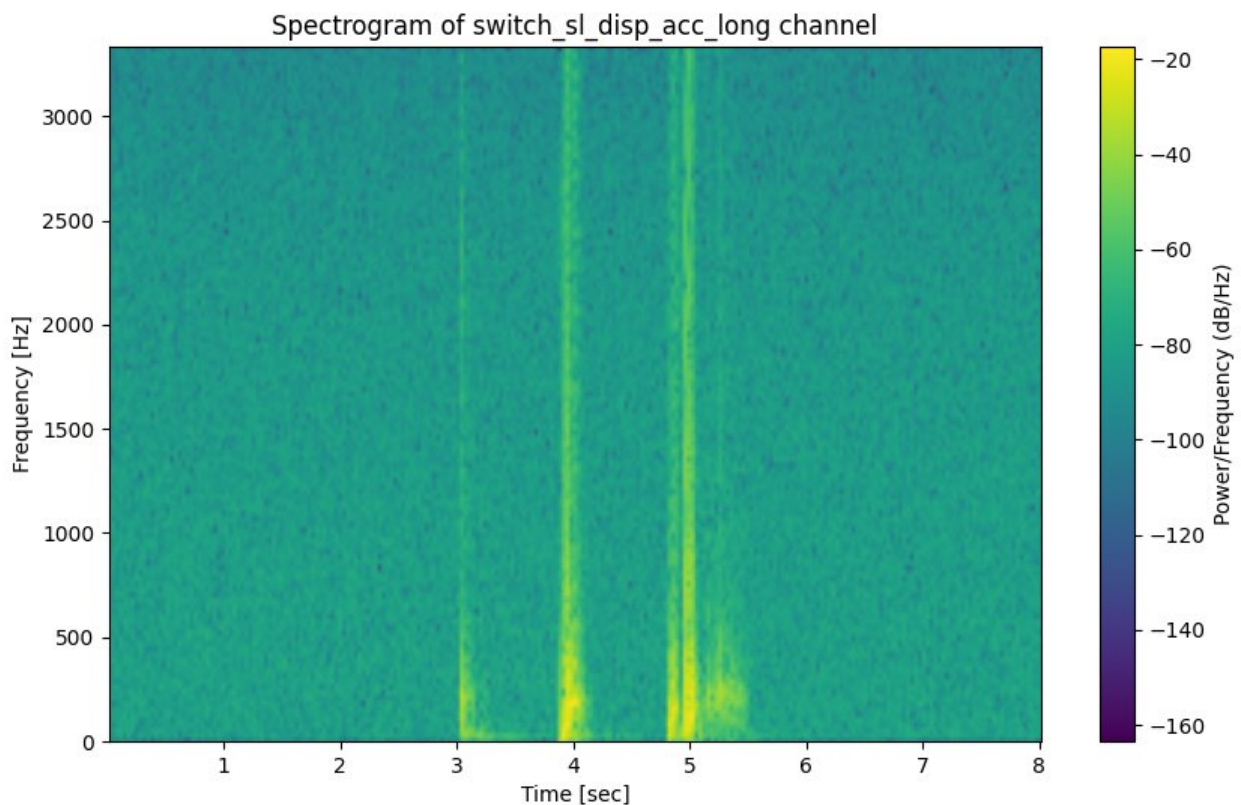


Figure 18-9: Spectrogram of the acceleration channel switch_sl_disp_acc_long of the switching area

The spectrogram data generated throughout the project is stored in the HDF5 file format. This

⁸ <https://docs.scipy.org/doc/scipy-1.15.2/reference/generated/scipy.signal.ShortTimeFFT.html>

format was selected because it allows for efficient storage and rapid access to large numerical datasets, which is critical for accelerating downstream data processing and machine learning workflows.

Figure 9 demonstrates that HDF5 and Avro file formats offer significantly higher read speeds compared to other commonly used formats, such as Pickle and Parquet. This performance advantage makes HDF5 particularly suitable for handling the large volumes of spectrogram data produced in this project.

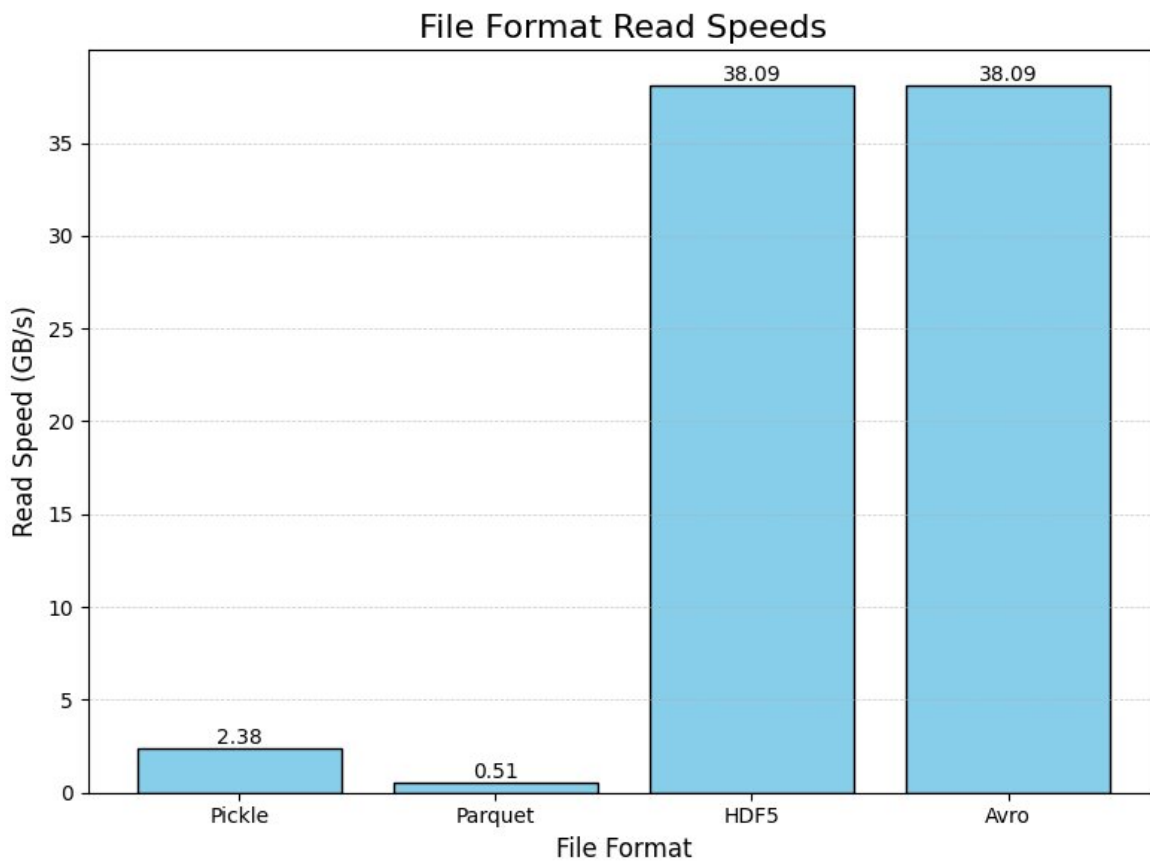


Figure 18-10: Comparing the read speeds of different file formats – Pickle, Parquet, HDF5 and Avro

The computation of spectrograms proved to be a computationally intensive task, particularly during the processing of the historical data collected since the inception of the project. To accelerate the data processing workflow, several optimization strategies were implemented, including improvements to the directory traversal mechanism for accessing the source data.

Specifically, the default Python library function for automatic recursive directory traversal was replaced by a custom implementation. This custom method constructs the file paths through manual string concatenation and records the names of the source files into a metadata file. By avoiding repeated and costly directory tree traversals, this approach significantly reduced the overhead associated with file access.

These optimizations were crucial, as the original directory traversal process alone required more than two hours to scan the directory structure containing the data files collected to date – which were stored on the local disk of our containerization server. Within the data preprocessing methodology, the directory structure must be traversed twice: first, to identify available source

files, and second, to determine which files have already been processed. This was optimized by storing all the filenames and paths within a common file, which allows us to skip the whole directory traversal step. Thus, optimizing this step was essential to achieve sensible runtimes and ensure the scalability of the preprocessing pipeline.

In the next phase, we will select relevant acceleration channels that exhibit consistent data recordings over defined time periods. Based on the visualizations presented above, two options for selecting the time frame have been identified.

18.1.4. Selection of Relevant Acceleration Channels Based on Data Availability

In the first case, by restricting the time frame to April through December, the available dataset includes recordings from nine acceleration channels:

- crossing_sl_b_disp_acc_lat
- crossing_sl_b_disp_acc_long
- crossing_sl_b_disp_acc_vert
- wingrail_r_b_acc_lat
- wingrail_r_b_acc_long
- wingrail_r_b_acc_vert
- wingrail_r_f_acc_lat
- wingrail_r_f_acc_long
- wingrail_r_f_acc_vert

Alternatively, if the selection is restricted to data from September onwards, eleven acceleration channels will be available. These include the nine channels listed above, along with two additional channels:

- crossing_sl_b_disp_acc_vert_100g
- crossing_sl_f_disp_acc_vert_100g

In either case, the corresponding spectrogram data from the selected acceleration channels will be utilized as feature representations for both supervised and unsupervised machine learning tasks.

18.2. Function: Model-based condition monitoring of switches and crossings

This section concerns efforts to develop simulation models that can provide a link between sensor structural response measurements to a condition assessment of the asset. Two different modelling approaches are covered. The first concerns a multi-body simulation model of a 1:50 swing nose crossing panel corresponding to the Spanish demonstrator in the FP3–IAM4RAIL project. The purpose of this model is to study the forces in the locking devices and the relationship between rail running surface irregularities and track responses. The second concerns a wave guide finite element model used to study where acoustic sensors should be mounted on rails to be able to detect cracks.

18.2.1. Multibody simulation model

The multibody simulation model consists of a track model representing the crossing panel of a high-speed turnout with a swing nose crossing. The length of the track model is limited to the area around the swing nose to save simulation time and therefore traffic is also represented by a single bogie. This approximation is considered acceptable for simulation of traffic in the through (straight) route where the curving characteristics of the train is not important. An overview of the model is presented in Figure 18-11 and the main parameters are given in Table 18-1. In the model, rails and sleepers are represented using Timoshenko beam elements. Ballast and rail fastenings are represented using linear bushing elements and contact elements are used to model contacts between the swing nose and base plates and swing nose and wing rails. The model outputs wheel-rail contact quantities such as contact forces as well as displacements and forces in the turnout structure itself.

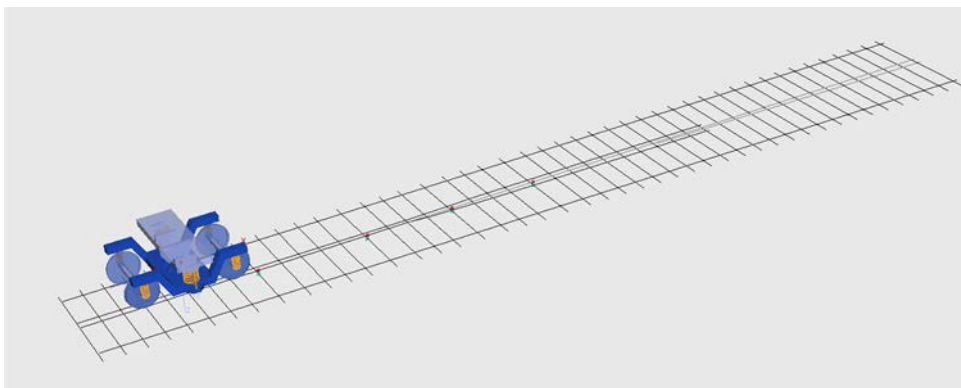


Figure 18-11: Multibody simulation model and bogie model in Simpack

Table 18-1: Specification of crossing panel and traffic conditions for multibody simulations

Speed	350 km/h
Axle load	18 Tonnes
Wheel profile	Nominal S1002
Crossing panel	1:50 swing nose panel with four locks
Rail pad stiffness	50kN/mm
Ballast stiffness	20kN/mm per metre of sleeper length

Example results

Example results from simulations are presented below. Figure 18-12 shows the vertical wheel-rail contact forces on the wing rail and swing nose for a bogie passage through the crossing panel. The transition from wing rail to crossing nose is smooth with a low dynamic amplification from the wheel transition from wing rail to swing nose. Further, the vertical contact forces between base plates and swing nose are presented in Figure 18-13 for the first 14 base plates covering the lock region. It can be observed that the forces are initially very low and then rise to a new baseline level around baseplate 6-7 where the wheels make the transition to the swing nose.

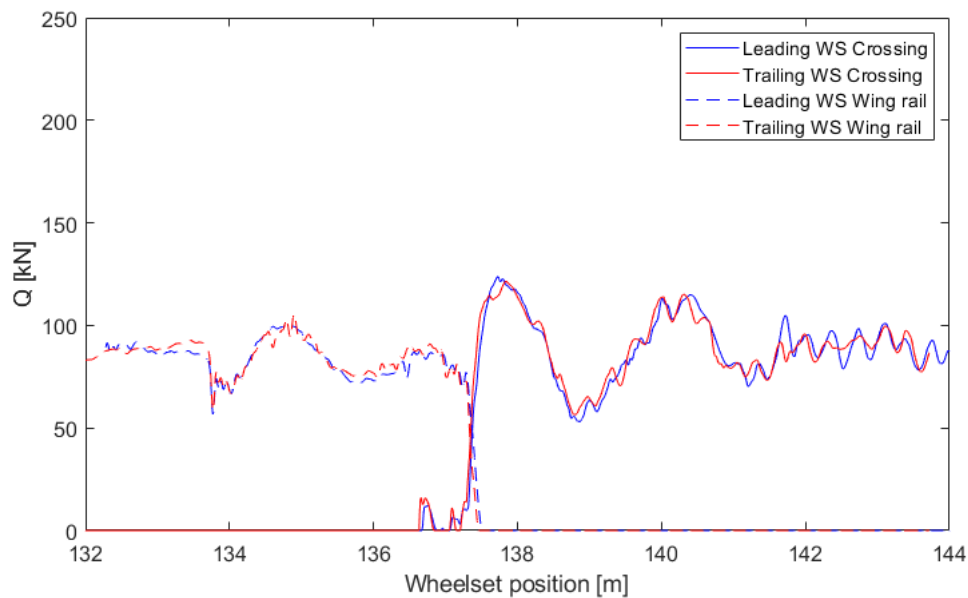


Figure 18-12: Vertical wheel-rail contact forces on wing rail and swing nose for leading and trailing wheel sets

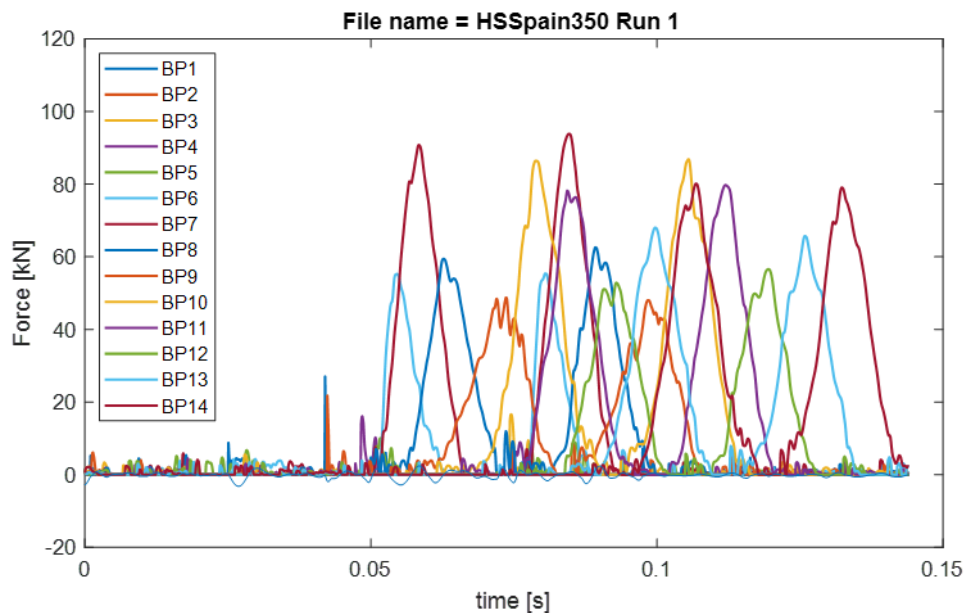


Figure 18-13: Normal contact forces between swing nose and the first 14 slide chairs/base plates along the swing nose. This region covers the distance from the first to the fourth lock.

18.2.2. Waveguide finite element model

Non-destructive rail testing is one way to ensure safety and reliability in railway systems. The growth of rail defects, such as surface cracks, fractures, and internal fissures, can generate acoustic emissions (AE). These high-frequency signals are used for condition monitoring in several contexts. Since the rails act as waveguides with very low energy losses, AE signals can be observed over long distances. A main challenge in this approach is the high background noise level due to the rolling noise. Previous work addressed this with various signal processing techniques. Instead, this work focuses on optimizing the position of the AE sensor based on the location and source mechanism

of the defect. This is achieved by high-frequency waveguide Finite Element simulations and analysis of the cross-sectional mode shapes. The first steps in this analysis can be found in a paper by Jannik Theyssen [17].

18.3. Function: Drive/Detector rod monitoring

The drive rod / detector rod monitoring use case is covered by multiple analogue acoustic sensors mounted on the hollow sleeper of the different setting levels. In the crossing level each hollow sleeper was equipped by a single sensor as the maintenance teams reported repeatedly occurring breaks in this area. Figure 18-14 shows the signals of the acoustic sensors mounted at the four hollow sleepers in the crossing level. It can be observed that generally the first hollow sleeper shows the highest peaks in the signals, which can be related to the expectable highest loads in this region. However, all signals show amplitudes in the same order of magnitude which indicated a similar loading situation and an overall good health state of all four setting levels.

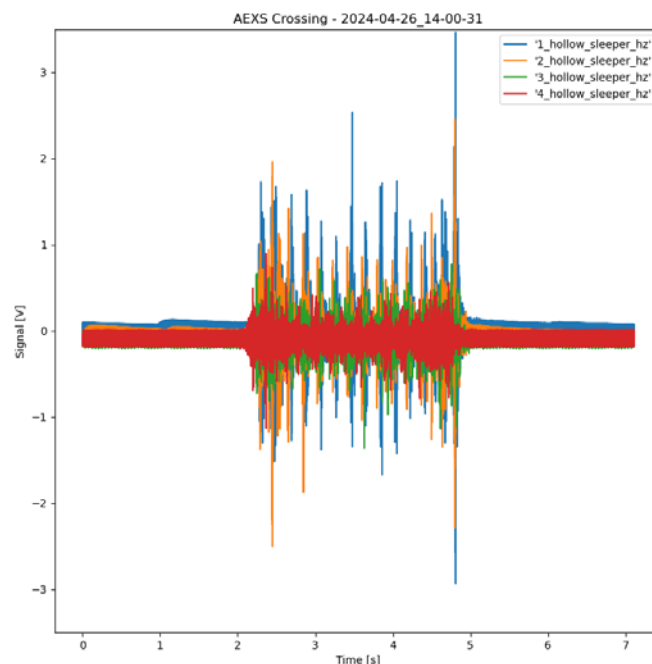


Figure 18-14: Acoustic emission signals of the acoustic sensors mounted on the hollow sleepers for detector rod monitoring in the crossing panel

Figure 18-14 shows the signals of the acoustic emission sensors mounted in the switch panel. Due to the high number of setting levels (10) and also less frequently reports about breaking rods in this area only every second setting level was equipped with an acoustic sensor. Which can be directly seen, in comparison to the figure before, is that the sensor in the switch panel measures a significantly lower signal. This can be related to generally lower vibrations levels and thus loads in the switch panel, which also correlates with the experience from the maintenance teams about fewer breaking rods in this area. Again, the first setting level shows slightly higher peak magnitudes compared to the other setting levels, however the signals are very moderate, and no faulty states could be observed so far.

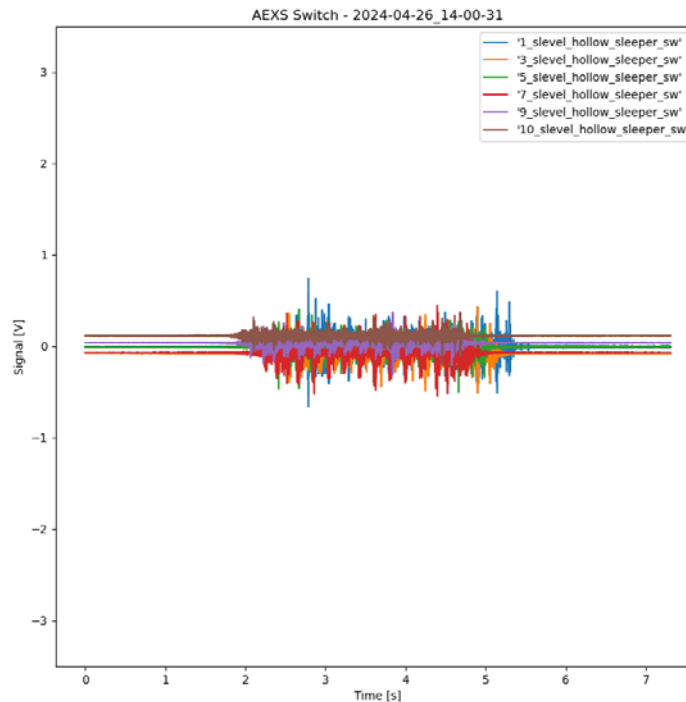


Figure 18-15: Acoustic signals of analogue acoustic sensors mounted on hollow sleepers in switch panel

18.4. Function: Switch assembly monitoring

The switch position monitoring use case is covered by 6 inductive sensors mounted in two cross sections of the switch panel. Figure 18-16 shows a plot of the measured data of one week at the beginning of May. The upper plot shows the distance between switch rail and stock rail of the closed switch rail. Considering the main operation route (through) mainly the right switch rail is in a closed position and therefore shows the most datapoints. It can be observed that both rail positions show values below 1.5mm, which can be defined as a very good state considering the total tolerance of 4mm. Furthermore, it can be observed that the left switch rail shows a single measurement point every 2 days which means the turnout is switches only once per two days. The lower plot shows the nearest flangeway of the left switch rail which is around 81mm. The critical value for this type of turnout is 70mm which means the nearest flangeway is in a good range. The schematic sensor arrangement is shown in Figure 4-12 and Figure 4-14 and Figure 4-16 show the sensor locations at the beginning of the switch and the nearest flangeway, respectively.

However, there are some outliers in the data which vary significantly from all other measurement points. Those can be caused either by a faulty operator or occur during maintenance and inspection tasks. Therefore, it can be concluded that it is of utmost importance for the monitoring system to obtain information about ongoing maintenance tasks in order to not provide any unnecessary alarms or warnings caused during maintenance.

Within this project the switch position development will be monitored over time and if any changes or trends in the data are recognised by the switch assembly health state model, the system will send out warning or alarms to the operator in order to perform maintenance and inspection tasks before the values yield safety critical values and affect the asset availability.

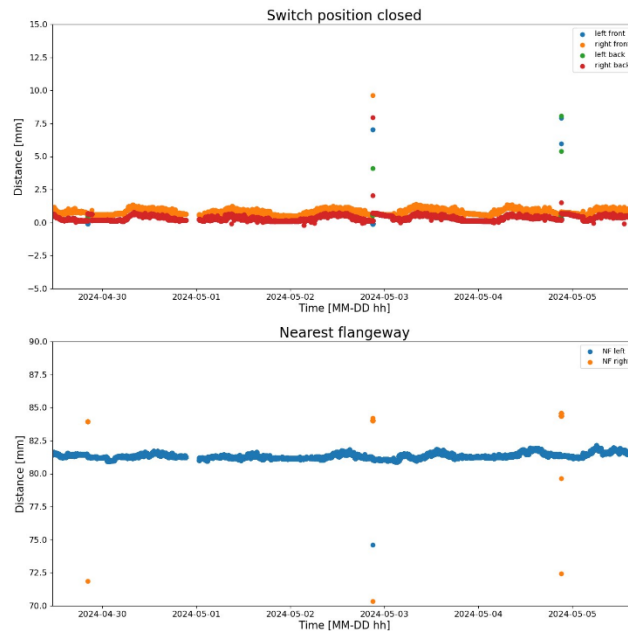


Figure 18-16: Switch position values for left and right switch rail in two cross sections (front and back).

18.5. Function: Track quality monitoring

The track quality monitoring is conducted by means of the multi-sensor introduced in section 5.2.1. The sensor estimates the sleeper displacement and tilt and thereby rates the quality of the ballast. Figure 18-17 shows the vertical sleeper displacement of the high-speed demonstrator turnout, in two cross sections of the switch panel and two cross sections of the crossing panel, respectively. It can be seen that the occurring vertical sleeper displacement are in a very low range, around 0.5 mm in the switch panel and around 1 mm in the crossing panel, which indicates an overall good health state of the ballast and a proper support for the turnout.

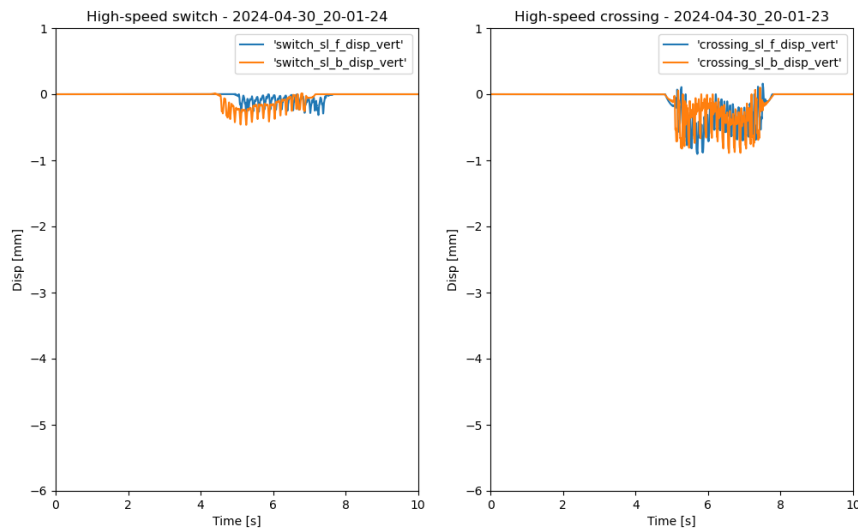


Figure 18-17: Vertical sleeper displacement recorded in two cross sections of switch- and crossing panel of the high-speed demonstrator located in Santa Cruz de la Zarza. All four positions show low displacements (below 1mm) which indicates a good ballast condition and high track quality.

Figure 18-17 shows the vertical sleeper displacement in the switch and the crossing panel of the mixed traffic demonstrator. It can be observed that the vertical sleeper displacements in the switch panel are again in a very low area, below 1mm, whereas the vertical displacement in the crossing area yields critically high values up to 5mm. This shows that a sufficient support of the ballast in the crossing area is not properly given, and the turnout requires maintenance, for example track tamping, as soon as possible. This high track displacements are not recommendable as they lead to significantly higher acceleration and dynamic forces on the crossing and thus can increase the damage to other mechanical components.

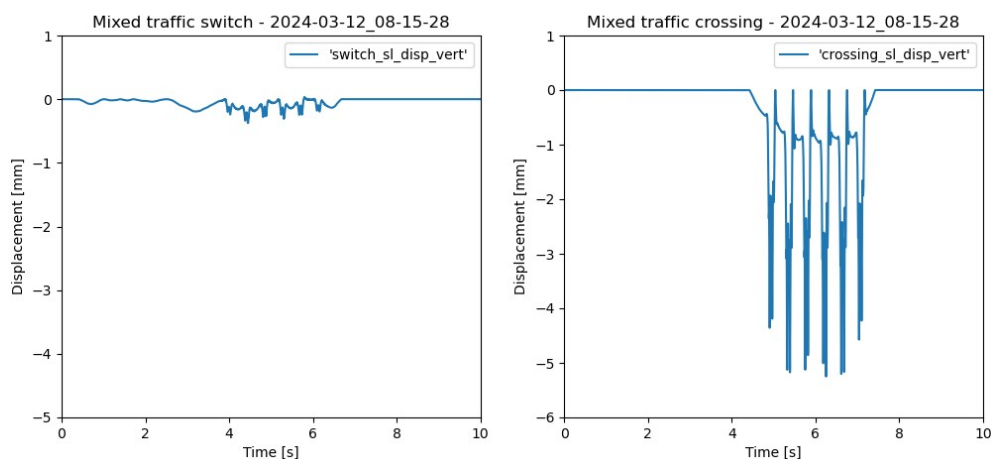


Figure 18-18: Vertical sleeper displacements recorded at switch- and crossing panel of the mixed traffic demonstrator located in Rifa/Tarragona (Catalunia). High displacements in crossing panel indicate poor ballast support at this sleeper

In addition, the acceleration signals on the wing rail and stock rail of the mixed traffic turnout are shown in Figure 18-19 to illustrate the influence of the high vertical displacements on the measured acceleration signals at the rail components. It can be observed that the vertical and lateral acceleration amplitude is moderate, around 50g, in the switch panel, whereas the acceleration amplitudes yield up to 300g in both directions, lateral and vertical, in the crossing panel. These high accelerations cause both damage to the rail components as well as a further degradation of the ballast below the crossing. Therefore, a timely maintenance action is highly recommendable.

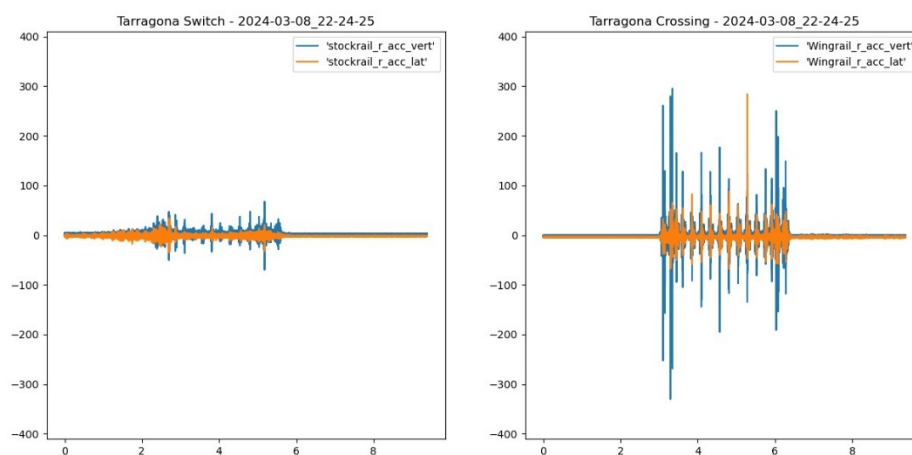


Figure 18-19: Vertical and lateral acceleration signal measured in switch and crossing panel of the mixed traffic demonstrator turnout in Rifa / Tarragona. The vertical and lateral acceleration magnitudes in the crossing area are very high and indicate a low asset health stat.

Comparing pictures from an on-site visit in June 2023, see Figure 18-20 and from the installation of the monitoring system in March 2024, see Figure 18-21, it can be observed that the surface of the crossing nose is subjected to considerable damage and a breakout has developed over these 9 months. The high vertical displacements and as a result the significant acceleration level are advancing the damage of the crossing.



Figure 18-20: Picture from mixed traffic demonstrator turnout from June 2023 during an on-site visit of the demonstrator



Figure 18-21: Picture from demonstrator turnout 9 months later in March 2024. The red box indicates initiated surface damage, a breakout, at the crossing nose running surface.

Figure 18-22 shows an evaluation of all recorded train passages at both demonstrators. The analysis shows in the upper plot a histogram of the highest recorded displacement value per passage for the mixed traffic demonstrator. The middle plot shows the same values for the high-speed demonstrator at the beginning of the switch and the lower plot the same value at the end of the switch area. It can be observed that all three sensors show similar maximum values and distributions.

Figure 18-23 shows the maximum displacement recorded per passage for the two demonstrators but in the crossing area. The upper plot shows the maximum displacement distribution at the mixed traffic demonstrator turnout in Rifa / Tarragona. It can be observed that the maximum displacements recorded at this turnout are at a very high level which shows a low asset health state.

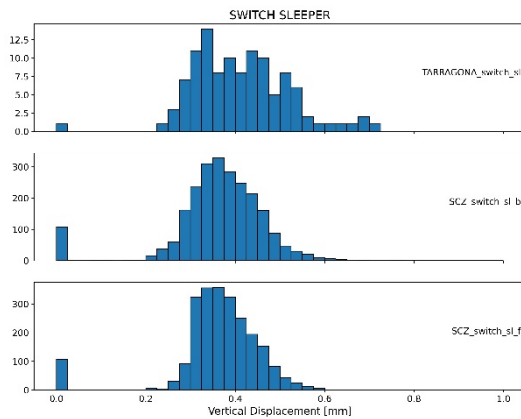


Figure 18-22: Maximum sleeper displacement in switch area per axle for (upper) mixed traffic turnout in Rifa / Tarragona and the high-speed demonstrator turnout in Santa Cruz de la Zarza (middle and lower plot)

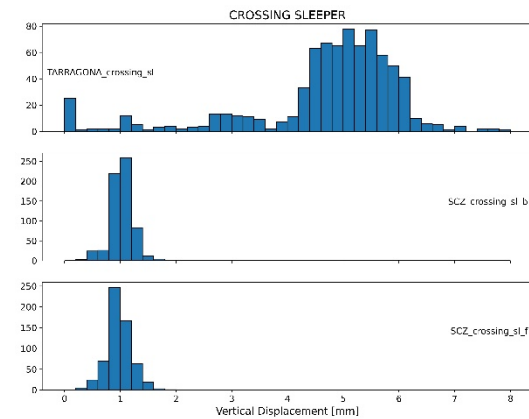


Figure 18-23: Maximum sleeper displacement in crossing area per axle for (upper) mixed traffic turnout in Rifa / Tarragona and the high-speed demonstrator turnout in Santa Cruz de la Zarza (middle and lower plot)

18.6. Function: Vehicle/track interaction and the resulting dynamic forces

The work is being carried out by Voestalpine in collaboration with its affiliated entity, Virtual Vehicle.

18.6.1. Brief introduction to the application

The application is focused on model-based condition monitoring of switch and crossing (S&C) components, with the aim of improving the current inspection and maintenance activities. The primary goal is to develop a detailed S&C model that can simulate the dynamic interaction of vehicles passing through a turnout. By analysing the vehicle/track interaction and the resulting dynamic forces, the model will provide valuable insights into the degradation behaviour of various track components, including the switch rails, and the frog area. This approach is aimed to identify potential issue and to provide knowledge to optimize the turnout inspections and maintaining.

18.6.2. Description of the technology

An S&C model is developed using the software SIMPACK. This model includes a detail representation of the turnout together with a vehicle car to simulate its passage through the turnout through route. The model is built according to the geometric layout and crossing nose geometry of the turnout installed in Rifa. To ensure accurate simulation results, the model is calibrated through a parameter study, comparing multibody dynamic (MBD) simulation results with the measurements acquired by the sensors. With the calibration process, some important unknown parameters can be estimated. Once the model is validated, the model is a meaningful tool, and the simulations can be used to analyse:

- Contact forces and accelerations experienced by the track components
- Identify the area subjected to the highest level of loading and forces
- Assessing the parameters influence (settlement changes, stiffness changes, surface defects and void, etc.)
- Simulating specific scenarios to understand the track behaviour under different conditions

18.6.3. Methodology

To simulate the vehicle excitation travelling through the turnout, a SIMPACK Multibody system model is developed. The model includes a detailed track model of the turnout (Figure 18-24) and a vehicle car (Figure 18-25) parametrised to represent the full fleet travelling through the turnout. The track model (Figure 18-26) is composed of two flexible rails supported by sleepers, which can be modelled as either rigid or flexible elements. The connection between the rails and the sleepers is made with spring-damper elements that represent the intermediate level and the fastening components. The sleepers are connected to the ground with spring-damper elements to simulate the ballast.

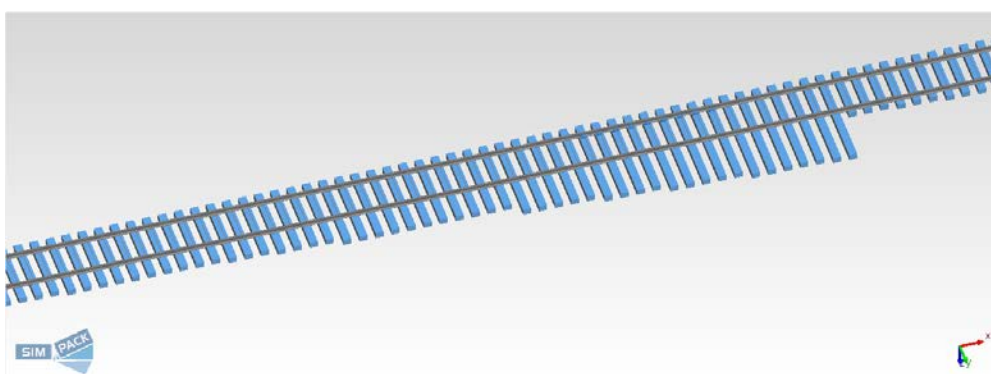


Figure 18-24: SIMPACK track model

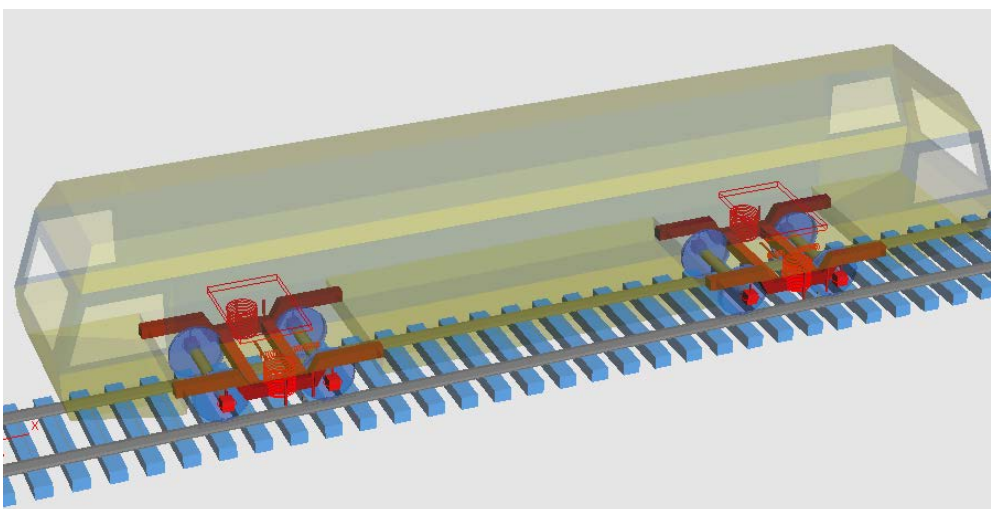


Figure 18-25: SIMPACK vehicle model

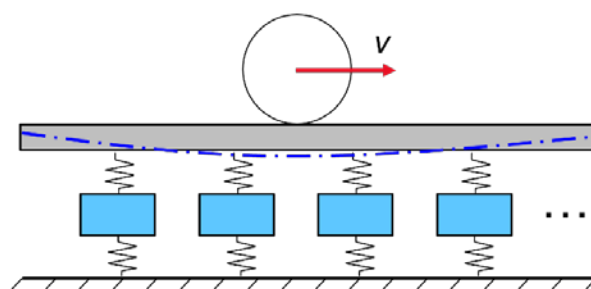


Figure 18-26: Track model

Each sleeper can be independently modelled with the option in defining whether it is a rigid or flexible element, as well as defining its length, mass, and stiffness values. This modelling approach enables a precise representation of the track dynamic behaviour and under various condition allowing the simulation of void under sleeper or sudden changes in the ballast stiffness. The crossing area is also modelled using rail profiles obtained from the cross-sections of the CAD model (Figure 18-27, Figure 18-28) provided. This allows for an accurate simulation of the complex interactions and forces occurring in this critical part of the track, providing valuable insights into the performance and potential degradation of the components involved.

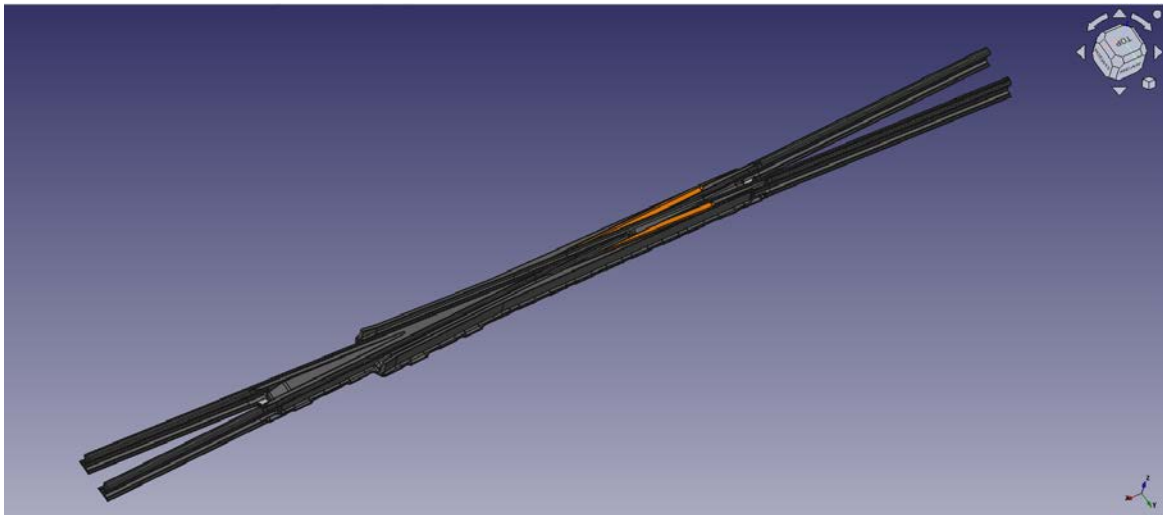


Figure 18-27: Crossing CAD model

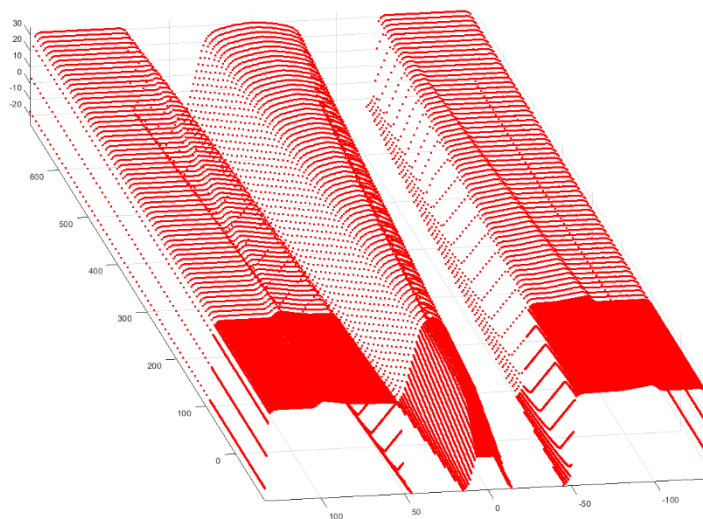


Figure 18-28: Frog sectioning

18.6.4. Description of the data

The input data for MBD simulations are:

- Turnout layout
- Geometry of the S&C

- Vehicles onboard measurements (for calibration)
- Vehicles operating conditions
- Wheel profiles
- Track irregularities
- Track surface defects

The output data of the MBD simulations are for example:

- Vertical acceleration of the Crossing Nose

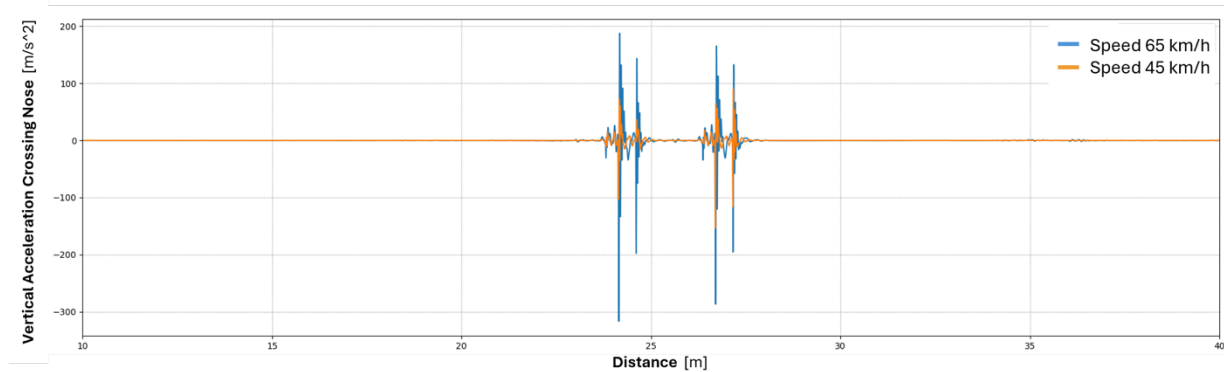


Figure 18-29: Crossing nose vertical acceleration - examples at 65 and 45 km/h

- Sleeper vertical displacement at the crossing nose

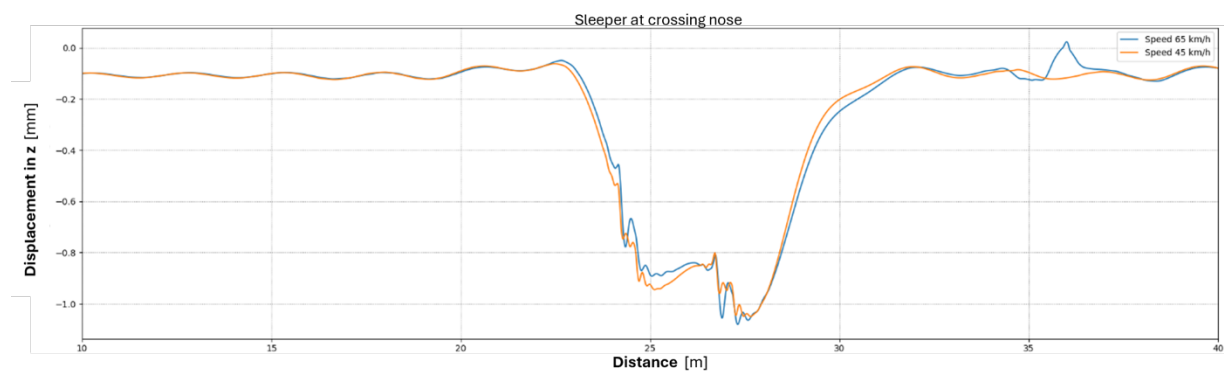


Figure 18-30: Sleeper vertical displacement at crossing nose - examples at 65 and 45 km/h

- Vertical Ballast Force at the crossing nose

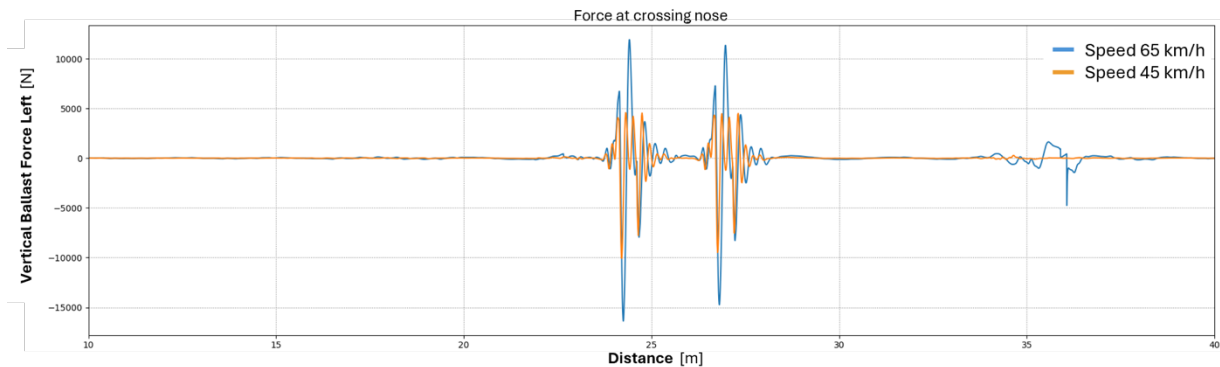


Figure 18-31: Vertical ballast force at crossing nose - examples at 65 and 45 km/h

18.7. Function: Frog / switch rail monitoring

This section provides detailed information on the type and specifications of the proposed multi-sensor system, which collects motion and vibration data.

The frog / switch rail monitoring use cases is covered by the multi-sensor described in section 5.2.1. This sensor system provides multiple channels in multiple directions and can be thus used for a wide range of applications at different rail components. The obtained signals are analysed in both time- and frequency domain to detect any changes in the material or structural response of the component, thereby detecting different damage patterns such as excessive plastic flow of the material, severe wear, break outs at the running surface or cracks. Especially foot cracks or internal cracks, which cannot be detected easily during regular inspection procedures shall be detected by this system as they can be safety critical for railway operators as they can grow and lead to total component failure if not recognised timely.

Figure 18-32 shows the acceleration signals (vertical and lateral) for a train passage at the mixed traffic demonstrator in the switch- and the crossing panel, respectively. Within the project the signals will be recorded and analysed for any changes over time, indicating changes in the structural response. Moreover, different model- and data drive approaches will be applied to the data with the aim of a holistic asset health state assessment.

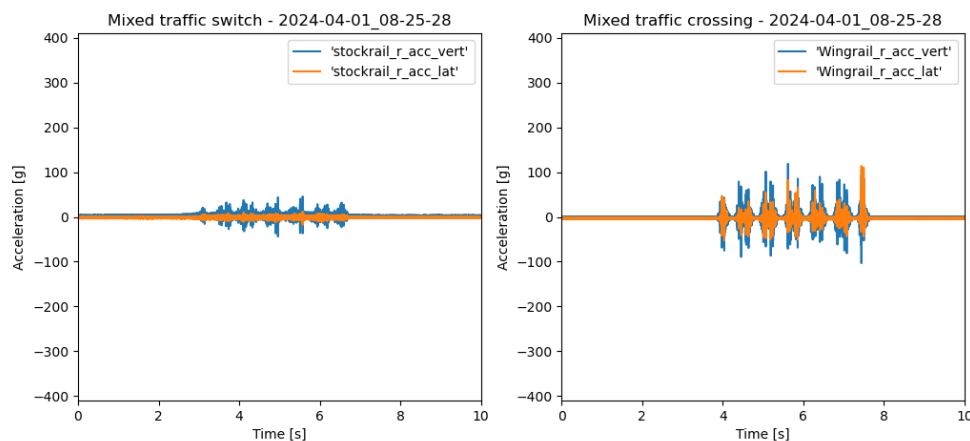


Figure 18-32: Vertical and lateral acceleration signals from switch- and crossing panel at the mixed traffic demonstrator located in Rifa/Tarragona (Catalunia). The signals are recorded from a commuter train.

The recorded acceleration at the high-speed turnout demonstrator, shown in Figure 18-33, generally yields higher acceleration amplitudes compared to the mixed traffic demonstrator, which can be attributed to the significantly higher train speed. Therefore, it is crucial and highly recommended to estimate train speed and train type of the passing vehicles and provide this information as an input variable to condition monitoring and health state assessment models in order to increase their accuracy and predictive capabilities.

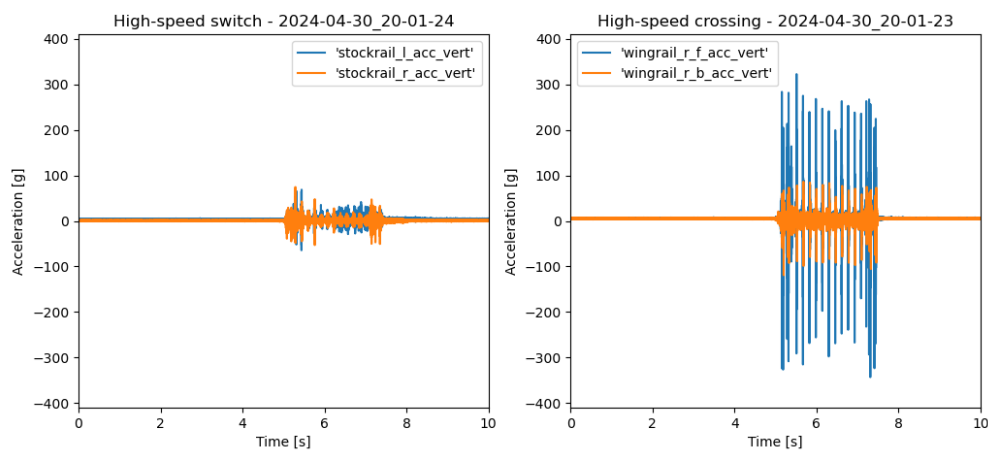


Figure 18-33: Vertical and lateral acceleration signals from switch- and crossing panel at the high-speed line demonstrator located in Santa Cruz de la Zarza (Toledo). The signals are recorded from a regular high-speed train.

Besides the acceleration signals, the acoustic emission signals represent a valuable source of information for the component health state assessment. As the sensor can be operated at very high sampling rates, it is able to detect even minor changes in the material and thereby indicate possible developing damages in the component. Figure 18-34 shows the acoustic emission signals recorded at two positions in switch and crossing panel of the high-speed demonstrators. The exact locations of these sensors are shown in section 18.8. It can be observed that the acoustic signals show the highest magnitudes for the sensor located at the tip of the swing nose, which is where the transition and thus the highest loads can be expected.

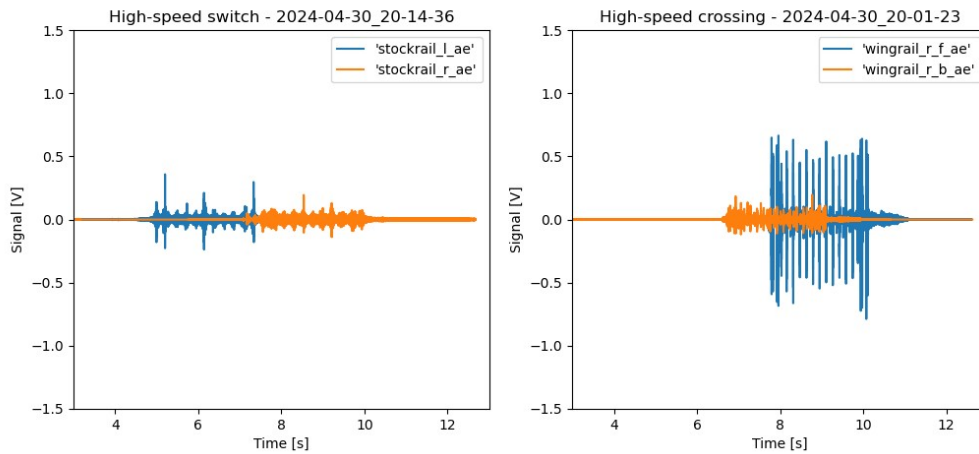


Figure 18-34: Acoustic emission signals recorded in switch and crossing panel of the high-speed demonstrator turnout.

Figure 18-35 shows the acoustic emission signals at the mixed traffic demonstrator turnout in the switch- and the crossing panel. It can be observed that the acoustic signal is significantly higher in the crossing panel than in the switch panel which correlates to the higher loads in the crossing panel. Furthermore, it is remarkable that the acoustic emission signal at the mixed traffic demonstrator shows higher amplitudes than in the high-speed demonstrator, although the acceleration signals are significantly higher at the high-speed demonstrator turnout. This high acoustic emission amplitudes could be facilitated by the surface break out, which is visible at the mixed traffic turnout in Rifa. However, this needs to be validated and confirmed by analyses of a larger set of measurements which will be conducted in WP11.

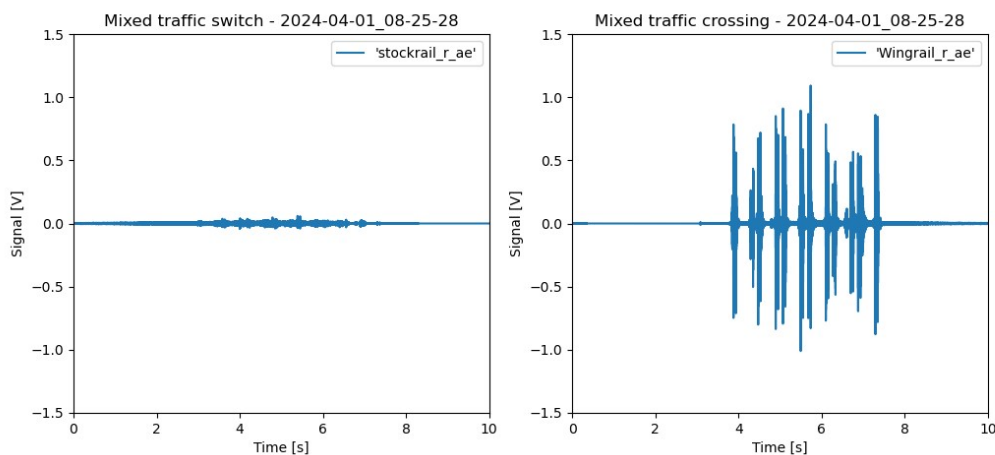


Figure 18-35: Acoustic emission signals recorded in switch panel and crossing panel at mixed traffic demonstrator

Figure 18-36 shows a histogram of the maximum acoustic emission per passage for all recorded passages at both demonstrator locations. The upper plot shows the data from the mixed traffic demonstrator in Rifa Tarragona whereas the middle plot shows the data recorded at the left switch rail at the high-speed demonstrator in Santa Cruz de la Zarza and the lower plot the right stock rail data. It can be observed that all three sensors provide similar maximum values and distribution

of the same.

Figure 18-37 shows the same analyses for the acoustic sensors in the crossing area. The upper contains the maximum values from the sensor mounted on the right-wing rail of the mixed traffic demonstrator. Generally, it is shown that the maximum values of this sensor show a very wide distribution, compared to the two lower plots from the (middle) sensor mounted at the spliced rail and (lower) at the swing nose tip at the high-speed demonstrator. Furthermore, it is observable that the sensor at the swing nose tip (lower plot) shows significantly higher maximum values than the sensor close to the spliced rail (middle plot).

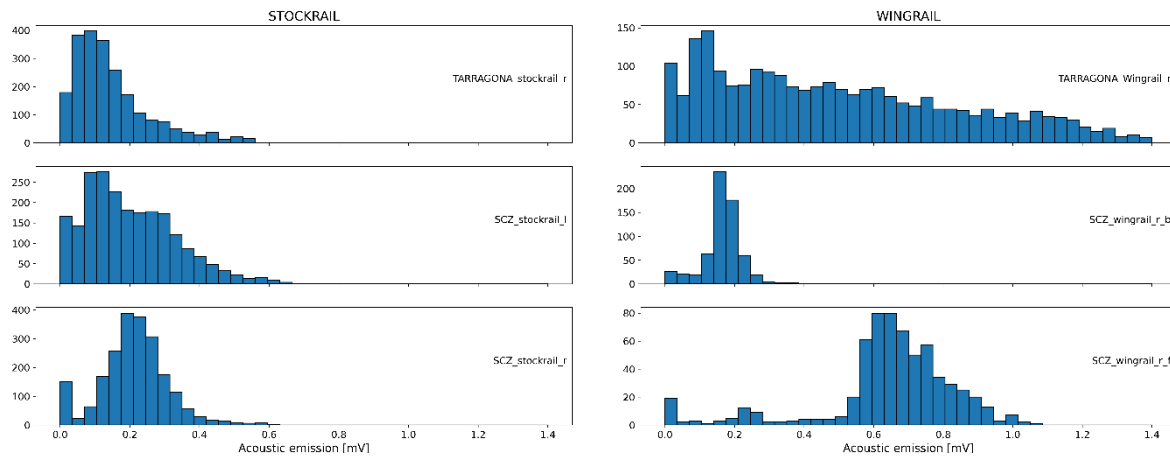


Figure 18-36: Maximum acoustic emission in switch area per passage for mixed traffic turnout in Rifa / Tarragona (upper plot) and the high-speed demonstrator turnout in Santa Cruz de la Zarza (middle – left stock rail and lower plot- right stockrail)

Figure 18-37: Maximum acoustic emission in crossing area per passage for mixed traffic turnout in Rifa / Tarragona (upper plot) and the high-speed demonstrator turnout in Santa Cruz de la Zarza (middle – at spliced rail and lower plot- at the swing nose tip)

Figure 18-38 shows a histogram of the maximum vertical acceleration recorded during every train passage at the switch panel of both demonstrators. Although the maximum values are comparable at all three sensor locations, the mixed traffic demonstrator data in the upper plot shows again a wider distribution. This parameter could be an additional parameter which could be influenced either by the overall condition of the asset as well as being influenced by certain vehicle parameters.

Figure 18-39 shows the same analyses for the crossing area. The analyses shows that the highest values can be observed at the swing nose tip of the high-speed turnout (lower plot) although the mixed traffic demonstrator shows also a certain number of passages with very high acceleration magnitudes up to 400g. Furthermore, it is visible that the distribution of the mixed traffic demonstrator sensor data shows a significantly wider distribution.

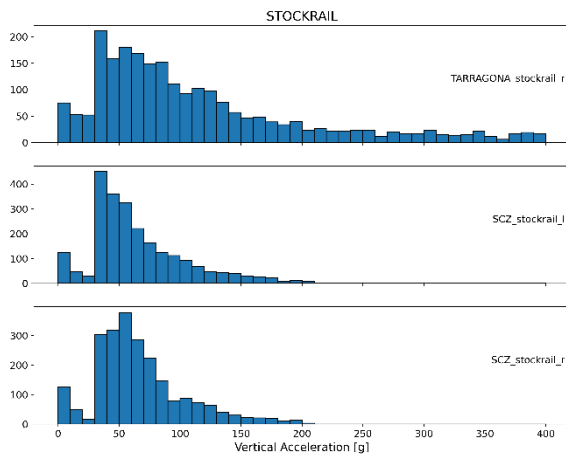


Figure 18-38: Maximum vertical acceleration switch area per passage for mixed traffic turnout in Rifa / Tarragona (upper plot) and the high-speed demonstrator turnout in Santa Cruz de la Zarza (middle – left stock rail and lower plot- right stockrail)

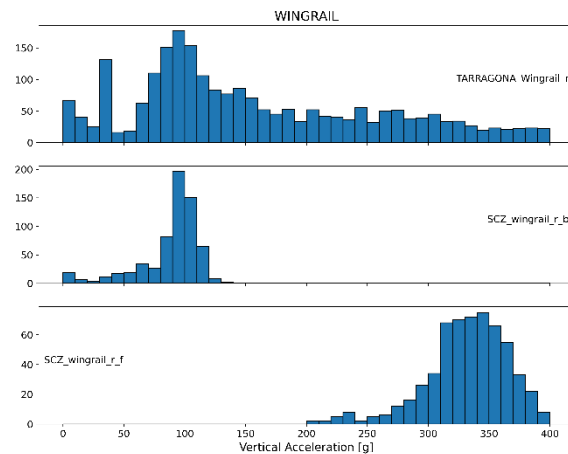


Figure 18-39: Maximum vertical acceleration in crossing area per passage for mixed traffic turnout in Rifa / Tarragona (upper plot) and the high-speed demonstrator turnout in Santa Cruz de la Zarza (middle – at spliced rail and lower plot- at the swing nose tip)

18.8. Function: Frog monitoring

This work has been carried out by Voestalpine in collaboration with its affiliated entity, the Materials Center Leoben.

As a first example, the frog condition will be assessed by means of vibration data. Depending on the wear state of frog and wheel, the transition point where the wheel contact point changes from the wing rail to the frog changes.

In previous work it has been shown via detailed finite element simulations and verified on a turnout (Figure 18-40) that the location of the transition point can be deduced from certain signal features of strain gages applied to the wing rails and frog.

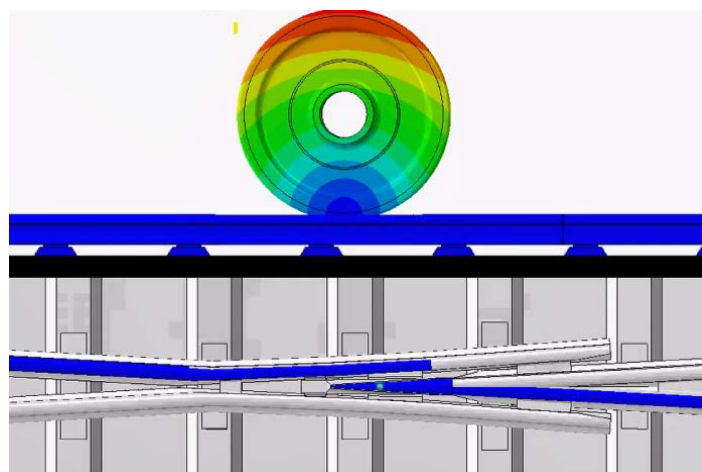


Figure 18-40: Numerical simulation of a wheel running over a turnout from left to right, side view (top) and top view (bottom, the wheel is hidden). This snapshot shows the moment where the wheel leaves the left wing rail and impacts the frog.

In the present work, this will be applied to acceleration signals of a cast turnout. In the current project, a digital twin of the Rifa Tarragona crossing (Figure 18-41) is being developed in order to derive the relations between the wear state of the frog and the acceleration signals, and

subsequently apply this knowledge to the evaluation of the measured acceleration signals.

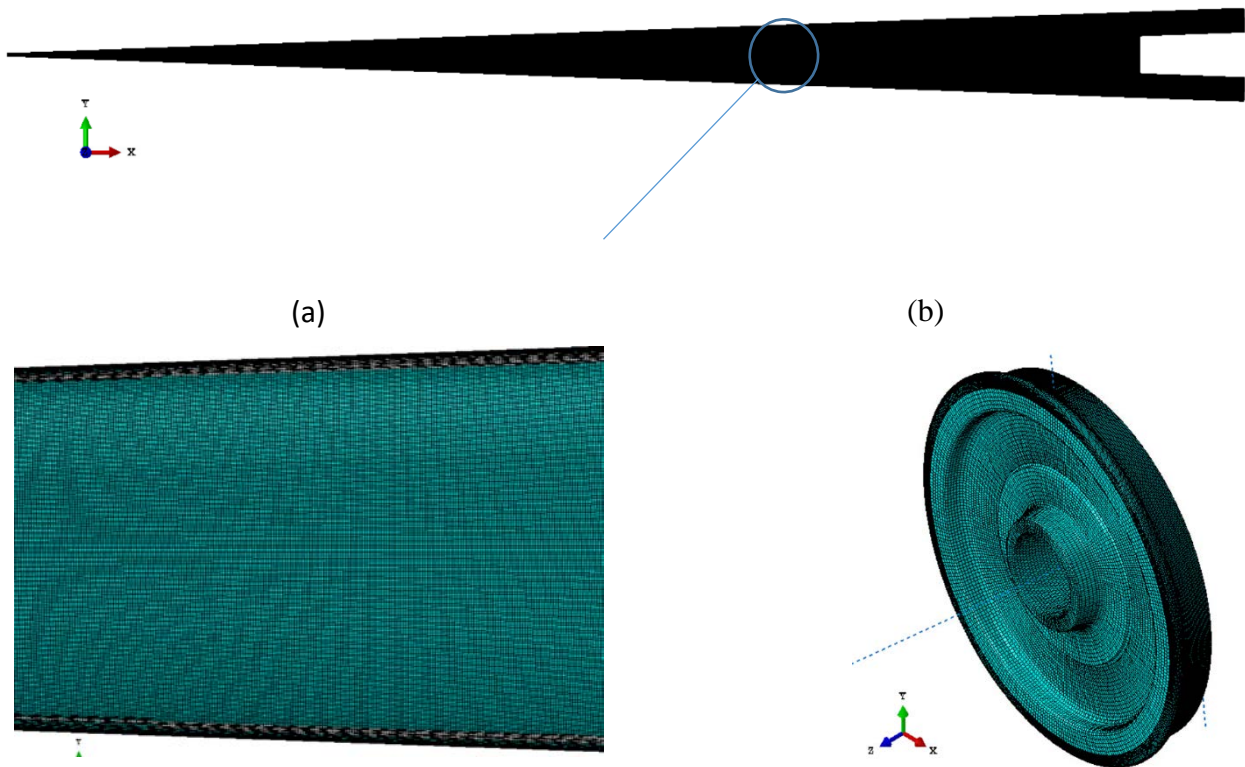


Figure 18-41 and 18-42: Hexahedral elements on (a) the contact surfaces of the rail head and (b) the wheel.

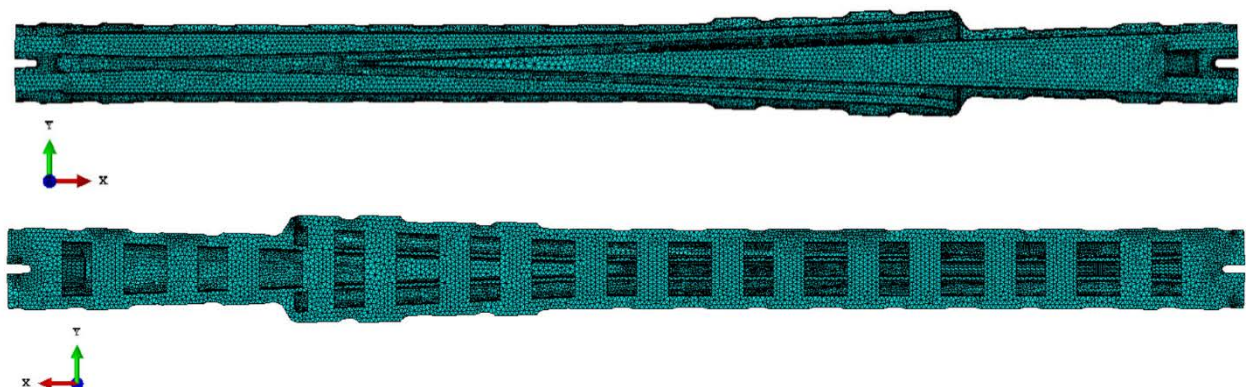


Figure 18-43 and 18-44: Tetrahedral elements on the web and foot of the rail (top view and bottom view)

The digital twin needs minimum computational effort at acceptable accuracy. Therefore, a careful meshing strategy has been designed to balance accuracy and computational efficiency. A hexahedral mesh is used for the wheel and head of the rail, specifically the contact surfaces where the wheel rolls over (Figure 18-41), to ensure high accuracy in capturing the stress and strain

distributions due to the wheel-rail contact. These elements provide superior performance in representing complex stress fields and offer better numerical stability and convergence. In the remainder of the rail, including areas with complex geometries (), tetrahedral elements are utilized to effectively manage the computational cost. These elements are versatile in meshing intricate geometries.

The model is currently being prepared for parameter studies and subsequent validation against on-site measurements.

19. CONCLUSIONS

Deliverable D10.2 presents the initial developments and preparatory work for the integrated demonstration within Flagship Project 3 FP3–IAM4RAIL, focusing on the progress achieved in Work Package 10 and its foundational impact on Work Package 11. This deliverable offers a detailed update on the groundwork and immediate progress of the multi-source/multi-purpose (MSMP) asset management platform, complementing the broader context provided in Deliverable D10.1. The report aims to provide essential summaries to maintain clarity and relevance, aligning with the overarching objectives of the MSMP IAMS and related research programs.

This work package builds on asset management solutions from previous EU projects such as IN2SMART and IN2SMART2, by deploying innovative solutions specifically for the rail infrastructure subsystem. It targets short-term asset management and off-site work preparation within the MSMP platform, providing continuous diagnostic and prognostic information through wayside and onboard sensors. This data supports daily decision-making by maintenance experts and asset managers. The scope encompasses all data acquisition processes for the rail infrastructure subsystem, with a particular focus on Switches and Crossings (S&Cs), ensuring a comprehensive 360-degree view around the track.

The objective of this deliverable is to address short-term asset management approaches for tracks and their surroundings. It involves defining pilot sites in Spain and the Netherlands for testing technologies based on two established use cases. A carefully selected set of applications, tailored to meet the needs of infrastructure managers such as ADIF and maintenance service providers such as Strukton, will serve as evaluation scenarios. These applications will be demonstrated and validated against expected Technology Readiness Levels (TRL) to ensure they meet operational and performance standards. Some of these applications have already been tested at the pilot sites and can be considered as quick wins.

Work packages 10 and 11 involve two primary use cases. Use Case 1 focuses on integrating new monitoring technologies with specific asset management issues for immediate problem-solving and quick wins. Use Case 2 involves combining monitoring data from various sources to enhance fault detection and diagnosis. Although this approach requires more effort, it provides deeper insights into infrastructure behaviour and condition. The development of specific applications relevant to end-users is guided by the high-level architecture of the prototype platform. These applications will be demonstrated at mixed-traffic and high-speed pilot sites in Spain and the Netherlands. Some applications, with higher maturity levels, have already demonstrated tangible results in operational environments, offering quick wins for end-users.

A total of 13 applications addressing practical issues in short-term asset management have been defined, with some reaching already the target TRL 6. Other technologies and their planned applications are intended to fill the innovation funnel, leading to further evaluation and development in subsequent project phases. This approach ensures that promising technologies are continuously assessed for future work based on their likelihood of success. By maintaining a pipeline of potential advancements, resources can be focused on the most promising developments, ensuring sustained progress in rail infrastructure management.

WP10 aimed to achieve initial developments with tangible results, presenting quick wins within the first two years. The defined 13 applications represent real-world use cases, with at least one, the reality model, already showing success in real-life pilots. Significant progress also includes



defining the pilot sites, installing technologies on-site, and initiating data exchange. This data is being used for various applications, representing early findings in these developments. Future work will continue in WP11, with alignment and integration with other work packages within cluster D of FP3-IAM4RAIL being a critical component of ongoing efforts.

20. WORKS CITED

- [1] H. Samson, J. Tiecken, A. Boogaard, B. Baasch, T. Neumann, J. Camacho de Migue, U. Alvarado, *Agile Multi-Sensor Platform Leonardo: Evaluation of new Monitoring Technologies in an Operational Environment*, TRA 2024, Dublin, Ireland (2024).
- [2] Samson, H.; Tiekcken, J; Nuemann, T.; Baasch, B; Cmacho de Miquel, J; Rodriques-Arana B; Alvarado , *Agile Multi-Sensor Platform LEONARDO: Evaluation of new monitoring Technologies in an Operational Enrinment*, TRA, 2024.
- [3] F.R. Redeker, *POSS®: Railway Condition Monitoring developed by a maintainer*, RCM 2011, Derby, UK (2011).
- [4] D. Narezo Guzmán, J. Heusel, N. Weik, S. Reetz, D. Buursma, A. van den Berg, G. Schrijver, T. Neumann, S. van den Broek, J. Groos, *Towards the automation of anomaly detection and integrated fault identification for railway switches in a real operational environment*, WCRR 2022, 6.-10. June 2022, Birmingham, UK, 2022.
- [5] D. Narezo Guzmán, E. Hadzic, B. Baasch, J. Heusel, T. Neumann, G. Schrijver, D. Buursma and J. C. Groos, *Anomaly Detection and Forecasting Methods Applied to Point Machine Monitoring Data for Prevention of Switch Failures*, Proceedings of the 32nd International Congress and Exhibition on Condition Monitoring and Diagnostic Engineering Management , 2019.
- [6] T. Neumann, J. Heusel, M del Alamo Ruiz, D. Narezo Guzmán, S. Reetz, *Modelling and simulating the atypical features of switch engine current curves*, SIGNALLING + DATA COMMUNICATION 1+2/2023, pp. 53-63, 2023).
- [7] T. Neumann, J. Tiecken, D. Buursma, B. Baasch, J. Camacho de Migue, B. Rodriguez, U. Alvarado, *Boosting holistic railway infrastructure monitoring and health prediction by integrated data sets and analysis*, Transport Research Arena 2024, 15.-18. April 2024, Dublin, Ireland, 2024.
- [8] Narezo Guzman, Daniela; Hadzic, Edin; Samson, Henk; van den Broek, Serge; Groos, Jörn Christoffer, *Detecting anomalous behavior of railway switches under real operation conditions: workflow and implementation*. In: TRA 2020 conference proceedings. Transport Research Arena 2020, 27-30 April 2020, Helsinki, Finland..
- [9] S. Reetz, T. Neumann, G. Schrijver, A. van den Berg A, D. Buursma, *Expert system based fault diagnosis for railway point machines*, Proceedings of the Institution of Mechanical Engineers, Part F: Journal of Rail and Rapid Transit. 2024;238(2):214-224.
- [10] K. Jahan; J. Pai Umesh; M. Roth, *Anomaly Detection on the Rail Lines Using Semantic Segmentation and Self-supervised Learning*, 2021 IEEE Symposium Series on Computational Intelligence (SSCI), Orlando, FL, USA, 2021, pp. 1-7, doi: 10.1109/SSCI50451.2021.9659920, 2022.
- [11] J. Niebling, B. Baasch, A. Kruspe, *Analysis of Railway Track Irregularities with Convolutional*

- Autoencoders and Clustering Algorithms*, Bernardi, S., et al. Dependable Computing - EDCC 2020 Workshops. EDCC 2020. Communications in Computer and Information Science, vol 1279. Springer, Cham. https://doi.org/10.1007/978-3-030-58462-7_7, 2020.
- [12] M. Hashmi, M.Ibrahim, I. Bajwa, H. Siddiqui, F. Rustam and E. Lee, *Railway Track Inspection Using Deep Learning Based on Audio to Spectrogram Conversion: An on-the-Fly Approach*, Sensors 2022, 22, 1983. <https://doi.org/10.3390/s22051983>.
- [13] H. Sun et al., *Looseness Detection of Rail Fasteners Using MEMS Sensor and Power Spectrum Entropy*, IEEE 1st International Conference on Micro/Nano Sensors for AI, Healthcare, and Robotics (NSENS), 2018. doi: 10.1109/NSENS.2018.8713630.
- [14] I. Bravo, U. Alvarado, J. Nieto and P. Ciáurriz, "Inspection and Condition Monitoring of Railway Tracks Using On-board Systems: A Systematic Review" - pending to be published.
- [15] E. Kassa, J. Saramota, and A. Skavhaug, *Monitoring of Switches and Crossings/Tracks Using Smart Sensors*, Springer Series in Reliability Engineering, Springer Science and Business Media Deutschland GmbH, 2021, pp. 149–166. doi: 10.1007/978-3-030-62472-9_9.
- [16] C. Hoelzl, V. Dertimanis, M. Landgraf, L. Ancu, M. Zurkirchen, and E. Chatzi, *On-board monitoring for smart assessment of railway infrastructure: A systematic review*, The Rise of Smart Cities: Advanced Structural Sensing and Monitoring Systems, Elsevier, 2022, pp. 223–259. doi: 10.1016/B978-0-12-817784-6.00015-1.
- [17] P. Salvador, V. Naranjo, R. Insa, and P. Teixeira, *Axlebox accelerations: Their acquisition and time-frequency characterisation for railway track monitoring purposes*, Measurement (Lond), vol. 82, pp. 301–312, Mar. 2016, doi: 10.1016/j.measurement.2016.01.012.
- [18] A. Chudzikiewicz, R. Bogacz, M. Kostrzewski, and R. Konowrocki, *Condition monitoring of railway track systems by using acceleration signals on wheelset axle-boxes*, Transport, vol. 33, no. 2, pp. 555–566, 2018, doi: 10.3846/16484142.2017.1342101.
- [19] M. Chen, W. Zhai, S. Zhu, L. Xu, and Y. Sun, *Vibration-based damage detection of rail fastener using fully convolutional networks*, Vehicle System Dynamics, vol. 60, no. 7, pp. 2191–2210, 2022, doi: 10.1080/00423114.2021.1896010.
- [20] Y. Xiao et al., *Evaluating the Effect of Rail Fastener Failure on Dynamic Responses of Train-Ballasted Track-Subgrade Coupling System for Smart Track Condition Assessment*, Materials, vol. 15, no. 7, Apr. 2022, doi: 10.3390/ma15072675.
- [21] M. Oregui, Z. Li, and R. Dollevoet, *Identification of characteristic frequencies of damaged railway tracks using field hammer test measurements*, Mech Syst Signal Process, vol. 54, pp. 224–242, Mar. 2015, doi: 10.1016/j.ymssp.2014.08.024.
- [22] Z. Zhan et al., "Wireless Rail Fastener Looseness Detection Based on MEMS Accelerometer and Vibration Entropy," IEEE Sens J, vol. 20, no. 6, pp. 3226–3234, Mar. 2020, doi: 10.1109/JSEN.2019.2955378.
- [23] A. P. Synodinos, *Identification of railway track components and defects by analysis of wheel-rail interaction noise*, Conference: 23rd International Congress on Sound & Vibration (ICSV),

July 2016.

- [24] Wei, Z., Sun, X., Yang, F., Ke, Z., Lu, T., Zhang, P., & Shen, C., Carriage interior noise-based inspection for rail corrugation on high-speed railway track, Vols. Applied Acoustics, 196, Article 108881. <https://doi.org/10.1016/j.apacoust.2022.108881>, Elsevier, 2022.
- [25] Baasch, B.; Oselin, P.; Groos, J. C., (2025) Ein digitaler Zwilling für die Analyse von dynamischen Fahrzeugreaktionen. SIGNAL + DRAHT, 42-49. DVV Media Group. ISSN 0037-4997.
- [26] Lohar, Shreya, Lei Zhu, Stanley Young, Peter Graf, and Michael Blanton., 2021. "Sensing Technology Survey for Obstacle Detection in Vegetation" Future Transportation 1, no. 3: 672-685. doi: 10.3390/futuretransp1030036.
- [27] Saleh, K., Szénási, S., & Vámosy, Z., 2021." Occlusion handling in generic object detection: A review". IEEE 19th World Symposium on Applied Machine Intelligence and Informatics (SAMI), pp. 000477-000484. doi: 10.1109/SAMI50585.2021.9378657..
- [28] Leibner P, Hampel F, Schindler C., 2023. "GERALD: A novel dataset for the detection of German mainline railway signals". Proceedings of the Institution of Mechanical Engineers, Part F: Journal of Rail and Rapid Transit. 237(10):1332-1342. doi:10.1177/09544097231166472.
- [29] Cordts, M., Omran, M., Ramos, S., Rehfeld, T., Enzweiler, M., Benenson, R., & Schiele, B., 2016. "The cityscapes dataset for semantic urban scene understanding". Proceedings of the IEEE conference on computer vision and pattern recognition, pp. 3213-3223. doi:10.48550/arXiv.1604.01685.
- [30] J. Y. Shih, P. Weston, M. Entezami, and C. Roberts, *Dynamic characteristics of a switch and crossing on the West Coast main line in the UK*, Railway Engineering Science, vol. 30, no. 2, pp. 183–203, Jun. 2022, doi: 10.1007/s40534-021-00269-4.
- [31] X. Liu, V. L. Markine, H. Wang, and I. Y. Shevtsov, *Experimental tools for railway crossing condition monitoring (crossing condition monitoring tools*, Measurement (Lond), vol. 129, pp. 424–435, Dec. 2018, doi: 10.1016/j.measurement.2018.07.062.
- [32] D. Fan, M. Sebès, E. Bourgeois, H. Chollet, and C. Pozzolini, *A fast co-simulation approach to vehicle/track interaction with finite element models of S&C*, 2021. [Online]. Available: <https://hal.science/hal-03367648>.
- [33] M. D. G. Milosevic, B. A. Pålsson, A. Nissen, J. C. O. Nielsen, and H. Johansson, *Condition Monitoring of Railway Crossing Geometry via Measured and Simulated Track Responses*, Sensors, vol. 22, no. 3, Feb. 2022, doi: 10.3390/s22031012.
- [34] S. Reetz; T. Najeh; J. Lundberg; J. Groos, *Analysis of Local Track Discontinuities and Defects in Railway Switches Based on Track-Side Accelerations*, Sensors 2024, 24, 477. <https://doi.org/10.3390/s24020477>, 2024.
- [35] Y. Wang and R. Zoughi, *Interaction of surface cracks in metals with open-ended coaxial probes at microwave frequencies*, Mater. Eval., vol. 2000, pp. 1228-1234.

- [36] T. Marazani, D. M. Madyira and E. T. Akinlabi, *Repair of cracks in metals: a review*, Proc. Manuf., vol 8, pp 673-679, 2017.
- [37] Y. Yao, S.-T.-E. Tung and B. Glisic, *Crack detection and characterization techniques—An overview*, Structural Control Health Monitor., vol. 21, no. 12, pp. 1387-1413, Dec. 2014.
- [38] M. U. Memon and S. Lim, *Review of electromagnetic-based crack sensors for metallic materials (recent research and future perspectives)*, Metals, vol. 6, no. 8, pp. 172, Aug. 2016.
- [39] McClanahan, S. Kharkovsky, A. R. Maxon, R. Zoughi and D. D. Palmer, "Depth evaluation of shallow surface cracks in metals using rectangular waveguides at millimeter-wave frequencies", IEEE Trans. Instrum. Meas., vol. 59, no. 6, pp. 1693-1704, Jun. 2010..
- [40] D. F. Cannon, K.-O. Edel, S. L. Grassie and K. Sawley, *Rail Defects: An Overview*, Fatigue Fract. Eng. Mater. Struct., vol. 26, pp. 865–886, 2003.
- [41] M. P. Papaelias, C. Roberts and C. L. Davis, *A Review on Non-Destructive Evaluation of Rails: State-of-the-Art and Future Development*, Proc. Inst. Mech. Eng. Part F J. Rail Rapid Transit, vol. 222, pp. 367–384, 2008.
- [42] R. Zoughi and S. Kharkovsky, *Microwave and millimeter wave nondestructive testing and evaluation—Overview and recent advances*, IEEE Instrum. Meas. Mag., vol. 10, no. 2, pp. 26-38, Apr. 2007.
- [43] K. Brinker, M. Dvorsky, M. T. Al Qaseer and R. Zoughi,, *Review of advances in microwave and millimetre-wave NDT&E: Principles and applications*, Phil. Trans. Roy. Soc. A Math. Phys. Eng. Sci., vol. 378, no. 2182, Sep. 2020.
- [44] M. Dvorsky, M. T. Al Qaseer and R. Zoughi, *Crack sizing using dual-polarized microwave SAR imaging*, Proc. IEEE Int. Instrum. Meas. Technol. Conf. (IMTC), pp. 1-6, May 2020.
- [45] R. J. Hruby and L. Feinstein, *A novel nondestructive noncontacting method of measuring the depth of thin slits and cracks in metals*, Rev. Sci. Instrum., vol. 41, no. 5, pp. 679-683, May 1970.
- [46] M. T. Ghasr, K. P. Ying and R. Zoughi, *SAR imaging for inspection of metallic surfaces at millimeter wave frequencies*, Proc. IEEE Int. Instrum. Meas. Technol. Conf. (IMTC), pp. 1202-1206, May 2014.
- [47] N. Qaddoumi, S. Ganchev and R. Zoughi, *A novel microwave fatigue crack detection technique using an open-ended coaxial line*, Proc. Conf. Precis. Electromagn. Meas. Dig., pp. 59-60, 1994.
- [48] S. Kharkovsky, M. T. Ghasr and R. Zoughi, *Near-field millimeter-wave imaging of exposed and covered fatigue cracks*, IEEE Trans. Instrum. Meas., vol. 58, no. 7, pp. 2367-2370, Jul. 2009.
- [49] Hu, Z. Ren, M. S. Boybay and O. M. Ramahi,, "Waveguide probe loaded with split-ring resonators for crack detection in metallic surfaces", IEEE Trans. Microw. Theory Techn., vol. 62, no. 4, pp. 871-878, Apr. 2014.

- [50] Q. Wang et al., *High-sensitivity dielectric resonator-based waveguide sensor for crack detection on metallic surfaces*, *EEE Sensors J.*, vol. 19, no. 14, pp. 5470-5474, Jul. 2019.
- [51] R. Zoughi, *Microwave Non-Destructive Testing and Evaluation*, The Netherlands: Kluwer Academic, 2000.
- [52] K. M. Donnell, A. McClanahan and R. Zoughi, *On the crack characteristic signal from an open-ended coaxial probe*, *EEE Trans. Instrum. Meas.*, vol. 63, no. 7, pp. 1877-1879, Jul. 2014.
- [53] M. Yadegari, R. Moini, S. H. H. Sadeghi and F. Mazlumi, "Output signal prediction of an open-ended rectangular waveguide probe when scanning cracks at a non-zero lift-off", *NDT E Int.*, vol. 43, no. 1, pp. 1-7, Jan. 2010..
- [54] F. Mazlumi, N. Gharanfeli, S. H. H. Sadeghi and R. Moini, *An open-ended substrate integrated waveguide probe for detection and sizing of surface cracks in metals*, *NDT E Int.*, vol. 53, pp. 36-38, Jan. 2013.
- [55] M. S. U. Rahman, O. S. Hassan and M. A. Abou-Khousa, *Crack detection and corrosion mapping using loaded-aperture microwave probe*, *IEEE Open J. Instrum. Meas.*, vol. 1, pp. 1-11, 2022.
- [56] M. R. Ramzi, M. Abou-Khousa and I. Prayudi, *Near-field microwave imaging using open-ended circular waveguide probes*, *EEE Sensors J.*, vol. 17, no. 8, pp. 2359-2366, Apr. 2017.
- [57] R. Zoughi and S. Kharkovsky, *Microwave and millimeter wave sensors for crack detection*, *Fatigue Fract. Eng. Mater. Struct.*, vol. 31, no. 8, pp. 695-713, 2008.
- [58] C.-Y. Yeh and R. Zoughi, *A novel microwave method for detection of long surface cracks in metals*, *IEEE Trans. Instrum. Meas.*, vol. 43, no. 5, pp. 719-725, Oct. 1994.
- [59] R. Z. S. Ganchev and C. Huber, *Microwave measurement-parameter optimization for detection of surface breaking hairline cracks in metals*, *Nondestruct. Test. Eval.*, vol. 14, no. 5, pp. 323-327, 1998.
- [60] N. Qaddoumi, E. Ranu, J. D. McColskey, R. Mirshahi and R. Zoughi, *Microwave detection of stress-induced fatigue cracks in steel and potential for crack opening determination*, *Res. Nondestruct. Eval.*, vol. 12, no. 1, pp. 87-103, 2000.
- [61] Balanis, *Advanced Engineering Electromagnetics*, Hoboken, NJ, USA: Wiley, 2012..
- [62] J. Bahr, "Using electromagnetic scattering to estimate the depth of a rectangular slot", *IEEE Trans. Antennas Propag.*, vol. AP-27, no. 6, pp. 738-746, Nov. 1979..
- [63] R. J. Hruby and L. Feinstein, *A novel nondestructive noncontacting method of measuring the depth of thin slits and cracks in metals*, *Rev. Sci. Instrum.*, vol. 41, no. 5, pp. 679-683, May 1970.
- [64] M. Dvorsky, M. T. A. Qaseer and R. Zoughi,, *Detection and orientation estimation of short cracks using circularly polarized microwave SAR imaging*, *IEEE Trans. Instrum. Meas.*, vol. 69, no. 9, pp. 7252-7263, Sep. 2020.

- [65] M. Chizh, A. Zhuravlev, V. Razevig and S. Ivashov, "Detection and orientation estimation of short cracks using circularly polarized microwave SAR imaging", IEEE Trans. Instrum. Meas., vol. 69, no. 9, pp. 7252-7263, Sep. 2020..
- [66] M. A. Abou-Khousa and M. S. U. Rahman, *Covered cracks detection using dual-polarization synthetic aperture radar imaging*, IEEE Trans. Instrum. Meas., vol. 70, pp. 1-4, 2021.
- [67] T. Watanabe and H. Yamada, *Orientation estimation of surface cracks in metals based on intensity maximization of polarimetric circular synthetic aperture radar images*, IEEE Trans. Instrum. Meas., vol. 70, pp. 1-14, 2021.
- [68] M. Chizh, A. Zhuravlev, V. Razevig and S. Ivashov, *Non-destructive testing of the rails rolling surface and joints with synthetic aperture radar*, Proc. 21st Int. Radar Symp. (IRS), pp. 112-116, Oct. 2020.
- [69] Liu, M. T. A. Qaseer and R. Zoughi, "Influence of antenna pattern on synthetic aperture radar resolution for NDE applications", IEEE Trans. Instrum. Meas., vol. 70, pp. 1-11, 2021..
- [70] M. T. Ghasr, B. J. Carroll, S. Kharkovsky, R. Zoughi and R. Austin, *Millimeter-wave differential probe for nondestructive detection of corrosion precursor pitting*, IEEE Trans. Instrum. Meas., vol. 55, no. 5, pp. 1620-1627, Oct. 2006.
- [71] M. A. Abou-Khousa, S. Kharkovsky and R. Zoughi, *Novel near-field millimeter-wave differential probe using a loaded modulated aperture*, IEEE Trans. Instrum. Meas., vol. 58, no. 5, pp. 1273-1282, May 2009.
- [72] J. Ye, E. Stewart, D. Zhang, Q. Chen, K. Thangaraj and C. Roberts, *Integration of multiple sensors for noncontact rail profile measurement and inspection*, IEEE Transactions on Instrumentation and Measurement, no. 70, pp. 1-12, 2021.
- [73] M. Ebadi, M. Bagheri, M. Lajevardi and B. Haas, *Defect detection of railway turnout using 3D scanning*, Sustainable Rail Transport: Proceedings of RailNewcastle 2017, pp. 1-18, 2017.
- [74] Wendong Gong , Muhammad Firdaus Akbar , Ghassan Nihad Jawad 2, Mohamed Fauzi Packeer Mohamed and Mohd Nadhir Ab Wahab , *Nondestructive Testing Technologies for Rail Inspection: A Review*.
- [75] Theyssen, j, *Observation of Acoustic Emission in Rails: Sensor position optimization*, DAGA 2024 - 50. Jahrestagung für Akustik, Hannover (Germany), March 18-21, 2024, 4 pages., pp. 5621-5628.
- [76] A. McClanahan, S. Kharkovsky, A. R. Maxon, R. Zoughi and D. D. Palmer, *Depth evaluation of shallow surface cracks in metals using rectangular waveguides at millimeter-wave frequencies*, IEEE Trans. Instrum. Meas., vol. 59, no. 6, pp. 1693-1704, Jun. 2010.
- [77] J. R. Gallion and R. Zoughi, *Millimeter-wave imaging of surface-breaking cracks in steel with severe surface corrosion*, IEEE Trans. Instrum. Meas., vol. 66, no. 10, pp. 2789-2791, Oct. 2017.
- [78] B. Hu, Z. Ren, M. S. Boybay and O. M. Ramahi, *Waveguide probe loaded with split-ring resonators for crack detection in metallic surfaces*, IEEE Trans. Microw. Theory Techn., vol.

62, no. 4, pp. 871-878, Apr. 2014.

- [79] A. M. Yadegari, R. Moini, S. H. H. Sadeghi and F. Mazlumi, *Output signal prediction of an open-ended rectangular waveguide probe when scanning cracks at a non-zero lift-off*, NDT E Int., vol. 43, no. 1, pp. 1-7, Jan. 2010.
- [80] M. R. Ramzi, M. Abou-Khousa and I. Prayudi, *Near-field microwave imaging using open-ended circular waveguide probes*, IEEE Sensors J., vol. 17, no. 8, pp. 2359-2366, Apr. 2017.
- [81] C. A. Balanis, *Advanced Engineering Electromagnetics*, Hoboken, NJ, USA: Wiley, 2012.
- [82] A. J. Bahr, *Using electromagnetic scattering to estimate the depth of a rectangular slot*, IEEE Trans. Antennas Propag., vol. AP-27, no. 6, pp. 738-746, Nov. 1979.
- [83] M. Chizh, A. Zhuravlev, V. Razevig and S. Ivashov, *Non-destructive testing of the rails rolling surface and joints with synthetic aperture radar*, Proc. 21st Int. Radar Symp. (IRS), pp. 112-116, Oct. 2020.
- [84] C. Liu, M. T. A. Qaseer and R. Zoughi, *Influence of antenna pattern on synthetic aperture radar resolution for NDE applications*, IEEE Trans. Instrum. Meas., vol. 70, pp. 1-11, 2021.
- [85] Y. Bezin et al., *Multibody simulation benchmark for dynamic vehicle-track interaction in switches and crossings: results and method statements*, Vehicle System Dynamics, vol. 61 no. 3, pp. 660-697, 2023, doi: 10.1080/00423114.2021.1959038.
- [86] K. Saleh, S. Szénási & Z. Vámosy, *Occlusion handling in generic object detection: A review*, IEEE 19th World Symposium on Applied Machine Intelligence and Informatics (SAMI), pp. 000477-000484. doi: 10.1109/SAMI50585.2021.9378657 2021.
- [87] P. Leibner, F. Hampel, C. Schindler, *GERALD: A novel dataset for the detection of German mainline railway signals*, Proceedings of the Institution of Mechanical Engineers, Part F: Journal of Rail and Rapid Transit. 237(10):1332-1342. doi:10.1177/09544097231166472, 2023.
- [88] M. Cordts, M. Omran, S. Ramos, T. Rehfeld, M. Enzweiler, R. Benenson, & B. Schiele, *The cityscapes dataset for semantic urban scene understanding*, Proceedings of the IEEE conference on computer vision and pattern recognition, pp. 3213-3223. doi:10.48550/arXiv.1604.01685, 2016.
- [89] S. Lohar, L. Zhu, S. Young, P. Graf, and M. Blanton, *Sensing Technology Survey for Obstacle Detection in Vegetation*, Future Transportation 1, no. 3: 672-685. doi: 10.3390/futuretransp1030036 2021.
- [90] A. P. Synodinos, *Identification of railway track components and defects by analysis of wheel-rail interaction noise*, Conference: 23rd International Congress on Sound & Vibration (ICSV), July 2016.
- [91] K. Jahan; A. Lähns; B. Baasch; J. Heusel; M. Roth, *Rail Surface Defect Detection and Severity Analysis Using CNNs on Camera and Axle Box Acceleration Data*, Kumar, U., Karim, R., Galar, D., Kour, R. (eds) International Congress and Workshop on Industrial AI and eMaintenance 2023. IAI 2023. Lecture Notes in Mechanical Engineering. Springer, Cham.



https://doi.org/10.1007/978-3-031-39619-9_31, 2024.

- [92] Baasch, B.; Oselin, P.; Groos, J. C., Model-based and Data-driven Digital Twins for Railway Vehicle-Track Interaction Monitoring,“ in ECCOMAS 2024.